Sandra Cristina Campos de Jesus

Adjuvant Nanocarriers for Hepatitis B Vaccine: Formulation Design and Mechanistic Studies

Setembro 2015

UNIVERSIDADE DE COIMBRA

Front page figure caption: Transmission electron microscopy images of Hepatitis B surface antigen virus-like particles, nanoparticles complexed with plasmid DNA, exosomes and simple nanoparticles (from left to right). Arrows illustrate the sequence of events involved in the systemic immune response generation after vaccination (from top to bottom).

Adjuvant Nanocarriers for Hepatitis B Vaccine: Formulation Design and Mechanistic Studies

Sandra Cristina Campos de Jesus

Candidature thesis for doctor degree in Pharmaceutical Sciences, submitted to the Faculty of Pharmacy of the University of Coimbra

Tese de candidatura ao grau de doutor em Ciências Farmacêuticas, apresentada à Faculdade de Farmácia da Universidade de Coimbra

FFUC FACULDADE DE FARMÁCIA
UNIVERSIDADE DE COIMBRA

Acknowledgments / Agradecimentos

A nível pessoal, não posso deixar de agradecer a todos os amigos e família pelo contributo prestado, uma vez que esta jornada seria sem dúvida muito mais difícil, ou até impossível, se tivesse sido feita sozinha.

Ao Tiago, agradeço pelo amor e apoio que me dá em tudo. Sei que não é fácil diariamente somar horas de viagem às longas horas de trabalho, sem se esquecer de ter paciência para ouvir todos os meus desabafos. A ele, um enorme obrigada por me ajudar a pôr na cara todos os dias um sorriso, mesmo naqueles momentos mais difíceis. O misto de reforço positivo e negativo foi sem dúvida imprescindível para chegar ao fim desta etapa.

Em jeito de conclusão, e de uma forma muito especial, deixo aqui um agradecimento aos meus pais, que não só agora, mas em todo o meu percurso de vida e académico, foram os principais pilares de tudo o que realizei. Sem os seus conselhos e incondicional apoio, principalmente ao longo destes 10 anos fora de casa, não seria nada do que sou hoje! Agradeço-lhes todas as condições e oportunidades que me deram para conseguir chegar aqui, e agradeço ainda o esforço que sempre fizeram nas inúmeras viagens, que tornam Coimbra também a sua segunda casa. É sem dúvida um privilégio ter pais assim!

Table of contents

Chapter 2. Production and evaluation of PCL/chitosan NPs as vaccine delivery systems

Part 1. New insights on chitosan and poly-ε-caprolactone based nanoparticles as a protein delivery system

II

Chapter 3. Poly-ε-caprolactone/chitosan nanoparticles provide an adjuvant effect for recombinant HBsAg but not for the encoding plasmid DNA   99

Chapter 4. PCL/chitosan nanoparticles as a vaccine adjuvant for HBsAg subcutaneous vaccination – evaluation of immunostimulatory co-adjuvants

Part 1. Adjuvant activity of PCL/chitosan nanoparticles characterized by mast cell activation in vitro and IFN-γ and IL-17 production in vivo

Chapter 5. Generation of an immune response with a reduced HBsAg recombinant protein dose, intranasally delivered by PCL/chitosan nanoparticles

179

List of Abbreviations

APC(s)	Antigen presenting cell(s)
ATP	Adenosine triphosphate
BCA	Bicinchoninic acid assay
BMDC(s)	Blood marrow dendritic cell(s)
BSA	Bovine serum albumin
C3	Complement component 3
C3b	Element of complement component 3
C48/80	Compound C48/80
CD	Circular dichroism spectroscopy
CD4 + T cell	T cell lymphocyte with CD4+ receptor
CD8 + T cell	T cell lymphocyte with CD8+ receptor
CLR(s)	C- type lectin receptor(s)
CLSM	Confocal laser scanning microscopy
CpG ODN	Oligodeoxynucleotides with repeating CpG-motifs containing cytosine and guanine moieties
CPH	1,6-bis(p-carboxyphenoxy)hexane
CPP	1,3-bis(p-carboxyphenoxy)propane
CPTEG	1,8-bis(p-carboxyphenoxy)-3,6-dioxaoctane
cryoSEM	Cryo-scanning electron microscopy
CTL	Cytotoxic T lymphocytes
DAMP(s)	Danger associated molecular pattern(s)
DC(s)	Dendritic cell(s)
DDA	degree of deacetylation
DLN	Draining lymph nodes
DLS	Dynamic light scattering
DMEM	Dulbecco's modified Eagle's medium
DMSO	Dimethyl sulfoxide
DNA	Deoxyribonucleic acid
DNase	Deoxyribonuclease
DSC	Differential scanning calorimetry
DTA	Differential thermal analysis
EDTA	Ethylenediaminetetraacetic acid
ELISA	Enzyme-linked immunosorbent assay

ELS	Electrophoretic light scattering
EMA	European medicines agency
EV(s)	Extracellular vesicle(s)
EXO	Exosomes
F12	Ham´s F12 nutrient medium
FACs	Fluorescence-activated cell sorting
FBS	Fetal bovine serum
FDA	Food and drug administration
FELASA	Federation of laboratory animal science associations
FITC	Fluorescein isothiocyanate
FTIR	Fourier transform infrared spectroscopy
FTIR-ATR	Fourier transform infrared spectroscopy with attenuated total reflection
GALT	Gut-associated lymphoid tissue
HBsAg	Hepatitis B surface antigen
HBV	Hepatitis B virus
HRP	Horseradish peroxidase
HSA	Human serum albumin
HSP	Heat sock protein
ID	Intradermal
IFN-γ	Interferon gamma
Ig	Immunoglobulin
IL-	Interleukin
IM	Intramuscular
IMDM	Iscove's modified Dulbecco's medium
IN	Intranasal
IP	Intraperitoneal
LC	Loading capacity
LE	Loading efficacy
LMW	Low molecular weight
LN	Lymph nodes
LPS	Lipopolysaccharide
MALT	Mucosa-associated lymphoid tissue
MC(s)	Mast cell(s)
MFI	Mean fluorescence intensity
MHC	Major histocompatibility complex
MMW	Medium molecular weight

MPLA	Monophosphoryl Lipid A
MTT	3-(4,5-dimethylthiazol-2-yl)-2,5-diphenyltetrazolium bromide
MVB(s)	Multivesicular body(ies)
MW	Molecular weight
MWCO	Molecular weight cut-off
MyD88	Myeloid differentiation primary response gene 88 protein
NALT	Nasopharyngeal-associated lymphoid tissue
NF-κβ	nuclear factor kappa-light-chain-enhancer of activated B cells
NK	Natural killer
NLR(s)	NOD-like receptor(s)
NP(s)	Nanoparticle(s)
OD	Optical density
OPD	o-Phenylenediamine
OVA	Ovalbumin
PAMP(s)	Pathogen associated molecular pattern(s)
PAS	Periodic acid : Schiff
PB	Phosphate buffer
PBMC(s)	Peripheral blood mononuclear cell(s)
PBS	Phosphate buffer saline
PBS-T	Phosphate buffer saline with tween™ 20
PCL	Poly- -caprolactone
pCMVluc	plasmid DNA encoding luciferase
pDNA	Plasmid DNA
PEG	Polyethylene glycol
PEI	Polyethylenimine
PGA	Polyglycolic acid
PI	Propidium iodide
PI (disambiguation)	Polydispersity index
PLA	Polylactic acid
PLGA	Poly(lactic-co-glycolic) Acid
PMSF	Phenylmethylsulfonyl fluoride
PMVA	Poly(N-methyl-N-vinylacetamide)
PPS	Poly(p-phenylene sulfide)
Prc/CMV-HBS	Plasmid DNA encoding HBsAg
PRR(s)	Pattern recognition receptors
PVA	Polyvinyl alcohol

PVM/MA	Polyvinyl methyl ether/maleic acid
RBITC	Rhodamine B isothiocyanate
RLU	Relative light units
RPMI	Roswell park memorial institute medium
SA	Sebacic acid
SC	Subcutaneous
SD	Standard deviation
SDS	Sodium dodecyl sulfate
SEM	Standard error of the mean
SEM (disambiguation)	Scanning electron microscopy
SGF	Simulated gastric fluid
SIF	Simulated intestinal fluid
sIgA	Secretory immunoglobulin A
SNF	Simulated nasal fluid
TEER	Transepithelial resistance
TEM	Transmission electron microscopy
TGA	Thermogravimetric analysis
Th1	T helper type 1
Th17	T helper type 17
Th2	T helper type 2
TLR(s)	Toll-like receptor(s)
TMC	Trimethyl chitosan
TNF-α	Tumor necrosis factor alpha
TPP	Tripolyphosphate
UV	Ultraviolet
VLP(s)	Virus-like particles

Abstract

Vaccination is a major achievement in global public health, with a huge impact on modern society. The development of safer formulations has instigated the use of small proteins and other molecules containing antigenic epitopes instead of the inactivated or killed microorganisms. Those antigens have reduced immunogenicity and their efficacy is dependent on the presence of immunological adjuvants. Over the last years, different polymeric nanoparticles (NPs) have been tested as vaccine adjuvants acting as delivery systems, which protect and enhance the recognition of the antigen and its internalization by the specialized immune system cells.

Given the aforementioned considerations, the studies underlying the present dissertation aimed at preparing and evaluating polymeric NPs, based on poly- -caprolactone (PCL) and chitosan, as adjuvants for hepatitis B vaccine. PCL/chitosan NPs, prepared by a nanoprecipitation technique, were characterized and their capabilities as a vaccine adjuvant tested through *in vitro* and *in vivo* assays.

When suspended in water, NPs measured approximately 200 nm and presented a positive zeta potential (+ 25 mV). These NPs, constituted by the physical blend of two polymers, demonstrated to be cytocompatible with various cell lines and primary cells and revealed a good cellular interaction and internalization. The presence of chitosan on the surface of the NPs mainly constituted by PCL, yielded particles with a high loading capacity for model proteins and DNA plasmids through surface adsorption.

Using mononuclear cells isolated from human peripheral blood, it was possible to demonstrate that PCL/chitosan NPs did not induce TNF- secretion, a cytokine linked to inflammatory response and sometimes related to adjuvants mechanism of action. On the other hand, it was observed that PCL/chitosan NPs are mast cell activators. By inducing the activation, NPs contribute to mast cell degranulation, favoring the release of immune mediators with an active role in the generation of a protective immune response. These discoveries are important contributions to the knowledge of the PCL/chitosan NPs adjuvant mechanism.

Vaccination studies were performed in C57BL/6 mice, allowing for the first time, the validation of PCL/chitosan NPs as an adjuvant for a vaccine against hepatitis B virus.

One of the approaches considered was the development of a DNA vaccine, in which a plasmid encoding for the hepatitis B surface antigen (HBsAg) recombinant protein was adsorbed on the surface of the PCL/chitosan NPs. However, this approach conducted to a negligible immune response. On the other hand, a formulation developed with the recombinant HBsAg protein adsorbed on NPs surface led to a strong humoral immune response when administered subcutaneously, superior to the response generated by vaccination with the commercial vaccine Engerix-B®, at the same dose. It was also found

that the response generated was dependent on the NPs dose since highest doses of the adjuvant caused a significant increase in the production of cytokines secreted by Th1 and Th17 lymphocytes. In another strategy, exosomes were used as co-adjuvants of the nanoparticulate formulation vaccine. In the literature, exosomes are described as effective immunological adjuvants for tumor vaccination strategies but they are not yet widely explored as vaccine adjuvants for recombinant antigens. The study developed in this thesis demonstrated an increase in mice innate immune response after subcutaneous vaccination with the formulation co-adjuvanted with exosomes, as illustrated by the high production of basal IFN- from splenocytes. However, this formulation showed no advantage in the specific immune response.

Finally, vaccination studies through the nasal route were developed, encouraged by the good results of the subcutaneous immunization, together with the results demonstrating the ability of this NPs to adsorb mucin, an abundant glycoprotein in the mucus, and to be retained in an artificial mucus layer produced *in vitro*. The results showed the possibility of using PCL/chitosan NPs for nasal vaccination against hepatitis B using very small amounts of antigen.

Overall, with the work herein developed and described, it was possible to characterize PCL/chitosan NPs and test their ability as a delivery system and immunostimulatory adjuvant for vaccination purposes. Despite the extrapolation of these results to other recombinant antigens presents some limitations, the conclusions drawn here are of great importance for future applications of PCL/chitosan NPs.

Resumo

A vacinação tem um papel essencial na área da saúde pública e um enorme impacto na sociedade moderna. O desenvolvimento de formulações mais seguras tem levado a que a investigação de vacinas baseadas em microorganismos vivos inativados ou mortos seja preterida em prol da utilização de pequenas proteínas ou de outras moléculas contendo epítopos antigénicos, cuja imunogenicidade é reduzida. Contudo, o sucesso dessas vacinas depende da presença de adjuvantes imunológicos, por forma a aumentar a resposta imune gerada. Ao longo dos últimos anos diversas nanoparticulas (NPs) poliméricas têm sido estudadas como sistemas adjuvantes de vacinas, funcionando como sistemas de entrega, protegendo os antigénios e aumentando o reconhecimento e internalização destes por parte de células especializadas do sistema imunológico.

Face ao exposto, o objetivo do trabalho subjacente à presente dissertação consistiu na preparação e avaliação de NPs poliméricas de poli- -caprolactona (PCL) e quitosano como adjuvantes de uma vacina para a hepatite B. As NPs preparadas através do método de nanoprecipitação foram pormenorizadamente caracterizadas e as suas capacidades como adjuvantes avaliadas através de ensaios *in vitro* e *in vivo*.

Quando suspensas em água, as NPs apresentaram um tamanho aproximado de 200 nm e um potencial zeta positivo (+ 25 mV). Estas NPs, constituídas pela mistura física dos dois polímeros, revelaram citocompatibilidade com diversas linhas celulares e células primárias, boa interação e internalização celular. A presença de quitosano na superfície das NPs maioritariamente constituídas por PCL, permitiu obter partículas com uma elevada capacidade de carregamento de proteínas modelo e de plasmídeos através de adsorção à superfície.

Usando células mononucleares isoladas a partir de sangue periférico humano, demonstrou-se que estas NPs não induzem a secreção do fator de necrose tumoral alfa (TNF-), uma citocina ligada a reações inflamatórias, que, por vezes, está também na base do mecanismo de ação de alguns adjuvantes. Por outro lado, descobriu-se que as NPs de PCL/quitosano são ativadoras de mastócitos. A ativação destas células leva à sua desgranulação, favorecendo a libertação de mediadores imunológicos que tem um papel activo na geração da resposta imune. Ambas as descobertas foram importantes contribuições sobre o mecanismo adjuvante das NPs de PCL/quitosano.

Neste trabalho, estudos de vacinação de murganhos C57BL/6 permitiram validar, pela primeira vez, a aplicação das NPs de PCL/quitosano como um sistema adjuvante na vacinação contra a infeção pelo vírus da hepatite B. Inicialmente, testou-se uma vacina de ADN, na qual o plasmídeo codificado para a expressão do antigénio de superfície do vírus da hepatite B (HBsAg) foi adsorvido à superfície das NPs. No entanto, a resposta imune obtida com esta abordagem foi negligível. Por sua vez, as

formulações desenvolvidas com a proteína recombinante HBsAg adsorvida à superfície das NPs levaram a uma forte resposta humoral quando administradas pela via subcutânea, superior à resposta gerada pela vacinação com a vacina comercial Engerix-B®, na mesma dose. A reposta gerada foi dependente da dose de NPs administrada, sendo que doses mais elevadas deste adjuvante nanoparticulado geraram um aumento estatisticamente significativo na produção de citocinas secretadas por linfócitos do tipo Th1 e Th17. Numa outra abordagem, foram ainda usados exosomas, adjuvantes imunológicos ainda pouco explorados para vacinas baseadas em proteínas recombinantes, mas cujas propriedades têm revelado vantagens em estratégias de vacinação contra tumores. Os resultados da vacinação subcutânea com exosomas como adjuvantes da formulação de NPs adsorvida com o HBsAg, demonstraram o aumento da resposta imune inata *in vivo*, ilustrada pelos níveis basais elevados de interferão gama (IFN-) secretado por esplenócitos. No entanto, a utilização desta formulação não se mostrou vantajosa na resposta imune específica.

Por fim, realizaram-se estudos de vacinação pela via nasal encorajados pelos bons resultados da vacinação subcutânea e pela capacidade que as NPs demonstraram de adsorverem mucina, uma glicoproteína abundante no muco e de ficarem retidas sobre uma camada artificial de muco produzida *in vitro*. Estes estudos mostraram a possibilidade da utilização das NPs de PCL/quitosano para vacinação nasal contra a hepatite B, utilizando quantidades muito reduzidas de antigénio.

Em suma, ao longo dos trabalhos realizados no âmbito da presente tese de doutoramento, foi possível caracterizar e testar com sucesso as NPs de PCL/quitosano como adjuvantes da vacinação, quer pelo efeito de transporte, quer pelo efeito imunoestimulante. Apesar da extrapolação dos resultados entre antigénios recombinantes apresentar limitações, as conclusões inferidas ao longo dos estudos são de grande importância para futuras aplicações deste sistema polimérico.

Palavras-chave: Nanopartículas, vacinas, PCL, quitosano, antigénio, proteína recombinante, hepatite B, ADN, exosomas, administração subcutânea, administração nasal, nanopartículas de PCL/quitosano.

Chapter 1. Introduction

1. Nanotechnology at the forefront of medicine

Nanotechnology is a thriving area in the materials science whose multidisciplinary applications comprise distinct fields, as for example computer and biomedical sciences, with a common purpose to improve modern society lifestyles [1]. In nanomedicine, polymeric nano-constructs are designed to act as biological mimetics, biomaterials, nanoscale microfabrication-based devices, sensors and laboratory diagnostics [2]. Accordingly, European Medicines Agency (EMA) [3] defined nanomedicine as the application of nanotechnology to improve or generate medical diagnosis, treat or prevent diseases. In a reflection paper about nanotechnology-based medicinal products for human use published in 2006 [3], they defined nanotechnology as *"the production and application of structures, devices and systems by controlling the shape and size of materials at nanometer scale"*, considering that *"the nanometer scale ranges from the atomic level at around 0.2 nm (2 Å) up to around 100 nm"*. A more broaden definition of nanotechnology focus on the different physical and chemical properties of the nanoscale materials comparatively to those properties presented by bulk materials and larger size particles [4]. Consequently, Food and Drug Administration (FDA) guidance for considering whether an FDA-regulated product involves the application of nanotechnology [5] refers that it should be considered *"the evaluation of materials or end products engineered to exhibit properties or phenomena attributable to dimensions up to 1000 nm, as a means to screen materials for further examination and to determine whether these materials exhibit properties or phenomena attributable to their dimension(s) and associated with the application of nanotechnology"*.

In scientific reports the nanoscale range (0.2 nm - 100 nm) is generally not followed for defining nanoparticles (NPs), and most of the times they are referred as submicron sized particles or colloidal systems with sizes inferior to 1000 nm.

2. Polymeric nanoparticles and their application in modern vaccines

Polymeric NPs may be defined as colloidal particulate entities, comprised of synthetic or natural polymers, with size ranging from 1 nm to 1000 nm [6, 7]. Several relevant characteristics, transversal to all types of polymeric NPs, contribute to their continuous development in the most different scientific fields. For instance, biomedical applications in the prevention and treatment of diseases, beneficiate from its ability to transport and protect proteins, peptides, nucleic acids, oligonucleotides, drugs, among others. Also, polymeric NPs support the co-deliver of more than one compound simultaneously, potentiating the biomedical outcome. NPs are without a doubt excellent delivery systems, with the ability to encapsulate, adsorb or covalently bind cargo molecules [6]. The encapsulation presents some benefits regarding the protection and integrity of the cargo against physiological pH conditions, or biological secretions containing enzymes [8]. Adsorption on particle surface, in turn, avoids the harsh conditions of encapsulation during NPs production, which can interfere with the cargo final biological activity. The adsorption phenomena results generally from hydrophobic or electrostatic interactions and compared to the encapsulation method, can be responsible for a faster delivery of the cargo [6]. Importantly, the controlled release of the transported molecules is also influenced by the physicochemical properties of the polymers constituting the NPs [9].

Vaccines are one of the most important accomplishments in medicine, playing a fundamental role in the prevention of numerous infectious diseases. The success of vaccination programs over the years allowed saving millions of lives. Since 1796, with the introduction of the smallpox vaccine by Edward Jenner [10], the vaccine field is under continuous development and improvement to achieve increasingly effective and safer formulations. As vaccines are often administered to young and healthy individuals, medical risks must be reduced to a minimum. Therefore, traditional inactivated or live attenuated pathogen vaccines are preferably substituted with highly purified recombinant antigens and even epitope sequences, known to be inductive of a protective immune response [11]. DNA vaccines are a modern approach to develop new and safer vaccines. These vaccines are based on a plasmid encoding the vaccine antigen, which is further expressed in the cellular machinery of the host [12, 13]. In "nanovaccinology", polymeric nanoparticles are used as vaccine adjuvants, either as delivery systems for antigens or as immunostimulant entities, increasing total antibody titers, fastening and prolonging immune responses, increasing protective and therapeutic responses among special populations (young, older and immunocompromised individuals), decreasing antigen dose and vaccine boosts while maintaining efficient immunization, inducing potent cell mediated and mucosal immune responses, balancing or redirecting the immune response (Th1, Th2 and Th17) and inducing cross-protection [14]. Therefore, weak recombinant antigens can benefit from nanotechnology and particularly from polymeric

NPs. Similarly, these delivery systems may be helpful for DNA vaccination strategies. In fact, the transfection efficiency of a DNA vaccine is easily achieved with viral vectors, but their use arises safety concerns [12, 13]. Consequently, non-viral delivery approaches have been tested over the years to increase DNA vaccination, including the use of particulate adjuvants as platforms for DNA delivery.

Due to their nanoparticulate nature, small size and shape, NPs can enter living cells using cellular endocytosis mechanism, in particular pinocytosis [6]. Moreover, NPs can improve antigen recognition by the immune system, particularly from antibody presenting cells (APCs), resulting in increased antigen uptake and presentation, stimulation of cytokine production, upregulation of costimulatory molecules, migration of mature APCs to the draining lymph nodes and enhanced T cell stimulatory capacity [15-22]. Ultimately, this cascade of events may evolve towards immunosuppression or immunostimulation [19]. Both phenomena may constitute desirable or undesirable effects. In fact, immunosuppression may be desirable for the treatment of autoimmune [23] and inflammatory diseases [24], for the prevention of allergies [25] and for the prevention of transplant rejections [26] but it can also reduce immune responses to infections. On the other hand, immunostimulation is the most studied effect derived from polymeric nanoparticles, in particular for prophylactic and therapeutic vaccine purposes. However they might generate hypersensitive or allergic reactions. When administered locally in the tissues, polymeric NPs are known to create a depot effect, contributing to a prolonged and improved immune response [27]. Synthetic biodegradable polymers like poly(L-lactic acid) (PLA), poly(D,L-lactic-co-glycolic acid) (PLGA), poly(glycolic acid) (PGA), poly- -caprolactone (PCL) and natural biodegrable polymers as chitosan and alginate, are among the most attractive and studied materials used within the scope of nanoparticulate vaccine delivery systems.

In this review it will be explored how the application of polymeric NPs as vaccine adjuvants influence the immune response generated and the discussion will be illustrated with examples from recently published reports. Previously, some important notions regarding vaccine immune response will be addressed.

3. The immune response generation after immunization

The antigen association with polymeric NPs influences the course of the adaptive immune response triggered by inducing the production of co-stimulatory molecules or by directly affecting the antigen processing and presentation. To support the general description of the immune response given throughout the next pages, a brief resume of the basic mechanisms involved are schematized in Figure 1.

3.1. Antigen presenting cells: recognition and T cell differentiation

After vaccine administration in a healthy individual, immune system cells recognize and process antigens. Among these cells, macrophages, dendritic cells (DCs) and B-lymphocytes are the most important antigen presenting cells (APCs) involved in immune response generation. Particularly, immature DCs surveille the organism and upon recognition of a foreign material they internalize and process it, becoming mature DCs, able to express co-stimulatory molecules (CD40, CD83, CD86, etc.) [28]. Simultaneously they produce co-stimulating factors (cytokines) and migrate through lymphatic vessels to lymph nodes [28]. Processed antigens or protein epitopes are presented to naïve T cells through major histocompatibility complex molecules class I (MHC I) or class II (MHC II), inducing CD8+ or CD4 + T cell differentiation, respectively [29]. Normally, exogenous processed antigens are presented in the context of MHC II [30]. The presentation through MHC I require either endogenously produced viral proteins (possible with DNA vaccination) or a secondary phenomenon called cross-presentation (discussed ahead) [30]. As an illustration of what was described, Uto and co-workers [31] confirmed that after the SC immunization of C57BL/6 mice with 200-250 nm -PGA NPs loaded with antigens, the vaccine was internalized by DCs inducing the cell maturation and its migration to regional lymph nodes. DCs internalizing antigen- -PGA NPs were found to be expressing costimulatory molecules (CD80, CD86, CD40 and CCR7) and upregulating MHC I molecules. These are indicators of DCs maturation and initiation of the adaptive immune response [31].

Antigen intrinsic properties and vaccine adjuvants can influence the DCs maturation and expression of co-stimulatory factors (costimulatory markers or cytokine production) contributing for a specific type of immune response. Vaccines interaction with DCs happens mostly through pattern recognition receptors (PPRs) [32], an extended receptor family which comprises, among others, toll-like receptors (TLRs), C-type lectin receptors (CLRs) and Nod-like receptors (NLRs) [32, 33]. These receptors are able to recognize pathogen and danger associated molecular patterns (PAMPs and DAMPs) [34] ultimately leading to the activation of different signaling pathways. For instance, TLRs

activation may induce the mitogen-activated protein kinase (MAPK), nuclear factor- (NF-κ) or interferon regulatory factors (IRFs) pathways [35].

As an example, Hamasaki et al. reported that -PGA NPs (lipopolysaccharides (LPS) free) interacted with TLRs present in blood marrow dendritic cells (BMDCs) and induced the production of IL12p49, TNF-, IL-1 and IL-6 through the MyD88-mediated NF-κ pathway [36]. The authors found the gene expression pattern induced by -PGA NPs similar to the one induced by LPS, cytosine-phosphodiester-guanine oligodeoxynucleotide (CpG-ODN) and Zymosan, three vaccine adjuvants, ligands of TLR-4, TLR-9 and TLR-2 respectively [36], suggesting this TLRs may be involved in the interaction with -PGA NPs.

To conclude, in order to efficiently induce T cell differentiation, dendritic cells generate 3 different signals all influencing the resultant immune response: 1) antigen presentation through MHC I or II complexes; 2) costimulatory molecules expression; and 3) cytokine release [37].

3.2. Th1, Th2 and Th17 CD4+ T cell lineages differentiation

As stated before, the activation of different PRRs may be translated in a specific cytokine production with distinct T cell polarizing effects [32, 33]. As a matter of fact, the expansion of CD4+ T cells can result into 3 principal subpopulations: T helper (Th) 1 cells, Th2 cells and Th17 cells.

After expansion, the Th2 CD4+ T cell lineage is responsible for the production of IL-4, IL-5, IL-10 and IL-13 cytokines, and for the co-stimulation of B-cells which originates short lived plasma cells, able to produce antibody specific immunoglobulins [29]. Activated B-cells are also able to induce the clonal proliferation of germinal centers, where cells differentiate into memory B cells [29]. Memory B cells and long lived plasma cells, mainly found in the bone marrow, depend on stromal cells for survival and are responsible for the specific immunologic memory maintenance after vaccination [38]. Consequently, a further exposition to the virus will induce a rapid immune response onset, preventing the establishment of the infection [38].

Th1 CD4+ T cell lineage contributes to the production of specific immunoglobulin classes, generally associated to opsonization and virus neutralization (Th1 immunoglobulins – IgG2 and IgG3), but is also involved in cellular immunity by producing cytokines with immunoregulatory functions or with direct impact on invading pathogens. In fact, through the production of mostly IFN- and IL-2, Th1 CD4+ T cells are able to mediate macrophage activation and kill infecting pathogens [29].

Only in recent years, the Th17 subset of CD4+T helper cells has been investigated as a crucial lineage for vaccine induced protection. This lineage is induced by co-stimulatory cytokines as IL-6, TNF- and TNF-, IL-21, IL-23 and IL-1 that are produced by the activated APCs. On its turn, Th17 cells

produce IL-21 and IL-17 responsible for neutrophil recruitment [39] which has an impact in the protective immunity against infectious diseases, particularly at mucosal sites [32, 39]. Nonetheless, Th17 cell lineage is negatively regulated by Th1 and Th2 cytokines. This limitation, appears to be fundamental since Th17 CD4+ T cells have the ability to mediate serious inflammatory reactions and were already associated to autoimmune processes [39].

3.3. CD8+T cells differentiation

CD8+ T cell differentiation depend on the antigen presentation by MHC I molecules. After MHC I antigen presentation and correct co-stimulation, naïve T cells mature into CD8+ cytotoxic T lymphocytes (CTL). These cells are mainly involved in the clearance of intracellular viruses, bacteria and parasites, a key factor for the efficacy of therapeutic vaccines [29, 30]. Actually, strategies relying on stimulation of virus-specific CTL activity may contribute to the development of immunotherapies against chronic viral infections with a worldwide expression such as the human immunodeficiency virus (HIV), the hepatitis B virus (HBV), and the hepatitis C virus (HCV) infections [30].

Usually, the best mechanism for recombinant antigens to be efficiently presented by MHC I molecules is through cross-presentation. However, a different situation occurs with DNA vaccines since they mediate the recombinant antigen expression in the host cellular machinery. If the transfection of the plasmid (antigen expression) happen in APCs, the antigen will be processed as an endogenous antigen, by MHC I molecules, favoring the induction of CD8+ T cells [40].

3.3.1. Cross-presentation of the antigen

As previously stated, CD8+ T cell differentiation results either from MHC I antigen presentation of endogenously produced viral proteins or from MHC I antigen presentation of exogenous antigens, by a phenomenon called cross-presentation [30]. Cross-presentation may occur by two different pathways: (1) the cytosolic pathway where antigens are degraded by the proteasome; (2) and the vacuolar pathway where both antigen degradation and MHC I presentation occur primarily in the endocytic compartment [30]. The cross-presentation mechanism is believed to be highly dependent on the DCs maturation stimulus, resultant from the interaction with a foreign antigen. For instance, the interaction mediated by C-lectin type receptors (CLR) and also Fc receptors (particularly Fc R) is known to facilitate further cross-presentation of the antigen in MHC I [30].

Some examples may be found in the literature, regarding the contribution of polymeric NPs for the cross-presentation phenomenon. In fact, 350 nm PLA NPs were found to increase the uptake of the hepatitis B surface antigen (HBsAg) by J774A.1 macrophages, as well as to be co-localized with the

antigen, both in the lysosome and in the cytosol of the cells. On its turn, the soluble antigen and the alum adjuvanted antigen were mostly localized inside the lysosome. The two different trafficking fates of the antigen when delivered by PLA NPs explain the reported expression of MHC II and MHC I molecules at the surface of the cells. Therefore, PLA NPs contribute to the activation of both CD4+ T cells and CD8+ T cells. Soluble or alum-HBsAg only induced the expression of MHC II molecules, resultant from the lysosomal digestion of the extracellular pathogen. These results were confirmed in vivo by the increased production of IFN- by CD8+ T cells (isolated from spleens of vaccinated mice), after re-stimulation with HBsAg [41]. In another study, -PGA NPs were also found to promote ovalbumin (OVA) cross-presentation in DCs, when administered by SC route in C57BL/6 mice [31]. They showed the higher expression of MHC class I molecules at the surface of DCs containing OVA loaded -PGA NPs and the increase of OVA specific CD8+T cells in the spleens of immunized mice, 7 days after a single immunization [31]. Shen et al. [42] reported that 500-1000 nm PLGA NPs loaded with OVA, were able to generate similar levels of MHC class I cross-presentation as a 1000-fold higher concentration of soluble OVA in KG1.kb cells, a human dendritic cell line. The cross-presentation phenomenon was further proved to be dependent on endosomal escape of the antigen to the cytosol. In this study, the encapsulation of OVA was fundamental since OVA adsorbed PLGA NPs did not induce cross-presentation [42]. A last example of cross presentation mediated by polymeric NPs refers to PLGA NPs loaded with OVA and coated with protamine [43]. The coated NPs significantly improved the OVA delivery efficiency to BMDCs and the IL12p70 production, which is indicative of a switch to a Th1 immune response and CTL activity [43]. The cross-presentation phenomenon in this case, was explained by the arginine positive groups of protamine, that bonded the acidic phospholipidic groups in the lysosome membrane causing cytoplasmic escape of OVA *in vitro* [43]. In this situation, the expression of MHC I molecules at the surface of BMDCs was not increased, but the existent MHC I molecules presented higher levels of the exogenous peptide [43].
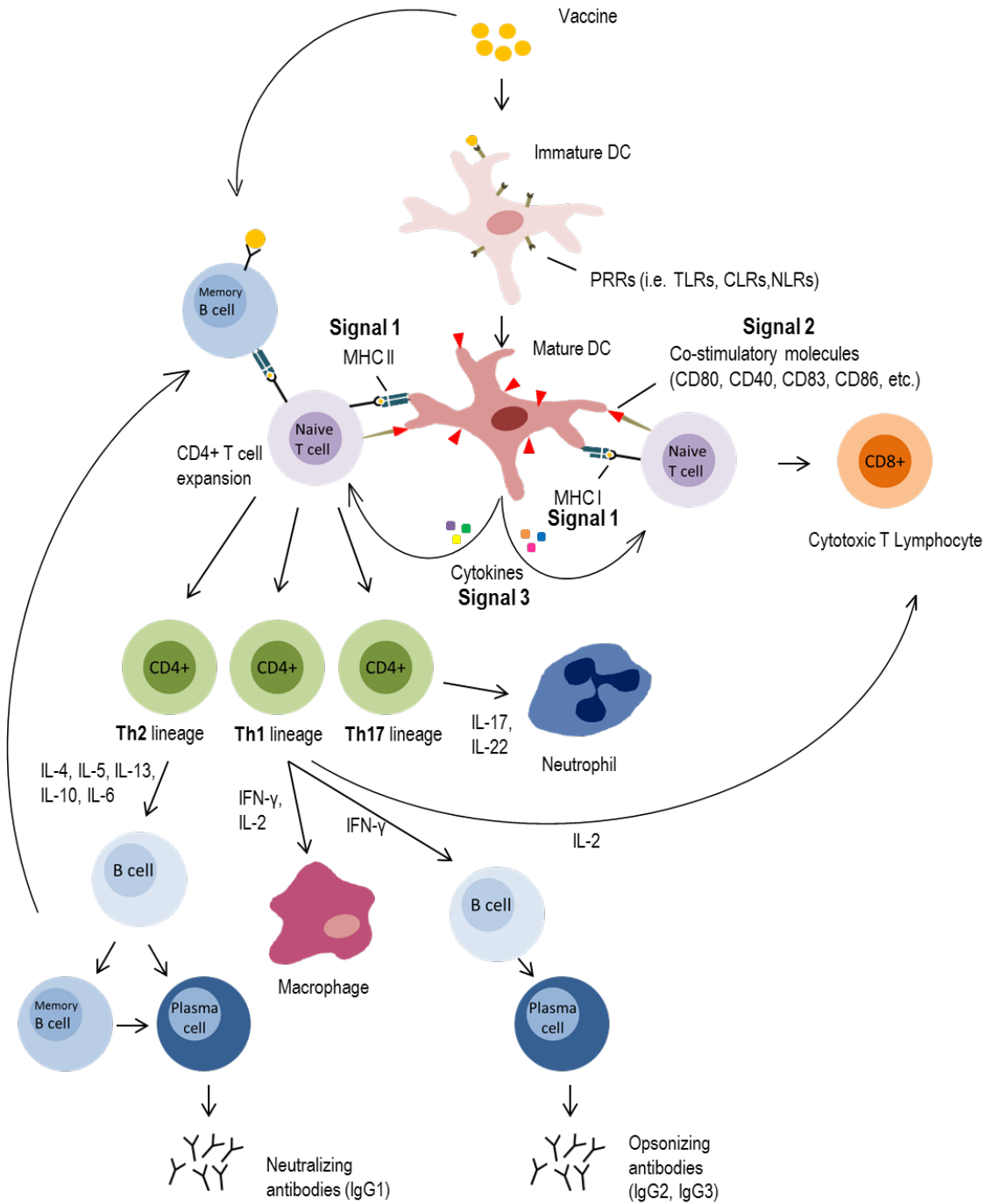
Figure 1: Schematic illustration of the general concepts regarding the immune response to vaccines. Following the arrows there is a brief overview of the T cell polarization involved in humoral and cellular immune responses. Antigens are recognized, processed and presented by dendritic cells (APCs) to naïve T cells. The antigen presentation through MHC molecules class I or II (signal 1) together with the presentation of co-stimulatory molecules (signal 2) and the secretion of cytokines (signal 3) dictate the expansion of the different CD4+ T cell lineages (Th2, Th1 and Th17) and the differentiation of CD8+ T cells. In turn, these cells release cytokines and

that stimulate the activity of B cells responsible for antibody production, macrophages, neutrophils and killer T cells.

3.4. Production of secretory IgA after mucosal vaccination

The mucosal (i.e. oral, rectal, vaginal, nasal, pulmonary) administration of vaccines is an important approach to the induction of antigen-specific IgA, an antibody that plays a critical role in mucosal immunity. Secretory immunoglobulin A (sIgA) differs from serum IgA by two additional features, the joining (J) chain and the secretory component [44]. The secretory component of sIgA among other functions protects the immunoglobulin from being degraded by proteolytic enzymes, so it can resist in the harsh mucosal environment [44]. Consequently, among antibodies present on mucosal surfaces, sIgA is able to block pathogen replication and is able to neutralize pathogen surface acting toxins [29].

In detail, when a vaccine is administered through mucosal routes, antigens are captured by cells from mucosal associated lymphoid tissues, particularly resident mucosal APC's (B-cells, macrophages and dendritic cells), and transported via afferent lymphatic vessels into regional lymph nodes where presentation to T-cells occurs. In addition to the systemic immune response developed, Th2 CD4+ T cells, induce IgA-committed-B cells, that migrate to effector mucosal sites [45]. IgA-committed-B cells together with IL-5 and IL-6 secreted by Th2 CD4+ cells, originate the production of dimeric IgA by plasma cells, which binds to polymeric immunoglobulin receptors present on mucosal epithelial cells, in order to be transported in the form of sIgA to the mucosal surface [29]. Therefore, both humoral systemic and mucosal immune responses are effectively generated.
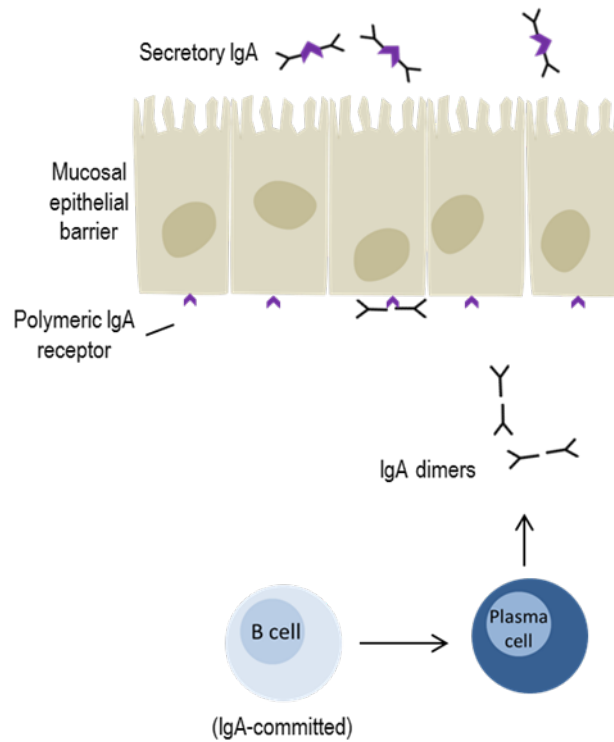
Figure 2: Secretory IgA production on mucosal effector sites. CD4+ T cells activated by mucosal-resident dendritic cells preferentially induce IgA-committed B cells. These cells, under the influence of co-stimulatory cytokines derived from Th2 CD4+ cells, are able to induce dimeric IgA production by plasma cells [29]. IFN-(produced by Th1 CD4+ T cells) on its turn, mediates the IgA receptor presence on epithelial cells, necessary to the transport of secretory IgA to mucosal surfaces [29].

4. Nanoparticle characteristics and its contribution to the type of immune response generated

As previously stated, polymeric nanoparticles (NPs), especially derived from biodegradable polymers are being widely investigated and used as antigen carriers, promoting specific humoral and cellular immune responses [6, 17, 46]. As vaccine adjuvants, polymeric NPs will act on the targeting, cell activation or antigen presentation, especially on high specialized APCs (macrophages and DCs) [28]. However, their exact immunological mechanism is poorly understood, particularly *in vivo* [31].

The particulate nature of the vaccine formulation has a great influence in the immune response outcome. One of the primordial mechanisms involved is the depot formation on the injection site. The deposition of the vaccine particulate formulation at the injection site is responsible for the destabilization of the local physiological micro-environment and most importantly contributes to the slow release of the antigens [27]. Authors of a study with a formulation containing OVA encapsulated into and mixed with PLGA NPs concluded that the free antigen (not encapsulated) is responsible for the initial immune system priming, while the encapsulated antigen depot, allowed for the continuous release of antigen over time [47]. Authors suggested the association of both effects were responsible for higher expression of both MHC molecules (MHC I and MHC II) and the co-stimulatory molecule CD86 on DCs as well as a higher frequency of follicular T helper cells in the draining lymph nodes [47]. The efficient CD4+ and CD8+ T cell expansion was associated with antigen prolonged supply [47, 48].

The APCs recognition and uptake of antigens transported by polymeric NPs is widely improved due to the formulations particulate nature [49]. The most probable explanation to this is the pathogen mimicking effect, since polymeric NPs are a foreign material resembling size and shape of a virus or bacteria. As soon as they are administered to an immunocompetent organism, surveilling APCs rapidly identify the antigen and process it. By improving the efficacy of the antigen delivery, NPs may also contribute to the reduction of the antigen dose as illustrated in some reports. Intramuscularly administered PLGA NPs loaded with a plasmid DNA for HSP65 (20 µg/mouse), were able to reduce inflammation, peribronchiolar and perivascular fibrosis and clearly lower the number of yeast cells and collagen deposition in lungs of animals infected with P. Brasiliensis [50]. These results were comparable to the ones induced by 400 µg of the same plasmid DNA without the use of the delivery system (naked) [50]. In another study, PLGA NPs loaded with tumor antigenic peptides originated a more robust CTL activity and a delayed and smaller tumor development than the same peptides administered in a concentration 63 fold higher, in the presence of incomplete Freund's adjuvant (IFA) [51]. However, caution must be taken when evaluating dose-sparing capacity of NPs. For example, killed porcine reproductive and respiratory syndrome virus entrapped into PLGA NPs elicited good neutralizing

antibody titers but were not able to induce viral clearance when the antigen dose was reduced 5 times [52].

Finally, some particulate adjuvants are also known to generate a local pro-inflammatory environment [22]. Although inflammation is considered a double edge sword contributing both to host defense and tissue damage, pro-inflammatory cytokines (IL-1- and TNF-) and chemokines (CCL4, CCL2, CXCL10, CXCL5 and CL5) may play a role in recruiting a variety of immune cells (monocytes, macrophages, DCs, neutrophils, NK and T memory cells) [53]. Carrilo-Conde et al. [54] referred that both mannose functionalized poly(anhydride) NPs as well as non-functionalized ones were able to stimulate DCs to secrete IL-6. This interleukin is important for both innate and adaptive immune responses contributing to a systemic inflammation and promoting humoral immune responses [54]. In some situations, blank NPs (without antigen) were found to generate non-specific immune responses with therapeutic outcome, which supports the intrinsic immunostimulator ability of some NPs. For instance, immunization with polyethylenimine (PEI)/ -PGA NPs coated with an empty plasmid DNA (vector), increased the survival rate of mice challenged with a lethal strain of Plasmodium yoelii17XL-parasitized red blood cells. This may be explained by the NPs stimulation of signaling pathways involved in the innate immunity. In fact, this empty plasmid delivery system was found to stimulate the production of IL12 and TNF- in an antigen independent manner [55].

Specific polymeric NPs characteristics such as polymer composition, hydrophobic-hydrophilic balance, surface charge and physical properties like the size and shape, are able to influence cellular interactions, immunomodulation activities and ultimately biocompatibility of the vaccine adjuvant [8]. Furthermore, targeting ligands or co-adjuvants may be used in an attempt to trigger specific immune mechanisms [8]. Although the further discussion will be focused on one characteristic at a time, it is important to consider a holistic approach when aiming vaccine design: the nanocarrier intrinsic chemical and physical properties, route of administration and temporal coordination (i.e., the host biological or disease temporal status and the cargo controlled release profile) [48, 56]. All factors are interconnected and together mediate one or multiple mechanisms responsible for initiating immune responses.

4.1. Composition as the primordial variable affecting nanoparticle ability as a vaccine adjuvant

Biodegradable polymers present advantages over non-biodegradable since they do not accumulate into cells and tissues inducing toxicity, and its degradation may be useful for a controlled release of the cargo molecules [7]. In detail, non-biodegradable polymers are eliminated from the organism through renal clearance which might induce some toxicity in the renal glomerular membrane, according to the

polymer's molecular weight (MW) and structure. By contrast, biodegradable polymers are degraded into smaller molecules by a metabolic clearance process and only then are eliminated by the kidney [57]. These polymers can derive from natural sources like chitosan (chitin) or proteins, or they can be synthetic like PLGA, PLA or PCL and normally allow for a slower cargo controlled release [8]. Briefly, some biodegradable polymer classes extensively used in NPs preparation will be described, together with some of their inherent characteristics in the context of vaccine adjuvants, as reported by other authors.

Polyesters are characterized by the presence of ester linkages in the main polymer chain, likely to be degraded by hydrolysis when subjected to physiological conditions. This biodegradability is conditioned by the length of the aliphatic chains between the ester bonds, and only the shorter lengths are degraded in useful time for biomedical approaches [8]. PLA, PGA, PLGA (copolymer) and PCL are polyesters commonly used in nanotechnology. PLA and PLGA are polylactides susceptible to be rapidly degraded by non-enzymatic hydrolysis [46]. This fast hydrolysis contributes to the accumulation of lactic and glycolic acids, which decrease the surrounding pH, eventually creating a harmful environment at release site [8]. In particular, PLGA has FDA approval for several clinical human applications [8] and PLGA NPs are widely attractive for the vaccine field due to its biocompatibility, size and controlled release that improve antigen uptake, presentation and cross-presentation by antigen presenting cells (APCs) [58]. PLGA NPs possess the ability to be taken up by Peyer´s patches (PPs) and efficiently target APCs leading to the activation of both CD8+ and CD4+ T cell immune responses [59]. PCL is a semicrystalline and highly hydrophobic polymer that presents slower degradation kinetics under physiological conditions when compared to polylactides. Therefore it avoids the physiological accumulation of degradation products and contributes to a prolonged release of the cargo compounds [57, 58]. PCL shows good *in vitro* stability and exceptional blend compatibility with other polymers, which can alter some of its mechanical, physical or ionic properties [60-62] and raises interest for a large set of different applications, from food packaging to tissue engineering [63-65]. Moreover it has FDA approval for some biomedical applications. At last, PCL hydrophobicity is known to increase the uptake by the nasal associated lymphoid tissue (NALT) [66].

Sebacic acid (SA), p-(carboxyphenoxy)propane (CPP), p-(carboxyphenoxy)hexane (CHP) and p-(carboxyphenoxy)dioxaoctane (CPTEG) are monomers that can form anhydride bounds between each other originating polyanhydride polymers [57]. Their degradation influences the controlled release of the cargo and generates non-toxic products [57]. The hydrophobicity degree of the constituting monomers is one of the main determinants of the polymers physical properties and stability [57, 67, 68]. Still regarding polyanhydrides, copolymers between methyl vinyl ether and maleic anhydride (PVMA) are being widely studied since their NPs preparation and consequent cargo loading can be achieved by a

mild process, due to the presence of anhydride reactive groups [8]. Also, Ulery et al. [69] proposed that when this polymer is degraded it exposes numerous hydroxyl end groups resembling pathogen-like characteristics (like the structural components of LPS), which explains its DC activating capacity.

Polyamides are polymers whose monomers are linked through amide bounds, such as proteins. These materials have excellent mechanical properties derived from the presence of amide groups and hydrogen bonds [57]. For instance, in the case of proteins the degradation rate depend on the hydrophilicity of the constitutive amino acids [57].

Polysaccharides are biodegradable and biocompatible polymers formed by glycosidic linkages of several monosaccharides. They constitute a very diverse group as polymers based on the same monosaccharide may differ in structure, conformation, length of the chain and the number of branches in it [57]. Chitosan for instance is the most described polysaccharide regarding polymeric NPs for the delivery of drugs, vaccines [70-72] and plasmids [73-75], among other biomedical applications [76-79]. Generically, chitosan-based formulations were reported to enhance antigen uptake and presentation and to have some intrinsic, direct immune-modulating activities [80-82]. Furthermore, chitosan is also known to be mucoadhesive and to promote the opening of intestinal and nasal mucosal tight junctions [80, 81]. This polymer is obtained through the partially N-deacetylation of chitin, which is extracted from cuticles of insect species or crustaceans such as crabs and shrimp [8]. The production process results in different polysaccharides with various molecular weights and deacetylation degrees, all known by the generic name chitosan [82] but presenting different properties. For instance, a report on 200 nm oily cores coated with chitosan (MW 125 kDa, 85.5 % deacetylation degree), showed they did not induce C3 complement cleavage important for the activation of the complement cascade [83] after interaction with complement factors present in PRRs (CLRs)[84]. Authors refer this fact as the result of the high degree of deacetylation of the chitosan used and although they did not test other chitosans they do not exclude the possibility of a different behavior with lower deacetylation degrees [83]. Derivatives of chitosan, such as tri-methyl chitosan (TMC) and glycol chitosan, are being produced to overcome its less attractive properties, like the low water solubility [82]. While chitosan at physiological pH loses its ability to enhance drug permeation and adsorption, TMC shows high solubility, bioadhesive properties and the ability to enhance permeation over a wide range of pHs [82]. The quaternization of the NH_2 group in TMC also increases the polymer positive charge when compared to chitosan. Nonetheless, different TMC synthesis methods can lead to different TMC derivatives and properties. Mangal et al. [85] reported that the tri-methylation of chitosan through a mild method was able to produce TMC with higher MW and intrinsic viscosity compared to the one produced by the traditional method. In fact, TMC NPs prepared with TMC produced by the mild method possessed increased zeta potential, better

mucoadhesive ability and induced stronger immune responses when were used to deliver HBsAg by intranasal (IN) route [85].

-Glucans are also an important group of polysaccharides with a key ability bind receptors present in the surface of macrophages, DCs, NK cells, monocytes or T-cells, such as dectin-1, TLRs, lactosylceramide, scavenger receptors and complement receptors, initiating and molding immune responses [86]. As in the case of chitosan, -glucans vary depending on the length and on branching structures of the assembled glucose monomers and therefore their effects in the immune system can be different [87]. In fact, Sonck et al. [87] studied the effect of different -glucans in the maturation of porcine BMDCs and concluded that they stimulate differently the DCs, since the profile of secreted cytokines diverged. Therefore, the -glucans should be carefully chosen according to their specific immunological effects.

4.2. The nanoparticle's size comparable to pathogens improves immune response to transported antigens

The NPs size is a major factor for cellular interaction. As previously referred, the NPs size comparable to pathogen size is believed to be important for APCs recognition and uptake, resulting in efficient induction of the immune system [6]. Pathogen size however is a broad concept, since virus size range from $\approx$ 30 nm to 200 nm and bacteria reaches few micrometers in length.

Small particles (< 200 nm) are able to drain freely from subcutaneous, muscular, and even mucosal sites of application directly to local lymph nodes [9, 48]. On its turn, particles with sizes higher than 200 nm must be phagocytosed by local or blood derived macrophages or DCs, in order to reach the draining lymph nodes [48]. However, some authors refer the 100 nm the border line size for lymph node free migration, instead of the 200 nm [6]. Particles with a size ranging from 20 nm to 200 nm are reported to be mostly taken up by DCs via clathrin-mediated endocytosis and are more likely to generate a virus like immune response with activation of CTL and Th1 cells [9], while those with 0.5 nm to 5 µm size range are primarily taken up by macrophages via macropinocytosis or phagocytosis and are more likely to generate humoral immune responses [6, 51, 88].

In non-phagocytic cell lines, only NPs measuring less than 100 nm are taken up by caveola- or clathrin- mediated endocytosis [48]. Therefore, the ideal size for NPs depends on the target cell type [48]. To test size influence, a great amount of studies have been performed in well-stablished cultured cell lines, like epithelial or immune system cell lines.

A report on chitosan particles with 2 different sizes (30-500 nm and 1000-6000 nm) demonstrated that both were efficiently taken up by DCs [89]. However, microparticles took longer to reach the

draining lymph nodes (DLN) in comparison to nanoparticles [89]. Despite this difference, both nano- and microparticles presented similar ability to induce antigen specific immune responses subcutaneously [89]. In this case, chitosan behavior as a charged polyelectrolyte seemed to overcome the size influence of the delivery system [89]. In order to explain the delayed arrival of microparticles to the DLNs, the authors compared their results with an observation from Manolova et al. [90] that found that polystyrene nanoparticles (20 nm and 200 nm) were preferably drained through the lymphatics to the DLNs, while microparticles (500 nm and 1000 nm) transport was cell mediated.

However, in the scientific literature it is possible to find conflicting reports about the effect of particles size on the triggered immune response. A review published in 2010 by Oyewumi et al. [91] extensively reported this situation. Briefly, in this review it was highlighted the contradictory results presented by different authors, some arguing that the strength of the immune responses induced is maximized with submicron particle sizes over those with larger sizes, and some arguing the opposite [91]. Moreover, the discussion extends to the type of immune response induced, which is also influenced by the particles size. Again, they mention conflicting data from different reports, hindering the exact conclusions on the relation between size and the triggered type of immune response [91].

4.3. Amphiphilic nanoparticles present advantages for the immune response triggering

Hydrophobicity is believed to be a damage-associated molecular pattern (DAMP) that causes PPR-dependent innate immune activation [92]. The rationale behind this theory results from the fact that hydrophobic cellular materials are only exposed in extracellular environment when pathological reactions occur (cell necrotic disruption) [93]. Therefore the presence of hydrophobic materials will also be regarded as a danger signal. However, Chavez-Santoscoy et al. [94] while evaluating the effects of di-mannose and galactose functionalization in poly(anhydride) NPs, referred that the hydrophilic properties of the formulation were also important to increase its uptake by alveolar macrophages. In fact, before the functionalization with the carbohydrates, they inserted a glycolic acid linker in the NPs, which caused them to lose part of their hydrophobic properties. This preliminary insertion of the spacer was enough to improve NPs uptake [94].

Furthermore, hydrophobic and amphiphilic poly(anhydride) co-polymers have different immunostimulatory properties. Ulery and co-workers [69] showed that DCs stimulated with CPH:SA 50:50 NPs (≈ 400 nm and hydrophobic) failed to increase the surface expression of MHC I and II and CD86 while CPTEG:CPH 50:50 NPs (≈200 nm and amphiphilic) increased these activation markers to levels similar to LPS stimulation. In a previous study, the same group showed poly(anhydride) NPs with

rich polymer chemistries both in SA and CPTEG were able to activate DCs. However, while the poly(SA) particles were believed to mimic a hydrophobic related danger signal, the CPTEG:CPH NPs present hydroxyl end groups to the APCs increasing their activation state [95]. Indeed, the superiority that hydrophobic surfaces demonstrate as cellular activators can be further enhanced by the presence of chemical groups such as $-NH_3^+$, $-OH^-$ or $-COOH^-$. An example of this influence was reported by Camacho et al. [96]. They found that the hydroxylated surface of PMVA NPs (poly(N-methyl-N-vinylacetaminde)), under physiological water conditions presented reactive hydroxyl nucleophiles able to form hydrogen bonds with C3b inducing the activation of the complement system, which is described as a key player for optimal T cell function [96].

Several strategies are reported in the literature in order to modify the hydrophobic/hydrophilic properties of the polymeric NPs, some of them based on the association of complementary polymers or surfactants. For instance, Binjawadagi et al. reported the incorporation of poloxamer 188 in PLGA NPs in order to give an hydrophilic nature to the aliphatic polyester particles [52]. These modifications changed the NPs hydrophobicity but also influenced its zeta potential, ultimately changing the formulation colloidal stability, mucoadhesion properties or protein adsorption ability [97].

4.4. Nanoparticle positive surface charge is important for cellular interaction

The surface charge of the NPs is a dynamic physicochemical property, highly influenced by the surrounding environment [48]. Besides the NPs size and its hydrophobic/hydrophilic character, the NPs surface charge also influences the efficiency and pathway of cellular uptake upon administration, by influencing the NPs interaction and adhesion to cells. Since cells membranes present negative charge, cationic particles are usually taken up more easily than anionic particles due to electrostatic interactions [6, 28]. Furthermore, although associated with some toxicity, cationic NPs tend to present a higher uptake by DCs mediated by clathrin receptors, while highly anionic NPs can be associated to immune tolerance, since they target MARCO scavenger receptors in macrophages and monocytes [48]. Importantly, the surface charge influence, in the generation of an immune response, is believed to be more determinant for bigger size NPs [6].

Neumman et al. [15], showed that the activation of the cytoplasmic NOD-like receptor called NLRP3 or NALP3, was not a general feature of all particulate vaccine adjuvants [15]. Activated NLRP3 binds to a caspase recruitment domain (ASC) and caspase-1 to form a protein complex called inflammasome able to stimulate the secretion of cytokines (IL-1 and IL-18) ultimately related to immune activation [15, 34]. By comparing the polymer-based chitosan NPs, lipid-based cubosomes, a water in oil emulsion of incomplete Freund's adjuvant (IFA) and alum formulations they concluded that only

chitosan NPs and alum formulations (formulations with positive charge) were able to induce IL-1 secretion *in vitro* [15]. In agreement they suggested that the positive charge could be the decisive factor for inflammasome activation upon NPs uptake by DCs and macrophages [15].

Another study showed that protein encapsulated PLGA NPs without coating (≈ - 15 mV), coated with chitosan or coated with glycol chitosan (both ≈ + 15 mV), induced different clearance rates from the nasal mucosa, induced different uptake profiles by epithelial and M cells at nasal mucosa surface and consequently induced different systemic uptake in blood and lymph nodes after nasal immunization [98]. Better results were found with positive charged NPs (coated), and originated better antibody titers and better cytokine levels [98]. As their size had no major differences (≈ 200 nm), the results were due to their better solubility and capacity to retain positive zeta potential at physiological pH, improving the interaction with the nasal mucosa [98].

Lastly, the cargo can also influence the formulation surface charge and consequently influence the vaccine efficacy. Oily core chitosan nanocapsules, with positive surface charges interact electrostatically with negatively charged HBsAg. Different ratios (w/w) between the nanocapsules and the antigen (ratio 1:0.25 vs ratio 1:12.8) generated similar sized delivery systems with opposite charges. As a result, positive or negative charged nanocapsules, containing the same HBsAg dose, administered through IM route, generated different immune responses. Only the positively charged formulation was able to generate a higher immune response than the one generated by HBsAg adjuvanted with alum (commercially available vaccines) [99].

4.5. Ability of nanoparticles to co-deliver immunopotentiators

An important characteristic of polymeric NPs is their ability to carry simultaneously the antigen and an additional adjuvant compound [28]. Although the particulate nature of polymeric NPs per se, and its characteristics result in the activation of PRRs as previously described, sometimes this activation is weak and unable to generate a proper immune response. Therefore, strategies involving the co-delivery of the antigen and immunomodulatory compounds using polymeric NPs, aims to increase and modulate immune responses. The most studied immunomodulatory molecules act as ligands for the most diverse PRR such as TLRs, NLRs and CLRs [100]. For instance, the TLR9 ligand CpG-ODN and the TLR4 ligand monophosphoryl lipid A (MPLA) are important adjuvants with comproved immunostimulatory effects [100]. Specifically, MPLA, a chemically modified derivative of LPS, when associated with aluminum salts constitutes the licensed adjuvant AS04, used in the commercially available Human papillomavirus (HPV) vaccine (from GlaxoSmithKline) [100].

The advantages of the co-delivery of immunopotentiator compounds with antigens in the same NP delivery system are reported in several articles. For instance, oily cores coated with chitosan with ≈ 200 nm only induced IL6, IL10 and TFN- cytokine release by peritoneal macrophages in vitro, when loaded with a TLR7 agonist (imiquimod) [83]. Without the co-adjuvant, nanocapsules only slightly increased the IL10 levels [83]. In another example, PLGA NPs co-encapsulating CpG-ODN and autoclaved *Leishmania major* antigen, originated a much stronger immune response in susceptible BALB/c mice, and a higher protection rate upon challenge with L. major, than NPs without the co-adjuvant [101]. Similarly, MPLA encapsulation into PLGA NPs together with OVA for oral administration leads increased systemic and mucosal immune responses in comparison to OVA encapsulated PLGA NPs with no extra adjuvant [59]. Still regarding PLGA NPs (copolymer ratio 50:50), J. Tel et al. [102] verified that antigen loaded NPs only induced the activation of human plasmacytoid DCs, characterized by the expression of costimulatory molecules essential for IFN- and induction of specific CD4+ and CD8+ T cell responses, when the R848 (TLR 7 agonist) was co-delivered in the formulation [102].

More than the use of a single TLR agonist on NPs, the co-entrapment of two TLR agonists may have a synergistic effect as demonstrated by Silva et al. [9]. They showed that the presence of both CpG-ODN and Poli-I-C (TLR 3 agonist) in OVA loaded aliphatic polyester NPs (constituted by a blend of PLGA, PEG-b-PLGA and PEG-b-PCL in a 70:15:15 w/w ratio) resulted in a more effective induction of a Th1 based immune response [9].

Adsorbing or encapsulating the adjuvant in the NPs is not the only strategy to use these immunopotentiators. For instance, the replacement of a crosslink with an immunopotentiator is also possible. Slutter and co-workers [103] aimed to produce OVA encapsulated TMC NPs using CpG-ODN as crosslink instead of TPP. The modification resulted in a more Th1 type response, while maintaining strong levels of mucosal and systemic antibodies, when the formulation was administered by the IN route. Important for the comparison, size and zeta potential of both systems were similar: ≈ 300 nm and + 20 mV [103].

4.6. Functionalization to improve nanoparticle capabilities as vaccine adjuvants

The functionalization of NPs with specific chemical moieties is used to achieve multiple objectives, such as the prevention of NPs interaction with the host media after administration, the prevention of agglomeration phenomena, the ability to transport specific cargo or the ability to target particular cells or cellular receptors, among others. Here, by NPs surface functionalization we intend to illustrate mostly the covalent conjugation and modification of NPs with ligands in order to potentiate immune system

recognition and activation. The strategy by which the ligand is attached to the NPs is the main difference when comparing to the co-delivery of adjuvants already described.

Aliphatic polyester NPs (constituted by a blend of PLGA, PEG-b-PLGA and PEG-b-PCL in a 70:15:15 w/w ratio) were functionalized with mannose in order to target C-type lectin receptor MR/CD206 on APCs, which is involved in the recognition and internalization of pathogens [9]. Results demonstrated increased antitumor efficacy compared to non-functionalized NPs. Likewise, the functionalization of poly(anhydride) NPs with specific carbohydrates (di-mannose and galactose) is expected to enable NPs to engage CLRs on alveolar macrophages and DCs, increasing immune responses of intranasal administered vaccines [54, 94]. While non-functionalized NPs interact with DCs mostly by its hydrophobic surface, as apoptotic cells or endogenous stressors would, functionalized NPs allow for a more robust responses induced by the microbial PAMPs [54]. Chavez-Santoscoy and co-workers [54, 94] showed that di-mannose or galactose functionalized poly(anhydride) NPs were able to enter alveolar macrophages and DCs more efficiently and comparatively to non-functionalized NPs, increasing surface expression of MHC I and II, CD86, CD40 as well as CLR. Nevertheless, only di-mannose functionalization enhanced IL12p40, IL1 and TNF- production, sustaining the activation of the NF-K pathway activation [94]. Galactose functionalization induced cytokine levels similar to non-functionalized NPs [94]. Another example is the functionalization of HBsAg encapsulated PLGA NPs, with -L-fucose specific *Tetragonolobus purpureas* or *Lotus tetragonolobus* (LTA) lectin ligand, which efficiently targeted M cells to Peyer´s patches after oral immunization, and improved the efficiency of the delivered vaccine [104].

Toll-like receptor agonists are also appreciated molecules for NPs functionalization. Bershteyn and co-workers [105] showed that the functionalization of PLGA (copolymer ratio 50:50) NPs, enveloped with a PEGilated phospholipid membrane containing lipophilic molecular danger signals (MPLA or/and - galactosylceramide (GC)), were able to elicit strong antibody titers at very low antigen doses, by SC route vaccination. Similarly, pluronic (F127)-stabilized poly(propylene sulfide) (PPS) NPs chemically conjugated with CpG-ODN are able to induce maturation markers (CD40, CD86 and MHCII) as well as inflammatory cytokines (IL12p40 and CXCL-10) in immature BMDCs in a dose dependent fashion [106]. As a final example of TLR functionalization, the grafting of a chitosan derivate (6-0-carboxymethyl-N,N,N-trimethylchitosan, with 23.2 % carboxymethylation and 33 % trimethylation) with PAM3Cys moiety, a TLR1/2 agonist, through a PEG spacer, induced IL-8 and TNF- increased expression in the basal compartment of a 3D cell culture system, which was used to mimic a human bronchial epithelial airway barrier [107]. The IL-8 increase is correlated with a possible adjuvant activity also observed *in vivo*, and the TNF- is correlated with a bias towards a Th1 type immune response [107].

As previously stated, NPs functionalization may also be used to mediate the conjugation of antigens. Indeed, the functionalization of choloacethyl groups in chitosan NPs is a strategy to covalently bind thiol-containing antigens to the NPs surface through a simple incubation under slightly basic conditions. This method present relative low costs and minimizes denaturing and degradation phenomena that may be associated to other encapsulation processes [89]. In the same way, the functionalization of pluronic stabilized poly(propylene) sulfide NPs with thiol reactive pyridyldisulphide groups allows for conjugation of thiol containing peptides and proteins under mild aqueous conditions. Additionally, this reduction sensitive dissulphide linkage is strongly beneficial for cross-presentation of antigens [108].

5. Factors non-inherent to adjuvant nanoparticles affect the immune response to vaccines

In addition to the NPs intrinsic characteristics, factors like the route of administration and immunization schedules may have a great impact in the vaccine efficacy and generation of a suitable immune response.

Considering the common vaccine administration routes, some important differences must be attended. Each route possesses unique profiles and subsets of APCs responsible for the activation of helper T cells, and for influencing B cell class switching to produce diverse antibody isotypes [28]. Subcutaneous and intramuscular routes, although widely employed for vaccination present some disadvantages as compared to dermal or mucosal routes. Indeed, little antigen presenting cells including DCs and macrophages essential to the immune response generation, are found in the muscle of healthy individuals [109]. In contrast, skin is very rich in cells involved in immune responses, including Langerhans cells (LCs), dermal fibroblasts (FBs), dendritic cells (DCs) and mast cells (MCs) [110]. Furthermore, skin is connected with local draining lymph nodes possessing T cells and B cells, through afferent and efferent lymph vessels [110]. Strategies like intradermal immunization or transcutaneous immunization are likely to be very effective. However, regarding transcutaneous immunization, methods to overcome the stratum corneum barrier are still under investigation [110]. Finally, mucosal vaccination presents an important advantage over all the other strategies: the induction of mucosal immunity. The vaccine delivery through the mucosa induces a systemic immune response, but also activates mucosal B and T lymphocytes, and stimulates secretory IgA antibody production, preventing pathogen infection through mucosal sites [111]. Moreover, mucosal vaccination presents advantages regarding patient compliance and simplified immunization procedures, with decreased risk of contamination, commonly related to injectable formulations.

As an example of the importance of the immunization route, pH responsive NPs constituted by di block copolymers that self-assemble into micellar structures were evaluated for ovalbumin vaccination with or without CpG-ODN, by subcutaneous and intradermal route (same dose and regimen). The increase in CD8+ T cell and Th1 responses was higher when the vaccine was intradermally administered [112]. Similarly, Influenza A H1N1 (A/California/7/2009) hemagglutinin (HA) antigen encapsulated in chitosan coated PCL NPs induced a more Th1 balanced immune response, when the same dose was administered by intranasal route compared to intramuscular route [66]. Mohanan et al. [113] studied the effect of the immunization route comparing the results from intradermal, intramuscular, subcutaneous or intralymphatic vaccination routes. Using 2 different formulations they reached the same conclusions. Both OVA encapsulated in TMC NPs and OVA encapsulated in PLGA microparticles

induced a higher IgG2a production when administered by the intralymphatic route in comparison to the other routes. However, in this study, they demonstrated that the IgG1 production is less affected by the immunization route, since both formulations induced similar IgG1 titers when administered by the 4 different routes [113]. Based on the results, Mohanan et al. demonstrated that the immunization route affects particularly the generation of a Th1 type immune response [113].

Apart from the immunization route, differences in the administration technique can be the reason for discrepant results, especially, the ones obtained from small animal models. For instance, some authors report nasal delivery of formulations by inserting (0.2 cm) into the nostril a small piece of tubing attached to a Hamilton syringe and ejecting 0.5 mL formulation into the nasal cavity [98]. However, Gupta et al. [66] used the same administration technique, but referred that administering 10 µL was the ideal volume to prevent divergent bioavailability, due to the deposition of the formulation into the lung and lower respiratory tract with higher volumes. Without inserting the piece of tubing, the simple deposition of the formulation in the mice nostrils, is also a common administration technique for nasal vaccines. Vicente et al. [83] referred the administration of 60 µL/mouse (10 µL per nostril x 3 administrations spaced with 5 min intervals. On its turn, Florindo and coworkers immunized BALB/c mice by instilling 50 µL of the formulations into the mice nostrils. In the same paper, they referred that a study developed by other authors, concluded that 40 % of the volume would passes to the lungs after a nasal administration [114].

Immunization routes in animal models may sometimes be unreliable. Intradermal immunization for instance, is expected to target a high density of Langerhans cells and dermal DCs. However, in mice, the reduced thickness of the dermis difficult the correct administration and sometimes the immunization may reach the subcutaneous level, originating erroneous experiment results [113].

Boost regimens more than improving the general outcome of vaccination may be also necessary to change the type of immune response generated. In fact, oily core chitosan nanocapsules adsorbed with HBsAg elicited a type of immune response dependent on the immunization regimen. A single dose of the formulation resulted in a predominant Th2 based immune response while the boost induced a Th1/Th2 balanced immune response [99]. A similar result was observed by Gupta and co-workers [66]. They reported that IgG2a antibody titers were only achieved after a second IN booster immunization.

Other factors, like the ones inherent to the production technique of similarly constituted NPs can influence the immune response generated by the formulation. As an example, De S. Rebouças et al. [115, 116] showed that poly(anhydride) NPs were more stable over time and presented an increased adjuvant effect when dried by spray-drying rather than freeze-drying. In fact, the higher stability of the spray-dried NPs originated a slower release of the antigen. The slower release is believed to be in the origin of the lower IgE induction in orally and intradermally immunized mice, and in the origin of the

increased IFN- production in intradermally immunized mice [115, 116]. They concluded that a more fast release of the antigen (in the freeze-dried NPs) originated a Th2 type immune response while the higher stability of the spray-dried NPs contributed to the prolonged interaction of the antigen with the APCs, directing to a more Th1 type immune response [116].

At last, endotoxins are widely present in the environment. Their negative charge derived from phosphate groups together with their hydrophobicity, are responsible for a strong interaction with most biomaterials, especially cationic or hydrophobic materials [117]. Lipopolysaccharide (LPS), is an endotoxin, a natural adjuvant derived from the cell membrane of gram-negative bacteria and generates an inflammatory environment during lymphocyte activation [118, 119]. It is heat-stable and binds to a LPS binding protein that promotes LPS presentation to CD14 receptors, which are responsible for its delivery to myeloid differentiation protein-2 (MD2). This protein activates signaling through TLR4 by both the MyD88-dependent and TRIF-dependent pathways, resulting in the release of inflammatory cytokines, including IL-1 , TNF- and IL-6, mainly secreted by immune cells such as macrophages and dendritic cells [118-120]. Therefore, LPS is also considered as a vaccine adjuvant [121] that under appropriate conditions supports the differentiation or function of Th1, Th2, Th17, or Treg subsets [118]. During production and usage of polymeric NPs, endotoxin contamination should be verified, in order to distinguish specific NPs effects from the ones mediated by endotoxins [120]. Natural origin biomaterials like chitosan, increase the struggle to avoid endotoxins contamination preventing false biomaterial-mediated immunostimulatory effects [82]. As an example of contamination results, Lieder and co-workers [122] have shown that chitosan oligosaccharides improved osteogenic differentiation and deposition of calcium hydroxyapatite crystals. However they observed that these effects were only observed when chitosan was endotoxin-contaminated and were abolished by its removal.

Still, a great number of reports on adjuvant polymeric NPs lack a proper evaluation of endotoxins content, hampering a correct assessment of the immunological effect of the biomaterials, especially in *in vitro* mechanistic studies [123].

6. Rationale behind the work developed

Despite the existence of a prophylactic vaccine against hepatitis B virus (HBV), recent data from World Health Organization (WHO) revealed that 2 billion people worldwide have been infected with the virus and presently, 240 million remain HBV chronic carriers [124]. Complications resultant from hepatitis B chronic infection, namely liver cirrhosis and hepatocellular carcinoma, are responsible for the death of an estimated 650 000 people every year [124]. An effective vaccine exists (90 % to 95 % efficacy) , however, transport logistics and administration requirements prevent many people to be efficiently vaccinated, particularly in developing countries. Actually, in sub-Saharan Africa and East Asia the prevalence of hepatitis B reaches 5 % to10 % of adult population [124]. For these reasons, HBV infection remains a major global health problem, motivating the continuous development of new prophylactic vaccines and efficient therapeutic vaccines [125].

The commercially available formulations against HBV contain the hepatitis B surface antigen (HBsAg) produced by recombinant DNA technology adsorbed on aluminum hydroxide gel, and follow an immunization schedule of 3 intramuscular boosts. In the presence of this adjuvant, DCs process HBsAg and present them to T cells, in the context of MHC II molecules. Activated CD4+ T cells proliferate and secrete Th2 cytokines (IL-4) which activate B cell differentiation into antibody producing cells (Th2 antibody isotype) [126]. In contrast to the commercially available formulations, a vaccine that elicits a robust Th1-based CD4+ T cell response, would be able to reverse the state of immune tolerance observed in chronic hepatitis B patients, and simultaneously activate anti-HBV CD8+ T cells necessary for viral clearance [126, 127]. This mechanism would therefore benefit a therapeutic vaccination approach during chronic HBV infection. So far, recombinant HBsAg vaccines have shown to be effective for prophylactic vaccination but they only elicit a momentary effect on viral replication, not enough for therapeutic purposes [126]. DNA vaccines on their turn, have already generated positive results for chronic hepatitis B therapeutic vaccination, ending immune tolerance and initiating viral clearance [126]. Nonetheless, safer non-viral vectors for efficient DNA vaccination are still under development.

In addition to the vaccine composition, improved immunization results may be achieved using different administration routes. Since the sexual contact is the major transmission route in low endemic areas, mucosal vaccines have advantages regarding the generation of sIgA at mucosal surfaces (i.e., vaginal mucosa), as discussed previously. Additionally, mucosal vaccination strategies would avoid the requirement for trained medical personnel for the administration procedure, reduce the risks of co-infections due to the reuse of needles and syringes and would increase patient compliance [128].

To date, several strategies using nanoparticulate delivery systems for hepatitis B vaccination were tested as an alternative to licensed vaccines. Delivery systems based on chitosan, PLGA and PLA

polymers have been extensively studied over the years, regarding this purpose. In particular, strategies including chitosan NPs, were previously studied by our group with success through subcutaneous [129], oral [130] and intranasal routes [131]. In those studies, recombinant HBsAg was efficiently encapsulated or adsorbed on chitosan NPs, and eventually coated with alginate, in order to increase their resistance in physiologic environment, specifically the gastrointestinal tract. The best results were found when CpG-ODN 1826 was used as a co-adjuvant of the formulations. A similar approach was recently tested by Sherstha et al. [132], but instead of alginate they used poly (vinyl alcohol) (PVA) as a non-digestive coating, inducing increased serum specific IgG levels in rats, after oral vaccination. For nasal vaccination against HBV, chitosan and its derivatives are also widely described, alone or in combination with PLGA or PLA. For instance, Pawar et al. [98, 133, 134] reported the nasal vaccination of mice with 10 µg of HBsAg loaded in chitosan NPs, glycol-chitosan NPs, chitosan-coated PLGA NPs, glycol-chitosan coated PLGA NPs or tri-methyl chitosan coated PLGA NPs. On its turn, Khatri et al. [135] tested intranasal vaccination of mice using chitosan NPs loaded with pDNA encoding for HBsAg and reported chitosan NPs as effective pDNA vaccine carrier and adjuvant. Strategies employing PLGA NPs have shown good results, nonetheless, the use of $Mg(OH)_2$ as a stabilizer is a requirement for the success of the formulation. As PLGA biodegradation results in the generation of an acidic environment, caused by lactic and glycolic acid, the addition of $Mg(OH)_2$ prevents the pH drop preventing HBsAg degradation during release [104, 136, 137].

In order to develop an improved HBV vaccine, PCL and chitosan, two well-known biodegradable polymers, were chosen to create a blend polymeric vaccine delivery system with immunostimulatory properties. During the design of the working strategy, one major concern was to achieve the final nanoparticulate vaccine formulation through technologically simple and attractive methods. Therefore, a nanoprecipitation technique was chose instead of the w/o/w emulsion diffusion solvent evaporation technique generally described for similar blend particles [66, 138, 139]. To the best of author's knowledge this was the first time the nanoprecipitation technique was used to prepare PCL/chitosan NPs with the intention to use as a vaccine delivery system for recombinant antigens. Moreover, among the known vaccination strategies previously reported for recombinant antigens with PCL particles modified with hydrophilic polymers, the cargo was encapsulated into the delivery system during the preparation of the particles [66, 138]. By contrast, we intend to load the PCL/chitosan NPs after preparation, by simple surface adsorption. Presumably, the external location of HBsAg recombinant protein will resemble virus surface epitopes enabling an effective recognition by immune system cells. Once more, this strategy has not been tested with recombinant proteins, which are generally less immunogenic and therefore more challenging to increase their specific immune responses. Despite the differences, previously published studies with related blend particles were the starting point and the

base of discussion for the development of an immunologically attractive formulation that exceeds the currently available vaccine options against hepatitis B infection.

6.1. Aim of the thesis

Polymeric NPs are with no doubt delivery systems with major abilities to develop successful vaccines. Accordingly, the aim of this thesis was to develop, characterize and evaluate *in vitro* and *in vivo*, PCL/chitosan NPs for different vaccination strategies against hepatitis B virus (HBV) infection.

6.2. Thesis outline

The first part of this work consisted in the preparation and extensive evaluation of PCL/chitosan NPs physical and chemical properties, as well as its behavior regarding model proteins and plasmid DNA. The discussion of PCL/chitosan NPs characteristics was enriched with direct comparisons to single polymer NPs (chitosan NPs and PCL NPs), prepared and tested under the same conditions. The comparison included also their different protein loading abilities and its release in simulated biological fluids. Regarding DNA complexation ability, studies were performed only with PCL/chitosan NPs and PCL NPs, since the chitosan capability as a gene delivery system is already extensively documented.

The incorporation of chitosan in PCL particles aimed to increase the immunomodulatory and mucoadhesive properties of the delivery system, as well as provide the particles an amphiphilic character and positive surface charge, important characteristics for immune cell recognition and cellular interaction. Consequently, comprehensive *in vitro* studies allowed the detailed analysis of the NPs cytotoxicity, cellular uptake, mucoadhesivity, transfection efficiency and possible immunostimulatory mechanisms involved in the immune response generation. For these purposes, different cell lines as the A549 and Calu-3 human lung epithelial cell lines, the Caco-2 human epithelial colorectal cell line, the HMC-1 human mast cell line and the THP-1 human monocyte cell line were used, as well as primary cells such as peripheral blood mononuclear cells isolated from the blood of healthy donors and splenocytes isolated from mice spleens.

After an extensive *in vitro* characterization of the polymeric delivery system, its adjuvant effect was validated with HBsAg through vaccination studies in mice. PCL/chitosan NPs loaded with HBsAg or pDNA encoding for HBsAg, were administered to C57BL/6 mice through the subcutaneous route and the immune responses generated were thoroughly evaluated. To assess the possibility of modulating the immune responses, CpG-ODN, a TLR9 agonist already used with success as adjuvant for HBsAg [129], was used as co-adjuvant in the recombinant vaccines prepared with PCL/chitosan NPs. Similarly, exosomes isolated from LPS stimulated monocytes were tested as adjuvants for free HBsAg

recombinant vaccine, and for HBsAg loaded PCL/chitosan NP vaccine. Finally, the positive results achieved by the subcutaneous route, allied to the suitable physicochemical properties of the delivery system, instigated the study of the prepared HBsAg loaded PCL/chitosan NP vaccine through the intranasal route of administration.

For each *in vivo* vaccination strategy, the humoral and cellular immune response generated was evaluated regarding its intensity and quality, focusing on the main objective of accomplishing an advantageous vaccine in comparison to the commercially available ones.

References

1.   Porter, A.L. and J. Youtie, *Where does nanotechnology belong in the map of science?* Nat Nano, 2009. **4**(9): p. 534-536.

2.   Moghimi, S.M., A.C. Hunter, and J.C. Murray, *Nanomedicine: current status and future prospects.* FASEB J, 2005. **19**(3): p. 311-30.

3.   European Medicines Agency (EMA). *EMEA/CHMP/79769/2006 - Reflection paper on nanotechnology-based medicinal products for human use.* European Medicines Agency (EMA) 2006 [Access 2015 July]; Available from: http://www.ema.europa.eu/docs/en_GB/document_library/Regulatory_and_procedural_guideline/2010/01/WC500069728.pdf.

4.   Hofmann-Amtenbrink, M., et al., *Nanotechnology in medicine: European research and its implications.* Swiss Med Wkly, 2014. **144**: p. w14044.

5.   Food and Drug Aministration (FDA). *Considering Whether an FDA-Regulated Product Involves the Application of Nanotechnology: Guidance for Industry.* Food and Drug Aministration (FDA) 2014 [Access 2015 July]; Available from: http://www.fda.gov/RegulatoryInformation/Guidances/ucm257698.htm.

6.   Zhao, L., et al., *Nanoparticle vaccines.* Vaccine, 2014. **32**(3): p. 327-37.

7.   Bolhassani, A., et al., *Polymeric nanoparticles: potent vectors for vaccine delivery targeting cancer and infectious diseases.* Hum Vaccin Immunother, 2014. **10**(2): p. 321-32.

8.   De Souza Reboucas, J., et al., *Nanoparticulate adjuvants and delivery systems for allergen immunotherapy.* J Biomed Biotechnol, 2012. **2012**: p. 474605.

9.   Silva, J.M., et al., *In vivo delivery of peptides and Toll-like receptor ligands by mannose-functionalized polymeric nanoparticles induces prophylactic and therapeutic anti-tumor immune responses in a melanoma model.* J Control Release, 2015. **198**: p. 91-103.

10.   Thomas, S. and B.A. Luxon, *Vaccines based on structure-based design provide protection against infectious diseases.* Expert Rev Vaccines, 2013. **12**(11): p. 1301-11.

11.   Brito, L.A. and D.T. O'Hagan, *Designing and building the next generation of improved vaccine adjuvants.* J Control Release, 2014. **190**: p. 563-79.

12.   Cordeiro, A.S., M.J. Alonso, and M. de la Fuente, *Nanoengineering of vaccines using natural polysaccharides.* Biotechnol Adv, 2015.

13.   Xiang, S.D., et al., *Delivery of DNA vaccines: an overview on the use of biodegradable polymeric and magnetic nanoparticles.* Wiley Interdiscip Rev Nanomed Nanobiotechnol, 2010. **2**(3): p. 205-18.

14.   Powell, B.S., A.K. Andrianov, and P.C. Fusco, *Polyionic vaccine adjuvants: another look at aluminum salts and polyelectrolytes.* Clin Exp Vaccine Res, 2015. **4**(1): p. 23-45.

15.   Neumann, S., et al., *Activation of the NLRP3 inflammasome is not a feature of all particulate vaccine adjuvants.* Immunol Cell Biol, 2014. **92**(6): p. 535-42.

16.   Moon, H.J., et al., *Mucosal immunization with recombinant influenza hemagglutinin protein and poly gamma-glutamate/chitosan nanoparticles induces protection against highly pathogenic influenza A virus.* Vet Microbiol, 2012. **160**(3-4): p. 277-89.

17.   Akagi, T., M. Baba, and M. Akashi, *Biodegradable Nanoparticles as Vaccine Adjuvants and Delivery Systems: Regulation of Immune Responses by Nanoparticle-Based Vaccine*, in *Polymers in Nanomedicine*, S. Kunugi and T. Yamaoka, Editors. 2012, Springer Berlin Heidelberg. p. 31-64.

18.   Tamayo, I., et al., *Poly(anhydride) nanoparticles act as active Th1 adjuvants through Toll-like receptor exploitation.* Clin Vaccine Immunol, 2010. **17**(9): p. 1356-62.

19.   Jiao, Q., et al., *Immunomodulation of nanoparticles in nanomedicine applications.* Biomed Res Int, 2014. **2014**: p. 426028.

20.	Gregory, A.E., R. Titball, and D. Williamson, *Vaccine delivery using nanoparticles.* Front Cell Infect Microbiol, 2013. **3**: p. 13.

21.	Joshi, V.B., S.M. Geary, and A.K. Salem, *Biodegradable particles as vaccine antigen delivery systems for stimulating cellular immune responses.* Hum Vaccin Immunother, 2013. **9**(12): p. 2584-90.

22.	Awate, S., L.A. Babiuk, and G. Mutwiri, *Mechanisms of action of adjuvants.* Front Immunol, 2013. **4**: p. 114.

23.	Heo, R., et al., *Hyaluronan nanoparticles bearing gamma-secretase inhibitor: in vivo therapeutic effects on rheumatoid arthritis.* J Control Release, 2014. **192**: p. 295-300.

24.	Yoo, D., et al., *Antioxidant polymeric nanoparticles as novel therapeutics for airway inflammatory diseases.* Int J Pharm, 2013. **450**(1-2): p. 87-94.

25.	Maldonado, R.A., et al., *Polymeric synthetic nanoparticles for the induction of antigen-specific immunological tolerance.* Proc Natl Acad Sci U S A, 2015. **112**(2): p. E156-65.

26.	Pan, Q., et al., *Corticosteroid-loaded biodegradable nanoparticles for prevention of corneal allograft rejection in rats.* J Control Release, 2015. **201**: p. 32-40.

27.	Zolnik, B.S., et al., *Nanoparticles and the immune system.* Endocrinology, 2010. **151**(2): p. 458-65.

28.	Leleux, J. and K. Roy, *Micro and nanoparticle-based delivery systems for vaccine immunotherapy: an immunological and materials perspective.* Adv Healthc Mater, 2013. **2**(1): p. 72-94.

29.	McNeela, E.A. and K.H. Mills, *Manipulating the immune system: humoral versus cell-mediated immunity.* Adv Drug Deliv Rev, 2001. **51**(1-3): p. 43-54.

30.	van Montfoort, N., E. van der Aa, and A.M. Woltman, *Understanding MHC class I presentation of viral antigens by human dendritic cells as a basis for rational design of therapeutic vaccines.* Front Immunol, 2014. **5**: p. 182.

31.	Uto, T., et al., *Uptake of biodegradable poly(gamma-glutamic acid) nanoparticles and antigen presentation by dendritic cells in vivo.* Results Immunol, 2013. **3**: p. 1-9.

32.	Lin, Y., S.R. Slight, and S.A. Khader, *Th17 cytokines and vaccine-induced immunity.* Semin Immunopathol, 2010. **32**(1): p. 79-90.

33.	McAleer, J.P. and A.T. Vella, *Educating CD4 T cells with vaccine adjuvants: lessons from lipopolysaccharide.* Trends Immunol, 2010. **31**(11): p. 429-35.

34.	Kuroda, E., C. Coban, and K.J. Ishii, *Particulate adjuvant and innate immunity: past achievements, present findings, and future prospects.* Int Rev Immunol, 2013. **32**(2): p. 209-20.

35.	Dalod, M., et al., *Dendritic cell maturation: functional specialization through signaling specificity and transcriptional programming.* Embo j, 2014. **33**(10): p. 1104-16.

36.	Hamasaki, T., et al., *Modulation of gene expression related to Toll-like receptor signaling in dendritic cells by poly(gamma-glutamic acid) nanoparticles.* Clin Vaccine Immunol, 2010. **17**(5): p. 748-56.

37.	Walsh, K.P. and K.H. Mills, *Dendritic cells and other innate determinants of T helper cell polarisation.* Trends Immunol, 2013. **34**(11): p. 521-30.

38.	Lambert, P.H., M. Liu, and C.A. Siegrist, *Can successful vaccines teach us how to induce efficient protective immune responses?* Nat Med, 2005. **11**(4 Suppl): p. S54-62.

39.	Dubin, P.J. and J.K. Kolls, *Th17 cytokines and mucosal immunity.* Immunol Rev, 2008. **226**: p. 160-71.

40.	Li, L., F. Saade, and N. Petrovsky, *The future of human DNA vaccines.* J Biotechnol, 2012. **162**(2-3): p. 171-82.

41.	Yue, H., et al., *The orchestration of cellular and humoral responses is facilitated by divergent intracellular antigen trafficking in nanoparticle-based therapeutic vaccine.* Pharmacol Res, 2012. **65**(2): p. 189-97.

42. Shen, H., et al., *Enhanced and prolonged cross-presentation following endosomal escape of exogenous antigens encapsulated in biodegradable nanoparticles.* Immunology, 2006. **117**(1): p. 78-88.

43. Han, R., et al., *Surface modification of poly(D,L-lactic-co-glycolic acid) nanoparticles with protamine enhanced cross-presentation of encapsulated ovalbumin by bone marrow-derived dendritic cells.* J Biomed Mater Res A, 2011. **96**(1): p. 142-9.

44. Corthésy, B., *Multi-Faceted Functions of Secretory IgA at Mucosal Surfaces.* Frontiers in Immunology, 2013. **4**: p. 185.

45. Kiyono, H. and S. Fukuyama, *NALT- versus Peyer's-patch-mediated mucosal immunity.* Nat Rev Immunol, 2004. **4**(9): p. 699-710.

46. Jain, N.K., et al., *Formulation and stabilization of recombinant protein based virus-like particle vaccines.* Adv Drug Deliv Rev, 2014.

47. Zhang, W., et al., *Immune responses to vaccines involving a combined antigen-nanoparticle mixture and nanoparticle-encapsulated antigen formulation.* Biomaterials, 2014. **35**(23): p. 6086-97.

48. Getts, D.R., et al., *Harnessing nanoparticles for immune modulation.* Trends Immunol, 2015. **36**(7): p. 419-27.

49. Correia-Pinto, J.F., N. Csaba, and M.J. Alonso, *Vaccine delivery carriers: insights and future perspectives.* Int J Pharm, 2013. **440**(1): p. 27-38.

50. Ribeiro, A.M., et al., *Nanobiotechnological approaches to delivery of DNA vaccine against fungal infection.* J Biomed Nanotechnol, 2013. **9**(2): p. 221-30.

51. Ma, W., et al., *PLGA nanoparticle-mediated delivery of tumor antigenic peptides elicits effective immune responses.* Int J Nanomedicine, 2012. **7**: p. 1475-87.

52. Binjawadagi, B., et al., *Adjuvanted poly(lactic-co-glycolic) acid nanoparticle-entrapped inactivated porcine reproductive and respiratory syndrome virus vaccine elicits cross-protective immune response in pigs.* Int J Nanomedicine, 2014. **9**: p. 679-94.

53. Fairley, S.J., et al., *Chlamydia trachomatis recombinant MOMP encapsulated in PLGA nanoparticles triggers primarily T helper 1 cellular and antibody immune responses in mice: a desirable candidate nanovaccine.* Int J Nanomedicine, 2013. **8**: p. 2085-99.

54. Carrillo-Conde, B., et al., *Mannose-functionalized "pathogen-like" polyanhydride nanoparticles target C-type lectin receptors on dendritic cells.* Mol Pharm, 2011. **8**(5): p. 1877-86.

55. Cherif, M.S., et al., *Nanoparticle formulation enhanced protective immunity provoked by PYGPI8p-transamidase related protein (PyTAM) DNA vaccine in Plasmodium yoelii malaria model.* Vaccine, 2014. **32**(17): p. 1998-2006.

56. Cheng, C.J., et al., *A holistic approach to targeting disease with polymeric nanoparticles.* Nat Rev Drug Discov, 2015. **14**(4): p. 239-47.

57. Vilar, G., J. Tulla-Puche, and F. Albericio, *Polymers and drug delivery systems.* Curr Drug Deliv, 2012. **9**(4): p. 367-94.

58. Manish, M., et al., *A single-dose PLGA encapsulated protective antigen domain 4 nanoformulation protects mice against Bacillus anthracis spore challenge.* PLoS One, 2013. **8**(4): p. e61885.

59. Sarti, F., et al., *In vivo evidence of oral vaccination with PLGA nanoparticles containing the immunostimulant monophosphoryl lipid A.* Biomaterials, 2011. **32**(16): p. 4052-7.

60. Dash, T.K. and V.B. Konkimalla, *Poly-epsilon-caprolactone based formulations for drug delivery and tissue engineering: A review.* J Control Release, 2012. **158**(1): p. 15-33.

61. Mahapatro, A. and D.K. Singh, *Biodegradable nanoparticles are excellent vehicle for site directed in-vivo delivery of drugs and vaccines.* J Nanobiotechnology, 2011. **9**: p. 55.

62. Silva, J.M., et al., *Immune system targeting by biodegradable nanoparticles for cancer vaccines.* J Control Release, 2013. **168**(2): p. 179-99.

63. Beltran, A., et al., *Characterization of poly(epsilon-caprolactone)-based nanocomposites containing hydroxytyrosol for active food packaging.* J Agric Food Chem, 2014. **62**(10): p. 2244-52.

64. Gloria, A., et al., *Magnetic poly(epsilon-caprolactone)/iron-doped hydroxyapatite nanocomposite substrates for advanced bone tissue engineering.* J R Soc Interface, 2013. **10**(80): p. 20120833.

65. Woodruff, M.A. and D.W. Hutmacher, *The return of a forgotten polymer—Polycaprolactone in the 21st century.* Progress in Polymer Science, 2010. **35**(10): p. 1217-1256.

66. Gupta, N.K., et al., *Development and characterization of chitosan coated poly-(varepsilon-caprolactone) nanoparticulate system for effective immunization against influenza.* Vaccine, 2011. **29**(48): p. 9026-37.

67. Torres, M.P., et al., *Amphiphilic polyanhydrides for protein stabilization and release.* Biomaterials, 2007. **28**(1): p. 108-16.

68. Joshi, V.B., et al., *Characterizing the antitumor response in mice treated with antigen-loaded polyanhydride microparticles.* Acta Biomater, 2013. **9**(3): p. 5583-9.

69. Ulery, B.D., et al., *Rational design of pathogen-mimicking amphiphilic materials as nanoadjuvants.* Sci Rep, 2011. **1**: p. 198.

70. Lebre, F., et al., *Progress towards a needle-free hepatitis B vaccine.* Pharm Res, 2011. **28**(5): p. 986-1012.

71. Panos, I., N. Acosta, and A. Heras, *New drug delivery systems based on chitosan.* Curr Drug Discov Technol, 2008. **5**(4): p. 333-41.

72. Baldrick, P., *The safety of chitosan as a pharmaceutical excipient.* Regul Toxicol Pharmacol, 2010. **56**(3): p. 290-9.

73. Lavertu, M., et al., *High efficiency gene transfer using chitosan/DNA nanoparticles with specific combinations of molecular weight and degree of deacetylation.* Biomaterials, 2006. **27**(27): p. 4815-24.

74. Picola, I.P.D., et al., *Effect of ionic strength solution on the stability of chitosan–DNA nanoparticles.* Journal of Experimental Nanoscience, 2012. **8**(5): p. 703-716.

75. Amaduzzi, F., et al., *Chitosan-DNA complexes: charge inversion and DNA condensation.* Colloids Surf B Biointerfaces, 2014. **114**: p. 1-10.

76. Fonte, P., et al., *Polymer-based nanoparticles for oral insulin delivery: Revisited approaches.* Biotechnol Adv, 2015.

77. Azuma, K., et al., *Anticancer and anti-inflammatory properties of chitin and chitosan oligosaccharides.* J Funct Biomater, 2015. **6**(1): p. 33-49.

78. Pallela, R., *Nutraceutical and pharmacological implications of marine carbohydrates.* Adv Food Nutr Res, 2014. **73**: p. 183-95.

79. Kerch, G., *The potential of chitosan and its derivatives in prevention and treatment of age-related diseases.* Mar Drugs, 2015. **13**(4): p. 2158-82.

80. Borges, O., et al., *Induction of lymphocytes activated marker CD69 following exposure to chitosan and alginate biopolymers.* Int J Pharm, 2007. **337**(1-2): p. 254-64.

81. Bakhru, S.H., et al., *Oral delivery of proteins by biodegradable nanoparticles.* Adv Drug Deliv Rev, 2013. **65**(6): p. 811-21.

82. Vasiliev, Y.M., *Chitosan-based vaccine adjuvants: incomplete characterization complicates preclinical and clinical evaluation.* Expert Rev Vaccines, 2015. **14**(1): p. 37-53.

83. Vicente, S., et al., *Co-delivery of viral proteins and a TLR7 agonist from polysaccharide nanocapsules: a needle-free vaccination strategy.* J Control Release, 2013. **172**(3): p. 773-81.

84. Bergmann-Leitner, E.S., W.W. Leitner, and G.C. Tsokos, *Complement 3d: from molecular adjuvant to target of immune escape mechanisms.* Clin Immunol, 2006. **121**(2): p. 177-85.

85. Mangal, S., et al., *Pharmaceutical and immunological evaluation of mucoadhesive nanoparticles based delivery system(s) administered intranasally.* Vaccine, 2011. **29**(31): p. 4953-62.

86. Devi, K.S., et al., *Heteroglucan-dendrimer glycoconjugate: a modulated construct with augmented immune responses and signaling phenomena.* Biochim Biophys Acta, 2014. **1840**(9): p. 2794-805.

87. Sonck, E., et al., *Varying effects of different beta-glucans on the maturation of porcine monocyte-derived dendritic cells.* Clin Vaccine Immunol, 2011. **18**(9): p. 1441-6.

88. Xiang, S.D., et al., *Pathogen recognition and development of particulate vaccines: does size matter?* Methods, 2006. **40**(1): p. 1-9.

89. Chua, B.Y., et al., *Chitosan microparticles and nanoparticles as biocompatible delivery vehicles for peptide and protein-based immunocontraceptive vaccines.* Mol Pharm, 2012. **9**(1): p. 81-90.

90. Manolova, V., et al., *Nanoparticles target distinct dendritic cell populations according to their size.* Eur J Immunol, 2008. **38**(5): p. 1404-13.

91. Oyewumi, M.O., A. Kumar, and Z. Cui, *Nano-microparticles as immune adjuvants: correlating particle sizes and the resultant immune responses.* Expert Rev Vaccines, 2010. **9**(9): p. 1095-107.

92. Woodrow, K.A., K.M. Bennett, and D.D. Lo, *Mucosal vaccine design and delivery.* Annu Rev Biomed Eng, 2012. **14**: p. 17-46.

93. Moyano, D.F., et al., *Nanoparticle hydrophobicity dictates immune response.* J Am Chem Soc, 2012. **134**(9): p. 3965-7.

94. Chavez-Santoscoy, A.V., et al., *Tailoring the immune response by targeting C-type lectin receptors on alveolar macrophages using "pathogen-like" amphiphilic polyanhydride nanoparticles.* Biomaterials, 2012. **33**(18): p. 4762-72.

95. Petersen, L.K., et al., *Activation of innate immune responses in a pathogen-mimicking manner by amphiphilic polyanhydride nanoparticle adjuvants.* Biomaterials, 2011. **32**(28): p. 6815-22.

96. Camacho, A.I., et al., *Poly(methyl vinyl ether-co-maleic anhydride) nanoparticles as innate immune system activators.* Vaccine, 2011. **29**(41): p. 7130-5.

97. des Rieux, A., et al., *Nanoparticles as potential oral delivery systems of proteins and vaccines: a mechanistic approach.* J Control Release, 2006. **116**(1): p. 1-27.

98. Pawar, D., et al., *Development and characterization of surface modified PLGA nanoparticles for nasal vaccine delivery: effect of mucoadhesive coating on antigen uptake and immune adjuvant activity.* Eur J Pharm Biopharm, 2013. **85**(3 Pt A): p. 550-9.

99. Vicente, S., et al., *A polymer/oil based nanovaccine as a single-dose immunization approach.* PLoS One, 2013. **8**(4): p. e62500.

100. Reed, S.G., M.T. Orr, and C.B. Fox, *Key roles of adjuvants in modern vaccines.* Nat Med, 2013. **19**(12): p. 1597-608.

101. Tafaghodi, M., A. Khamesipour, and M.R. Jaafari, *Immunization against leishmaniasis by PLGA nanospheres encapsulated with autoclaved Leishmania major (ALM) and CpG-ODN.* Parasitol Res, 2011. **108**(5): p. 1265-73.

102. Tel, J., et al., *Targeting uptake receptors on human plasmacytoid dendritic cells triggers antigen cross-presentation and robust type I IFN secretion.* J Immunol, 2013. **191**(10): p. 5005-12.

103. Slutter, B. and W. Jiskoot, *Dual role of CpG as immune modulator and physical crosslinker in ovalbumin loaded N-trimethyl chitosan (TMC) nanoparticles for nasal vaccination.* J Control Release, 2010. **148**(1): p. 117-21.

104. Mishra, N., et al., *Lectin anchored PLGA nanoparticles for oral mucosal immunization against hepatitis B.* J Drug Target, 2011. **19**(1): p. 67-78.

105. Bershteyn, A., et al., *Robust IgG responses to nanograms of antigen using a biomimetic lipid-coated particle vaccine.* J Control Release, 2012. **157**(3): p. 354-65.

106. Thomas, S.N., et al., *Targeting the tumor-draining lymph node with adjuvanted nanoparticles reshapes the anti-tumor immune response.* Biomaterials, 2014. **35**(2): p. 814-24.

107. Heuking, S., et al., *Fate of TLR-1/TLR-2 agonist functionalised pDNA nanoparticles upon deposition at the human bronchial epithelium in vitro.* J Nanobiotechnology, 2013. **11**: p. 29.

108. Stano, A., et al., *PPS nanoparticles as versatile delivery system to induce systemic and broad mucosal immunity after intranasal administration.* Vaccine, 2011. **29**(4): p. 804-12.

109. Sawaengsak, C., et al., *Chitosan nanoparticle encapsulated hemagglutinin-split influenza virus mucosal vaccine.* AAPS PharmSciTech, 2014. **15**(2): p. 317-25.

110. Hansen, S. and C.M. Lehr, *Nanoparticles for transcutaneous vaccination.* Microb Biotechnol, 2012. **5**(2): p. 156-67.

111. Srivastava, A., et al., *Mucosal vaccines: a paradigm shift in the development of mucosal adjuvants and delivery vehicles.* APMIS, 2015. **123**(4): p. 275-88.

112. Wilson, J.T., et al., *pH-Responsive nanoparticle vaccines for dual-delivery of antigens and immunostimulatory oligonucleotides.* ACS Nano, 2013. **7**(5): p. 3912-25.

113. Mohanan, D., et al., *Administration routes affect the quality of immune responses: A cross-sectional evaluation of particulate antigen-delivery systems.* J Control Release, 2010. **147**(3): p. 342-9.

114. Eyles, J.E., et al., *Analysis of local and systemic immunological responses after intra-tracheal, intra-nasal and intra-muscular administration of microsphere co-encapsulated Yersinia pestis sub-unit vaccines.* Vaccine, 1998. **16**(20): p. 2000-9.

115. De, S.R.J., et al., *Immunogenicity of peanut proteins containing poly(anhydride) nanoparticles.* Clin Vaccine Immunol, 2014. **21**(8): p. 1106-12.

116. Reboucas Jde, S., et al., *Development of poly(anhydride) nanoparticles loaded with peanut proteins: the influence of preparation method on the immunogenic properties.* Eur J Pharm Biopharm, 2012. **82**(2): p. 241-9.

117. Lieder, R., P.H. Petersen, and O.E. Sigurjonsson, *Endotoxins-the invisible companion in biomaterials research.* Tissue Eng Part B Rev, 2013. **19**(5): p. 391-402.

118. McAleer, J.P. and A.T. Vella, *Understanding how lipopolysaccharide impacts CD4 T cell immunity.* Crit Rev Immunol, 2008. **28**(4): p. 281-99.

119. Moyle, P.M. and I. Toth, *Modern subunit vaccines: development, components, and research opportunities.* ChemMedChem, 2013. **8**(3): p. 360-76.

120. Smulders, S., et al., *Contamination of nanoparticles by endotoxin: evaluation of different test methods.* Part Fibre Toxicol, 2012. **9**: p. 41.

121. van den Berg, J.H., et al., *Lipopolysaccharide contamination in intradermal DNA vaccination: toxic impurity or adjuvant?* Int J Pharm, 2010. **390**(1): p. 32-6.

122. Lieder, R., et al., *Endotoxins affect bioactivity of chitosan derivatives in cultures of bone marrow-derived human mesenchymal stem cells.* Acta Biomater, 2013. **9**(1): p. 4771-8.

123. Dobrovolskaia, M.A. and S.E. McNeil, *Handbook of Immunological Properties of Engineered Nanomaterials.* 2013: World Scientific.

124. World Health Organization (WHO). *Guidelines for the prevention, care and treatment of persons with chronic hepatitis B infection.* World Health Organization (WHO) 2015 [Access 2015 August]; Available from: http://apps.who.int/iris/bitstream/10665/154590/1/9789241549059_eng.pdf?ua=1&ua=1.

125. MacLachlan, J.H. and B.C. Cowie, *Hepatitis B Virus Epidemiology.* Cold Spring Harb Perspect Med, 2015. **5**(5).

126. Michel, M.L. and P. Tiollais, *Hepatitis B vaccines: protective efficacy and therapeutic potential.* Pathol Biol (Paris), 2010. **58**(4): p. 288-95.

127. Zuckerman, J.N., *Protective efficacy, immunotherapeutic potential, and safety of hepatitis B vaccines.* J Med Virol, 2006. **78**(2): p. 169-77.

128. Borges, O., et al., *Mucosal vaccines: recent progress in understanding the natural barriers.* Pharm Res, 2010. **27**(2): p. 211-23.

129. Borges, O., et al., *Alginate coated chitosan nanoparticles are an effective subcutaneous adjuvant for hepatitis B surface antigen.* Int Immunopharmacol, 2008. **8**(13-14): p. 1773-80.

130. Borges, O., et al., *Evaluation of the immune response following a short oral vaccination schedule with hepatitis B antigen encapsulated into alginate-coated chitosan nanoparticles.* Eur J Pharm Sci, 2007. **32**(4-5): p. 278-90.

131. Borges, O., et al., *Immune response by nasal delivery of hepatitis B surface antigen and codelivery of a CpG ODN in alginate coated chitosan nanoparticles.* Eur J Pharm Biopharm, 2008. **69**(2): p. 405-16.

132. Shrestha, B. and J.P. Rath, *Poly(vinyl alcohol)-coated chitosan microparticles act as an effective oral vaccine delivery system for hepatitis B vaccine in rat model.* IET Nanobiotechnol, 2014. **8**(4): p. 201-7.

133. Pawar, D. and K.S. Jaganathan, *Mucoadhesive glycol chitosan nanoparticles for intranasal delivery of hepatitis B vaccine: enhancement of mucosal and systemic immune response.* Drug Deliv, 2014: p. 1-11.

134. Pawar, D., et al., *Evaluation of mucoadhesive PLGA microparticles for nasal immunization.* Aaps j, 2010. **12**(2): p. 130-7.

135. Khatri, K., et al., *Plasmid DNA loaded chitosan nanoparticles for nasal mucosal immunization against hepatitis B.* Int J Pharm, 2008. **354**(1-2): p. 235-41.

136. Thomas, C., et al., *Aerosolized PLA and PLGA nanoparticles enhance humoral, mucosal and cytokine responses to hepatitis B vaccine.* Mol Pharm, 2011. **8**(2): p. 405-15.

137. Gupta, P.N., et al., *M-cell targeted biodegradable PLGA nanoparticles for oral immunization against hepatitis B.* J Drug Target, 2007. **15**(10): p. 701-13.

138. Jimenez-Ruiz, E., et al., *Low efficacy of NcGRA7, NcSAG4, NcBSR4 and NcSRS9 formulated in poly-epsilon-caprolactone against Neospora caninum infection in mice.* Vaccine, 2012. **30**(33): p. 4983-92.

139. Florindo, H.F., et al., *The enhancement of the immune response against S. equi antigens through the intranasal administration of poly-epsilon-caprolactone-based nanoparticles.* Biomaterials, 2009. **30**(5): p. 879-91.

Chapter 2. Production and evaluation of PCL/chitosan NPs as vaccine delivery systems

Part 1. New insights on chitosan and poly-ε-caprolactone based nanoparticles as a protein delivery system

Abstract

Three carrier systems, chitosan nanoparticles (NPs), poly- -caprolactone (PCL) NPs, and the corresponding blend (PCL/chitosan) NPs were extensively characterized and directly compared. The main objective was to enumerate the real transposable advantages of each system and their abilities to promote non-parenteral delivery of proteins, based on physical and chemical properties, so far not systematically compared. Thermal analysis suggested the blend NPs were more stable than the isolated polymers. Moreover, while chitosan NPs presented non-freezable water adsorbed to chitosan NPs, indicative of its hydrophilic character, PCL and PCL/chitosan NPs did not. The blend NPs showed an intermediate spleen cells toxicity profile compared to single polymer NPs. PCL/chitosan NPs were the ones that showed higher protein adsorption efficacy (84 %) in low shear stress and aqueous environment, suggesting a synergistic effect of chitosan positive charges and PCL hydrophobicity for protein interaction. Moreover, the hydrophobic binding, may also be responsible for the higher ellipticity loss of the protein secondary structure, evaluated during 6-month storage by circular dichroism, when compared to chitosan NPs adsorbed protein. In simulated biological fluids, PCL and PCL/chitosan NPs showed an advantageous release profile for oral delivery, while due to its lower resistance at acidic conditions, chitosan NPs may be more indicated for intranasal route. In conclusion the combination of both polymers characteristics makes PCL/chitosan NPs a good approach as a protein/antigen delivery system.

Keywords*: Biodegradable, nanoparticles, poly- -caprolactone, chitosan, protein delivery systems, adsorption.

1. Introduction

Proteins and peptides, including recombinant antigens, are of great importance for the pharmaceutical industry and, over the years, improved analytical methods have promoted numerous discoveries in this field. Likewise, molecular biology and genetic engineering have enabled large-scale production of polypeptides, and are continuously searching for new and better protein expression systems. Lastly, there is a better understanding of the role of regulatory proteins and peptides in the pathophysiology of human diseases [1, 2]. Proteins, particularly recombinant proteins, are very important for vaccination strategies, since they may present epitopes capable of eliciting a protective immune response against a specific microorganism [3]. Regardless of this great interest, the clinical usage of proteins and peptides is dependent on the development of adequate formulations, since these biomolecules are highly vulnerable with short *in vivo* half-lives and chemical and physical instability (formation/breaking of covalent bindings and changes in higher-order structures, respectively), which results in poor bioavailability [4, 5]. From the practical point of view, most of these peptides and proteins are administered by injection, generally though intramuscular, subcutaneous or intravenous routes [2, 6]. The new protein formulations are, most of the times, delivery systems, that efficiently protect proteins or peptides, stabilize them in physiological medium, allow a controlled release, avoid potential side effects generated by burst releases and permit a non-parenteral administration [2, 4, 6]. Moreover, these delivery systems also protect proteins from enzymatic degradation, increase protein interactions with epithelial membranes and/or mucosae, and increase the residence time, promoting higher uptake of biomolecules of interest [2, 7]. Polymeric delivery systems, namely nanoparticles (NPs), can efficiently transport and protect protein and peptides whether through encapsulation or by simple adsorption. Using the simple adsorption method the stabilization and protection of cargo molecules can be achieved through the surface activity, preferential exclusion, steric hindrance of protein-protein interactions and increased solution viscosity - limiting the protein structural movement [5]. Moreover, this method presents advantages over encapsulation, as protein and peptides are not submitted to harsh conditions during the NPs production, which might lead to loss of activity.

Chitosan is a cationic polymer, non-toxic, biodegradable and biocompatible [8]. Extensive research has been directed towards its use in medical applications such as drug and vaccine delivery [9, 10]. Chitosan is also known to be mucoadhesive and its ability to stimulate cells of the immune system has been shown in many studies [11, 12]. PCL on its turn, is a synthetic semicrystalline biodegradable and highly hydrophobic polymer, that shows good *in vitro* stability and exceptional blend compatibility. This polymer is degraded slowly in physiological environments, does not lead to the accumulation of toxic

metabolites and is inexpensive [13, 14]. PCL properties, among others, have raised interest for a large set of different applications, ranging from food packaging to tissue engineering [15-17].

The aim of this work was to prepare and extensively characterize PCL/chitosan NPs in order to evaluate in depth its ability as a protein delivery system. The inclusion of chitosan, a hydrophilic polymer, on PCL NPs intended to increase the immunomodulator and mucoadhesive properties of the particles, two advantageous characteristics for particulate antigen delivery systems, particularly for mucosal administration of vaccines. Moreover, a certain degree of hydrophilicity is expected to be conferred to particles, which consequently would increase their stability in aqueous mediums. Not only blend NPs, but also single-polymer systems (chitosan NPs and PCL NPs) were physically and chemically assessed, using the same methodologies in order to direct establish comparisons. Ovalbumin (OVA) was chosen as a model protein, having in mind its extensive use as an antigen model to test NPs adjuvant ability. Moreover, OVA was adsorbed to the NPs after production, in low shear stress and aqueous environment. In addition to previously explained adsorption advantages, the model antigen surface localization is also important as it mimics pathogen microorganisms improving the formulation recognition by immune system. Therefore, it is our intention to enumerate the real transposable advantages of each of these systems and their capabilities in the future to promote non-parenteral delivery of proteins, based on their physical and chemical properties.

Previous reports addressing the simultaneous use of PCL and chitosan or chitosan derivatives (trimethyl chitosan or glycol chitosan) are based on water/oil/water emulsion diffusion evaporation techniques using PVA as stabilizer [18-22], excepting the article published by Bilensoy et al. [23] and another published by Mazzarino et al [24] where the production method is nanoprecipitation. However, in these reports, the cargo (hydrophilic drug mitomycin C or hydrophobic curcumin, respectively) is added during NPs production [23, 24]. Besides commonly assessed parameters as size and zeta potential, these articles do not undertake a systematic analysis of the chemical and physical parameters related to the NPs, nor do they study extensive comparisons with single-polymer NPs, or cargo adsorption characterization. Moreover, results with specific drug molecules cannot be lightly transposable for proteins. In the present paper, we describe and compare FTIR spectra, TGA and DSC profiles for all delivery systems at their final arrangements. Moreover, we evaluate NPs toxicity in a primary cell culture of spleen cells, a good representative of immune system cells involved in responses to vaccines. To complete our analysis, we evaluate protein conformation when adsorbed at NPs surface, and further investigate protein release in different simulated biological fluids, assays which to the authors knowledge, have not been done before for PCL/chitosan NPs.

2. Materials and methods

2.1. Materials

Chitosan (ChitoClear™ - 95 % DD and 8 cP viscosity measured in 1 % solution in 1 % acetic acid) was purchased from Primex Bio-Chemicals AS (Avaldsnes, Norway). PCL (average M_w 14000), D-(+)-Trehalose dehydrate (≥ 98.5 %), ovalbumin - albumin from chicken egg white (≥ 98 %), RPMI 1640 medium and MTT (3-[4,5-dimethylthiazol-2-yl]-2,5-diphenyl tetrazolium bromide) were obtained from Sigma-Aldrich Corporation (St. Louis, MO, USA). Pierce™ Bicinchoninic acid (BCA) protein assay kit, FBS and PenStrep from Gibco® were purchased from Thermo Fisher Scientific Inc., Waltham, MA, USA). Spectra®Por cellulose ester dialysis membrane, MWCO 300.000 was purchased from Spectrum Europe B.V. (Breda, NL). All the other chemicals were from normal suppliers, but always of analytical grade.

2.2. Methods

2.2.1. Preparation of nanoparticles

2.2.1.1. Chitosan NPs

Chitosan NPs were prepared by a method previously described with slight modifications [25]. Briefly, a volume of 200 mL of an aqueous solution of chitosan 0.25 % (w/v) in 0.1 % (v/v) acetic acid and 0.1 % (w/v) Tween™ 80 were placed under a high speed homogenizer (Ystral X120, Ballrechten-Dottingen, DE) with simultaneous ultrasound agitation; meanwhile, 3.5 mL of sodium sulfate were added dropwise over one minute. After the addition, homogenization was stopped but the ultrasound was kept on 30 min further. The NPs were matured under magnetic agitation for further 2 h and finally were washed and freeze dried directly or in the presence of a cryoprotectant - trehalose. The trehalose was added so that the final powder has a percentage of 10 % of NPs (FreezeZone 6, Labconco Corporation, Kansas City, MO, USA).

2.2.1.2. PCL NPs

The preparation of PCL NPs were prepared by a method already described by us [26]. Briefly, an aqueous solution containing 0.1 % (v/v) acetic acid and 5 % (w/v) Tween™ 80 was placed under a high speed homogenizer. The organic phase, consisting of 0.2 % (w/v) PCL diluted in acetone, was added dropwise to the first solution at a ratio of 1:3 (v/v) to give a final volume of 18 mL. Agitation was continued for 1 min after the complete mixture of both phases. At this point, the particle suspension was formed and was placed under magnetic swirl for 45 min to achieve maturation. The NPs suspended in the original medium were isolated by centrifugation at 16000 g, for 75 min at 4 °C. To achieve minimal

particle aggregation, after the centrifugation, a 200 L glycerol bed for each batch was placed inside centrifuge tubes. After the centrifugation, particles were placed for 48 h under dialysis against water to remove the glycerol. Then, the resulting suspension was freeze dried as previously described.

2.2.1.3.   PCL/chitosan NPs

PCL/chitosan NPs were prepared by the same technique as described for PCL NPs with the exception that the aqueous solution of 0.1 % acetic acid and 5 % Tween 80 also contained 0.1 % (w/v) of purified chitosan (see Figure A from supplementary material chapter 2 for schematic illustration).

2.2.1.4.   Adsorption of Ovalbumin by Nanoparticles

After dialysis, NPs suspended in water were incubated with a solution of ovalbumin (OVA) for 30 min under rotational agitation. Ratio of 2:1 (NP:ovalbumin, (w/w)) was used for all formulations. The amount of OVA adsorbed was calculated by the difference between the total protein and the protein that remained in solution which was quantified by a colorimetric assay, BCA protein assay. Nevertheless, non-bound protein was not removed from the suspension and the resulting formulations were freeze dried as described previously and further used for morphological and structural analysis, *in vitro* release studies and circular dichroism analysis.

2.2.2. Morphological and structural analysis

Delsa™ Nano C particle analyzer (Beckman Coulter, Brea, CA, USA) was used to measure the particle size by Dynamic light scattering (DLS), and the zeta potential through electrophoretic light scattering (ELS). Transmission electron microscopy (TEM) was performed using a JEOL JEM 1400, 120 kV (JEOL, Peabody, MA, USA). For TEM visualization, the particles were resuspended in water and centrifuged to eliminate the cryoprotector in solution. Then, a drop of the sample was dried out in a mesh grid before visualization. FTIR was performed using KBr tablets in a Vertex 70V from Bruker (Bruker Biosciences Corporation, Billerica, MA, USA) and the data collected in OPUS software. The analysis was performed under vacuum. A FTIT ATR (attenuated total reflectance) was performed in the pure NP powder using a FTS 7000 from Varian (Varian Medical Systems, Palo Alto, CA, USA) with the support of a UMA 600 microscope from Varian.

2.2.3. *In vitro* nanoparticle toxicity

The cytotoxicity of chitosan, PCL and PCL/chitosan NPs were evaluated on a primary line of spleen cells using MTT cytotoxicity assay. Female C57/BL6 mice (13-week old) were purchased from Charles

River (Saint-Germain-Nuelles, FR), provided with food and water ad libitum and all experiments were in accordance with FELASA guidelines and approved by the Animal Care Committee of the Center for Neuroscience and Cell Biology of Coimbra. Mice were sacrificed by cervical dislocation and spleens were aseptically removed, dissociated with cell strainers (70 µm pore, white, DB Biosciences, Bedford, MA, USA) and the resulting cell suspensions washed twice with RPMI 1640. The final suspension was adjusted to a final concentration of 1×10^7 cells/mL in complete RPMI 1640 medium (supplemented with 10 % (v/v) fetal bovine serum, 2 mM glutamine, 1% (v/v) PenStrep and 20 mM HEPES buffer). Cytotoxicity assays were performed in a 96-well plate at a density of 10^6 cells per well. Serial dilutions of the freeze dried NPs (with trehalose), were prepared in serum-free RPMI for a final particle concentration ranging between 0.15 g/mL and 150 g/mL on the well. The samples were allowed to incubate with the cells for 24 h, at 37 ℃ and 5 % CO_2. After this period, 20 µL of MTT solution (5 mg/mL) in PBS) were added to each well followed by additional 4 h incubation. To ensure dissolution of the formazan crystals, 200 µL of the culture medium was replaced by same volume of DMSO and the OD of the resultant colored solution was measured at 570 nm. Cell viability (%) was calculated by the following equation:

$$\text{cell viability } (\%) = \frac{(\text{OD sample (540nm) - OD sample (630nm))}}{(\text{OD control (540nm)- OD control (630nm))}} \qquad \text{(Eq. 1)}$$

The inhibitory concentration for 50 % of cell viability (IC_{50}) was calculated by plotting the log concentration of the NPs versus inhibition percentage of cell viability and extrapolating the value from a non-linear regression.

2.2.4. Thermal analysis

Thermogravimetric analysis (TGA) was performed under a nitrogen atmosphere using a Q50 thermogravimetric analyzer (TA Instruments, New Castle, DE, USA) from room temperature to 1000 ℃ with a heating rate of 10 ℃/min. Differential scanning calorimetry (DSC) was performed using a Q20 differential scanning calorimeter (TA instruments, New Castle, DE, USA) starting at 0 ℃ with a heating rate of 10 ℃/min until the degradation temperature accessed previously by TGA (200 ℃). Freeze dried NPs (without trehalose) were used for thermal analysis.

2.2.5. Circular Dichroism

The secondary structures of native and adsorbed protein were analyzed using a J-815 circular dichroism (CD) analyzer (JASCO Analytical Instruments, Easton, MD, USA) in the wavelength range of

190 nm to 260 nm. NPs were analyzed in a total mass concentration of 61.25 µg/mL corresponding to a protein concentration of 9 µg/mL for chitosan NP and 3 µg/mL for PCL NP and PCL/chitosan NP formulations. Measurements were performed in ultrapure water at room temperature.

2.2.6. *In vitro* release studies

The protein release from nanoparticulate systems was assessed using various simulated biological fluids over 6 h at 37 ºC and under 140 strokes/min. Freeze dried formulations (25 mg with 5.8 % NPs, 2.9 % protein and 91.3 % trehalose) were dispersed in 5 mL of media previously equilibrated at 37 ºC and 300 µL aliquots were collected over time. These samples were centrifuged at 21000 g for 10 min and 150 µL supernatant gathered for non-bound protein quantification through BCA protein assay. Simulated gastric (SGF) and intestinal (SIF) fluids were used, and their compositions are described in USP 33 (2010). Enzymes were excluded from the fluid composition to prevent interferences in the protein quantification. Simulated nasal fluid (SNF) was used and prepared according to Martinac et al. [27]. All pH were measured prior to the assays using a inoLab® pH Benchtop Meter with a SenTix® pH electrode from WTW GmbH (Weilheim, DE).

3. Results and Discussion

3.1. Morphological and structural properties of nanoparticulate carriers

Three particulate systems and their respective conjugates with ovalbumin were successfully produced. Table 1 shows the detailed results for size and zeta potential. Chitosan NPs present a mean hydrodynamic diameter around 546 nm with and without protein adsorbed on its surface. However, TEM analysis showed that particles larger than 600 nm were also formed (Fig. 1A). On the other hand, PCL NPs were smaller, with mean diameter of 202 nm for the NPs and 155 nm for the ovalbumin/NP conjugates (Table 1 and Fig. 1B). Simple and protein adsorbed PCL/chitosan NPs have a mean diameter of 539 nm and 186 nm, respectively, clearly suggesting that PCL has a predominant role on the blend. It is noteworthy that, especially for PCL and PCL/chitosan NPs, protein adsorbed at their surface stabilized the particulate systems, and aggregation tendency that was present after dialysis process, disappeared. This is confirmed by Figure 1C, where it is possible to observe aggregates of PCL/chitosan NPs. Moreover, this phenomenon is documented on the DLS analysis intensity distribution graphics (data not shown). Without protein, the formulations present two peaks, one for simple NPs and another for larger entities concordant with aggregates. With adsorbed protein, the larger size peak disappears and only the peak correspondent to the actual particle-protein conjugates hydrodynamic size is present. Although polysorbate 80 (Tween™ 80), a nonionic surfactant, was included in particle formation medium in order to stabilize the suspension and thus to avoid the formation of aggregates, in particle isolation (centrifugation and dialysis), a great part of the polysorbate was eliminated and the suspension became less stabilized. More evident for PCL/chitosan NPs, stabilization was increased after adding the protein during the adsorption process: proteins because their hydrophobic and hydrophilic domains worked like a surfactant [28]. The reason why PCL based NPs (both PCL and PCL/chitosan NPs) rely on the presence of surfactants to avoid agglomeration is due to the hydrophobic nature of PCL, while chitosan NPs due to the chitosan highly positive domains is rather stabilized by electrostatic repulsion.

Table 1: Sizes and zeta potentials of chitosan, PCL and PCL/chitosan NPs in water. Results were presented by mean ± SD from at least 3 independent batches.

NPs	Simple NPs			Protein adsorbed NPs		
	Size (nm)	Polidispersity (PI)	Zeta Potential (mV)	Size (nm)	Polidispersity (PI)	Zeta Potential (mV)
Chitosan	545.9 ± 9.5	0.12 ± 0.01	26.0 ± 0.4	546.2 ± 8.5	0.11 ± 0.03	25.7 ± 0.5
PCL	201.7 ± 27.5	0.29 ± 0.04	1.4 ± 4.6	154.6 ± 1.5	0.09 ± 0.02	17.6 ± 3.7
PCL/chitosan	539.1 ± 113.7	0.25 ± 0.04	21.7 ± 0.5	186.0 ± 2.7	0.22 ± 0.01	15.0 ± 0.6
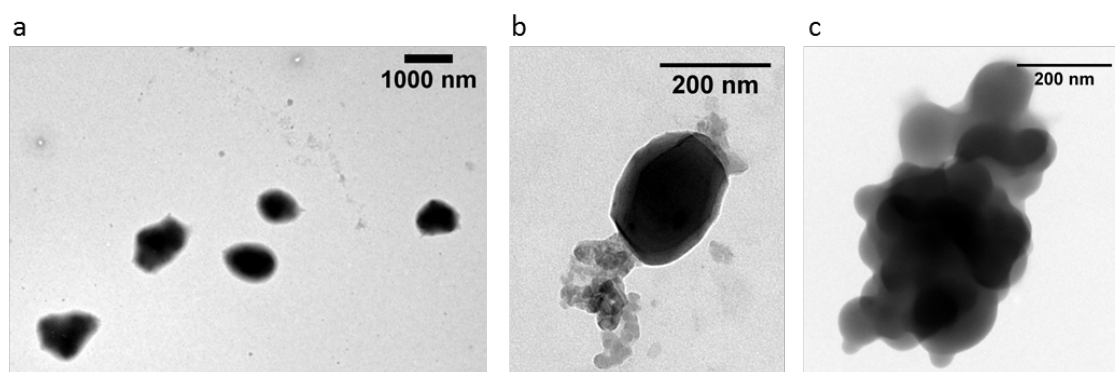
Figure 1: TEM images of NPs after resuspension of the freeze dried power in water and elimination of trehalose by centrifugation. A) Chitosan NPs; B) PCL nanoparticle with adsorbed ovalbumin; C) Simple PCL/chitosan NPs aggregate, before protein adsorption process.

Concerning zeta potential, chitosan and PCL/chitosan NPs presented a positive charge when in water (pH ≈ 5), while PCL NPs presented a neutral charge. When the protein is adsorbed, the negative charge of the protein turns PCL and PCL/chitosan NPs into negative surface-charged. For PCL/chitosan NPs situation this can be an indication that the protein is binding chitosan residues that are at the particle surface and for that reason its contribution for positive charge is annulled. For chitosan NPs the zeta potential remained the same (≈ + 27 mV) [25]. Electrostatic interactions between protein negative hydrophilic domains and chitosan protonated amine groups were responsible for protein adsorption. Therefore, positive surface charge probably the resulted from non-bonded chitosan amine groups and positive hydrophilic domains of the protein that will be localized on protein corona surface.

FTIR has been used to have an insight on the hypothetical structural changes occurring in NPs when compared with native chitosan and PCL (Fig. 2A) [29, 30]. Chitosan displayed a broad band at 3450 cm^1 assigned to O–H and N–H stretching vibrations, two bands at 1650 and 1590 cm^1 due to N–H bending vibrations, and a peak at 1090 cm^1 (C–O–C stretching vibrations) [31-34]. For PCL a well resolved spectrum was obtained being possible to identify, for instance, the asymmetric CH_2 stretching at 2942 cm^1, the carbonyl stretching at 1730 cm^1 and the OC-O stretching at 1180 cm^1 [35].

Considering the spectra for chitosan NPs the OH and NH broad band was observed at the same wavenumber 3450 cm^{-1}. However, the bands assigned to N–H bending vibrations are slightly displaced to 1640 and 1530 cm^{-1}, respectively, and are more clearly defined. This change is closely related to the protonation of chitosan in the amine function on acidic medium and is characterized by the presence of two peaks, both attributed to the NH_3^+. The protonation of the amine groups suggest a possible electrostatic interaction mechanism with the cross-link sodium sulfate [36]. For PCL/chitosan and PCL NPs, the characteristic peaks presented in the spectra fit with that of PCL. Considering spectra from pure ovalbumin it is possible to identify bands at 3300, 1650 and 1535 cm^{-1} assigned to the stretching

51

vibrations of the amide A (mainly NH stretching vibration), amide I (C=O stretching) and amide II (CN stretching, NH bending), respectively. Comparing to the NP-OVA conjugates, these characteristic peaks are still present [37-39].

Despite the previous discussion, it was not possible to observe, in FTIR spectra shown in the Figure 2A, any band characterizing the presence of chitosan in the PCL/chitosan NPs. A possible explanation can be the small amount of chitosan into sample NPs that is masked by the higher amount of PCL. In fact, by comparing the NPs yield from PCL NPs production and PCL/chitosan NPs, only a small difference of 10 % between them is verified. That is, by freeze drying PCL/chitosan NPs without cryoprotector, 10 mg of particles are obtained per batch. On its turn, a batch of PCL NPs contains 9 mg of particles, which is in line with the precipitation of all used PCL for NPs production stated also by Haas et al. [18]. In their report, Haas and coworkers estimated 70 % of the NPs mass was attributable to PCL and 30 % of the NPs mass was the result of PVA and chitosan incorporation. This PVA and chitosan incorporation only corresponds to 35 % of the amount used during production. In our case, the estimated amount of 10 % of chitosan (7.4 % of the total chitosan used for production) may not be enough for detection.

In order to overcome FTIR limitation with KBr tablets, the more versatile attenuated total reflectance (ATR)-FTIR [30, 40] has been used to assess NPs spectra as shown in the Figure 2B. With this methodology it is possible to compare the FTIR PCL/chitosan NPs spectrum with that of PCL NPs. The broad band occurring around 3217 cm^{-1} on the chitosan NPs spectra was marginally detected in the PCL/chitosan NPs spectra. This band is indicative of the NH and OH stretching vibrations from chitosan. The remote possibility that the band is indicative of water presence, is not considered since thermal analysis described further ahead did not show water content in the PCL/chitosan NPs, and the sample was the same (freeze dried NPs without trehalose). Other visible difference is the appearance of a peak at 1610 cm^{-1} typical from the amide I band [38]. Finally the band at 1045 cm^{-1} seems to be appearing in the PCL/chitosan NP spectra masking the bands from the PCL powder. Nevertheless, other typical vibrational PCL modes can be observed at 2940 and 1727 cm^{-1} bands for both samples: PCL NPs as well as for PCL/chitosan NPs. These results demonstrate, as expected, the incorporation of chitosan in the blend NPs.

A)
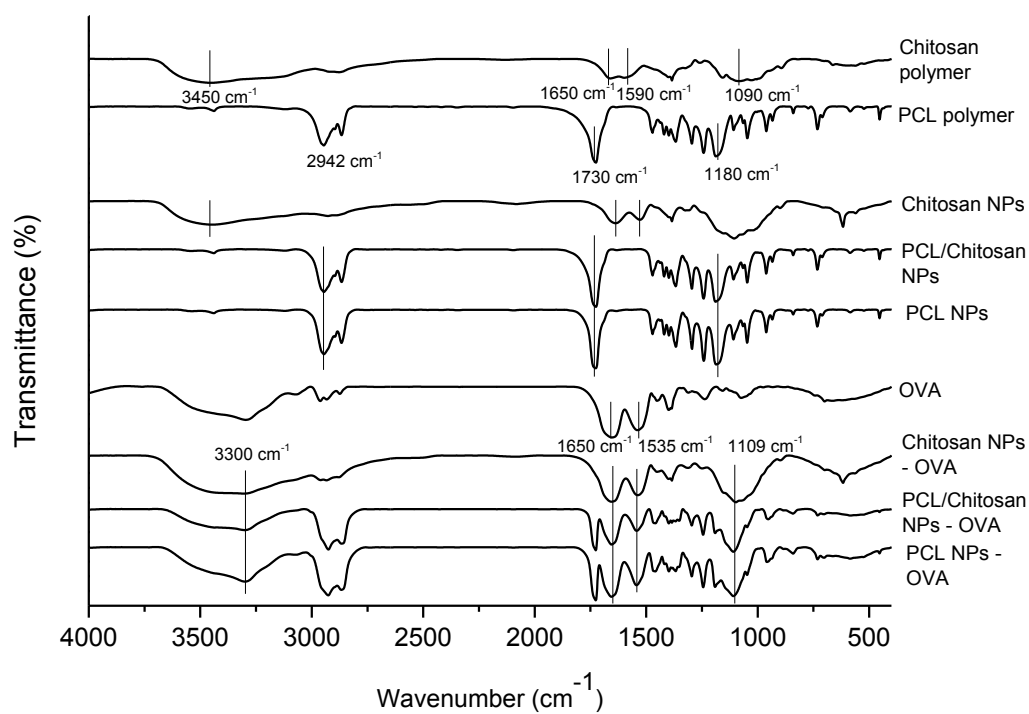
B)
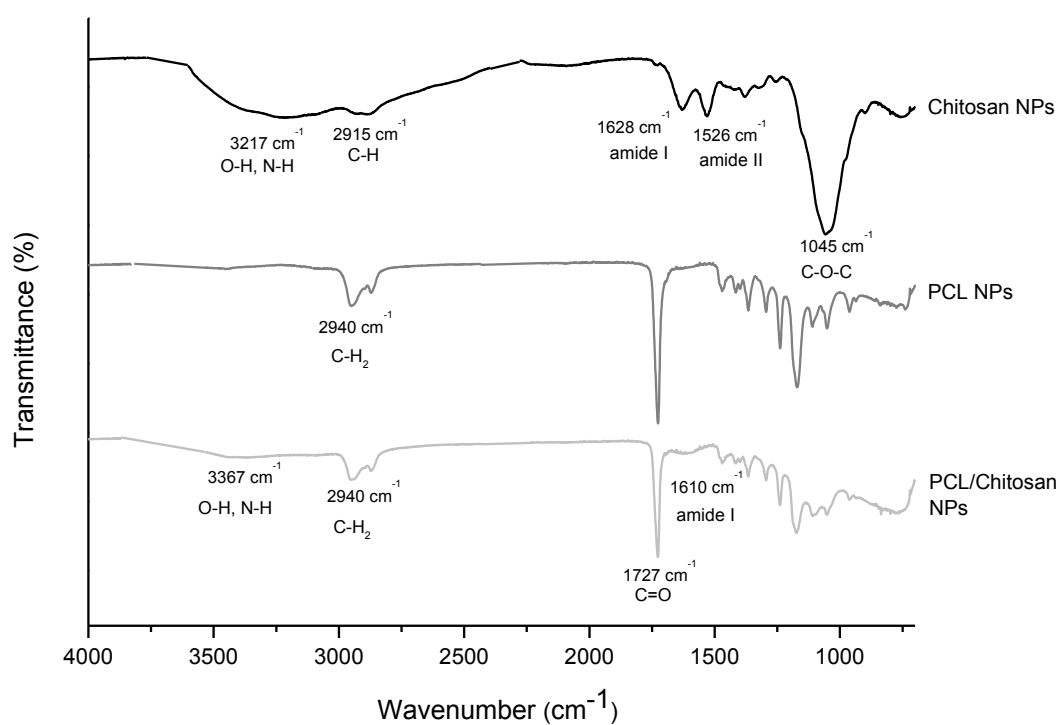
Figure 2: A) FT-IR spectra of chitosan, PCL, Ovalbumin, chitosan NPs, PCL NPs and PCL/chitosan NPs and all NP systems adsorbed with ovalbumin. B) FTIR-ATR spectra of chitosan NPs, PCL NPs and PCL/chitosan NPs.

3.2. Incorporation of chitosan into PCL nanoparticles improved its *in vitro* toxicity profile

In vitro toxicity gives an indication of a particle toxic profile that may be observed *in vivo*. MTT is a rapid and precise assay that measures the metabolic activity of living cells. Cell metabolism of 3-(4,5-dimethylthiazol-2-yl)-2,5-diphenyl tetrazolium bromide leads to the generation of insoluble crystals of formazan. Their dissolution in DMSO generates a purple signal, measured by colorimetry [41]. The NPs described were prepared with the objective of delivering proteins and vaccine antigens to immune system cells. A primary culture of spleen cells were used since they are a good cell model and also representative of the cells of the immune system. Cytotoxicity results for the three systems showed a good cytocompatibility profile (Fig. 3). However, for concentrations above 37.5 g/mL, PCL NPs showed to induce an accentuated decrease in cell viability, with 50 % decrease in cell viability (IC_{50}) at approximately 99 µg/ml. On its turn, chitosan NPs presented a gentle decrease, being the IC_{50} predicted at 1160 µg/ml and PCL/chitosan NPs an intermediate profile (IC50: 193 µg/ml). So, the incorporation of chitosan into the PCL NPs increased the biocompatibility of the nanoparticulate system with cells from the immune system.
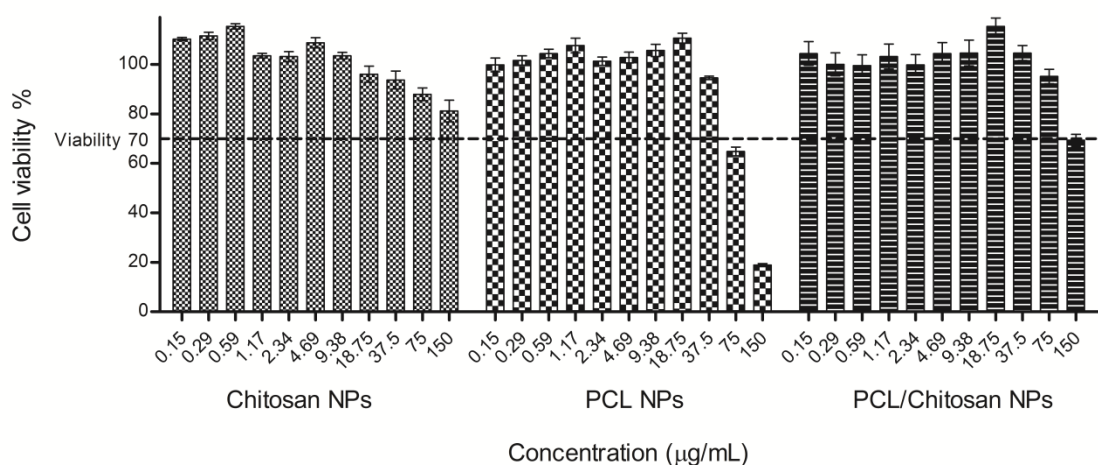
Figure 3: *In vitro* spleen cell viability after 24 h incubation with different concentrations (g/mL per well) of chitosan, PCL and PCL/chitosan NPs. (Mean ± SEM, n=4).

3.3. Thermal Analysis

The physical-chemical characterization of the NPs has been completed by TGA and DSC analysis [42, 43]. TGA curves obtained for all materials are shown in Figure 4A. The initial degradation temperatures (T_{ini}) determined at 5 % weight loss and the maximum degradation temperatures (T_{max}) obtained for all materials are shown in Table 2. From the analysis of Figure 4A, it is possible to notice

the water desorption on chitosan powder and chitosan NPs corresponding to a weight loss of 10 % and 12 %, respectively, at temperatures below 200 ºC. These results are easily justified by the highly hydrophilic character of chitosan and indicate the presence of non-freezable water inside materials [44]. On the other hand, PCL-containing materials do not show such features as a consequence of the PCL hydrophobic character. Concerning the specific case of PCL/chitosan NPs, it seems that the amount of chitosan in the blend is not enough to enhance the hydrophilic character of NP, as has been previously seen by Ciardelli et al. on PCL/polysaccharides blends [45]. Comparing the water loss for chitosan either as powder or as NP (Fig. 4A and Table 2), it can be observed that the onset degradation temperature ($T_{ini\ 5\ \%}$) is significantly lower (49 ºC) for NPs than for simple polymer sample (93 ºC), indicating that the chemical modification caused the cross-linking affects the chitosan structure with a consequent increase of the free volume of water [44]; an increase in the water content also lead to a plasticization effect on chitosan structure with a consequent decrease in the T_{max} from 277 ºC to 256 ºC.

Comparing thermograms for chitosan materials another observation is worth of notice: whilst for chitosan powder just one main degradation step is found (T_{max}= 277 ºC) for chitosan NPs the degradation occurs in two steps (219 ºC and 256 ºC); the latter can be justified by a chemical reaction between chitosan and the cross-linker which further decreases its thermal stability [44]. The analysis of PCL powder thermogram shows a main degradation temperature at 388 ºC; however, a more detailed analysis of DTG shows a further transition at 486 ºC. Persenaire et al. [46] referred that the first mechanism as the pyrolysis of the polymer and a second one via an unzipping mechanism [45, 46]. When PCL is arranged into NPs (simple and with chitosan) the second peak present on the DTG curve at 486 ºC does not exist. Probably, the unzipping mechanism was not happening due to the absence of free hydroxyl end groups derivate from the nanoparticle structure arrangement [46]. The formation of nanoparticulate systems with PCL powder increased the polymer thermal stability. For simple PCL NPs the maximum degradation rate temperature increased from 388 ºC to 392 ºC and for PCL/chitosan NPs increased to 391 ºC. Although the T_{max} of the blend is controlled by the PCL NPs, the $T_{ini\ 5\ \%}$ for this blend shows a synergetic effect of both chitosan and PCL, showing initial temperature of degradation at 339 ºC, suggesting that the blend was a more stable structure than the isolated polymers.

DSC measurements can be predictive of degree of miscibility, degree of intermolecular interactions and degree of crystallization [42, 47]. Figure 4B(a) shows the DSC curves of chitosan either as powder or as NPs. Endothermic peaks are observed at 103 ºC and 114 ºC, respectively. The shift to higher temperature accompanied by higher enthalpy can be attributed to stronger interactions of water molecules with this material. The crosslink interaction leads to a reduction in the amino groups available to react with water. On its turn, water molecules form hydrogen bindings with hydroxyl groups and

therefore more energy is needed for their removal [44]. This result is in agreement with TG data discussed before.

For PCL powder and based NPs the endothermic phase transition showed in DSC analysis corresponds to its melting transition (T_m). Compared to PCL powder the phase transition temperature of PCL NPs decreased from 65 ºC to 57 ºC, which is related to the physical state of the polymer or a lower crystallinity of PCL due to NP formation (Fig. 4B(b)). For PCL/chitosan NPs there are two endothermic transitions: one at 57 ºC and the second one at 148 ºC (Fig. 4B(c)). The former can be easily justified as due to PCL NP, whilst the latter may be indicative of a potential interaction between the two polymers [48]. It is also worth noting that PCL/chitosan NPs, when compared with PCL NPs, are essentially amorphous, as can be justified by the significant decrease in the enthalpy of transition [49].

A)

B)
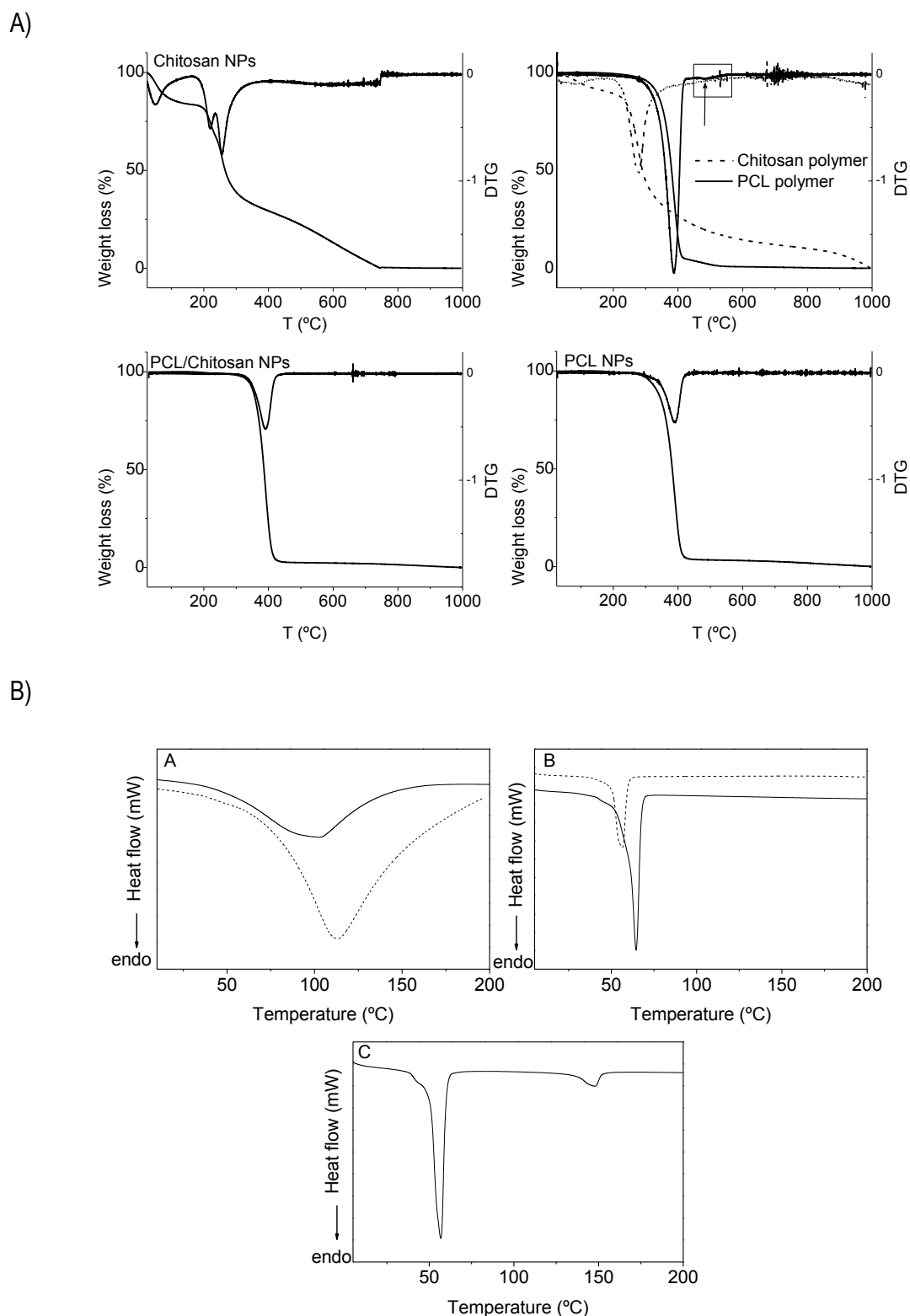
Figure 4: Thermal analysis. A) Thermogravimetric profiles of chitosan and PCL based NPs and pure polymers (left Y axis) and their derivative thermogravimetric curves (DTG) (right Y axis). For further details about the meaning of the arrow, please check the text. B) Differential scanning calorimetry (DSC) of chitosan (a) and PCL (b), as polymer (solid lines) or NPs (dashed lines), and PCL/chitosan blend NPs (c).

57

Table 2: Thermal properties of chitosan- and PCL-based materials.

	TG/DTG Analysis		DSC Analysis		
	$T_{ini\ 5\%}$ (ºC)	T_{max} (ºC)	T_{onset} (ºC)	T_m (ºC)	ΔH (J/g)
Chitosan Polymer	93	84 277	48	103*	299.40
PCL powder	309	388 486	60	65	89.4
Chitosan NPs	49	50 219 256	76	114*	442.2
PCL NPs	313	392	51	57	74.58
PCL/chitosan NPs	339	391	51 138	57 148	58.30 6.123

* desorption of the absorbed moisture.

.

3.4. Analysis of the protein secondary structure when adsorbed to the NPs by circular dichroism (CD)

Circular dichroism spectroscopy (CD) can be used to obtain information about the secondary structure of proteins [50]. The spectra of proteins are so dependent on their conformation that CD can be used to estimate the structure of unknown proteins and monitor conformational changes that can occur due to temperature, mutations, heat, denaturants, interaction with molecules or adsorption onto particles surface [51-53]. The nanoparticle surface can modify the structure and therefore the function of the adsorbed protein, in some cases in an irreversible manner. Furthermore, the formulation uptake can either be inhibited or increased due to loss of protein structure or unfolding of the native protein [54, 55].

Ovalbumin is known as a -protein meaning that it binds weakly in its native conformation compared to -proteins [56]. In the "w" shaped spectra obtained for the native protein (Figs. 5A, 5B and 5C) it shows a typical -helical structure with negative peaks in the range between 208 nm to 222 nm. When the protein is adsorbed to a nanoparticle it loses part of its ellipticity and this happened for all the systems tested. This phenomenon has been reported for protein conjugates at the boundary surface of NPs resulting in the partial loss of the two major bands referred and the spectra more similar to a typical rich structure represents a transformation from -helix to a -sheet structure conformation [57-59]. This fact was especially visible for the chitosan NP-OVA system, which presented a slight dislocation of the 222 nm peak to higher values, together with the loss of ellipticity (Fig. 5A).
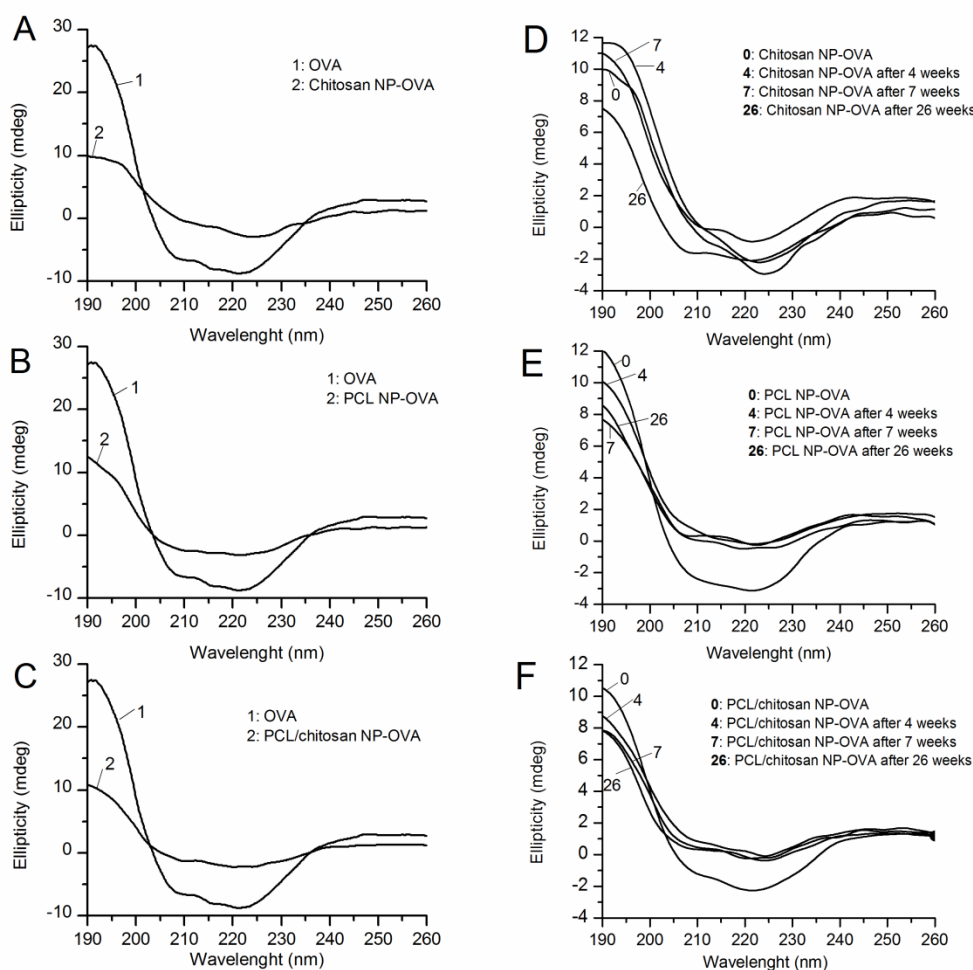
Figure 5: Circular dichroism analysis. The left graphics represent CD spectra of ovalbumin adsorbed to chitosan NPs (A), PCL NPs (B) and PCL/chitosan NPs (C) compared to CD spectra of the native form of ovalbumin. The right graphics represent CD spectra of ovalbumin adsorbed to the different NPs over time at room temperature (D - chitosan NPs; E – PCL NPs; F - PCL/chitosan NPs). Storage temperatures of 4 ºC and 40 ºC were also tested and graphics are shown on supplementary material. All this formulations were stored freeze dried with trehalose.

Freeze dried NPs with protein adsorbed in the presence of trehalose were stored at room temperature (Figs. 5D, 5E and 5F), at 4 ºC and at 45 ºC (supplementary material, Fig.B and C) for a period of 26 weeks. In the graphics it is possible to see that chitosan NPs adsorbed with protein (Fig. 5D) were the most stable ones with a lower decrease in the ellipticity, when stored at room temperature. Nevertheless, it is also possible to verify that the -sheet conformation of the protein resultant of the adsorption to the NPs is markedly returning to -helix (the main conformation in solution), which we may speculate to be indicative of some desorption of the bound protein. For PCL and PCL/chitosan NP-OVA systems, the loss of ellipticity was much higher for all the conditions tested which might be result of the hydrophobic binding not present in chitosan NPs. We might say that the ellipticity losses were more

gradual for PCL/chitosan NP system than for PCL NP system, which differences were evident between the time 0 and 4 weeks.

3.5. *In vitro* ovalbumin release profile differs among analyzed particles

The hydrophilic/hydrophobic characteristics of the NPs can be modulated by the design of blend NPs performed with polymers with opposite characteristics. These characteristics would influence the protein adsorption and subsequently, protein desorption observed during a protein release study. In fact, different ovalbumin adsorption efficacies were obtained for each system: 43 % for chitosan NPs, 58 % for PCL NPs and 84 % for PCL/chitosan NPs. Moreover, a direct comparison of ovalbumin release from the 3 different delivery systems was performed on diverse simulated biological fluids. In SGF, immediate total protein release from chitosan particles was observed (Fig. 6A). In fact, during the experiment it was possible to observe a variation of the color of the suspension from milky aspect to transparent color which indicates that particles were destroyed in acid environment and consequently protein was released to medium. A similar observation was previously reported by our group [60].
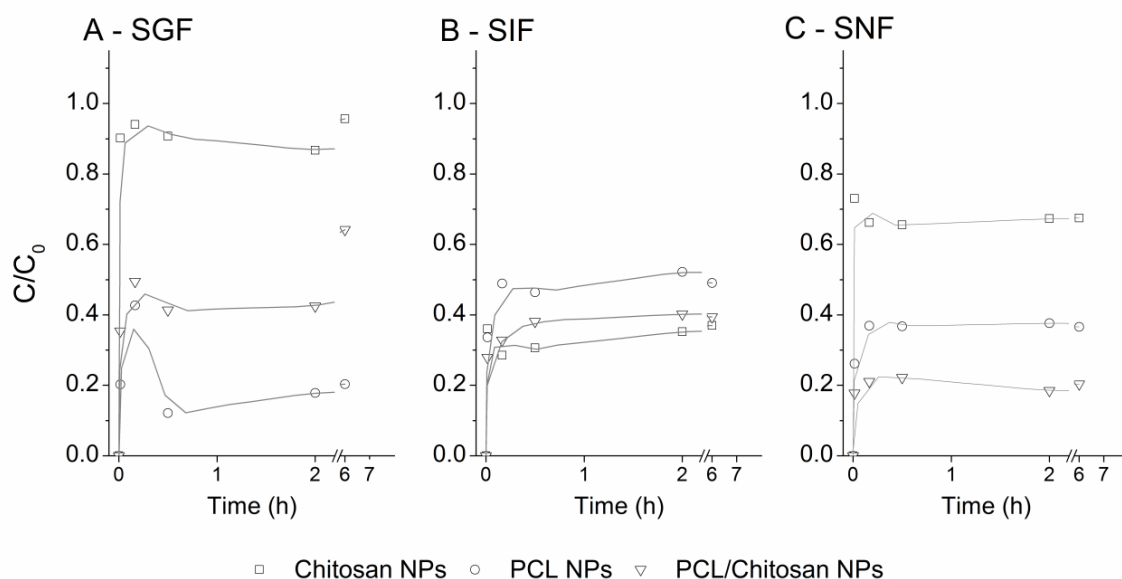
Figure 6: Ovalbumin release from chitosan, PCL and PCL/chitosan NPs when re-suspended in Simulated gastric fluid pH 1.2 (A), Simulated intestinal fluid pH 6.8 (B) and Simulated Nasal Fluid pH 6.8 (C), at 37 °C. The mean ratio of 3 results are presented where C = free protein concentration and C_0 = total protein concentration (g/mL).

By the contrary, the release ratio of the protein from particles containing PCL was less than 0.4 for both cases. Simple PCL NPs presented almost no release (about 0.2) of the protein and PCL/chitosan NPs presented an intermediate ratio between the two simple polymeric NPs. In fact, after the first 2 h of

the release assay, new adsorption equilibrium occurred as a result of the original NPs suspension dilution when added to the release fluid at 37 ºC. To summarize, in SGF, PCL NPs were the ones that retained more protein adsorbed on its surface. The inclusion of chitosan into PCL NPs, decreases its ability to maintain protein adsorbed on surface which could be a disadvantage for oral delivery of proteins. A different phenomenon was found with SIF (Fig. 6B). After the establishment of the new equilibrium, all delivery systems provided a similar protein release ratio that was near 0.4. In SNF (Fig. 6C), differences among the delivery systems were observed once again. The protein released from chitosan NP leaded to the highest protein release. A ratio near 0.7 was observed at 10 min assay and the value was maintained during the following 6 h. The release of the ovalbumin from the two based PCL NPs (simple and with chitosan included) were much less and occurred on the first minutes of the assay. Ratios about 0.4 and 0.2 were observed for PCL and PCL/chitosan NP, respectively which indicate superior capacity of these delivery systems to maintain the protein adsorbed on its surface. Direct comparison to similar published studies was not possible. To the author's knowledge, this is the first assessment of PCL/chitosan NPs release in simulated biological fluids. However, analyzing a study performed by Bilensoy and co-workers [23] with similar PCL/chitosan NPs opposite results to ours were found. In fact, they studied the release of mytomicin C from PCL/chitosan NPs production and chitosan NPs production (prepared by ionotropic gelation with tripolyphosphate (TPP)) on phosphate buffer pH 6.0 and observed that PCL/chitosan NPs after 1 h released 80 % of the drug load, while chitosan NPs only released 10 %, and those results stayed constant throughout the 6 hours of the assay. However, their release buffer is different from ours, and the influence of the cargo nature may be of high importance, limiting the transposition of the results. In fact, the authors suggest the mytomicin C hydrophilicity causes the drug to be localized at the surface of the particles (independently of the encapsulation method during NPs production) and leads to an higher tendency of the drug to escape from the PCL hydrophobic core and be released [23].

In our study, the ovalbumin release from NPs was dependent on the composition/pH of the release fluid for chitosan NPs, was less dependent for the case of PCL/chitosan NPs and had almost no influence on protein released from PCL NPs. That observation is explained, in part, by the predominant hydrophobic nature of the interaction, between protein and the surface of PCL NPs, less liable to be disturbed by the pH and the ionic strength of the fluids used on this study when compared with the hydrophilic interactions between chitosan NPs and the ovalbumin.

Mucoadhesive NPs prolong the residence time of the formulation in the nasal cavity and improve the uptake of loaded particles by epithelial and antigen presenting cells. Chitosan is known for its mucoadhesive properties and chitosan NPs are consequently expected to present advantages for nasal delivery of proteins and antigens [61]. However they have a limited colloidal stability particularly in

biological fluids and dissociate before reaching the absorption site [7]. In fact due to its rapid water adsorption and high swelling degree in aqueous environment chitosan is not the ideal for sustained release [62]. For oral administration, chitosan NPs, particularly the ones cross-linked with sodium sulfate, present another disadvantage. In the presence of an acidic medium, like the gastric fluid, the equilibrium is shifted towards dissolution of chitosan and the particles dissolve [63]. This theory was in accordance with our results: chitosan NPs are less indicated delivery system for oral delivery, if not included into a gastro-resistant capsule. On other hand, PCL and PCL/chitosan NPs present a profile that indicates a protein controlled release possibly, which may protect part of the cargo until the protein loaded delivery system reach the target tissue. As PCL is insoluble in water, PCL based NPs are more stable on biological fluids including the gastric fluid. In fact, the degradation of PCL in comparison to polyglycolic acid is slow, making it suitable for long-term/controlled delivery [64, 65].

Long-term ovalbumin release studies could present a higher cumulative release of the protein. Nevertheless, the time of the assay was planned in concordance with the predictable maximum retention times for oral and nasal deliveries. During this release time, on an *in vivo* situation the protein loaded NPs would be internalized by cells and therefore protein would be released through cellular degradation mechanisms.

4. Conclusions

The nanoprecipitation technique, a simplified method for PCL/chitosan NPs production when compared to those previously described [18-22], showed to be suitable for protein adsorption leading to a controlled released in all simulated biological fluids tested. Considering PCL based NPs, they present a release profile in simulated gastric fluid likely to be suitable for an oral administration of the nanoparticle-protein conjugate formulation. It induces a low release even when subjected to harsh conditions making these particles suitable for reaching the intestine without being destroyed or releasing protein. Chitosan NPs on their turn, produced by the conventional method with no further modifications, are not indicated for oral delivery since they are destroyed in acidic conditions. In all cases, the protein adsorption on NPs leads to an expected loss of protein ellipticipy, but with no major alterations (i.e. random coil).

All studied particles showed suitable sizes for cellular uptake and to cross M cells present on mucosae (intestinal and respiratory tract) and so, theoretically able to be taken up by the lymphatic system [66]. Additionally, the positive zeta potential of chitosan NPs even with adsorbed protein is a favorable characteristic for cellular uptake distinctive from PCL based NPs. Positive charges can interact with negatively charged cell membranes promoting the uptake [67].

In conclusion, nanoprecipitated PCL/chitosan NPs constitute a good approach to adsorb and deliver proteins as it combines positive characteristics of both polymers. In fact, they present improved thermal degradation profile, good chemical resistance, adequate biomolecule sustained release in simulated biological fluid, and initial positive charge. These are important aspects that would allow to better design future specific applications (i.e., real antigen) and the subsequent *in vitro* and *in vivo* studies.

References

1. Hudson, L.C., et al., *Soybean seeds: a practical host for the production of functional subunit vaccines.* Biomed Res Int, 2014. **2014**: p. 340804.
2. Shaji, J. and V. Patole, *Protein and Peptide drug delivery: oral approaches.* Indian J Pharm Sci, 2008. **70**(3): p. 269-77.
3. Junqueira-Kipnis, A.P., L.M. Marques Neto, and A. Kipnis, *Role of Fused Immunogens and Adjuvants in Modern Tuberculosis Vaccines.* Front Immunol, 2014. **5**: p. 188.
4. Tan, M.L., P.F. Choong, and C.R. Dass, *Recent developments in liposomes, microparticles and nanoparticles for protein and peptide drug delivery.* Peptides, 2010. **31**(1): p. 184-93.
5. Al-Tahami, K. and J. Singh, *Smart polymer based delivery systems for peptides and proteins.* Recent Pat Drug Deliv Formul, 2007. **1**(1): p. 65-71.
6. Degim, I.T. and N. Celebi, *Controlled delivery of peptides and proteins.* Curr Pharm Des, 2007. **13**(1): p. 99-117.
7. Amidi, M., et al., *Chitosan-based delivery systems for protein therapeutics and antigens.* Adv Drug Deliv Rev, 2010. **62**(1): p. 59-82.
8. Baldrick, P., *The safety of chitosan as a pharmaceutical excipient.* Regul Toxicol Pharmacol, 2010. **56**(3): p. 290-9.
9. Lebre, F., et al., *Progress towards a needle-free hepatitis B vaccine.* Pharm Res, 2011. **28**(5): p. 986-1012.
10. Panos, I., N. Acosta, and A. Heras, *New drug delivery systems based on chitosan.* Curr Drug Discov Technol, 2008. **5**(4): p. 333-41.
11. Borges, O., et al., *Induction of lymphocytes activated marker CD69 following exposure to chitosan and alginate biopolymers.* Int J Pharm, 2007. **337**(1-2): p. 254-64.
12. Bakhru, S.H., et al., *Oral delivery of proteins by biodegradable nanoparticles.* Adv Drug Deliv Rev, 2013. **65**(6): p. 811-21.
13. Singh, J., et al., *Diphtheria toxoid loaded poly-(epsilon-caprolactone) nanoparticles as mucosal vaccine delivery systems.* Methods, 2006. **38**(2): p. 96-105.
14. Benoit, M.A., B. Baras, and J. Gillard, *Preparation and characterization of protein-loaded poly(epsilon-caprolactone) microparticles for oral vaccine delivery.* Int J Pharm, 1999. **184**(1): p. 73-84.
15. Beltran, A., et al., *Characterization of poly(epsilon-caprolactone)-based nanocomposites containing hydroxytyrosol for active food packaging.* J Agric Food Chem, 2014. **62**(10): p. 2244-52.
16. Gloria, A., et al., *Magnetic poly(epsilon-caprolactone)/iron-doped hydroxyapatite nanocomposite substrates for advanced bone tissue engineering.* J R Soc Interface, 2013. **10**(80): p. 20120833.
17. Woodruff, M.A. and D.W. Hutmacher, *The return of a forgotten polymer—Polycaprolactone in the 21st century.* Progress in Polymer Science, 2010. **35**(10): p. 1217-1256.
18. Haas, J., et al., *Preparation and characterization of chitosan and trimethyl-chitosan-modified poly-(epsilon-caprolactone) nanoparticles as DNA carriers.* AAPS PharmSciTech, 2005. **6**(1): p. E22-30.
19. Florindo, H.F., et al., *Streptococcus equi antigens adsorbed onto surface modified poly-epsilon-caprolactone microspheres induce humoral and cellular specific immune responses.* Vaccine, 2008. **26**(33): p. 4168-77.
20. Gupta, N.K., et al., *Development and characterization of chitosan coated poly-(varepsilon-caprolactone) nanoparticulate system for effective immunization against influenza.* Vaccine, 2011. **29**(48): p. 9026-37.
21. Florindo, H.F., et al., *The enhancement of the immune response against S. equi antigens through the intranasal administration of poly-epsilon-caprolactone-based nanoparticles.* Biomaterials, 2009. **30**(5): p. 879-91.

22. Jimenez-Ruiz, E., et al., *Low efficacy of NcGRA7, NcSAG4, NcBSR4 and NcSRS9 formulated in poly-epsilon-caprolactone against Neospora caninum infection in mice.* Vaccine, 2012. **30**(33): p. 4983-92.

23. Bilensoy, E., et al., *Intravesical cationic nanoparticles of chitosan and polycaprolactone for the delivery of Mitomycin C to bladder tumors.* Int J Pharm, 2009. **371**(1-2): p. 170-6.

24. Mazzarino, L., et al., *Elaboration of chitosan-coated nanoparticles loaded with curcumin for mucoadhesive applications.* J Colloid Interface Sci, 2012. **370**(1): p. 58-66.

25. Borges, O., et al., *Preparation of coated nanoparticles for a new mucosal vaccine delivery system.* Int J Pharm, 2005. **299**(1-2): p. 155-66.

26. Jesus, S., G. Borchard, and O. Borges, *Freeze Dried Chitosan/ Poly- e-Caprolactone and Poly-e-Caprolactone Nanoparticles: Evaluation of their Potential as DNA and Antigen Delivery Systems.* J Genet Syndr Gene Ther 2013. **4**(164).

27. Martinac, A., et al., *Development and bioadhesive properties of chitosan-ethylcellulose microspheres for nasal delivery.* Int J Pharm, 2005. **291**(1-2): p. 69-77.

28. Rahman, M., et al., *Nanoparticle and Protein Corona*, in *Protein-Nanoparticle Interactions*. 2013, Springer Berlin Heidelberg. p. 21-44.

29. Bhargava, R., S.Q. Wang, and J.L. Koenig, *FTIR Microspectroscopy pf Polymeric Systems.* Adv Polym Sci, 2003. **163**: p. 137-191.

30. Dole, M.N., et al., *Advance applications of fourier transform infrared spectroscopy.* Int J Pharm Sci Rev Res, 2011. **7**(2).

31. Roozbahani, F., et al., *Effects of Chitosan Alkali Pretreatment on the Preparation of Electrospun PCL/Chitosan Blend Nanofibrous Scaffolds for Tissue Engineering Application.* Journal of Nanomaterials, 2013. **2013**: p. 6.

32. Gregorio-Jauregui, K.M., et al., *One-Step Method for Preparation of Magnetic Nanoparticles Coated with Chitosan.* Journal of Nanomaterials, 2012. **2012**: p. 8.

33. Duarte, M.L., et al., *An optimised method to determine the degree of acetylation of chitin and chitosan by FTIR spectroscopy.* Int J Biol Macromol, 2002. **31**(1-3): p. 1-8.

34. Jang, M.K., et al., *The preparation and characterization of low molecular and water soluble free-amine chitosan.* Bull. Korean Chem. Soc., 2002. **23**(6).

35. Elzubair, A., et al., *The physical characterization of a thermoplastic polymer for endodontic obturation.* J Dent, 2006. **34**(10): p. 784-9.

36. Zhetcheva, V.D.K. and L.P. Pavlova, *Synthesis and spectral characterization of a decavanadate/chitosan complex.* Turk. J. Chem., 2011. **35**: p. 215-223.

37. Yang, H.Y., et al., *One-pot synthesis of water-dispersible Ag2S quantum dots with bright fluorescent emission in the second near-infrared window.* Nanotechnology, 2013. **24**(5): p. 055706.

38. Kong, J. and S. Yu, *Fourier transform infrared spectroscopic analysis of protein secondary structures.* Acta Biochim Biophys Sin (Shanghai), 2007. **39**(8): p. 549-59.

39. Chakraborty, S., et al., *Contrasting effect of gold nanoparticles and nanorods with different surface modifications on the structure and activity of bovine serum albumin.* Langmuir, 2011. **27**(12): p. 7722-31.

40. Kazarian, S.G. and K.L. Chan, *ATR-FTIR spectroscopic imaging: recent advances and applications to biological systems.* Analyst, 2013. **138**(7): p. 1940-51.

41. Mosmann, T., *Rapid colorimetric assay for cellular growth and survival: application to proliferation and cytotoxicity assays.* J Immunol Methods, 1983. **65**(1-2): p. 55-63.

42. Acharyulu, S.R., T. Gomathi, and P.N. Sudha, *Physico-chemical characterization of cross linked chitosan-polyacrylonitrile polymer blends.* Der Pharmacia Lettre, 2013. **5**(2): p. 354-363.

43. Xiao, Y., *Characterization and Implications of Surface Hydrophobicity in Nanoparticle Fate and Transport*, in *Civil and Environmental Engineering*. 2012, Duke University.

44. Neto, C.G.T., et al., *Thermal analysis of chitosan based networks.* Carbohydrate Polymers, 2005. **62**(2): p. 97-103.

45. Ciardelli, G., et al., *Blends of poly-(epsilon-caprolactone) and polysaccharides in tissue engineering applications.* Biomacromolecules, 2005. **6**(4): p. 1961-76.

46. Persenaire, O., et al., *Mechanisms and kinetics of thermal degradation of poly(epsilon-caprolactone).* Biomacromolecules, 2001. **2**(1): p. 288-94.

47. Mohamed, A., et al., *Thermal Properties of PCL/Gluten Bioblends Characterized by TGA, DSC, SEM, and Infrared-PAS.* Journal of Applied Polymer Science, 2008. **110**(5): p. 3256-3266.

48. das Neves, J., et al., *Assessing the physical-chemical properties and stability of dapivirine-loaded polymeric nanoparticles.* International Journal of Pharmaceutics, 2013. **456**(2): p. 307-314.

49. Correlo, V.M., et al., *Properties of melt processed chitosan and aliphatic polyester blends.* Materials Science and Engineering: A, 2005. **403**(1–2): p. 57-68.

50. Li, X.M., et al., *Interaction of bovine serum albumin with self-assembled nanoparticles of 6-O-cholesterol modified chitosan.* Colloids and Surfaces B-Biointerfaces, 2012. **92**: p. 136-141.

51. Huang, R.X., et al., *Protein-nanoparticle interactions: the effects of surface compositional and structural heterogeneity are scale dependent.* Nanoscale, 2013. **5**(15): p. 6928-6935.

52. Greenfield, N.J., *Using circular dichroism spectra to estimate protein secondary structure.* Nature Protocols, 2006. **1**(6): p. 2876-2890.

53. Kelly, S.M. and N.C. Price, *The Use of Circular Dichroism in the Investigation of Protein Structure and Function.* Current Protein & Peptide Science, 2000. **1**(4): p. 349-384.

54. Saptarshi, S.R., A. Duschl, and A.L. Lopata, *Interaction of nanoparticles with proteins: relation to bio-reactivity of the nanoparticle.* Journal of Nanobiotechnology, 2013. **11**.

55. Treuel, L. and M. Malissek, *Interactions of nanoparticles with proteins: determination of equilibrium constants.* Methods Mol Biol, 2013. **991**: p. 225-35.

56. Ghosh, G., L. Panicker, and K.C. Barick, *Selective binding of proteins on functional nanoparticles via reverse charge parity model: an in vitro study.* Mater. Res. Express, 2014. **1**(1).

57. Shang, L., et al., *pH-dependent protein conformational changes in albumin:gold nanoparticle bioconjugates: a spectroscopic study.* Langmuir, 2007. **23**(5): p. 2714-21.

58. Zhou, H.S., et al., *Conformational change of protein cytochrome b-562 adsorbed on colloidal gold particles; absorption band shift.* Chem. Commun., 1997(6): p. 605-606.

59. Ranjbar, B. and P. Gill, *Circular Dichroism Techniques: Biomolecular and Nanostructural Analyses- A Review.* Chemical Biology & Drug Design, 2009. **74**(2): p. 101-120.

60. Borges, O., et al., *Uptake studies in rat Peyer's patches, cytotoxicity and release studies of alginate coated chitosan nanoparticles for mucosal vaccination.* J Control Release, 2006. **114**(3): p. 348-58.

61. Sogias, I.A., A.C. Williams, and V.V. Khutoryanskiy, *Why is chitosan mucoadhesive?* Biomacromolecules, 2008. **9**(7): p. 1837-42.

62. Sonia, T.A. and C.P. Sharma, *Chitosan and Its Derivatives for Drug Delivery Perspective.* Chitosan for Biomaterials I, 2011. **243**: p. 23-53.

63. Sinha, V.R., et al., *Chitosan microspheres as a potential carrier for drugs.* International Journal of Pharmaceutics, 2004. **274**(1-2): p. 1-33.

64. Mahapatro, A. and D.K. Singh, *Biodegradable nanoparticles are excellent vehicle for site directed in-vivo delivery of drugs and vaccines.* Journal of Nanobiotechnology, 2011. **9**.

65. Kumari, A., S.K. Yadav, and S.C. Yadav, *Biodegradable polymeric nanoparticles based drug delivery systems.* Colloids and Surfaces B-Biointerfaces, 2010. **75**(1): p. 1-18.

66. Kulkarni, S.A. and S.S. Feng, *Effects of particle size and surface modification on cellular uptake and biodistribution of polymeric nanoparticles for drug delivery.* Pharm Res, 2013. **30**(10): p. 2512-22.

67.   Xiang, S.D., et al., *Delivery of DNA vaccines: an overview on the use of biodegradable polymeric and magnetic nanoparticles.* Wiley Interdiscip Rev Nanomed Nanobiotechnol, 2010. **2**(3): p. 205-18.

Part 2. Freeze dried chitosan and poly-ε-caprolactone nanoparticles: evaluation of their ability as DNA and antigen delivery systems

Abstract

Nanoparticles (NPs) prepared from natural or synthetic polymers have shown capacity for antigen and DNA vaccine delivery to mucosal surfaces. The purpose of this research was to prepare poly-ε-caprolactone (PCL)/chitosan NPs and PCL NPs and compare their ability as DNA and protein/vaccine delivery systems. Both preparation methods resulted in particles with low cytotoxicity and sizes apparently ideal to be taken up by cells (199 ± 62 nm and 165 ± 35 nm, respectively for PCL/chitosan and PCL NPs). However, PCL/chitosan NPs offered considerable advantages over PCL NPs as antigen and plasmid DNA (pDNA) delivery system. Namely, higher loading efficacies for model antigens studied (myoglobin, BSA, ovalbumin, lactalbumin, α-casein and lysozyme), much higher uptake by A549 cells and great ability to form stable complexes, protecting DNA from nucleases. However, in spite of good pDNA and protein loading capabilities, PCL/chitosan NPs showed much better qualities as a protein delivery system since transfection rates achieved with the complexes were low.

Keywords: Polymeric nanoparticles; Chitosan; Poly-ε-caprolactone; DNA vaccine; Recombinant antigens.

1. Introduction

In developing countries traditional vaccines are mostly administered by injection, which potentially results in a significant transmission of viral infections, due to the reuse of material and unsafe injection practices. Developing needle free vaccination methods to render the administration of vaccines safer is therefore a priority [1]. The nasal mucosa is considered to be a valuable vaccination route due to its relatively large surface area, permeable endothelium, high total blood flow, avoidance of first pass metabolism, avoidance of harsh environmental conditions of the gastrointestinal tract, and ease of administration due to its accessibility [2]. Nevertheless, when a vaccine is administered mucosally it encounters the same host defense barriers as do microbial pathogens and other foreign macromolecules. They are diluted in mucosal secretions, retained and cleared in mucus gels, attacked by proteases and nucleases and barred by the epithelial barrier, which leads to a poor and limited contact of the formulations with the nasal mucosal epithelium itself [2, 3]. Even so, this region presents advantages that are worth exploiting for nasal immunization, for instance the high amount of lymphoid tissue in the nasal passages and the capacity to elicit both mucosal and systemic immune responses [2].

Protein based vaccines are widely used and present good efficacy for the prevention of a wide range of infections; however, they generally induce antibody mediated responses (humoral responses) and often require periodic booster injections. This immune response induced is therefore not indicated for the clearance of intracellular pathogens, because it requires the generation of cytotoxic T lymphocytes, which might also be crucial in the protection against some diseases that currently have no prophylactic treatment available [4-6].

DNA vaccines can produce a coordinated activation of both humoral and cell mediated responses that result from the intracellular synthesis of the encoded antigen within the host's cells. The encoding sequence may be translated into antigen protein sequences by antigen presenting cells (APC) and then processed and presented by the major histocompatibility complex (MHC) class I, making it recognizable by the receptor of cytotoxic CD8+ T cells; or it may be expressed in other cells, being released into the extracellular space and then captured by APC, processed and presented by MHC class II and recognized by the CD4+ receptors of T helper cells, which facilitate humoral as well as cellular responses [4, 7-9]. DNA vaccines also present no propensity for the antigen reverse to virulence, the initiation of long lasting immunity, the possibility of widespread use even in immunocompromised individuals, are inexpensive, versatile, extremely stable and relatively easy to produce [7, 10]. The main obstacle concerning DNA vaccination lies with the necessary intracellular delivery of the encoding sequence. Several factors make this task a difficult one to accomplish: the protection of plasmid DNA

(pDNA) from degradation, low clearance from the interstitial space, transport through the extracellular matrix to the surface of target cells, internalization by target cells, escape from the endosomal / phagosomal compartment and, once in the cytoplasm, translocation of DNA into the nucleus, transcription and then translation into the protein antigen [4].

Encapsulation or complexation of pDNA with a biomaterial can significantly enhance pDNA stability, its cellular uptake and ultimately protein expression [4]. Polymeric NPs have shown the capacity to deliver DNA vaccines, as they are able to protect pDNA from extracellular degradation, can accommodate larger size plasmids, viruses and immunostimulatory agents simultaneously, possess the ability to offer a phagocytosis-based passive targeting of APC and the ability to be conjugated with appropriate functionalities to enhance cellular targeting and uptake [10]. The ability to co-deliver an immunopotentiator that for instance acts by binding to specific receptors is an essential feature as the immunogenicity and transfection efficiency of DNA vaccines is low, especially in humans [8, 10, 11].

Chitosan is a cationic polymer consisting of -(1-4)-linked D-glucosamine (deacetylated unit) and N-acetyl-D-glucosamine (acetylated unit) monomers that can be obtained by deacetylation of chitin [12]. It has been considered as a non-toxic, biodegradable and biocompatible polymer [13], and extensive research has been directed towards its use in medical applications such as drug and vaccine delivery [14-17]. Chitosan is also known to be mucoadhesive and its ability to stimulate cells of the immune system has been shown in many studies [18]. When applied to cells, the positively charged polyplexes will mediate transfection via a multistage process that includes cationic binding to the negatively charged cell membrane, which facilitates entrance into the cytoplasm. However, a high density of positive charges leads to an increased cytotoxicity [10]. Moreover, the results of mucosal DNA vaccination studies using chitosan NPs as vectors already described in the scientific literature are in general not very encouraging. The strong interaction between chitosan and pDNA in complexes may not allow for a subsequent dissociation of the complex and unpacking of the DNA, which is necessary for gene expression and may therefore be a possible reason for the low transfection efficiency reported [19, 20]. Current knowledge suggests a balanced and moderate interaction between the carrier and the pDNA as one of the key factors to successful therapeutics (extensively reviewed elsewhere [19]).

The introduction of chitosan during the preparation of poly-ε-caprolactone (PCL) particles, e.g., a synthetic biodegradable and hydrophobic polymer, will allow to obtain more amphiphilic particles in which the chitosan-DNA interaction is expected to be modified, and therefore the gene expression be may be improved. Other advantages are present when synthetic polymers such as PCL are considered for DNA delivery applications. Their chemical composition, total molecular weight and block length ratios can easily be adjusted to allow to control the size and morphology of the polymeric carriers [10]. PCL was also chosen due to its higher hydrophobicity, which could further enhance uptake of NPs by the

nasal mucosal immune system (NALT) and their *in vitro* stability, lower costs, and allow for the safe elimination of PCL metabolites, lactic and glycolic acid [21].

The purpose of this research was to optimize the preparation of PCL/chitosan NPs and simple PCL NPs in order to obtain two possible freeze dried vaccine delivery systems. Their properties were studied and compared to determine their aptitude for antigen loading and delivery, DNA loading and delivery, as well as transfection efficiency.

2. Materials and methods

2.1. Chitosan purification

Chitosan (ChitoClear™) was purchased from Primex BioChemicals AS (Avaldsnes, Norway). According to the provider's specifications, the degree of deacetylation was 95 % (titration method) and the viscosity 8 cP (measured in 1 % solutions in 1 % acetic acid). The polymer was purified by a technique adapted from [22]. Briefly, 1 g of chitosan was suspended in 10 mL NaOH 1 M solution. This suspension was heated to between 40-50 ºC under continuous magnetic stirring for 3 h. After this time, at room temperature, it was filtered using a Buchner funnel. Insoluble chitosan on the filter was washed with water and then recovered to be dissolved in 200 mL 1 % acetic acid solution, and stirred for 1 h at room temperature. The chitosan solution was then filtered through a 0.45 µm filter and 1 M NaOH solution was used to adjust the pH value of the filtrate to pH 8.0. The precipitate was then washed with deionized water through 3 consecutive 30 min centrifugations at 4500 x g. The precipitate was recovered and freeze dried.

2.2. Preparation of the delivery systems

2.2.1. Nanoparticle production method

The procedure for the preparation of PCL/chitosan particles in our laboratory resulted from the adaptation of different techniques described in the literature, with special consideration to the one described by Bilensoy [23] based on the nanoprecipitation technique patented by Fessi [24]. Briefly, an aqueous phase of acetic acid containing 0.1 % chitosan and 5 % Tween™ 80 was placed under a high speed homogenizer (homogenizer Ystral X120, Ballrechten-Dottingen, DE). The organic phase, consisting of 0.2 % PCL (Sigma Aldrich Corporation, St. Louis, MO, USA) diluted in acetone, was added drop wise to the first solution at a ratio of 1:3 (v/v) to give a final volume of 18 mL. Agitation was continued for 1 min after the complete mixture of both phases. At this point, the particle suspension was formed and was placed under magnetic swirl for 45 min to achieve maturation. Finally, the organic phase was removed by evaporating acetone with a nitrogen flux in a water bath (40 ºC maximum). The NPs suspended in the original medium were isolated, resuspended and concentrated in other diluents by centrifugation at 16000 x g, for 75 min at 4 ºC. To achieve minimal aggregation of the particles after the centrifugation, a 200 L glycerol bed for each 18 mL batch is recommended. Another methodology for particles isolation is dialysis of the original medium against water for 48 h, using Spectra®Por cellulose ester dialysis membrane, MWCO 300.000 (Spectrum Europe B.V., Breda, NL). Then, to the resulting solution trehalose (Sigma Aldrich Corp., MO, USA) was added to a final concentration of 2.5 %

(w/v), so that a freeze-drying process (FreezeZone 6, Labconco Corporation, Kansas City, MO, USA) was successfully achieved maintaining the particle original properties.

PCL particles were produced using the methodology described above, by replacing the 0.1 % chitosan solution by a simple acetic acid solution with 5 % of Tween 80™.

2.2.2. Production of nanoparticle-protein conjugates

Model proteins were adsorbed to NPs, previously resuspended in buffer, by simple incubation at variable protein:NPs (w/w) ratios and incubation times, with slight agitation at room temperature.

2.2.3. Production of nanoparticle-DNA complexes

Plasmid DNA (pCMVluc) encoding luciferase was amplified in *E. coli* strain DH 5 and purified using QIAGEN Plasmid Giga kit (QIAGEN, Hilden, DE). The purified pDNA was dissolved in MiliQ water and its concentration and purity assessed by UV spectrophotometry by measuring the absorbance at 260/280 nm. Nanoparticle-pDNA (NP-pDNA) complexes were prepared by mixing equal volumes of a nanoparticle suspension in phosphate buffer (PB) pH 5.7 (several concentrations) with a 100 µL/mL luciferase plasmid solution during an incubation time of 30 min. NP-pDNA complexes with surface-adsorbed protein were prepared by adsorbing human serum albumin (HSA, 96 % fraction V, Sigma Aldrich Corporation, St. Louis, MO, USA), to the NPs, through simple incubation (several ratios tested). The resulting suspension was mixed with an equal volume of 100 µL/mL luciferase plasmid solution during an incubation time of 30 min at room temperature.

2.3. Characterization of the delivery systems

2.3.1. Surface appearance

Cryo Scanning Electron Microscopy (CryoSEM) was performed on a FE-CryoSEM/EDS, JEOL JSM 6301F (CEMUP - Materials Centre of the University of Porto, Portugal). Particles were prepared as described above, acetone was evaporated with a nitrogen flux and a 48 hour dialysis accomplished. After the dialysis samples were treated with liquid nitrogen, fractured and then observed.

2.3.2. Size and Zeta potential measurements

Delsa™ Nano C particle analyzer (Beckman Coulter, Madrid, ES) was used to measure the particle size by Dynamic Light Scattering (DLS), and their zeta potential by electrophoretic light scattering (ELS). For the size, analyzes were performed at 25 °C and scattered light collected at a 165° angle. Particle

suspensions were characterized in the production medium, after centrifugation and after the resuspension of the freeze dried particles.

An MPT-2 autotitrator coupled to a ZetaSizer Nano ZS (Malvern Instruments, Ltd., Worcestershire, UK) was used to measure the zeta potential and intensity of the particles versus a wide range of pH values of the suspension medium. The NPs, freeze-dried in the presence of trehalose were resuspended in water and placed in the sample tube connected to a clear disposable cuvette. The assay was performed automatically at 25 ºC and the titrants used were NaOH 0.25 M, HCl 0.25 M and HCl 0.01 M. pH ranged from 2 to 11 during approximately 6 h, and the final volume of added titrants was approximately 0.5 mL.

2.3.3. Protein adsorption studies

Bovine serum albumin (BSA, 96 % fraction V), ovalbumin (98 %), myoglobin from equine skeletal muscle (95 %-100 %), -casein (>70 %), lysozyme (≥ 80 %), lactalbumin from bovine milk (≈ 80 %) (Sigma Aldrich Corporation, St. Louis, MO, USA) were incubated with fresh NPs, centrifuged and resuspended in phosphate buffer (PB) pH 7.4. PCL/chitosan and PCL NPs were used at a protein:NP (w/w) ratio of 1.5:1 and 1.6:1, respectively. The incubation was extended for 3 h maximum and at different times, aliquots of the particle suspension were centrifuged at 16000 x g for 30 min and the supernatant collected for non-bound protein quantification. Pierce^{TM} bicinchoninic acid (BCA) protein assay (Thermo Fisher Scientific Inc., Waltham, MA, USA) was performed in microplates.

The percentage of loading efficacy (% LE) and the percentage of loading capacity (% LC) of the NPs was calculated using the following equations (Eq. 1 and Eq. 2, respectively):

$$\text{LE (\%)} = \frac{\text{(total amount of protein (µg/mL)-non bound protein(µg/mL))}}{\text{total amount of protein(µg/mL)}} \times 100 \qquad \text{(Eq. 1)}$$

$$\text{LC (\%)} = \frac{\text{(total amount of protein (µg/mL)−non bound protein(µg/mL))}}{\text{weight of the particles (µg/mL)}} \times 100 \qquad \text{(Eq. 2)}$$

2.3.4. Cytotoxicity of the nanoparticles

A549 cells (American Type Culture Collection, ATCC, Barcelona, ES) were cultured at 37 ºC and 5 % CO_2, in Nutrient mixture F12 Ham (Sigma Aldrich Corporation, St. Louis, MO, USA) with 10 % FBS supplemented with 1 % PenStrep having a final pH of 7.2 to 7.4. Subcultures were performed by detaching the cells with trypsin (Live Technologies Corporation, Paisley, UK). Cytotoxicity assays were performed after 18 h incubation of 100 µL A549 cell suspension seeded in a 96-well plate at a density of

10^5 cells/mL. Serial dilutions of the NPs, freeze-dried with trehalose, were prepared in serum-free F12 Ham's at a concentration range between 0.29 µg/mL and 300 µg/mL. Prior to the addition of the NPs, the medium was removed and 100 µL of new medium was added. 100 µL of each sample was added and allowed to incubate with the cells for 24 h, at 37 ºC and 5 % CO_2. After 24 h, an MTT cytotoxicity assay was performed (MTT reagent, Sigma Aldrich Corporation, St. Louis, MO, USA). The relative cell viability (%) related to control (cells in culture medium without NPs) was calculated by the following equation (Eq. 3):

$$\text{cell viability (\%)} = \frac{\text{OD sample (540nm) - OD sample (630nm)}}{\text{OD control (540nm)- OD control (630nm)}} \times 100 \qquad \text{(Eq. 3)}$$

Cytotoxicity assays were performed also with pDNA complexes following the incubation time as for transfection assays (described below).

2.3.5. DNA complexation assay / Gel retardation assay

To evaluate the complexation of pDNA with the NPs an electrophoresis in agarose gel was performed. Samples were diluted with PB pH 5.7 at a ratio of 1:4 and 10 µL of each resulting sample was added to 2 µL of a loading buffer containing bromophenol blue to monitor the run. 6 µL of each sample were placed in individual wells in a 1 % agarose gel, stained with 1 % ethidium bromide for the electrophoresis run (horizontal DNA electrophoresis System, Bio-Rad, Hercules, CA, USA). The electrophoresis was set to 45 min at 100 V. The control was pDNA solution at 12.5 µg/mL. Data analysis was performed in a UV transilluminator (UVITEC Cambridge, Cambridge, UK).

2.3.6. DNA protection assay /DNase I assay

Different NP-pDNA complexes were incubated with several concentrations of a DNase I solution (Sigma Aldrich Corporation, St. Louis, MO, USA) for 15 minutes at 37 ºC. DNase I was maintained in a buffer solution with 50 Mm Tris-HCL, 10 mM $MnCl_2$ and 50 µg/mL BSA. The reaction was stopped by using an EDTA 0.5 M solution (1 µL/unit of DNase I). Controls using inactivated DNase I were performed after its inactivation with EDTA, at the same theoretical concentrations for 15 min at 37 ºC. To evaluate DNase I activity on the DNA complexed with the particles, an electrophoresis in agarose gel was performed as described above.

2.3.7. *In vitro* uptake studies

To perform uptake studies with simple PCL/chitosan NPs, chitosan was labeled with fluorescein isothiocyanate (FITC) (Santa Cruz Biotechnology, Heidelberg, DE) according to a protocol described

previously with some modifications [25]. Briefly, 35 mL of dehydrate methanol containing 25 mg of FITC was mixed with 25 mL of a 1 % w/v chitosan in 0.1 M of acetic acid and incubated for 3 hours, at room temperature in the dark. FITC labeled chitosan was then precipitated with 0.2 M NaOH to pH 10, and centrifuged for 30 minutes at 4500 x g. The resulting pellet was washed with a mixture of methanol and water (70:30, v/v) three times. Labeled chitosan was resuspended in 15 mL of 0.1 M acetic acid solution and stirred overnight. Polymer solution was dialyzed in 2.5 L of distilled water for 3 days under darkness, before freeze-drying. The resulting powder was used to prepare 0.1 % chitosan solution used in the nanoparticle production method as described above.

The formulations analyzed for cellular uptake consisted of FITC-labeled NPs, FITC-labeled NP-pDNA complexes and FITC-labeled NPs adsorbed with protein.

For flow cytometry studies A549 cells were seeded on glass coverslips on 48 well plates at a density of 5×10^4 cells/well and cultured at 37 °C in 5 % CO_2 for 48 hours. The medium was then replaced with serum free medium and cells were incubated with different formulations for 4 hours. Following the uptake period, medium containing NPs was removed and cells were washed and trypsinized with 50 μL of Trypsin-EDTA. The cells of six wells were collected into one tube and the medium replaced with 300 μL of PBS pH 7.4. Cells were kept at 4 °C until analysis. Prior to analysis on a BD FACSCalibur Flow Cytometer (BD Biosciences, Bedford, MA, USA), 1.5 μL propidium iodide solution (PI) 50 μg/mL (Sigma Aldrich Corporation, St. Louis MO, USA) was added to the samples. The mean fluorescence data for a population of 20000 cells were collected and results processed by CellQuest Modfit LT software (BD Biosciences).

For confocal laser scanning microscopy (CLSM) studies, A549 cells were seeded on glass coverslips in 12 well plates at a density of 1.2×10^5 cells/well and cultured at 37 °C in 5 % CO_2 overnight. After approximately 16 h incubation, the medium was replaced with serum free medium and cells were incubated with different formulations for 4 h. Following the uptake period, medium containing NPs was removed, cells washed with phosphate buffer saline (PBS) pH 7.4 and fixed with 4 % paraformaldehyde in PBS for 15 min at 37 °C. Plasma membrane and cell nucleus of the pre-fixed cells were labeled with image-It™ LIVE Plasma membrane and nuclear labeling kit (Live Technologies Corporation, Paisley, UK), according to manufacturer's instructions. Nucleus were stained with a cell permeable nucleic acid (Hoechst 33342), and their plasma membranes stained with cell impermeable Alexa Fluor 594 wheat germ agglutinin, that binds selectively to N-acetylglucosamine and N-acetylneuraminic (sialic) acid residues on the cell membrane [26]. After labeling, cells were washed twice with PBS and coverslips mounted on microscope slides with DAKO mounting medium, and examined under an inverted laser scanning confocal microscope (Zeiss LSM 510 META, Carl Zeiss, Oberkochen, DE) equipped with imaging software (LSM 510 software, Carl Zeiss).

2.3.8. Transfection studies

Transfection studies were performed in order to assess the suitability of the complexes (PCL/chitosan NP-pDNA) to efficiently mediate gene transfer. A549 cells were seeded in a volume of 500 µL at a density of 5 x 10^4 cells/well on 48-well plates, and incubated for 48 hours, at 37 ºC and with 5 % CO_2, prior to the transfection assay. After this period, the cells were adherent and the F12 Ham´s medium was replaced for serum free F12 medium or complete F12 medium. Different ratios of NP:HSA:pDNA (w/w/w) were prepared and added to cells based on the previous pDNA complexation and protection assays, ensuring a volume containing 1 µg of pDNA per well. The incubation of complexes with the cells lasted for 4 hours at 37 ºC. A solution of pDNA was used as negative control. After incubation, the medium was replaced by F12 Ham's medium and cells were cultured for another 48 hours in the incubator to allow gene expression. To determine the transfection efficiency of the complexes, after the incubation time, the culture medium was removed, the cells washed with PBS pH 7.4 and the adherent cells lysed with lysis buffer (1 mM DTT, 1 mM EDTA, 25 mM Tris-phosphate pH 7.8, 8 mM MgCl2, 15 % glycerol, 1 % (v/v) Triton X-100, 100 µL/well). The resulting lysate was the centrifuged and the supernatant used to quantify the luciferase expression, using 50 µL, placed in a white 96-well plate. The samples platted in a 96-well plate, were analyzed in a Lmax II 384 Luminometer (Molecular Devices, Sunnyvale, CA, USA), by adding 100 µL of D-Luciferin sodium salt solution and 100 µL of ATP (Sigma Aldrich Corp., MO, USA) at 37 ºC. Immediately after the luminescence emitted was read. To normalize the luminescence values, the total protein content of the samples was also measured from the resulting supernatant with the BCA protein assay described above. Luminescence values were expressed in Relative Light Units (RLU)/µg of protein present in the 50 µL of sample.

2.4. Statistical Analysis

Results are expressed as mean values ± standard deviation (SD). Data analyzes and determination of significance ($p < 0.05$) were determined using SPSS software (IBM Corporation, New York, NY, USA) for protein adsorption studies and GraphPad software (GraphPad Software, Inc., La Jolla, CA, USA) for all other data.

3. Results

3.1. Characteristics of the nanoparticles

The chitosan purification process did not induce any modification in the acetylation degree as confirmed by Fourier Transform Infrared Spectroscopy (FTIR) (data not shown). The precipitation technique allowed us to efficiently produce two different types of NPs: PCL/chitosan NPs and PCL NPs.

First of all, it was also possible to conclude that the inclusion of chitosan into PCL particles did neither alter their size (statistical analysis not shown), nor their morphology. In fact, the morphology of the particles, evaluated by Cryo Scanning Electron Microscopy (Fig. 1A), revealed small, round shaped NPs for both PCL/chitosan and PCL formulations. The scale bar in the image allowed us to observe particles with sizes around 250 nm with low polydispersity.

Particle size was measured right after preparation in the original medium and after the two particle isolation/purification steps tested, during the development and optimization of the particle preparation method: method 1 – centrifugation; method 2- dialysis. In the latter case, the size was not measured immediately after the dialysis, but was measured after the subsequent step, the lyophilization.

As clearly shown in Figure 1B, both particle isolation methods, applied in order to eliminate unreacted compounds, did not result in any alteration of the size of the PCL/chitosan particles (Fig. 1B1). Therefore, the sizes obtained during the three phases of the preparation of the particles were 199.5 ± 62.0 nm (polydispersity index (PI) 0.162), 235.7 ± 96.4 nm (PI 0.180), 282.5 ± 36.7 nm (PI 0.248), respectively for size measured in the original medium (immediately after production) and size measured after the isolation methods, centrifugation and dialysis. PCL particles were of similar size in the original medium and after centrifugation using a glycerol bed, showing values of 165.3 ± 35.1 nm (PI 0.152) and 151.2 ± 8.3 nm (PI 0.098), respectively. Nevertheless, after freeze-drying of the dialyzed PCL particles, the size increased significantly to a medium size of 323.0 ± 155.7 nm and a polydispersity index (PI) of 0.205, which also reflects poor reproducibility of the freeze-drying process. The results also suggest that the concentration of trehalose used appears to be adequate for the PCL/chitosan particles and probably needs to be optimized for the PCL particles.

A1

A2

B1

B2
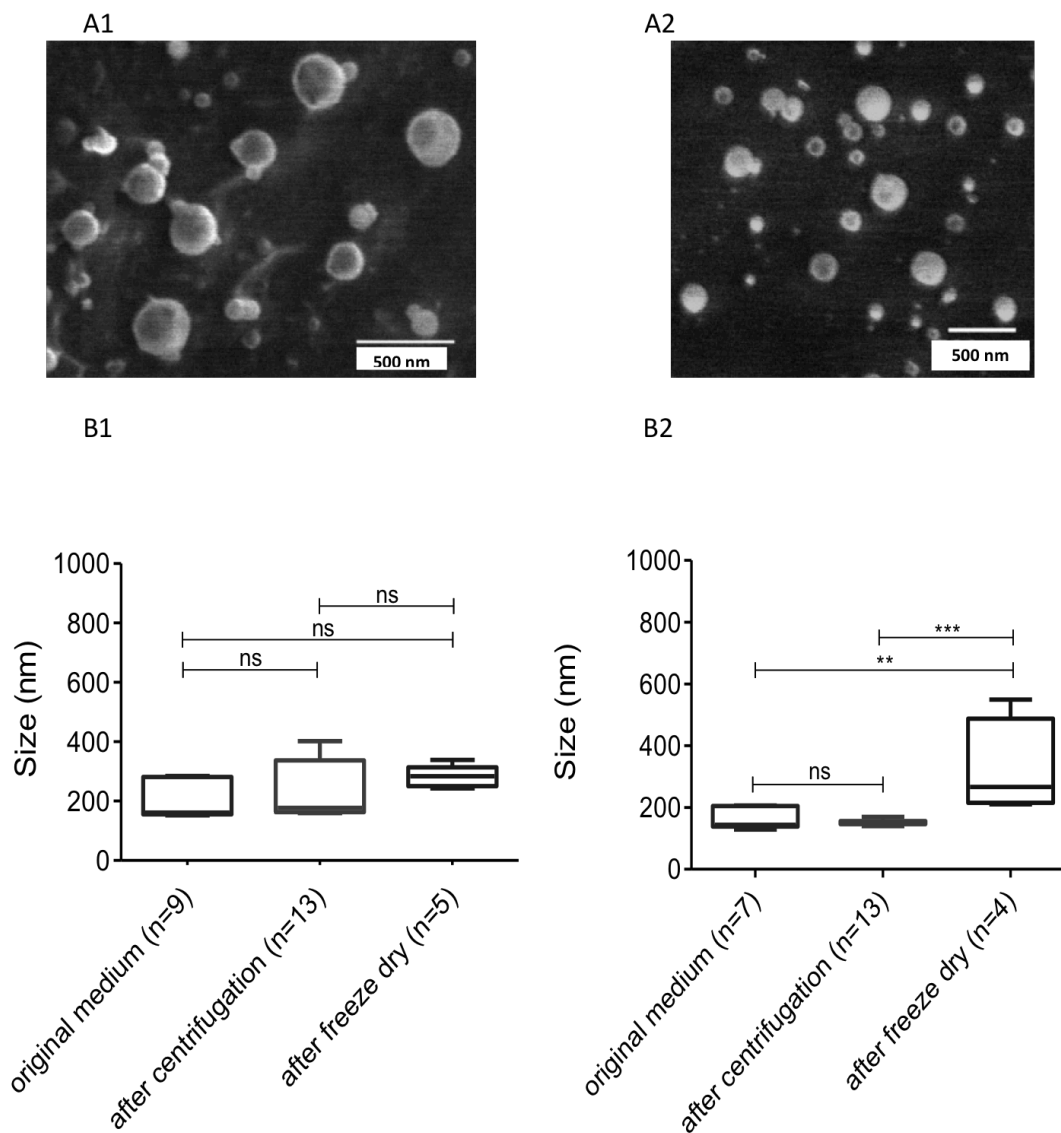
Figure 1: A) Particles observed by CryoSEM after a 48 hours dialysis against water. (A1) PCL/chitosan NPs; (A2) PCL NPs. Length of scale bar: 500 nm. B) Particles size distribution on the original medium and after re-suspension in water after two different isolation procedures. Box and whiskers graphics showing maximum, minimum, median and 75th and 25th percentiles (B1) PCL/chitosan NPs; (B2) PCL NPs. Caped lines above boxes and whiskers represent comparison above isolation procedures: ns "no statistical difference"; ** p<0.05; *** p<0.01.

Zeta potential depends on the ionic strength, pH and ion type of the medium in which particles are suspended [27]. PCL/chitosan and PCL NPs, when suspended in phosphate buffer (0.1 M; pH 7.4) showed similar values for zeta potential with no statistical significant differences (-10.1 ± 3.6 mV and -11.9 ± 3.1 mV, respectively; p<0.05).

In order to study surface properties under different conditions for both nanoparticle species a zeta potential titration over a pH range from 2 to 11 was performed. Zeta potential and size data were recorded.

PCL/chitosan NPs titration

A   **B**

PCL NPs titration

C   **D**
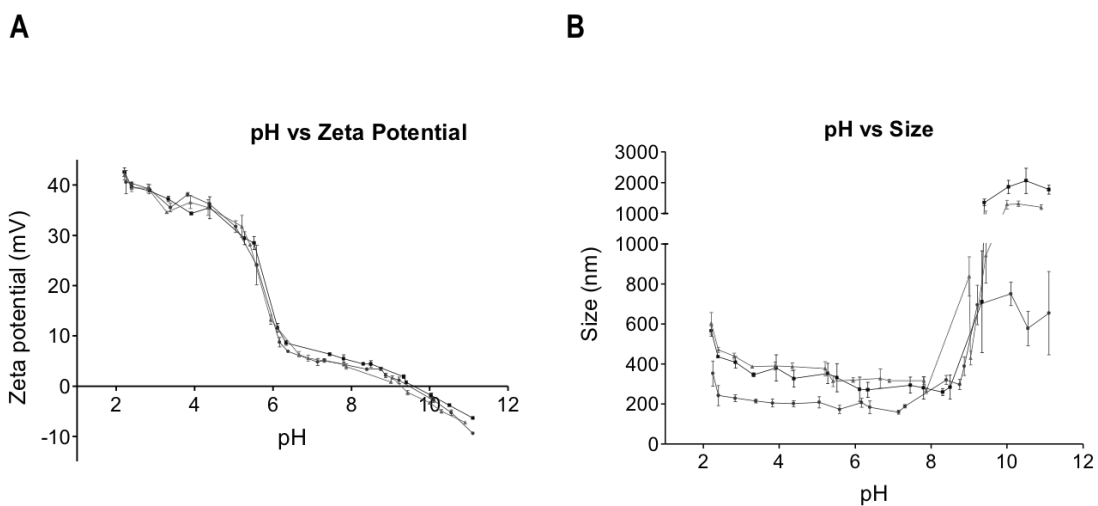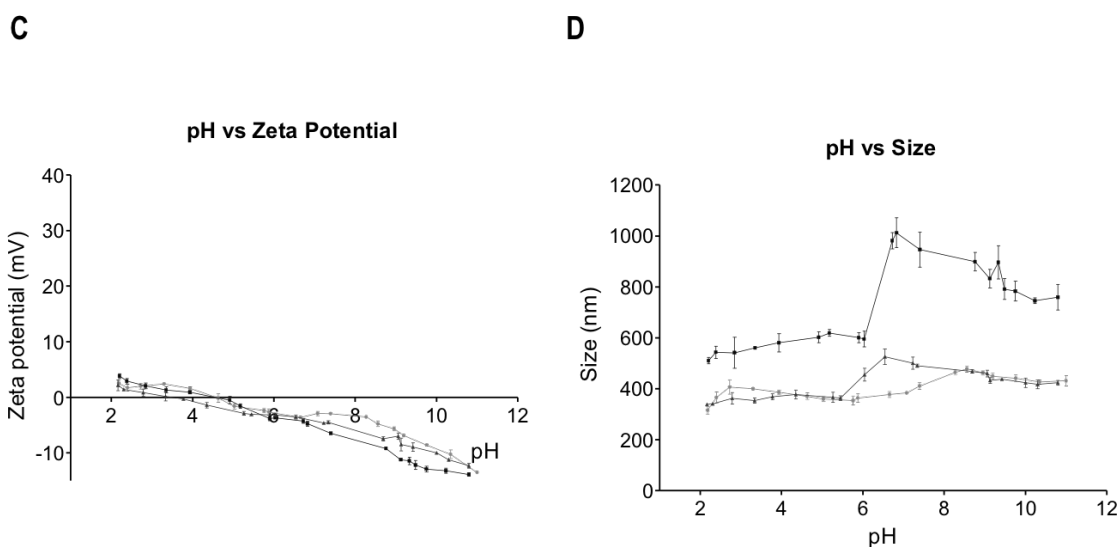
Figure 2: Titration of lyophilized PCL/chitosan NPs (A,B) and PCL NPs (C,D) zeta potential and size according to the pH of the medium. pH changed from 2 to 11 following alkalization with NaOH 0,25 M. A) PCL/chitosan NPs zeta potential according to pH; B) PCL/chitosan NPs size according to pH; C) PCL NPs zeta potential according to pH; D) PCL NPs size according to pH. Each curve represents an independent assay.

We observed two different zeta potential titration curves corresponding to each nanoparticle type. As illustrated in Figure 2, PCL/chitosan NPs are highly positively charged from pH 2 to pH 6, slightly positive from pH 6 to pH 9 and negatively charged at higher pH values (Fig. 2A). PCL NPs presented slightly positive (almost zero) zeta potential values between pH values from 2 to 4.5 and negative values up to pH 11 (Fig. 2B). These zeta potential titration curves were expected and indicated the presence of chitosan adsorbed to the surface of the PCL/chitosan particles. In fact, the zeta potential titration curve of chitosan particles are similar (data not shown) at low pH values, so it is possible to conclude that chitosan is contributing to the positive charge of the particles observed at low pH values of the curve, which is absent in PCL NPs. The zeta potential titration curves also allow the determination of the isoelectric point of the particles, corresponding to the pH value at which the zeta potential is zero. This property is especially important since it gives an indication at which pH value the particles are usually unstable (isoelectric point ± 2 pH units) [28]. Instable particles tend to flocculate or agglomerate, which may be incorrectly viewed as a simple increase of particle size. In fact, observing graphs B and D in figure 2, a high increase in size occurred when the isoelectric point was achieved, approximately at pH 9 for the PCL/chitosan particles and larger sizes were maintained for the pH values above that point. PCL NPs also showed the same tendency, although the increase in size varied between batches, and was in general a minor variation. It may therefore be concluded that the incorporation of chitosan in PCL/chitosan NPs decreased particle stability at pH values above 9.

3.2. Both delivery systems have high protein loading capacities

The adsorption of antigens to the particle surface has been recognized as a very convenient method to load particles. One of the reasons is because the process can be performed in water or in buffer maintaining the bioactivity of the biomolecules. The inclusion of a hydrophilic polymer, chitosan, into PCL particles certainly modifies the surface properties of these particles and thus the adsorption of antigens. With the intention to study the differences between the two particle species, six model antigens (proteins) with different iso-electric points were used to perform the adsorption studies. A fixed concentration of particles was incubated with 500 μg/mL of protein solution resulting in a ratio of 1:1.5 PCL/chitosan NPs:protein and a (w/w) ratio of 1:1.6 PCL NPs:protein. The incubation time lasted for a maximum of 3 h, and loading efficacy and loading capacity of the particles were assessed at different times. The results are shown in Figures 3A and 3B, allowing a comparison between the two nanoparticle formulations.

PCL/chitosan NPs showed higher loading efficacies than PCL NPs for 5 of the 6 proteins studied. The only protein that showed similar adsorption was myoglobin. Nevertheless, for PCL/chitosan NPs the loading efficacies were superior to 50 %, only with the exception of lysozyme, the protein with the

highest isoelectric point. PCL NPs presented loading efficacies of less than 50 % for almost all proteins assayed.
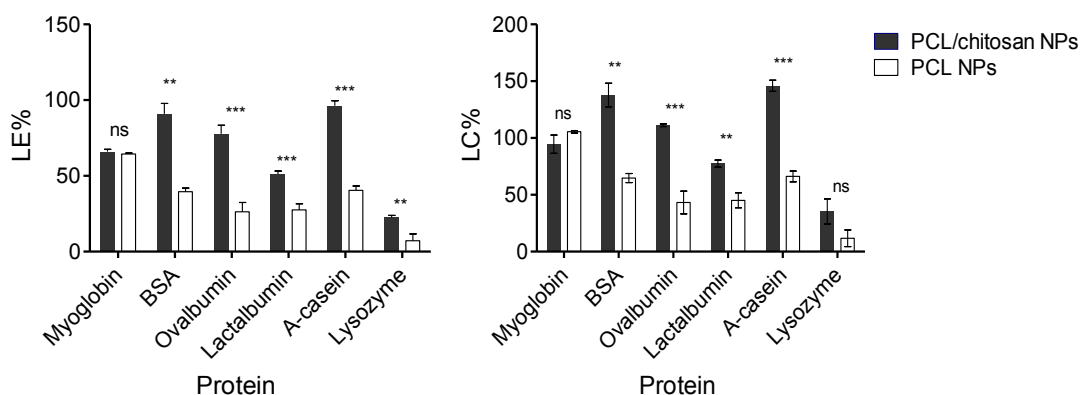
Figure 3: Loading efficacy (LE) and loading capacity (LC) results of freshly prepared NPs, isolated by centrifugation. (A) Maximum LE (%) observed on PCL/chitosan NPs and PCL NPs for different proteins; (B) Maximum LC (%) observed on PCL/chitosan NPs and PCL NPs for different proteins (**p<0.01, ***p<0.001, ns p>0.05).

Normalization between loading efficacy values and the nanoparticle concentration for the PCL/chitosan and PCL formulations in each case allowed for a more realistic comparison between the two delivery systems. As the concentrations of both particle species are only slightly different, loading capacity results show the same profile as those for loading efficacy. Nevertheless, it is noteworthy that PCL/chitosan nanoparticle loading capacity exceeded 100 %, confirming the superiority of these NPs as a protein delivery system as compared to PCL NPs.

3.3. Both freeze-dry delivery systems have low cytotoxicity

The effects of freeze dried PCL/chitosan and PCL NPs on A549 cells were investigated by performing the MTT viability assay. To determine the concentrations suitable for subsequent *in vitro* studies at minimal toxicity, a serial dilution for each nanoparticle suspension was prepared. These nanoparticle formulations contain a high amount of trehalose to prevent agglomeration during the process of resuspension of the particles in the culture medium, however, previous cytotoxicity studies at high concentrations of trehalose were performed and no decrease in cell viability was observed (data not shown). As illustrated in Figure 4, PCL/chitosan NPs and PCL NPs present a similar profile, with concentrations superior to 18.8 µg/mL per well resulting in significant toxicity (cellular viability below 50 %).
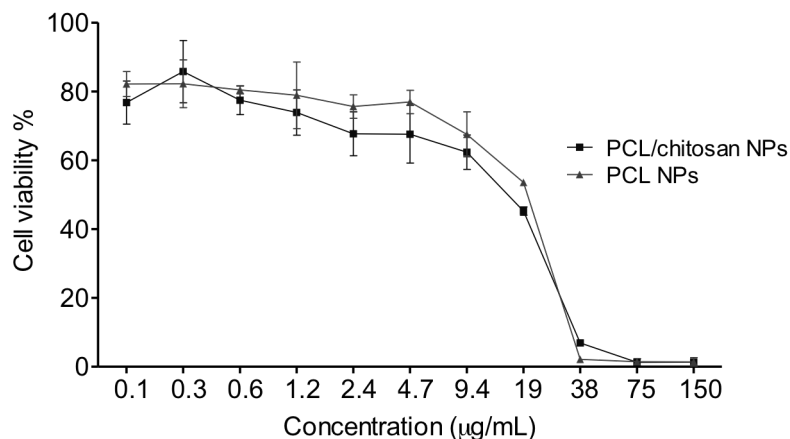
Figure 4: Cytotoxicity induced by different concentration of PCL/chitosan NPs and PCL NPs on A549 cell line. NPs concentration refers to the dilution on the well and the incubation was maintained for 24 hours. Error bars represent standard deviation of the mean, n=4.

3.4. Only PCL/chitosan particles are able to form complexes with DNA

As already stated, our main goal was not only to optimize particle preparation methods but also to evaluate the suitability of the particles to deliver both, pDNA and protein antigens. For the studies with NP-pDNA complexes, freeze-dried NPs were preferred instead of freshly centrifuged ones due to increased stability of the former [29].
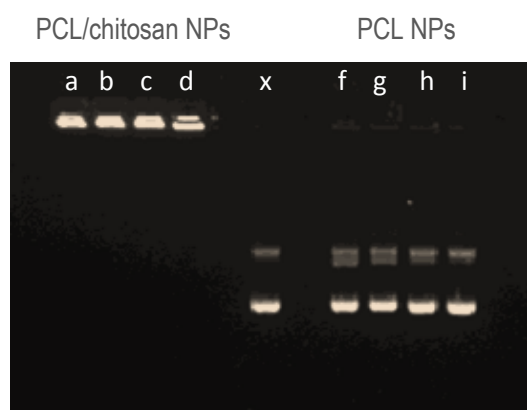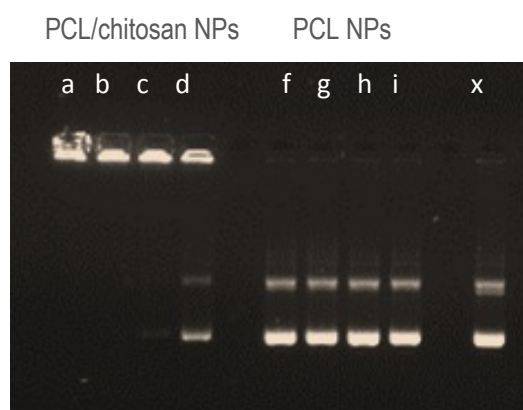
Figure 5: Electrophoresis in agarose gel illustrating the capability of plasmid DNA immobilization by PCL/chitosan NPs (lane a,b,c,d) and PCL NPs (lane f,g,h,i). A) Different (w/w) ratios NPs:pDNA: a and f) 20:1; b and g) 15:1; c and h) 10:1; d and i) 5:1; control presented on lane x (free pDNA). B) Different (w/w) ratios NPs:HSA:pDNA: a

and f) 2.5:2.5:1; b and g) 1.875:1.875:1; c and h) 1.25:1.25:1; d and j) 0.6:0.6:1; control presented on lane x (free pDNA).

Therefore, the suitability of particles to efficiently complex DNA was assessed through an agarose electrophoresis assay. In the initial experiments PCL/chitosan and PCL NPs were compared, using large amounts of NPs to complex lesser amounts of DNA. Immediately differences were found between the two formulations. Using ratios from 20:1 to 5:1 (NP:pDNA) PCL/chitosan NPs revealed total efficiency in complexing pDNA, resulting in no free pDNA in the agarose gel (Fig. 5A, wells a to d). PCL NPs were not able to efficiently complex pDNA, which is possible to infer from the migration of free pDNA visible in wells f to i (Fig. 5A).

In order to assess the suitability of particles to efficiently deliver pDNA and to promote gene transfer, the particles were modified. Human serum albumin (HSA) has been studied for its capacity of increasing transfection efficacy of lipoplexes and polyethyleneimine complexes [30], and therefore HSA was previously adsorbed to particles at a ratio of 1:1 (NP:HSA) immediately before the complexation with pDNA. The binding capacity of the modified NPs was assessed as described for unmodified NPs. In this case it was decided to use only lower NP:pDNA ratios in order to reduce potential toxic particle concentrations in future cell uptake studies. The results were similar to what was observed before. PCL/chitosan NPs adsorbed with HSA presented total complexation activity, except for the lowest NP:pDNA ratio (0.6:1) and in contrast, PCL particles confirmed once more their unsuitability to form complexes with DNA (Fig. 5 B).

The successful NP:pDNA complexes presented here were very stable maintaining pDNA adsorbed as freshly formed complexes when incubated in different culture media for 1 h at 37 ºC (data not shown). Therefore, complexes prepared with PCL/chitosan NPs were subsequently used in subsequent studies. In contrast, PCL NPs, which showed their relative inferiority, were not used in the majority of the subsequent studies. So, considering these earliest comparative studies, it can be concluded that PCL NPs did not present suitable properties for DNA delivery system and inclusion of chitosan into these particles have increased its capacity to complex DNA. Therefore, additional methods were performed with the aim to evaluate if complexes are able to protect DNA from nucleases and if, effectively, complexes would facilitate the transfection.

The protection by complexation with PCL/chitosan particles was assessed by agarose gel electrophoresis. A NP:pDNA ratio of 2.5:1 was used for the complex preparation and protection of complexed DNA submitted to different concentrations of DNase I was evaluated. The highest concentrations of DNase I tested (lane a and c, Fig. 7 A) were able to degrade pDNA when complexed with the NPs. Parallel experiments using pre-inactivated DNase I showed no degradation of pDNA.

When using 1.25×10^{-2} U DNase I/µg DNA or lower concentrations the nanoparticulate system was able to efficiently protect the plasmid (lane g, i and k, Fig. 6 A).
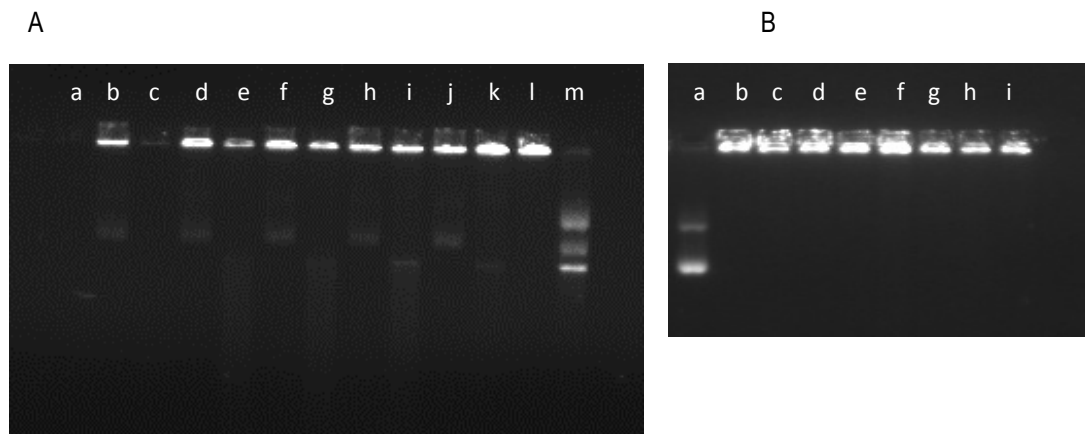
Figure 6: Electrophoresis in agarose gel illustrating the ability of pDNA protection by PCL/chitosan NPs. A) Protection revealed by a (w/w) ratio of 2.5:1 NPs:pDNA when submitted to different concentrations of DNase I: a) 0.25 U DNase I/µg DNA; b) $3.125X10^{-2}$ U DNase I/µg DNA; e) $1.25X10^{-2}$ U DNase I/µg DNA; g) $6.25X10^{-3}$ U DNase I/µg DNA; i) $1.25X10^{-3}$ U DNase I/µg DNA; k) $1.25X10^{-4}$ U DNase I/µg DNA; b, d, f, h, j, l are the respective controls with inactivated DNase I. Control is presented on lane m (free pDNA). B) Protection revealed when different ratios NPs:HSA:pDNA are submitted to a concentration of $1.25X10^{-2}$ U DNase I/µg DNA: b) 1.25:0.1:1 NPs:HSA:pDNA; d) 1.25:0.075:1 NPs:HSA:pDNA; f) 1.25:0.05:1 NPs:HSA:pDNA; h) 1.25:0.025:1 NPs:HSA:pDNA; c, e, g, i are the respective controls with inactivated DNase I. Control is presented on lane A (free pDNA).

Considering 1.25×10^{-2} U DNase I/µg DNA to be the highest concentration of DNase I that is not able to degrade DNA protected by PCL/chitosan NPs, a new protection assay was performed using a lower NPs:pDNA ratio and HSA adsorbed to the surface of the particles. This assay revealed the ability of chitosan to deliver pDNA into the cells and all NPs:HSA:pDNA ratios tested protected pDNA from degradation (Fig. 6B).

3.5. Enhanced uptake of PCL/chitosan NP by A549 cells

The particulate delivery systems should allow to concentrate and protect biomolecules against degradation during administration. This property is especially important when the administration is performed by one of the mucosal routes where physiological barriers restrict to the entrance of foreign species, like microorganisms, dust, allergens or particulate delivery systems. Moreover, particles potentially increase the cell internalization of the bioactive molecules, which is important for its function. In particular, protein antigens should be taken up by antigen presenting cells (APC's) to be processed and DNA vaccines to express the antigen. Therefore, our first studies to evaluate cell uptake and

intracellular localization of the NPs were performed using A549 cells and later visualized by confocal laser scanning microscopy (CLSM). The A549 cell line is a well-characterized human lung carcinoma cell line utilized for a variety of scientific studies, including respiratory immunotoxicity test, protein expression and apoptosis, etc. and was the cell line available in our laboratory at the time of these preliminary comparative experiments. Images of individual cells (Fig. 7A1 and 7A2) confirmed that PCL/chitosan particles were extensively internalized by A549 cells and were localized in the cytoplasm (Fig. 7A1). In contrast, confocal cell images of PCL particle uptake studies showed (Fig. 7A2) that PCL NPs were only marginally internalized by these cells. In case of PCL particles were stained with bovine serum albumin-FITC by adsorption, as we previously observed that PCL particles are able to adsorb on its surface diverse model vaccines, although with a lower loading capacity when compared with the PCL/chitosan particles. However, we found that PCL particles are not capable of transporting protein into cells. This fact was decisive to finally conclude that PCL NPs are of reduced interest as antigen delivery systems. Therefore, the quantitative analysis of particle internalization was made solely with PCL/chitosan particles.

Flow cytometry analysis of particle uptake was performed in order to achieve quantifiable results of the internalization of the PCL/chitosan NPs. NPs loaded with protein and NPs loaded with pDNA (Fig. 7B) were used. Initially, non-loaded NPs were tested at 4 different concentrations (1000, 500, 250 and 100 µg/mL). The uptake was successful in 98.5 ± 1.9 % and 95.6 ± 1.6 % of the cells for the 2 higher concentrations, respectively, and it decreased to 31.27 ± 5.3 % when concentration reached 250 µg/mL. At the same time, the cytotoxicity of the uptake was assessed with propidium iodide staining and it was observed that although the uptake of the 1000 and 500 µg/mL suspension had no statistical difference, the use of less NPs decreased cytotoxicity from 75.0 ± 4.7 % to 44.5 ± 8.8 %.

The same study was performed with protein adsorbed at the surface of the NPs, using a 1:1 ratio of NP:protein. The results for the formulations with 1000 and 500 µg/mL NPs presented an uptake of 92.8 ± 6.1 % and 95.9 ± 1.9 % of the cells, respectively. When the concentration was 250 µg/mL, the uptake decreased to 63.1 ± 28.3 %, an increase over the non-loaded NPs. The cytotoxicity results showed the same tendency as for non-loaded NPs. Therefore, the percentage of cell viability is directly related to particle uptake.

A1

A2

B

C
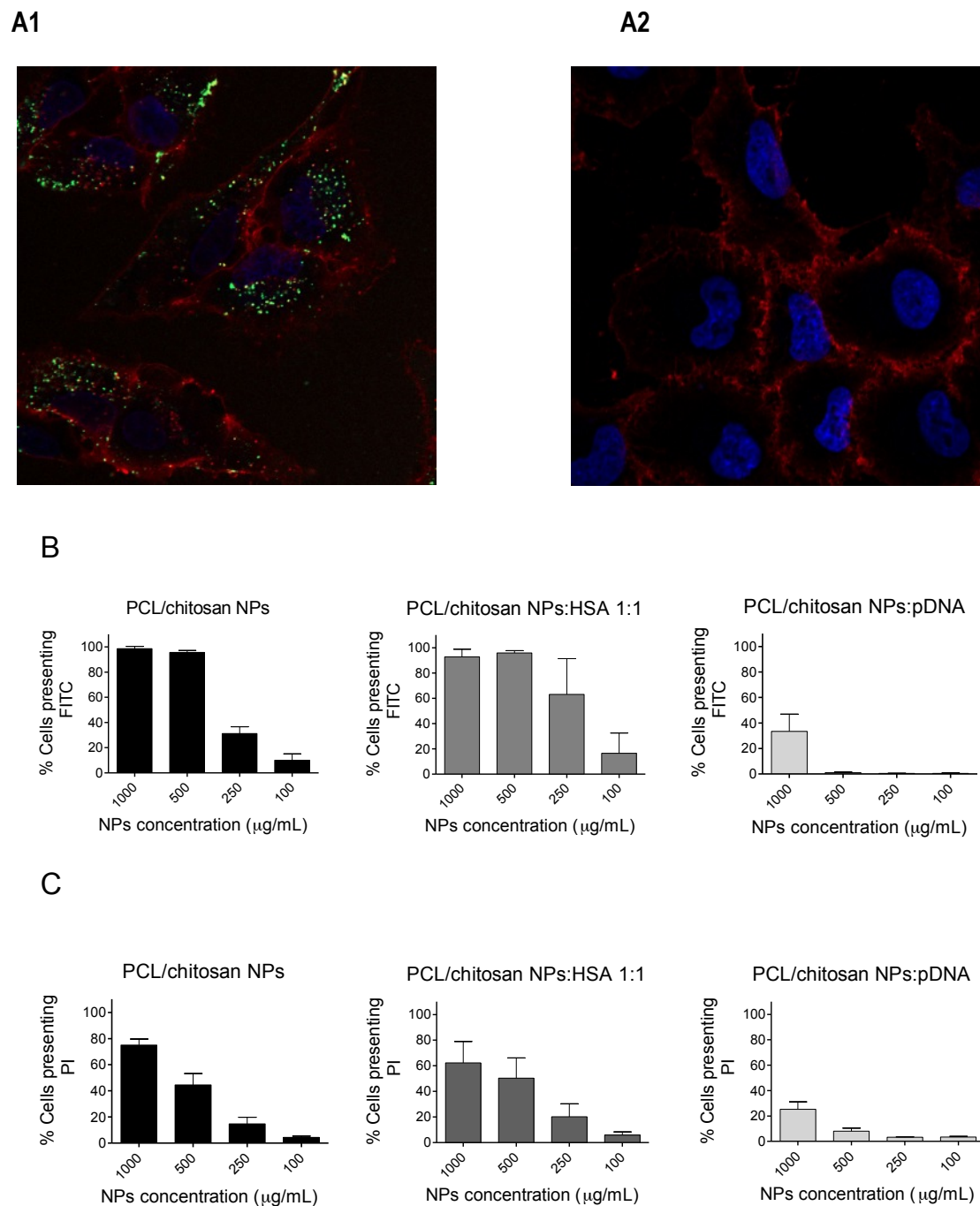
Figure 7: Uptake and cytotoxicity studies of NPs on A549 cells after 4 hours incubation. A) Cells were stained with Alexa Fluor 594 (blue fluorescence – nucleus) and with Hoechst 33342 (red fluorescence – plasmatic membrane). Images representing two different assays performed in duplicate. A1) Chitosan/PCL nanoparticles, produced with Chitosan covalently linked to FITC. A2) PCL nanoparticles adsorbed with BSA covalently linked to FITC. Flow cytometry analysis of the uptake (B) and cytotoxicity (C) on A549 cells after 4 hours incubation. For the uptake studies it was assessed the percentage of cells presenting FITC derived from chitosan labeling. For cytotoxicity studies it was assessed the percentage of cells presenting propidium iodide (PI). For each

formulation, 4 different NPs concentrations were tested (from 1000 to 100 µg/mL initial concentration). (Error bars represent standard deviation of the mean, n=3).

When PCL/chitosan NPs were complexed with pDNA, the uptake decreased significantly. The NP concentrations tested were the same as before, and the amount of pDNA was constant, generating NP:DNA ratios of 1:0.1, 1:0.2, 1:0.4 and 1:1. The results showed an uptake of 33.4 ± 13.6 % for the highest concentration added to cells (1000 µg/mL) and almost no uptake for the others. It is also important to note that in this experiment we also varied the concentration of DNA and curiously, in the other groups, we had less NPs but more DNA. Most probably, in the first group we also had some NPs, stained with fluorescein, not associated with DNA. So, we must not exclude that some particles that entered into cell were the above mentioned particles. Consequently, we can conclude that PCL/chitosan NPs have excellent characteristics to be taken up by cells and to transport model antigens into cells. However, same particles seem do not have the same ability when associated with DNA. We believed that this is because DNA confers a negative charge to particles limiting the interaction of the delivery system with the cell membrane and consequently, their internalization.

3.6. Modest improvement of transfection by association of DNA with particles

The results obtained with PCL NPs (complexes NP:DNA) in the transfection studies were disappointing (data not shown), with measurements similar to the ones obtained with naked DNA. These results were anticipated following the results obtained previously. Therefore, the results shown in this report correspond to transfection studies performed with the more promising complexes (PCL/chitosan NPs-pDNA) selected in previous studies.

The objective of the experiment was to study the influence of different NPs:pDNA ratios, the presence of HSA and its different concentrations in the complexes, and the presence of fetal bovine serum at a concentration of 10 % in Ham's F12 culture medium. The results illustrated in Figure 9 are representative of the best results obtained until now. As predictable, naked pDNA included as a negative control on the experiments did not produce any luminescence signal. The association of the NPs with DNA improved the transfection rates with the best results observed with NPs:pDNA ratios of 2.5:1 and 1.25:1 in serum-free cell medium. In order to improve these results, increasing amounts of human serum albumin were added prior to complex formation with pDNA. The results are shown in Figure 9.
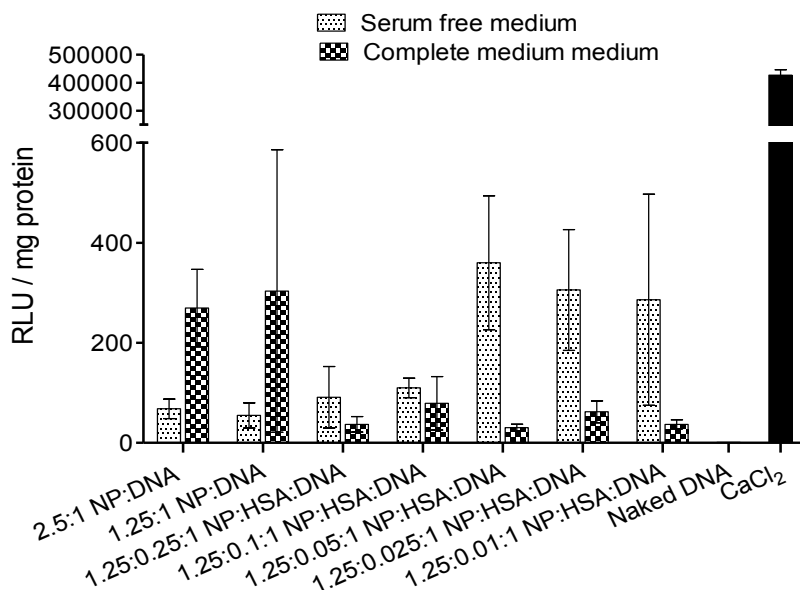
Figure 8: Transfection efficiency of PCL/chitosan NPs. After an exhausting study evaluating the ratio NPs:pDNA that led to better transfection results 2.5:1 and 1.25:1 where selected. In order to improve the results, HSA was adsorbed to the surface of the NPs at different concentrations, previously to the complexation with pDNA at the ratio 1.25:1 NPs:pDNA. The influence of the serum in the transfection media was also assessed. Results were compared with naked DNA and $CaCl_2$ (positive control). The results are representative of 4 different assays for NP:DNA and 2 different assays for NP:HSA:DNA . Transfection is presented in relative light units (RLU) / μg protein (Error bars represent standard error, n=3).

From the analysis of the results we concluded that the inclusion of the protein in complexes did lead to better results under serum free medium conditions.

Comparing the results with the positive control we can conclude that complexes, able to protect pDNA, allowed cell transfection, however, at rates lower than observed for the positive control. Therefore, further experiments are in progress to definitively evaluate the utility of the chitosan-PCL particles as a gene delivery vector.

4. Discussion

The differences observed in our transfection studies are partially in accordance with published data. When nanoparticle-DNA complexes are incubated with cells in a serum containing culture medium, transgene expression tends to be higher than under serum free conditions. On the other hand, nanoparticle-DNA complexes with HSA showed slightly better transfection results when serum free conditions were established.

In order to explore the causes that led to low transfection, viability assays with PCL/chitosan nanoparticle-DNA complexes were performed. When applying the same concentrations and conditions as for the transfection studies the results showed a percentage of cell survival of around 70 % (data not shown). Considering the 48 h of the transfection assay, including the 4 h incubation with the particles, this result was expected, and the observed cytotoxicity is not considered to be the cause for low transfection results.

As was reported for the uptake studies, lower zeta potential values may have caused low internalization rates of the complexes. In addition, the increasing size of the complexes compared to non-loaded NPs may play a role. In fact, the complexes, when suspended in F12 Ham's medium (in the presence or absence of serum), presented sizes of around 1 µm, a large size for the complex to be taken up extensively by endocytosis [31]. The complexes had a low NPs:DNA ratio, therefore the contribution of the negative charge of the DNA present at the nanoparticle surface was superior to the positive charges of chitosan, which lead to an overall negative zeta potential for the complexes. When suspended in F12 Ham's medium, complexes presented zeta potentials below –30 mV. The electrostatic interaction between the complexes and the cell membrane of target cells is not favorable under these conditions.

Uptake studies revealed the internalization of complexes containing luciferase plasmid and the successive expression of the reporter gene. Published data refer that the transfection efficiency achieved by DNA/chitosan complexes depend on several factors, such as the degree of deacetylation (DDA) and molecular weight (MW) of chitosan, pH of the medium, protein interactions, charge ratio of chitosan to DNA, cell type, nanoparticle size, interactions with cells, preparation techniques of chitosan/nucleic acid particles and routes of administration [20, 32]. Nevertheless, although there is a consensus on the multitude of factors, there is controversy on which affect the practical results. For instance when we consider the MW, Sato et al. [33] conclude that chitosan of a molecular weight of 10 KDa to 50 KDa is an excellent gene transfer reagent as compared to higher MW chitosan. Lavertu et al. [34] found a correlation between MW and DDA, and concluded that maximum transgene expression occurred at DDA:MW values that run along a diagonal from high DDA/low MW to low DDA/high MW.

The interaction with proteins can also have several interpretations as far as transfection efficiency is concerned. The presence of HSA in lipoplexes can be associated with the binding to nonspecific cell receptors, which mediate endocytosis, resulting in transfection enhancement by facilitating the escape of DNA from the endolysosomal pathway [35]. On the other hand, transfection efficiency can be decreased due to the interaction of the DNA complexes with serum proteins present in the culture medium [35, 36]. Due to this phenomenon, *in vitro* transfection studies are frequently performed under serum-free conditions, which is not the best model for results extrapolation and also cause the serum deprived cells to grow slower, diminishing transgene expression [32, 35]. Some promising results, however, have been published referring that chitosan can be used for transfection studies in the presence of serum since chitosan does not experience the inhibitory effects generated by the medium serum, and rather benefits from the increased cell metabolism [32, 33].

According to our studies, poly-ε-caprolactone (PCL) NPs are not a good gene vectors. The addition of a cationic polymer, such as chitosan to PCL appears to be a viable strategy; however, additional work has to be done in order to increase transfection rates.

To our knowledge, this is the first time that the preparation of PCL/chitosan NPs-pDNA complexes are described and evaluated as a gene delivery system. A study published by Jochen [37] describes the preparation of PCL NPs by an emulsion-diffusion-evaporation method using a blend of poly-(vinyl alcohol) and trimethyl chitosans with varying degrees of quaternization. The inclusion of the two stabilizers forced authors to adopt a more complex and time-consuming method in order to obtain particles. Particles obtained by these authors appeared to have size and zeta potential values similar to the ones detected in this study. The transfection results showed that the complexes or the conditions of the transfection assay needed to be improved. Complexes were superior to naked DNA, however, inferior to the transfection results obtained by the positive control and not comparable with our results since they were presented as fluorescence units.

5. Conclusions

PCL/chitosan NPs presented advantages over PCL NPs in terms of protein loading and pDNA complexation. These particles were shown to be stable in a freeze-dried formulation, suitable for antigen loading, antigen transport and delivery to epithelial cells *in vitro*. These new NPs may be considered as an antigen delivery system in terms of stability of the NPs and antigen adsorption efficiency, so work is scheduled in our laboratory aiming at *in vivo* evaluation of PCL/chitosan NPs as a vaccine (recombinant protein/antigen) adjuvant.

Although PCL/chitosan NPs-pDNA complexes were shown to be very stable and capable to protect pDNA from nucleases, more *in vitro* work has to be done before starting immunization studies using these NPs as DNA vaccine delivery systems.

References

1. Friede, M. and M.T. Aguado, *Need for new vaccine formulations and potential of particulate antigen and DNA delivery systems.* Adv Drug Deliv Rev, 2005. **57**(3): p. 325-31.

2. Jadhav, K.R., et al., *Nasal Drug Delivery System - Factors Affecting and Applications.* Current Drug Therapy, 2007. **2**: p. 27-38.

3. Neutra, M.R. and P.A. Kozlowski, *Mucosal vaccines: the promise and the challenge.* Nat Rev Immunol, 2006. **6**(2): p. 148-58.

4. Nguyen, D.N., et al., *Polymeric Materials for Gene Delivery and DNA Vaccination.* Adv Mater, 2008. **20**: p. 1-21.

5. Seder, R.A. and A.V. Hill, *Vaccines against intracellular infections requiring cellular immunity.* Nature, 2000. **406**(6797): p. 793-8.

6. He, Y. and L.D. Falo, *Induction of T cell immunity by cutaneous genetic immunization with recombinant lentivector.* Immunol Res, 2006. **36**(1-3): p. 101-17.

7. McCluskie, M.J. and H.L. Davis, *Mucosal immunization with DNA vaccines.* Microbes Infect, 1999. **1**(9): p. 685-98.

8. Starodubova, E.S., M.G. Isaguliants, and V.L. Karpov, *Regulation of Immunogen Processing: Signal Sequences and Their Application for the New Generation of DNA-Vaccines.* Acta Naturae, 2010. **2**(1): p. 53-60.

9. Mahapatro, A. and D.K. Singh, *Biodegradable nanoparticles are excellent vehicle for site directed in-vivo delivery of drugs and vaccines.* J Nanobiotechnology, 2011. **9**: p. 55.

10. Xiang, S.D., et al., *Delivery of DNA vaccines: an overview on the use of biodegradable polymeric and magnetic nanoparticles.* Wiley Interdiscip Rev Nanomed Nanobiotechnol, 2010. **2**(3): p. 205-18.

11. O'Hagan, D.T. and N.M. Valiante, *Recent advances in the discovery and delivery of vaccine adjuvants.* Nat Rev Drug Discov, 2003. **2**(9): p. 727-35.

12. Illum, L., *Chitosan and its use as a pharmaceutical excipient.* Pharm Res, 1998. **15**(9): p. 1326-31.

13. Baldrick, P., *The safety of chitosan as a pharmaceutical excipient.* Regul Toxicol Pharmacol, 2010. **56**(3): p. 290-9.

14. Lebre, F., et al., *Progress towards a needle-free hepatitis B vaccine.* Pharm Res, 2011. **28**(5): p. 986-1012.

15. Panos, I., N. Acosta, and A. Heras, *New drug delivery systems based on chitosan.* Curr Drug Discov Technol, 2008. **5**(4): p. 333-41.

16. van der Lubben, I.M., et al., *Chitosan for mucosal vaccination.* Adv Drug Deliv Rev, 2001. **52**(2): p. 139-44.

17. Gao, W., J.C. Lai, and S.W. Leung, *Functional enhancement of chitosan and nanoparticles in cell culture, tissue engineering, and pharmaceutical applications.* Front Physiol, 2012. **3**: p. 321.

18. Borges, O., et al., *Induction of lymphocytes activated marker CD69 following exposure to chitosan and alginate biopolymers.* Int J Pharm, 2007. **337**(1-2): p. 254-64.

19. Viola, J.R., et al., *Non-viral nanovectors for gene delivery: factors that govern successful therapeutics.* Expert Opin Drug Deliv, 2010. **7**(6): p. 721-35.

20. Mao, S., W. Sun, and T. Kissel, *Chitosan-based formulations for delivery of DNA and siRNA.* Adv Drug Deliv Rev, 2010. **62**(1): p. 12-27.

21. Singh, J., et al., *Diphtheria toxoid loaded poly-(epsilon-caprolactone) nanoparticles as mucosal vaccine delivery systems.* Methods, 2006. **38**(2): p. 96-105.

22. Gan, Q. and T. Wang, *Chitosan nanoparticle as protein delivery carrier--systematic examination of fabrication conditions for efficient loading and release.* Colloids Surf B Biointerfaces, 2007. **59**(1): p. 24-34.

23. Bilensoy, E., et al., *Intravesical cationic nanoparticles of chitosan and polycaprolactone for the delivery of Mitomycin C to bladder tumors.* Int J Pharm, 2009. **371**(1-2): p. 170-6.

24. Fessi, H., et al., *Process for the preparation of dispersible colloidal systems of a substance in the form of nanoparticles* 1992: US.

25. Huang, M., et al., *Uptake of FITC-chitosan nanoparticles by A549 cells.* Pharm Res, 2002. **19**(10): p. 1488-94.

26. Wright, C.S., *Structural comparison of the two distinct sugar binding sites in wheat germ agglutinin isolectin II.* J Mol Biol, 1984. **178**(1): p. 91-104.

27. Salgın, S., *Zeta Potentials and Isoelectric Points of Biomolecules: The Effects of Ion Types and Ionic Strengths.* International Journal of Electrochemical Science, 2012. **7**: p. 12404-12414.

28. Kosmulski, M., *Chemical properties of material surfaces.* Surfactant science series (vol. 102) Vol. VIII. 2001, New York: Marcel Dekker. 753.

29. Abdelwahed, W., et al., *Freeze-drying of nanoparticles: formulation, process and storage considerations.* Adv Drug Deliv Rev, 2006. **58**(15): p. 1688-713.

30. Simoes, S., et al., *Human serum albumin enhances DNA transfection by lipoplexes and confers resistance to inhibition by serum.* Biochim Biophys Acta, 2000. **1463**(2): p. 459-69.

31. Prabha, S., et al., *Size-dependency of nanoparticle-mediated gene transfection: studies with fractionated nanoparticles.* Int J Pharm, 2002. **244**(1-2): p. 105-15.

32. Nimesh, S., et al., *Enhanced gene delivery mediated by low molecular weight chitosan/DNA complexes: effect of pH and serum.* Mol Biotechnol, 2010. **46**(2): p. 182-96.

33. Sato, T., T. Ishii, and Y. Okahata, *In vitro gene delivery mediated by chitosan. effect of pH, serum, and molecular mass of chitosan on the transfection efficiency.* Biomaterials, 2001. **22**(15): p. 2075-80.

34. Lavertu, M., et al., *High efficiency gene transfer using chitosan/DNA nanoparticles with specific combinations of molecular weight and degree of deacetylation.* Biomaterials, 2006. **27**(27): p. 4815-24.

35. Faneca, H., S. Simoes, and M.C. Pedroso de Lima, *Association of albumin or protamine to lipoplexes: enhancement of transfection and resistance to serum.* J Gene Med, 2004. **6**(6): p. 681-92.

36. Ross, P.C. and S.W. Hui, *Lipoplex size is a major determinant of in vitro lipofection efficiency.* Gene Ther, 1999. **6**(4): p. 651-9.

37. Haas, J., et al., *Preparation and characterization of chitosan and trimethyl-chitosan-modified poly-(epsilon-caprolactone) nanoparticles as DNA carriers.* AAPS PharmSciTech, 2005. **6**(1): p. E22-30.

Chapter 3. Poly-ε-caprolactone/chitosan nanoparticles provide an adjuvant effect for recombinant HBsAg but not for the encoding plasmid DNA

Abstract

Poly- -caprolactone (PCL) based nanoparticles (NPs) are hydrophobic, which is a key characteristic for activating receptors of pathogen associated molecular patterns (PAMPs). The purpose of the present work was to investigate the adjuvant effect of PCL/chitosan NPs as an adjuvant for the recombinant hepatitis B antigen (HBsAg) and plasmid DNA (pDNA) encoding HBsAg (pRC/CMV-HBs). In both cases, antigen was adsorbed onto pre-formed NPs. Results of immunization studies in C57BL/6 mice revealed HBsAg adsorbed NPs formulation was able to generate strong specific anti-HBsAg IgG titers, mainly of the IgG1 isotype. Interestingly, this formulation also induced antigen-specific IL-17 secretion by spleen cells. In contrast, immunization with pRC/CMV-HBs loaded NPs generated merely a weak serum antibody response. Efficient adsorption of pDNA onto NPs resulted in negative zeta potential values, which may explain the low *in vitro* and *in vivo* transfection. Results obtained showed PCL/chitosan NPs are a good adjuvant for HBsAg when administered by subcutaneous (SC) route but apparently the same adjuvant effect is not obtained for pDNA vaccines.

Keywords: Adjuvant, nanoparticles, poly- -caprolactone, chitosan, vaccines, hepatitis B, recombinant protein, plasmid DNA.

1. Introduction

Vaccine adjuvants are fundamental to boost the immune response against highly purified recombinant antigens, which lack immunogenicity. While the first vaccine adjuvants such alum were based on empirical discovery, adjuvants are developed today based on increasing knowledge of the (innate) immune system applying a more rational design [1].

In the last decade, polymeric nanoparticles (NPs) prepared with biodegradable polymers inspired extensive research in the vaccine field. These vaccine carriers interact with proteins, peptides, pDNA and low molecular weight compounds through electrostatic forces, hydrogen bounds, hydrophobic interactions and van-der-Waal forces. Besides their loading capacity and delivery properties, these systems are emerging as immunostimulant adjuvants capable to activate and enhance immune responses [2, 3]. Their cellular interaction with antigen presenting cells (APCs) is attributed to their particulate nature [4]. Many receptors of pathogen associated molecular patterns (PAMPs) or damage associated molecular patterns (DAMPs) have evolved to recognize and react to hydrophobic portions of molecules [5]. Consequently, several studies have revealed that hydrophobicity of particulate adjuvants and antigens is a major factor for initiating immune responses [6]. However, various reports on the rational design of "pathogen-mimicking" NPs for vaccine delivery suggest that not only hydrophobicity is responsible for activating APCs, but a variety of factors including surface chemistry and composition may be responsible to increase immunomodulation and thus lead to protection against a wide range of pathogens. In this view, amphiphilic particles may represent the best approach as "pathogen-mimicking" entities for vaccine delivery [7-9].

Hepatitis B surface antigen (HBsAg) is a recombinant protein that self-assembles into 22 nm virus-like particles (VLPs) of some intrinsic immunogenic ability, but require the concomitant use of immunostimulant molecules for an efficient immunization [10]. Over the last years, a new approach to HBV vaccination has been discussed and involves the use of a plasmid DNA based vaccine encoding for HBsAg [11-13]. The use of pDNA vaccines is known to activate both humoral and cellular arms of an immune response, which could be advantageous in the generation of a therapeutic immune response [11]. Nevertheless, naked pDNA is not efficient to generate this response and a carrier system that confers protection against enzymatic degradation and hydrolysis, increase cellular uptake, endosomal escape and nucleic acid release, is necessary to assure antigen delivery, expression and presentation [14].

The basis of our work was to take advantage of the individual characteristics of 2 polymers to create a vaccine delivery system with immunostimulatory adjuvant properties. Chitosan is a cationic, biocompatible and biodegradable biopolymer, which is derived from chitin by deacetylation. Chitosan

has been described to have intrinsic, direct immune-modulating activities and chitosan-based formulations were reported to enhance antigen uptake and presentation [15]. Moreover, chitosan has been extensively studied as a vehicle for gene delivery [16-18]. PCL is a synthetic aliphatic polyester and highly biocompatible polymer with FDA approval for some biomedical applications. It is hydrophobic and its degradation under physiological conditions occurs slowly and with minimal toxicity [19-23]. PCL is an extremely versatile polymer, with ability to blend with other polymers, altering some of its mechanical, physical or ionic properties [23]. The blend of PCL and chitosan has been suggested to increase the amphiphilic character of the material [23]. As previously described, a more amphiphilic particle that possesses not only hydrophobic moieties resembling pathogens but also hydrophilic groups will be able to potentiate vaccine delivery. Moreover, we have previously shown that non-modified PCL NPs were not able to complex pDNA and the presence of chitosan was fundamental for pDNA delivery using PCL [24]. Considering protein based vaccines, PCL particles modified with chitosan and its derivatives have been evaluated, and a few reports are found in scientific literature. One study was published by Florindo and co-workers [25, 26], who tested PCL nano- and microspheres modified with glycol chitosan and different molecular weight chitosans as an adjuvant for *Streptococcus equi* antigens (enzymatic extract). In a second study, influenza A virus H1N1 hemagglutinin antigen (HA) was encapsulated into PCL nanoparticles modified with chitosan [27]. Both reports confirmed superior performance of chitosan-modified PCL particles in comparison to the non-modified PCL carrier or free antigens.

Our approach consists in the use of a different and easier methodology for NPs preparation (nanoprecipitation instead of emulsion diffusion evaporation), followed by the antigen loading under aqueous conditions, with the intention to present antigen epitopes at the NPs surface, possibly increasing APC recognition and immune response priming, in the absence of further adjuvants.

We tested poly- -caprolactone (PCL)/chitosan NPs as vaccine adjuvant for different hepatitis B virus (HBV) immunization strategies based on a recombinant protein antigen and a plasmid DNA (pDNA) encoding antigen. As far as we know, this is the first time PCL/chitosan NPs were tested *in vivo* for pDNA vaccination, and the first report describing immune responses generated by the administration of hepatitis B antigens (or DNA pRC/CMV-HBs) adsorbed onto PCL/chitosan NPs. With this study we intended to reveal the advantages PCL/chitosan NPs can offer to HBV vaccination strategies. Moreover, these first insights may constitute the basis for future new approaches regarding other immunization routes (i.e. non parenteral).

2. Materials and Methods

2.1. Materials

Chitosan (ChitoClear™ - degree of deacetylation 95 %; viscosity 8 cP (1 % solution)) was purchased from Primex Bio-Chemicals AS (Avaldsnes, Norway). PCL (average MW 14000), D-(+)-trehalose dehydrate (≥ 98.5 %), F12 Ham nutrient mixture, D-luciferin sodium salt, adenosine triphosphate (ATP) and o-phenylenediamine (OPD) were obtained from Sigma-Aldrich Corporation (St. Louis, MO, USA). Fetal bovine serum (FBS), PenStrep from Gibco® and Pierce™ BCA protein assay kit were purchased from Thermo Fisher Scientific Inc. (Waltham, MA, USA). Formvar coated nickel and copper grids (300 mesh) were obtained from TAAB Laboratories Equipment Ltd. (Berkshire, UK). Spectra®Por cellulose ester dialysis membrane (MWCO 300.000) was purchased from Spectrum Europe B.V. (Breda, NL). Cell strainers with 70 µm pores were obtained from DB Biosciences (Bedford, MA, USA). pDNA encoding luciferase (pCMVluc) was amplified in *E. coli* bacteria and further purified using QIAGEN Plasmid Giga Kit (QIAGEN, Hiden, Germany). The purified pDNA was dissolved in MilliQ water and concentration/purity determined by UV spectrophotometry by measuring the absorbance at 260/280 nm. pDNA encoding HBsAg (pRC/CMV-HBs) and HBsAg, subtype adw with approximately 25 kDa, were acquired from Aldevron (Fargo, ND, USA). Murine IL-4, IFN- and IL-17 standard ABTS ELISA development kits were obtained from PeproTech (Rocky Hill, NJ, USA). IgG horseradish peroxidase (HRP) and IgA HRP were obtained from Bethyl Laboratories (Montgomery, TX, USA). IgG2c HRP was acquired from GeneTex (Irvine, CA, USA). IgG1 HRP was obtained from Rockland Immunochemicals Inc. (Limerick, PA, USA). IgE HRP was obtained from Nordic Immunological Laboratories (Susteren, NL). All other chemicals and reagents were of analytical grade.

2.2. Methods

2.2.1. Nanoparticle preparation

Chitosan purification and PCL/chitosan NPs preparation were performed as previously described by us, with minor modifications concerning the NPs isolation steps [24]. After particle preparation and maturation, NPs suspended in the original medium were isolated and concentrated by centrifugation at 16000 x g, for 75 min at 4 °C with a 200 L glycerol bed. Glycerol was eliminated by dialysis of the suspension against water for 48 h. The resulting suspension was either added to a trehalose solution and freeze dried (FreezeZone 6, Labconco Corporation, Kansas City, MO, USA), or further centrifuged in 1.5 mL tubes to concentrate the NPs for *in vivo* studies. When freeze-dried the resulting powder contained 5.71 % of NPs. Size and zeta potential of NPs were measured with a Delsa™ Nano C (Beckman Coulter, Madrid, ES). NPs stored in paraformaldehyde 4 % were observed by transmission

electron microscopy. Samples were placed in a microscopy grid and observed under a FEI-Tecnai G2 Spirit Biotwin, a 20-120 kV transmission electron microscope (TEM) (FEI Company, Hillsboro, OR, USA).

2.2.2. HBsAg and adsorption to NPs

In order to prepare the formulations for the vaccination studies, PCL/chitosan NPs were incubated with HBsAg recombinant protein for 30 min under low shear stress conditions. Final formulations contained 4035 g/mL NPs and 15 g/mL HBsAg, or 26900 g/mL NPs and 667 g/mL HBsAg. The amount of protein adsorbed was calculated by the difference between the total protein added and the protein that remained in solution (after centrifugation), quantified by Pierce^{TM} BCA protein assay according to manufacturer's instructions. Characterization of obtained NPs was performed as described above.

2.2.3. pRC/CMV-HBs adsorption to NPs

DNA formulations were obtained by simple incubation of the pDNA solution with HBsAg loaded or unloaded NPs, for 30 min under low shear stress conditions. The resulting formulations herein referred to as NPs-HBsAg/pDNA and NPs-pDNA complexes, presented the following composition: (1) 4035 g/mL NPs, 15 g/mL HBsAg and 200 g/mL pRC/CMV-HBs; (2) 4035 g/mL NPs and 200 g/mL pRC/CMV-HBs. Characterization of obtained NPs was performed as described above.

2.2.4. Immunization studies

Female C57BL/6 mice (8-week old) were purchased from Charles River (Saint-Germain-Nuelles, FR). Animals were provided with food and water ad libitum and all experiments were in accordance with FELASA guidelines and approved by the Animal Care Ethical Committee of the Center for Neuroscience and Cell Biology of Coimbra. Groups of 5 mice were used to test different subcutaneous (SC) vaccine formulations, whose composition and immunization schedules are resumed in table 1. Immunizations were performed under slight isoflurane anesthesia, by injecting 100 L of the formulations subcutaneously.

Table 1: Hepatitis B vaccine formulations: composition and immunization schedule.

Group number	Formulation name	PCL/chitosan NPs (µg/animal)	pRC/CMV-HBs (µg/animal)	HBsAg (µg/animal)	Immunization schedule (SC) (day)	Euthanasia (day)
I	HBsAg	-	-	1.5	0, 14	42
II	NPs-HBsAg 1.5	403.5	-	1.5	0, 14	42
III	NPs-HBsAg/pDNA complexes	403.5	20	1.5	0, 14 and 42 (IN)*	64
IV	NPs-pDNA complexes	403.5	20	-	0, 14 and 42 (IN)*	64

* Mice from group III and IV received an intranasal (IN) vaccine boost at day 42, containing 403.5 g NPs and 10 g HBsAg (NPs-HBsAg 10 formulation). Immunizations were performed under isoflurane anesthesia by depositing 7.5 L of the formulation in each mouse nostril. Each drop was only deposited after the previous one had been inhaled/dried out.

2.2.4.1. Biological sample collection

Blood was collected by submandibular lancet method at day 42 for groups I and II, and at day 42 and 64 for groups III and IV under isoflurane anesthesia. After coagulation, blood was centrifuged at 4500 x g for 10 min for serum collection. On the sacrifice day, after blood collection anesthetized mice were euthanized by cervical dislocation and their spleens were aseptically removed. Vaginal washes were collected at day 41 and 42 for group I and II, and at day 63 and 64 for group III and IV. Vaginal washes were collected by instilling 100 µL of sterile PBS onto the vaginal cavity and flush the lavage fluid a few times before collection. Samples supplemented with phenylmethylsulfonyl fluoride and sodium azide (1mM and 0.01 %, respectively), were centrifuged at 3300 x g during 10 min, supernatants collected and stored at 80 °C until further analysis.

2.2.4.2. Determination of serum and mucosal immunoglobulins

For the determination of serum immunoglobulins, HBsAg coated high-binding 96-well plates (Nunc MaxiSorp®, Thermo Fisher Scientific Inc., Waltham, MA, USA) were obtained by overnight incubation at 4 °C, of 0.1 µg/well HBsAg in 50 mM sodium carbonate/bicarbonate, pH 9.6. Plates were washed 5 times with PBS-T and blocked for 1 h at 37 °C. After washing, serial dilutions of serum, starting at 1:64 (IgG and IgG1), at 1:32 (IgA) and 1:16 (IgG2c and IgE), were applied and incubated for 2 h at 37 °C. Following extensive washing, specific antibodies were detected by HRP conjugated goat anti-mouse IgG, IgG1, IgG2c, IgE or IgA respectively, for 30 min at 37 °C. Next, OPD solution (5 mg OPD to 10 mL citrate buffer and 10 µL H_2O_2) was incubated for 10 min at room temperature. Reaction was stopped with 1 M H_2SO_4 and absorbance was determined at 492 nm with a microplate reader. For mucosal

samples, HBsAg-specific and total IgA were measured in concentrated vaginal samples by a similar protocol with little modifications. A second plate was coated with IgA (10 µg/mL) for the total IgA determination, and mouse IgA serum reference was used to obtain calibration curves. Results for serum IgG, IgG1 and IgG2c are presented as the end-point titer, which represents the antilog of the last log 2 dilution, for which the absorbance were at least two-fold higher than the value of the naive sample equally diluted. Results for serum IgA are presented in absorbance when the measurement was at least two-fold higher than the value of the naïve sample equally diluted. Concentrations of total and anti-HBsAg mucosal IgA were extrapolated from absorbance values, using the calibration curves. Vaginal IgA results are presented as the ratio between specific anti-HBsAg IgA and total IgA for each mouse. Only mice whose IgA ratio was two-fold higher than naïve mice ratio average were considered as responders.

2.2.4.3. Cytokine production

Individual mice spleen cells suspensions were prepared as described in [28] without erythrocytes lysis. Spleen cell suspensions (0.25×10^6 cells/well) were platted in a 96-well culture plates, for incubation with and without stimulation of concanavalin A (con A) (1.25 g/well) and HBsAg (1 g/mL). Duplicates of each condition were incubated at 37 ºC with 96 % relative humidity (RH) in the presence of 5 % CO_2, for 48 h and 72 h. After 48 h or 72 h, plates were centrifuged and the clear supernatants stored at –80 ºC until analysis of IL-4 or IFN- and IL-17, respectively. Cytokines were measured by ELISA technique according to ELISA kit manufacturer's instructions.

2.2.5. *In vitro* transfection studies

A549 cells were acquired from the American Type Culture Collection (ATCC) (Barcelona, ES) and were cultured and plated as we previously described for transfection studies [24]. Complexes containing pDNA encoding luciferase (pCMVluc) were prepared as NPs-pDNA(pRC/CMV-HBs) complexes. 3 ratios NPs:pDNA were used: 10:1, 5:1 and 1:1 (w/w) and plated so that 1 µg of pCMVluc was present per well. During the 4 h transfection, different media were used: F12 medium with 10 % serum pH 5.5, F12 medium with 10 % serum pH 6.5, F12 medium with 10 % serum pH 8 and F12 serum free medium pH 8. Free pCMVluc was used as a negative control and calcium phosphate/pCMVluc precipitate was used as positive control. After 4 h incubation, formulations were removed and replaced with complete medium pH 8 for another 48 h incubation period. To determine luciferase activity, cells were washed with PBS and 100 L of lysis buffer (1 mM DTT, 1 mM EDTA, 25 mM Tris-phosphate pH 7.8, 8 mM $MgCl_2$, 15 % glycerol, 1 % (v/v) Triton X-100) was added to each well. The level of gene expression (luciferase) in the

lysates was evaluated by measuring relative light units (RLU) in a luminometer (Synergy HT, multimode microplate reader, BioTek Instruments, Inc., Winooski, VT, USA), according to standard protocols and normalized against total protein content, measured with BCA protein assay kit.

2.2.6. pDNA complex stability in culture medium

Complexes used for transfection studies were characterized by assessing their sizes and zeta potential as previously described, in water as well as suspended in serum-free cell culture medium pH=8 (transfection conditions). Agarose gel retention assay was performed to examine the adsorption of pDNA on NP surface immediately after preparation, and after incubation for 2 h and 4 h in cell culture medium, at 37 ºC, reproducing transfection conditions.

2.2.7. Statistical analysis

Results were expressed as mean ± standard error of the mean (SEM). Data were analyzed with GraphPad Prism v 5.03 (GraphPad Software Inc., La Jolla, CA, USA) by ANOVA, followed by a Tukey´s post-test for multiple comparisons test. A value of $p < 0.05$ was considered statistically significant.

3. Results and Discussion

In this work, PCL/chitosan NPs were tested as a vaccine adjuvant delivery system for HBsAg, a recombinant protein, and for pDNA encoding HBsAg (pRC/CMV-HBs). Adsorption is an advantageous process for antigen loading on polymeric carriers, as opposed to encapsulation, which is frequently performed under harsh conditions (i.e., use of organic solvents, high shear rates). Initial characterization revealed that unloaded PCL/chitosan NPs have a round shape, a size of approximately 200 nm and a positive zeta potential (> + 20 mV) (Fig. 1A). This positive zeta potential gives indication that some chitosan is present at the NPs surface contributing to the overall positive charge, as without chitosan, simple PCL NPs present neutral or slightly negative zeta potential. In fact, this observation was also described by other studies [25, 27].

A) PCL/chitosan NPs

Size (nm) [b]	PI [c]	Zeta (mV) [d]
255.1 ± 1.8	0.15 ± 0.01	+23.0 ± 0,2

B) PCL/chitosan NPs-HBsAg

w/w [a]	Size (nm) [b]	PI [c]	Zeta (mV) [d]	LE (%) [e]
403.5:10	191.6 ± 2.2	0.12 ± 0.01	-30.4 ± 1.2	>96
403.5:1.5	201.7 ± 5.2	0.18 ± 0.01	+ 18.6 ± 2.3	>96

C) PCL/chitosan NPs-pDNA(pRC/CMV-HBs)

w/w [a]	Size (nm) [b]	PI [c]	Zeta (mV) [d]
403.5:20	203.6 ± 3.1	0.16 ±0.01	-36.2 ± 0.6
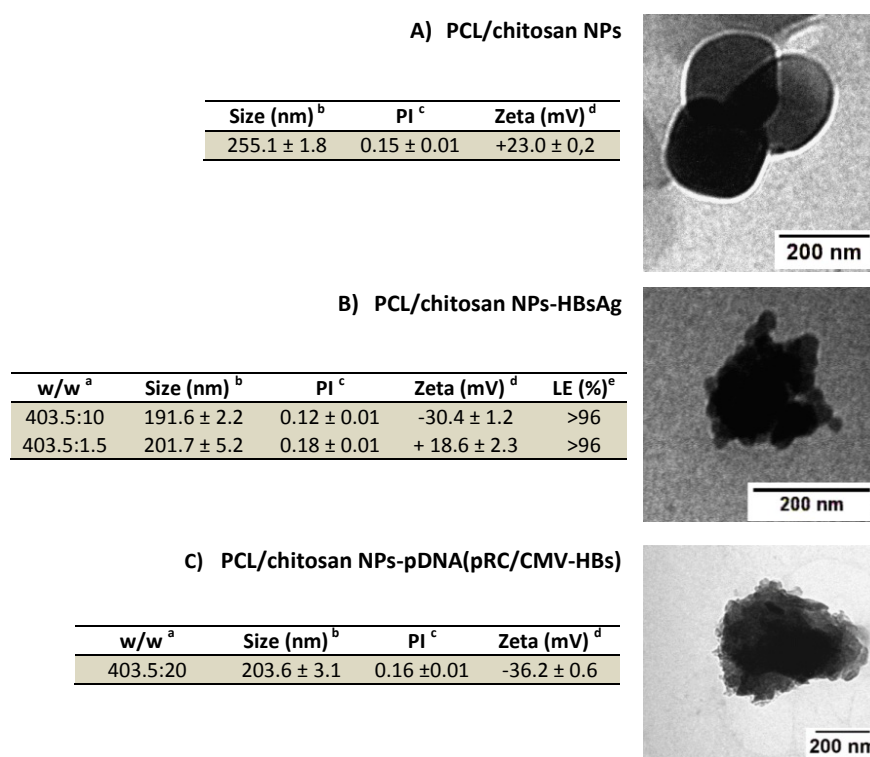
[a] Ratio NPs/antigen; [b] Formulation average size; [c] Polydispersity index; [d] Zeta Potential; [e] Loading Efficacy

Figure 1: Characterization of the PCL/chitosan NPs and formulations used in vaccination studies. (A) PCL/chitosan NPs; (B) PCL/chitosan NPs-HBsAg; and (C) PCL/chitosan NPs-pDNA(pRC/CMV-HBs) complexes. TEM images on the right side of the table are representative of the respective system (A, B or C).

In order to use the same amount of NPs in all immunization studies, and knowing the nasal vaccine would need a superior antigen dose, different amounts of HBsAg were adsorbed at the NPs surface.

When using a lower NPs:HBsAg (w/w) ratio (403.5:10), zeta potential appeared negative (- 30.36 mV). However, increased ratios (403.5:1.5) caused a positive surface charge as for unloaded NPs (+ 18.55 mV). The TEM image of the HBsAg loaded NPs (Fig. 1B) shows 22 nm VLPs adsorbed on PCL/chitosan NPs to a great extent. In both situations high loading efficacies (superior to 96 %), were achieved. PCL/chitosan NPs complexed with pRC/CMV-HBs complexes also presented a negative zeta potential of -36.18 ± 0.55 mV (Fig. 1C). pDNA (pRC/CMV-HBs) is a negative molecule containing phosphate groups, which are expected to interact electrostatically with the positive groups of chitosan. In fact, this interaction is the origin of pDNA condensation, caused by the neutralization of its negative phosphate groups [29]. This observation is similar to what was described by Haas et al. [30], who prepared pDNA complexes with chitosan and trimethyl chitosan coated PCL NPs and found that NPs surface was saturated with pDNA chains and the phosphate groups determined the measured surface charge.

3.1. SC vaccination of C57BL/6 mice demonstrates capacity of PCL/chitosan NPs to increase immune responses

As stated before, the recombinant HBsAg self-assembles into VLPs and generates antibody titers in immunized mice on administration by SC route due to its intrinsic immunogenicity [31, 32]. Nonetheless, for efficient vaccination, commercially available vaccines include aluminum hydroxide or alum as adjuvant. Despite their efficacy, aluminum salts are known to induce IgE antibodies and are associated to the occurrence of granulomas [1]. The use of PCL/chitosan NPs as HBsAg delivery system is intended to potentiate anti-HBsAg immune response as an alternative to aluminum salts. To the best knowledge of the authors, this is the first report on the validation of PCL/chitosan NPs as adjuvant for HBsAg. Animals from group I were immunized with free HBsAg and as expected generated a specific antibody immune response illustrated by titers shown in Figure 2. Hitherto, mice immunized with the NPs-HBsAg 1.5 formulation (group II) revealed approximately 40-fold higher specific IgG titers than mice immunized with free HBsAg. A previous report described intramuscular immunizations (IM) using chitosan coated PCL NPs encapsulating influenza antigen [27]. The application of those NPs resulted in significantly higher IgG antibodies than the soluble antigen, suggesting the particles had an intrinsic immunostimulatory effect by the IM route [27]. Also, chitosan coated PCL microspheres to which *Streptococcus equi* antigens were adsorbed were found to generate a higher IgG response than free antigens when applied subcutaneously.

The group III was planned to test the hypothesis of synergism between pDNA (pRC/CMV-HBs) and recombinant protein (HBsAg), both associated with NPs. Comparing group II and III, both revealed high

titers, however, no statistical differences between the two groups were detected. The presence of pRC/CMV-HBs in the formulation did not contribute to higher IgG titers. With regard to group IV, 1 animal presented detectable anti-HBsAg IgG titers. Most likely, the 4 non-responders were not able to efficiently process the DNA plasmid encoding the antigen, which prevented the staging of an immune response against the HBsAg. A possible control group with free pRC/CMV-HBs was not included as literature extensively describes naked pDNA as unable to generate biological effects [14].

Group number	NPs (µg/animal)	pRC/CMV-HBs) (µg/animal)	HBsAg (µg/animal)
I	-	-	1.5
II	403.5	-	1.5
III	403.5	20	1.5
IV	403.5	20	-
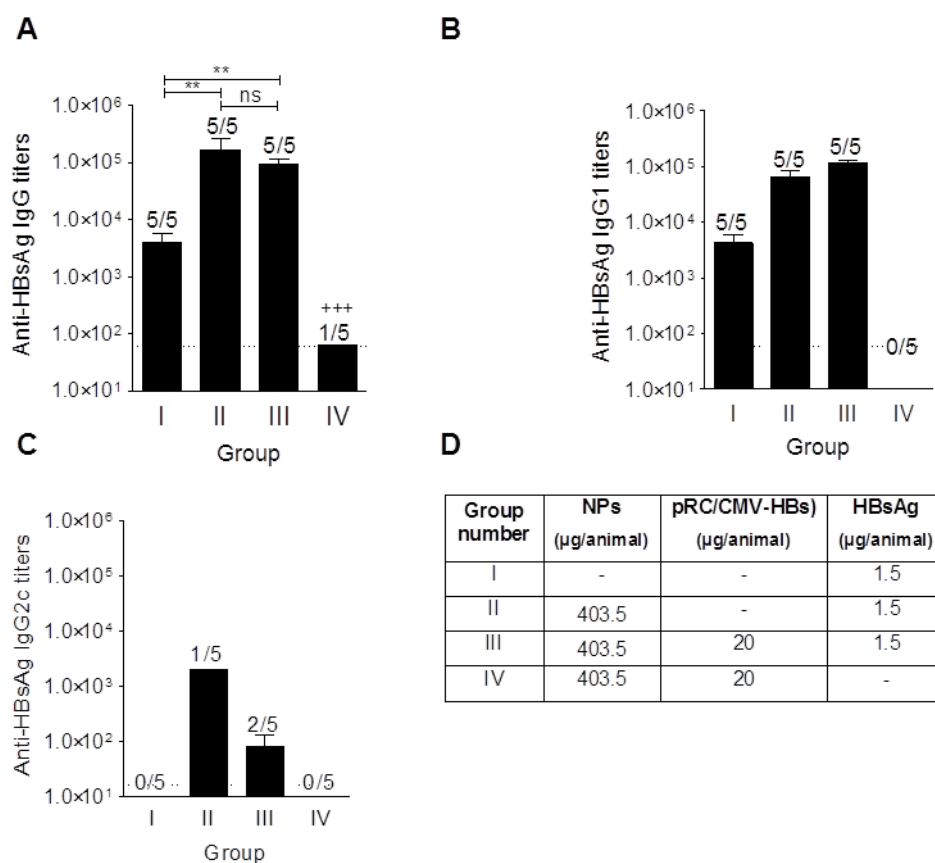
Figure 2: Immune response of SC immunized mice. Serum anti-HBsAg IgG (A), IgG1 (B), IgG2c (C) titers of mice of group I, II, III and IV (formulation composition described in table D), immunized on days 0 and 14. Blood was collected on day 42. Antibody titers were determined by ELISA as described in 'Materials and methods'. The end-point titer presented in the results represents the antilog of the last log 2 dilution for which the absorbance were at least two-fold higher than the value of the naive sample equally diluted. Dotted line represents the detection limit for each assay. Numbers above bars represent the number of mice in which antibody levels were detected. Data (mean ± SEM) represents groups of 5 mice each. **$p \leq 0.01$ indicates values that differ significantly from each other, ns indicates non-statistical differences and +++ $p \leq 0.001$ indicates a value that differs from all the other groups.

The evaluation of specific IgG subtypes in serum demonstrated IgG1 predominance, with titers comparable to specific IgG titers for each group. In fact, no major differences concerning the IgG1/IgG2c ratio was observed for either NPs-HBsAg 1.5 formulation or NPs-HBsAg/pDNA complexes. The only difference to be pointed out is the fact that with free HBsAg, no mice presented IgG2c (group I), while with the NPs based formulation groups at least 1 mouse/group was shown to produce IgG2c. Comparing these results to the literature some hypothesis can be drawn. In one study, *Streptococcus equi* proteins adsorbed on chitosan coated PCL microspheres administered by the SC route increased the IgG1/IgG2a humoral immune response balance [25]. Nevertheless, besides the different antigen and particle preparation method, this NPs-based vaccine formulation had sizes around 2 m, which may have influenced the immune response generated. In another study, PCL NPs encapsulating HA and coated with chitosan (125 nm), generated a balanced IgG1/IgG2 immune response only on intranasal (IN) administration. In fact, the same formulation administered through IM route was not able to induce detectable IgG2a titers in all BALB/c mice even after 3 immunizations [27]. Therefore, we can conclude the administration route may also have influence on the quality of the immune response generated by a given vaccine delivery system. As a consequence, it may be proposed that the properties of such systems need to be carefully adapted to their site of administration.

In contrast to aluminum salts, new and safer adjuvants, ideally, should not activate IgE production as this may induce anaphylactic reactions [33]. We therefore tested whether PCL/chitosan NPs would induce IgE production in immunized mice. Until day 42 post vaccination, none of the formulations induced detectable IgE titers in mice sera (data not shown).

With the objective to further evaluate the influence of the administration route on the generation of the immune response, group III and IV received an additional boost with NPs-HBsAg 10 formulation (table 1). The amount of antigen required to prime a mucosal immune response is generally higher than for parenteral vaccination, as molecules need to overcome the mucus barrier to activate immune system cells [34]. Therefore, taking into consideration that a 403.5 g/dose of NPs resulted in an adjuvant effect by the SC route we tested the same amount of NPs, adsorbing 10 g of HBsAg at their surface (NPs:HBsAg 403.5:10). Generally, mucosal immunization requires boosts in order to result in efficient immune responses. In our work, successive to the initial SC priming of the immune system, a single IN immunization was expected to induce mucosal antibody titers. Results 3 weeks after the IN boost showed anti-HBsAg IgG titers were not different from those obtained at day 42 (data not shown). Gupta and co-workers achieved higher serum HA-specific IgG titers with a single IN vaccination than the ones achieved with intramuscular (IM) vaccination [27]. Their particulate delivery system comprised the recombinant HA antigen from influenza virus encapsulated into chitosan coated PCL NPs and not

adsorbed on the surface. Therefore, positive amino groups of chitosan were available to interact with mucus and cells. In our work, HBsAg was adsorbed at the NPs surface decreasing the zeta potential to strongly negative values (- 30.36 mV), indicating the blocking of chitosan cationic amino groups available for cell interaction. However, in another study, *Streptococcus equi* antigens were adsorbed at the surface of PCL NPs modified with glycol chitosan, or unmodified. The glycol chitosan/PCL NPs formulation presented positive charges (+ 5.4 mV), while PCL NPs formulation had a negative surface charge (- 32.7 mV), and both formulations induced similar IgG titers after a single IN immunization [26]. Nonetheless, the enzymatic extract of *S. equi* antigens contained bacterial components likely to have adjuvant activity, and therefore might have increased the formulation's immunogenicity.
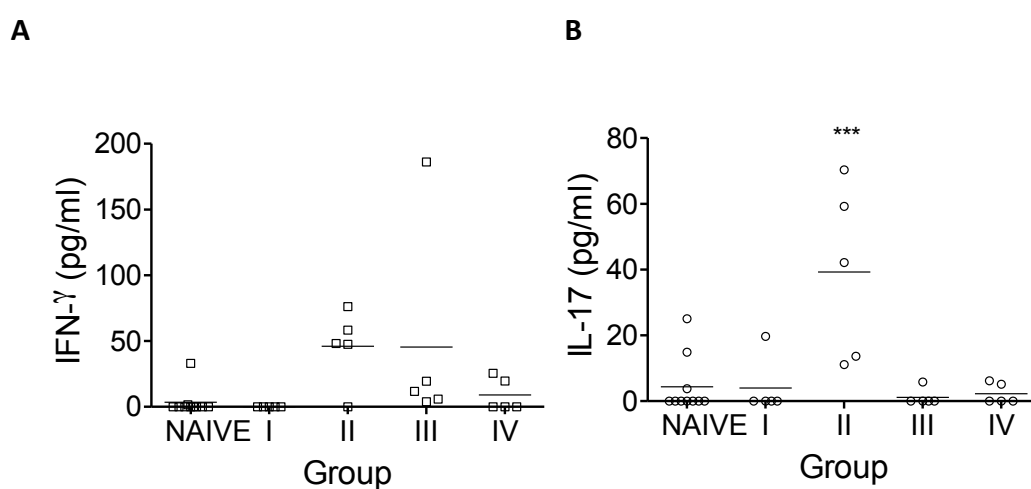
Figure 3: IFN- and IL-17 cytokine production. Spleen cells (0.25×10^6 cells/ well) from both immunized and naïve C57BL/6 mice were stimulated with 1 g HBsAg as described in 'Materials and methods'. Mice from group I and II were immunized SC on day 0 and day 14 and spleens collected at day 42. Mice from group III and IV were SC immunized at day 0 and day 14, boosted at day 42 with a single IN dose and spleens collected at day 64. Supernatants were collected 72 h after incubation and tested for IFN- (A) and IL-17 (B) titers. Results are shown as mouse cytokine concentrations minus basal concentration. Groups contain 5 mice, except for naïve group which comprises 10 mice. ***$p \leq 0.001$ indicates values that differ significantly from naive group.

Spleen cells from immunized mice were stimulated *in vitro* with the HBsAg. Main results of cytokine production are shown in Figure 3. Concerning IL-4 titers, the results were not included in the figure since the re-stimulation with HBsAg did not result in IL-4 production. Results from group I and naïve animals showed no increase over basal IFN- titers (Fig. 3A). This is in agreement with published data reporting that free HBsAg or HBsAg adjuvanted with aluminum salts do not induce the production of IFN- [12]. The groups containing PCL/chitosan NPs (II, III and IV) yielded different results. Although there was a

great variability within the groups, a tendency to produce higher levels of IFN- was observed. IFN-concentrations between 50 µg/mL and 75 µg/mL were observed in 4 out of 5 mice in group II. The marked higher level of IFN- of 1 mouse in group III may suggest the influence of DNA present in the formulation. However, the fact that only 1 mouse showed such increased titers limits the discussion of this hypothesis. With these data we may suggest the adjuvant activity of PCL/chitosan NPs may include the induction of CD4+ T cell proliferation and secretion of a Th1 cytokine, IFN-. In fact, it was not the first time that PCL microparticles associated with antigens allowed the induction of IFN-. A hot saline antigenic extract from *Brucella ovis* encapsulated into PCL induced increased levels of IFN- important for vaccination against *B. ovis* infection when administered SC [35]. Furthermore, PCL microspheres modified with chitosan and adsorbed *Streptotocus equi* antigen, induced higher IFN- titers than unmodified PCL microspheres through SC route [25]. The generation of a strong humoral immune response balanced with an efficient cellular Th1 immune response would be suitable for therapeutic vaccination in chronic HBV carriers [12, 13].

More recently, vaccination studies began to assess IL-17 production by CD4+ T cells after immunization with diverse NP formulations. For instance antigens like heparin-binding haemagglutinin (HBHA) [36], inactivated dengue virus type 2 [37] or *Chlamydia trachomatis* major outer-membrane protein peptide [38] induced higher IL-17 titers when delivered in NP based formulations. Our results of IL-17 production by mice spleen cells under HBsAg stimulation revealed no increase over basal concentration for groups I, III and IV compared to the naïve mice. Nevertheless, spleen cells in group II (particularly 3 out of 5 mice), were effectively stimulated on producing significantly higher levels of IL-17 in the presence of HBsAg (Fig. 3B). The fact that group III showed no increase in IL-17 titers compared to group II motivates some questions, as both delivery systems consist of NPs adsorbed with HBsAg and the difference is group III also includes pDNA. Further studies are required to evaluate the influence of PCL/chitosan NPs in the development of Th17 cytokine response. In fact, the traditional dichotomy Th1/Th2 subset of CD4+ T cells expressing effector cytokines has been changed by the crescent importance of the Th17 subset. This third subset of CD4+ T cells produces IL-17, whose role is believed to be important for protective cellular and memory immune responses [36, 39]. The Th17 promoting effect has already been reported by our group for other polymeric NPs based on chitosan [28].

Despite the positive results obtained by PCL/chitosan NPs as a vaccine adjuvant, the use of pRC/CMV-HBs appears not to have advantage for mice serum titers, neither for the IN boosts.

IN boosts in group III and IV with PCL/chitosan NPs adsorbed with HBsAg were performed with the objective to generate mainly a vaginal mucosal immune response, characterized by the production of secretory IgA (sIgA). Mucosal vaccination requires high amounts of HBsAg and boosts, and is known to

114

be variable between individuals. To assess whether a single IN boost was effective after 2 SC vaccine doses, anti-HBsAg IgA (at day 64) measured in mucosal washes was normalized for each mice according to their total IgA production. Comparisons were made with the groups I and II, SC immunized (IgA at day 42). Results are presented in Figure 4A. In group III, we observed that 3 out of 5 mice generated anti-HBsAg IgA in the mucosal washes. To note, 1 mouse presented a ratio of mucosal anti-HBsAg IgA/total IgA of around 0.5, a ratio considerably higher than all the rest. Comparing this result from group III with the result from group II (without IN boost), the mucosal anti-HBsAg IgA/total IgA ratio had no statistical differences. In group II, also 3 out of 5 mice developed a positive ratio. SC immunization is not expected to generate specific mucosal antibody titers, but transudation of serum IgA to mucosal sites seems to be dependent on the intensity of the serum IgA immune response observed [40]. This is, higher anti-HBsAg IgA serum titers would lead to higher mucosal anti-HBsAg IgA. Accordingly, in Figure 4B, the OD (492 nm) for the serum anti-HBsAg IgA levels in immunized mice at the same time point of vaginal washes is presented. The serum IgA was elevated for group II and III, explaining the similar results found. On the other hand, group IV does not present serum HBsAg-specific IgA titers. Therefore, in this group, vaginal IgA titers cannot be attributed to transudation from serum. However, only 1 mouse presented a positive ratio around 0.16.
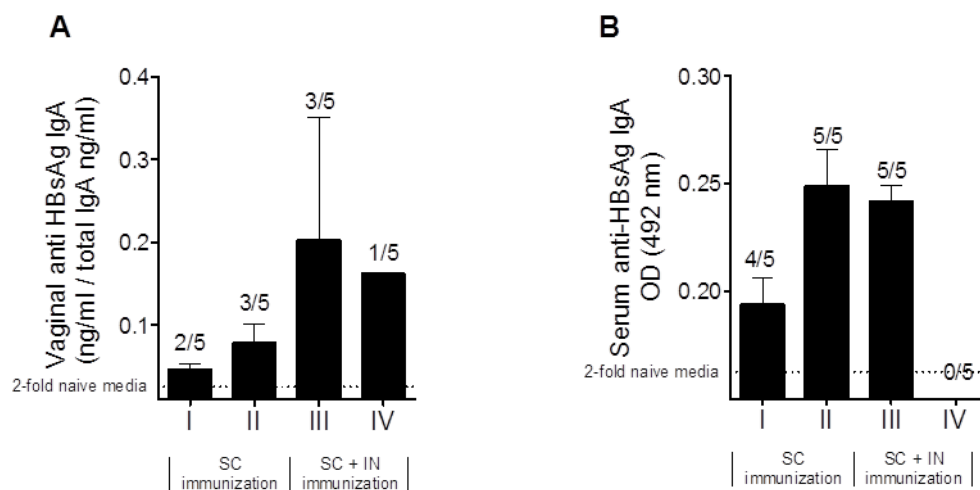
Figure 4: Vaginal (A) and serum (B) IgA concentration of immunized mice. Data represent mice from group I, II immunized SC on days 0 and 14 (see table 1) and mice from group III and IV immunized SC on days 0 and 14 and IN on day 42 (see table 1). (A) Vaginal anti-HBsAg IgA concentration of each mouse was normalized against total vaginal IgA. A pool of vaginal secretions was collected at day 41 and day 42 for group I and II, and at day 63 and 64 for group III and IV. Antibody concentrations were determined by ELISA as described in 'Materials and methods'. Positive results were only considered for ratios 2-fold higher than naïve media ratios. (B) Serum anti-HBsAg IgA levels of immunized mice. Blood was collected on day 42 and 64, respectively. Antibody levels were

determined by ELISA as described in 'Materials and methods'. Absorbance at 492 nm represents the immunoglobulin levels for a dilution of 1:32. Positive results were only considered for ODs 2-fold higher than naïve media ODs. Numbers above bars represent the number of mice for which antibody levels were considered positive. Data (mean ± SEM) are obtained from groups of 5 mice each.

Vaccination results demonstrated the adjuvant capacity of PCL/chitosan NPs to increase the antibody immune response against HBsAg when used as a delivery system for SC immunization. Also, promising results were found for the Th1 and Th17 cytokine production after HBsAg spleen cells re-stimulation. Nonetheless, overall results concerning PCL/chitosan NPs as a pDNA vaccine delivery system were not supportive.

3.2. Strongly negative zeta potential of PCL/chitosan NPs-pDNA complexes inhibits *in vitro* transfection

Preliminary transfection studies did not show encouraging results. In a previous report we described that low NPs:pDNA (w/w) ratios (2.5:1 and 1.25:1) were not able to generate significant transfection, even when using human serum albumin at the NPs surface, which was formerly described as a factor for increasing transfection efficiency in lipoplexes [24]. In an attempt to improve the transfection and therefore achieve good vaccination results, increased NPs:pDNA ratios were used.

The first aspect considered was the zeta potential of the complexes, which is a primary influence for cell uptake. In the previous study [24], we suspended the NPs in phosphate buffer prior to the pDNA complexation. The presence of the phosphate ions resulted in a negative zeta potential of the unloaded particles ($\approx$ 10 mV) [24]. Alternatively, as is visible in Figure 5A, PCL/chitosan NPs when dispersed in water presented a positive zeta potential (22.94 ± 1.09 mV), mostly derived from the positively charged amino groups of chitosan present at the surface of the delivery system. However, even in water, PCL/chitosan NPs-pDNA complexes showed a zeta potential of -18.90 ± 0.31 mV, -20.61 ± 1.87 mV and -32.97 ± 3.49 mV for ratios (w/w) NPs:pDNA 10:1, 5:1 and 1:1, respectively (Fig. 5A). This is justified as in order to complex pDNA in a NPs polymeric system, the negative charges of pDNA phosphate groups need to be neutralized, promoting pDNA condensation [14]. Therefore, complexation with PCL/chitosan NPs occurs due to the neutralization of pDNA negative phosphate groups by chitosan's cationic amino groups [29]. Without chitosan, PCL NPs were not able to complex pDNA [24]. In this case, the change to negative values appears to be gradual, so we might imply that increasing NPs:pDNA ratios would leave free more chitosan amino groups contributing at some point to a positive zeta potential. However, even a ratio of 500:1 (data not shown) results in a surface charge value of -14.74 ± 0.69 mV. Moreover, for *in vitro* or *in vivo* studies higher ratios than this are not suitable to be

used due to cytotoxicity and manufacturing related issues. Therefore, 10:1 was the maximum ratio that we were able to test.

Different NPs:pDNA (w/w) ratios might also have an impact on pDNA stability. In regard to chitosan:pDNA complexation and stability several authors report that a too low or too high amine to phosphate ratio (N:P) may be the cause of poor transfection due to physically unstable or too stable complexes, respectively [16]. Therefore, the complexation ability of the PCL/chitosan NPs in water was assessed using agarose gel electrophoreses retention assay as illustrated in Figure 5B. At both 10:1 and 5:1 ratios all the pDNA appears to be complexed, while the ratio 1:1 is not able to complex all pDNA and some is detected as free pDNA. Haas et al. reported on chitosan-modified PCL nanoparticles prepared by emulsion-difusion-evaporation method using poly-vinyl-alcohol as stabilizer, and complexation with pDNA was fully achieved for ratios higher than 2:1 NPs:DNA (w/w) [30].

To assess the pDNA unpacking dynamics from NPs, complexes were incubated in F12 medium for 2 h or 4 h (maximum of transfection studies) at 37 ºC followed by agarose gel retention assay. Figure 5C and 5D represent the state of complexation after the respective incubation times in F12 medium. After 2 h, all NPs-pDNA complexes effectively adsorbed pDNA with minor liberation. When the 4 h were completed all complexes were not retaining pDNA, which is illustrated by the signals comparable to free pDNA. From this assay we excluded the hypothesis of difficult pDNA unpacking as a factor limiting transfection results. This result was expected, as PCL/chitosan NPs were projected to be good pDNA delivery systems since the opposite charges of chitosan and PCL were likely to balance the interaction with pDNA generating complexes suitable for transfection. Highly cationic polymers like chitosan are known to efficiently form polycation/pDNA complexes, but their wide electrostatic interaction may hinder the pDNA unpacking crucial for its activity. Here, hydrophobic interactions were also involved between the carrier and the pDNA, and their weaker nature is known to counterbalance electrostatic forces [14, 41].
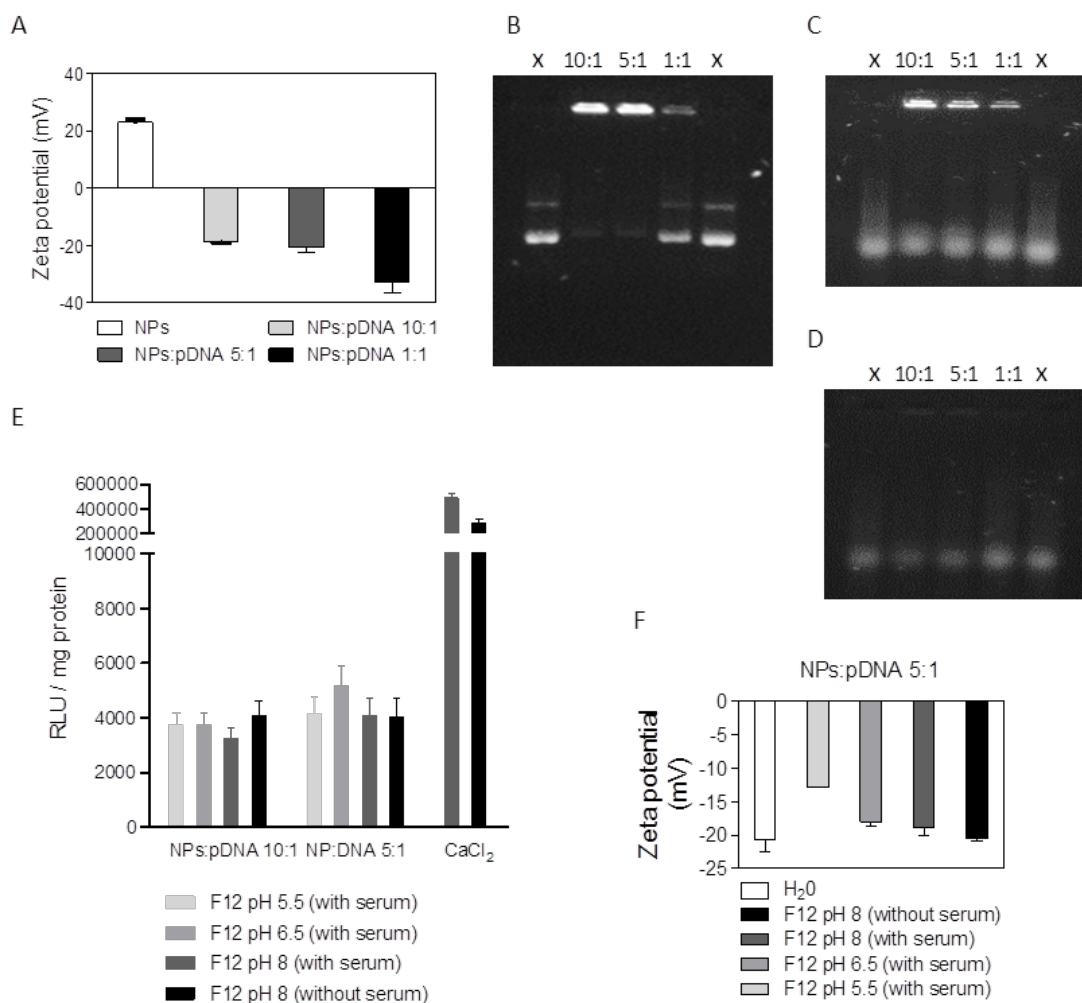
Figure 5: PCL/chitosan NPs as gene delivery system. Evaluation of pDNA-complex characteristics and transfection efficiency. A) Zeta potential (mV) of PCL/chitosan NPs and PCL/chitosan NPs complexed with different amounts of pDNA in water (pH ≈ 5). Conditions are described according to NPs:pDNA (w/w) ratios. Values represent 3 measurements performed with the same sample, illustrative of a minimum of 3 independent batches. (B) Agarose gel retention assay performed with the same NPs-pDNA complexes. Control of free pDNA is represented in (*x*) columns. C and D) Agarose gel retention assay performed with the NPs-pDNA and control already described and incubated in cell culture medium at 37 °C for 2 h (C) and 4 h (D). (E) Transfection efficiency of PCL/Chitosan NP complexes (w/w) ratios 10:1 and 5:1 evaluated under different conditions. Culture medium characteristics during transfection were experimental variables. Results were compared with CaCl$_2$ (positive control). Transfection is presented in relative light units / g protein (error bars represent standard deviation of the mean, n=8, from 2 independent assays). (F) Zeta potential of PCL/chitosan NPs complexes ratio (w/w) 5:1 when suspended in water (pH ≈ 5) and in cell culture media used for transfection experiments.

To transfect human lung adenocarcinoma (A549) cells *in vitro,* NPs-pDNA complexes with (w/w) ratios 10:1 and 5:1 were used. Transfection results denote a common slight increase in transfection at both NPs:pDNA ratios tested for all transfection media used. However, these increases were very low when compared to the positive control calcium chloride (Fig. 5E). To note, this positive control was only tested with unmodified cell culture medium (pH 8) as we had previously established high transfection results with it. The lower complex ratio (1:1) had already been tested without success [24], probably due to the lack of available chitosan amino groups, as they were all neutralizing pDNA. In these new experiments, based on the slightly increased zeta potentials at higher ratios, we speculated some chitosan was available to mediate cell interactions and increase transfection efficiency. Also, we questioned whether different media conditions would influence transfection and therefore 4 different conditions were tested: (1) F12 medium with 10 % serum, pH 5.5; (2) F12 medium with 10 % serum, pH 6.5; (3) F12 medium with 10 % serum, pH 8; and (4) F12 medium with 10 % serum, pH 8. Importantly, cytotoxicity studies were previously performed to guarantee that these different media pH values did not decrease cell viability during the assay (data not shown). It is known that transfection media characteristics like pH and serum concentration have a great influence on transfection efficiency of polyionic vectors [41, 42]. In fact, Sato et al. reported that transfection of A549 cells with chitosan/pDNA complexes was higher at pH 6.9 than at pH 7.6 due to the higher state of protonation of chitosan [43]. Several studies reported that when pH increases, the neutralization of chitosan amino groups leads to more negative zeta potentials [16, 42, 43]. To test this hypothesis, we assessed the influence of chitosan protonation in the PCL/chitosan NPs-pDNA complexes at the different media pH values (Fig. 5F). The most significant difference to note is at pH 5.5, where chitosan has a higher state of protonation and consequently less negative zeta potential. However, as in water, in all culture media conditions tested the overall charge of chitosan is less than the anionic charge of the pDNA in the complexes.

In the case of our formulations, the possible reason for the low transfection efficiency of NPs-pDNA, considering pDNA unpacks from the complexes, can be attributed to a challenging cell internalization due to their negative zeta potential not favoring interaction with cell membranes important for transfection [43]. Despite the change in media pH, an overall positive charge of complexes was never achieved. In addition, mean diameters of the complexes when suspended in cell culture media were around 1000 nm for all NPs:pDNA ratios tested. Although the uptake by antigen presenting cells (APCs) is possible with particles ranging between 20 and 5000 nm [3], 1000 nm is not ideal for endocytosis, especially by epithelial cell lacking phagocytic capacity [44].

Due to their safety profile, non-viral vectors are very attractive as pDNA delivery systems. Particularly, polymeric NPs are expected to allow the formation of small defined particles suitable for effective uptake

by target cells and also to confer pDNA protection and stabilization until intracellular delivery [14, 45]. However, low transfection rates are often observed with these systems [46]. Furthermore, some authors consider *in vitro* transfection assays difficult to correlate with *in vivo* studies [14]. Our vaccination results though are in line with the low transfection results obtained. Size increase in culture media may be a factor that inhibited A549 cells transfection, but based on *in vivo* and *in vitro* results we may speculate that the most likely cause for the overall low transfection results is the zeta potential. The lack of positive surface amino groups of chitosan limits cell interaction and consequently plasmid delivery and expression.

4. Conclusions

Polymeric NPs based on biodegradable materials are emerging as alternatives to currently available vaccine adjuvants. These NPs are widely studied systems for drug delivery and their evaluation in the vaccine field allows for new improvements and eventually to the establishment of an optimal approach. With this work we demonstrated the adjuvant capacity of PCL/chitosan NPs as a vaccine delivery system, enhancing systemic humoral and cellular immune responses. In fact, the immune response to NPs-HBsAg immunization by SC route was largely improved. Furthermore, a different cellular mediated immune response, with the production of IFN- and IL-17 was observed and may be an advantage when compared to the commercially available HBsAg vaccines. However, vaccination with PCL/chitosan NPs-pRC/CMV-HBs complexes did not generate efficient immune responses.

Overall, PCL/chitosan NPs proved to be a good adjuvant for HBsAg SC vaccination. Increased ratios of NPs:HBsAg (w/w) may allow us to evaluate whether the adjuvant effect may be dose-dependent and if it further enhances the Th1/Th17 mediated cellular immune responses. Moreover, increased NPs:HBsAg (w/w) ratios may be able to generate a humoral systemic immune response when administered by the nasal mucosa. To answer these questions further studies are being developed.

References

1. Powell, B.S., A.K. Andrianov, and P.C. Fusco, *Polyionic vaccine adjuvants: another look at aluminum salts and polyelectrolytes.* Clin Exp Vaccine Res, 2015. **4**(1): p. 23-45.
2. Akagi, T., M. Baba, and M. Akashi, *Biodegradable Nanoparticles as Vaccine Adjuvants and Delivery Systems: Regulation of Immune Responses by Nanoparticle-Based Vaccine*, in *Polymers in Nanomedicine*, S. Kunugi and T. Yamaoka, Editors. 2012, Springer Berlin Heidelberg. p. 31-64.
3. Zhao, L., et al., *Nanoparticle vaccines.* Vaccine, 2014. **32**(3): p. 327-37.
4. Tamayo, I., et al., *Poly(anhydride) nanoparticles act as active Th1 adjuvants through Toll-like receptor exploitation.* Clin Vaccine Immunol, 2010. **17**(9): p. 1356-62.
5. Seong, S.Y. and P. Matzinger, *Hydrophobicity: an ancient damage-associated molecular pattern that initiates innate immune responses.* Nat Rev Immunol, 2004. **4**(6): p. 469-78.
6. Shima, F., T. Akagi, and M. Akashi, *Effect of Hydrophobic Side Chains in the Induction of Immune Responses by Nanoparticle Adjuvants Consisting of Amphiphilic Poly(gamma-glutamic acid).* Bioconjug Chem, 2015. **26**(5): p. 890-8.
7. Ulery, B.D., et al., *Rational design of pathogen-mimicking amphiphilic materials as nanoadjuvants.* Sci Rep, 2011. **1**: p. 198.
8. Petersen, L.K., et al., *Activation of innate immune responses in a pathogen-mimicking manner by amphiphilic polyanhydride nanoparticle adjuvants.* Biomaterials, 2011. **32**(28): p. 6815-22.
9. Jiao, Q., et al., *Immunomodulation of nanoparticles in nanomedicine applications.* Biomed Res Int, 2014. **2014**: p. 426028.
10. Jain, N.K., et al., *Formulation and stabilization of recombinant protein based virus-like particle vaccines.* Adv Drug Deliv Rev, 2014.
11. Cova, L., *Advances and challenges in the development of therapeutic DNA vaccines against hepatitis B virus infection.* Curr Gene Ther, 2014. **14**(3): p. 149-60.
12. Michel, M.L. and P. Tiollais, *Hepatitis B vaccines: protective efficacy and therapeutic potential.* Pathol Biol (Paris), 2010. **58**(4): p. 288-95.
13. Zuckerman, J.N., *Protective efficacy, immunotherapeutic potential, and safety of hepatitis B vaccines.* J Med Virol, 2006. **78**(2): p. 169-77.
14. Viola, J.R., et al., *Non-viral nanovectors for gene delivery: factors that govern successful therapeutics.* Expert Opin Drug Deliv, 2010. **7**(6): p. 721-35.
15. Vasiliev, Y.M., *Chitosan-based vaccine adjuvants: incomplete characterization complicates preclinical and clinical evaluation.* Expert Rev Vaccines, 2015. **14**(1): p. 37-53.
16. Lavertu, M., et al., *High efficiency gene transfer using chitosan/DNA nanoparticles with specific combinations of molecular weight and degree of deacetylation.* Biomaterials, 2006. **27**(27): p. 4815-24.
17. Picola, I.P.D., et al., *Effect of ionic strength solution on the stability of chitosan–DNA nanoparticles.* Journal of Experimental Nanoscience, 2012. **8**(5): p. 703-716.
18. Amaduzzi, F., et al., *Chitosan-DNA complexes: charge inversion and DNA condensation.* Colloids Surf B Biointerfaces, 2014. **114**: p. 1-10.
19. Dash, T.K. and V.B. Konkimalla, *Poly-epsilon-caprolactone based formulations for drug delivery and tissue engineering: A review.* J Control Release, 2012. **158**(1): p. 15-33.
20. Mahapatro, A. and D.K. Singh, *Biodegradable nanoparticles are excellent vehicle for site directed in-vivo delivery of drugs and vaccines.* J Nanobiotechnology, 2011. **9**: p. 55.
21. Silva, J.M., et al., *Immune system targeting by biodegradable nanoparticles for cancer vaccines.* J Control Release, 2013. **168**(2): p. 179-99.
22. Ulery, B.D., L.S. Nair, and C.T. Laurencin, *Biomedical Applications of Biodegradable Polymers.* J Polym Sci B Polym Phys, 2011. **49**(12): p. 832-864.

23.   Dash, T.K. and V.B. Konkimalla, *Polymeric modification and its implication in drug delivery: poly-epsilon-caprolactone (PCL) as a model polymer.* Mol Pharm, 2012. **9**(9): p. 2365-79.

24.   Jesus, S., G. Borchard, and O. Borges, *Freeze Dried Chitosan/ Poly- e-Caprolactone and Poly-e-Caprolactone Nanoparticles: Evaluation of their Potential as DNA and Antigen Delivery Systems.* J Genet Syndr Gene Ther 2013. **4**(164).

25.   Florindo, H.F., et al., *Streptococcus equi antigens adsorbed onto surface modified poly-epsilon-caprolactone microspheres induce humoral and cellular specific immune responses.* Vaccine, 2008. **26**(33): p. 4168-77.

26.   Florindo, H.F., et al., *The enhancement of the immune response against S. equi antigens through the intranasal administration of poly-epsilon-caprolactone-based nanoparticles.* Biomaterials, 2009. **30**(5): p. 879-91.

27.   Gupta, N.K., et al., *Development and characterization of chitosan coated poly-(varepsilon-caprolactone) nanoparticulate system for effective immunization against influenza.* Vaccine, 2011. **29**(48): p. 9026-37.

28.   Bento, D., et al., *Development of a novel adjuvanted nasal vaccine: C48/80 associated with chitosan nanoparticles as a path to enhance mucosal immunity.* Eur J Pharm Biopharm, 2015. **93**: p. 149-64.

29.   Wang, Y., X. Zhang, and G. Yang, *Single molecular analysis of the interaction between DNA and chitosan.* RSC Advances, 2015. **5**(37): p. 29594-29600.

30.   Haas, J., et al., *Preparation and characterization of chitosan and trimethyl-chitosan-modified poly-(epsilon-caprolactone) nanoparticles as DNA carriers.* AAPS PharmSciTech, 2005. **6**(1): p. E22-30.

31.   Chroboczek, J., I. Szurgot, and E. Szolajska, *Virus-like particles as vaccine.* Acta Biochim Pol, 2014. **61**(3): p. 531-9.

32.   Boisgerault, F., G. Moron, and C. Leclerc, *Virus-like particles: a new family of delivery systems.* Expert Rev Vaccines, 2002. **1**(1): p. 101-9.

33.   Chung, E.H., *Vaccine allergies.* Clin Exp Vaccine Res, 2014. **3**(1): p. 50-7.

34.   Neutra, M.R. and P.A. Kozlowski, *Mucosal vaccines: the promise and the challenge.* Nat Rev Immunol, 2006. **6**(2): p. 148-58.

35.   Murillo, M., et al., *A Brucella ovis antigenic complex bearing poly-epsilon-caprolactone microparticles confer protection against experimental brucellosis in mice.* Vaccine, 2001. **19**(30): p. 4099-106.

36.   Verwaerde, C., et al., *HBHA vaccination may require both Th1 and Th17 immune responses to protect mice against tuberculosis.* Vaccine, 2014. **32**(47): p. 6240-50.

37.   Hunsawong, T., et al., *A novel dengue virus serotype-2 nanovaccine induces robust humoral and cell-mediated immunity in mice.* Vaccine, 2015. **33**(14): p. 1702-10.

38.   Dixit, S., et al., *Poly(lactic acid)-poly(ethylene glycol) nanoparticles provide sustained delivery of a Chlamydia trachomatis recombinant MOMP peptide and potentiate systemic adaptive immune responses in mice.* Nanomedicine, 2014. **10**(6): p. 1311-21.

39.   Lin, Y., S.R. Slight, and S.A. Khader, *Th17 cytokines and vaccine-induced immunity.* Semin Immunopathol, 2010. **32**(1): p. 79-90.

40.   Meckelein, B., et al., *Contribution of serum immunoglobulin transudate to the antibody immune status of murine intestinal secretions: influence of different sampling procedures.* Clin Diagn Lab Immunol, 2003. **10**(5): p. 831-4.

41.   Bolhassani, A., et al., *Polymeric nanoparticles: potent vectors for vaccine delivery targeting cancer and infectious diseases.* Hum Vaccin Immunother, 2014. **10**(2): p. 321-32.

42.   Nimesh, S., et al., *Enhanced gene delivery mediated by low molecular weight chitosan/DNA complexes: effect of pH and serum.* Mol Biotechnol, 2010. **46**(2): p. 182-96.

43.   Sato, T., T. Ishii, and Y. Okahata, *In vitro gene delivery mediated by chitosan. effect of pH, serum, and molecular mass of chitosan on the transfection efficiency.* Biomaterials, 2001. **22**(15): p. 2075-80.

44.   Prabha, S., et al., *Size-dependency of nanoparticle-mediated gene transfection: studies with fractionated nanoparticles.* Int J Pharm, 2002. **244**(1-2): p. 105-15.

45.   Xiang, S.D., et al., *Delivery of DNA vaccines: an overview on the use of biodegradable polymeric and magnetic nanoparticles.* Wiley Interdiscip Rev Nanomed Nanobiotechnol, 2010. **2**(3): p. 205-18.

46.   Kim, T.K. and J.H. Eberwine, *Mammalian cell transfection: the present and the future.* Anal Bioanal Chem, 2010. **397**(8): p. 3173-8.

Chapter 4. PCL/chitosan nanoparticles as a vaccine adjuvant for HBsAg subcutaneous vaccination – evaluation of immunostimulatory co-adjuvants

Part 1. Adjuvant activity of PCL/chitosan nanoparticles characterized by mast cell activation *in vitro* and IFN-γ and IL-17 production *in vivo*

Abstract

Polymeric nanoparticles (NPs) are extremely attractive vaccine adjuvants able to promote antigen delivery and presentation and in some cases hold intrinsic immunostimulatory properties. With this study we demonstrated that hepatitis B virus surface antigen (HBsAg) loaded poly-ε-caprolactone (PCL)/chitosan NPs, when administered through subcutaneous (SC) route, were able to induce higher specific antibody titers than a commercially available vaccine, without increasing IgE. Results also revealed the NPs capacity to promote a cellular immune response against HBsAg based on the production of IFN-γ and IL-17 by spleen cells. Moreover, preliminary mechanistic studies revealed that poly-ε-caprolactone (PCL)/chitosan NPs promoted mast cell (MC) activation and did not induce inflammatory TNF-α secretion by monocytes. Altogether, our results confirm the ability of PCL/chitosan NPs as a vaccine adjuvant.

Keywords: Nanoparticles, immunological adjuvant, Poly-ε-caprolactone, chitosan, recombinant vaccine, HBsAg, subcutaneous administration, immune response, CpG-ODN, Engerix-B.

1. Introduction

Vaccine adjuvants are an essential puzzle piece for vaccine efficacy. They increase the immune responses against highly purified recombinant protein antigens which present an excellent safety profile, but lack immunogenicity when compared to traditional vaccines based on inactivated or live attenuated pathogens. For a long time, adjuvants were classified as antigen delivery systems and immunopotentiators, sometimes used in combination. Currently, the scientific community knows that many antigen delivery vehicles act not only by modifying antigen bioavailability but by stimulating antigen presenting cells (APC's) directly, potentiating antigen immune responses. Particularly, polymeric nanoparticles (NPs), derived from synthetic or natural biodegradable polymers have been used as vaccine adjuvants since they protect antigens, create depot effect and increase the antigen presentation to dendritic cells (DCs), ultimately enhancing antigen specific humoral and cellular immune responses [1, 2].

The most studied mechanisms triggered by vaccine adjuvants, rely on the activation of pattern recognition receptors (PRRs), localized both at the surface and/or in the cytoplasm of immune cells, particularly DCs and macrophages [3]. However, recent studies show that other cell types, like mast cells (MCs), also have an important physiological role on the modulation of appropriate immune responses. MCs are considered the sensory arm of the immune system, capable of activating both innate and adaptive immune responses. This fact is probably related with the ability of MCs to rapidly release stored inflammatory mediators such as tumor necrosis factor (TNF), histamine and - hexosaminidase within minutes of activation [4]. Moreover, MCs release insoluble granular particles composed of heparin proteoglycans and proteases that once internalized by DCs, increase their ability to present antigens to the naive T cells [5, 6]. These granules are also able to reach lymph nodes and contribute its structural modification which favors DCs interaction with lymphocytes essential for the generation of adaptive immune responses [5, 6]. Up to now, mast cell (MC) activation capacity by small molecules, like compound 48/80 (C48/40), has been well characterized, and these molecules ability to increase vaccine immune responses was already documented [7, 8]. In the literature, there are no reports concerning the polymeric NPs intrinsic ability to activate MCs, except for the one recently published by our group about chitosan NPs [7]. We were able to confirm the ability of chitosan NPs as MC activators, creating new insights into the adjuvant mechanism of chitosan NPs [7]. Likewise, studies with other polymeric NPs may elucidate about their MC activation ability and possible vaccine immunostimulant adjuvant skills.

In the light of the above mentioned, our main objective was to evaluate the adjuvant ability of PCL/chitosan NPs for hepatitis B vaccination proposes. Poly- -caprolactone (PCL) is biocompatible and

132

was already approved by Food and Drug Administration (FDA) for biomedical applications. This highly hydrophobic polyester undergoes a slow degradation process, avoiding the generation of an acidic harmful environment at the site of administration [9]. PCL ability to blend with other polymers to form composite nanoparticles may also modulate some of its mechanical, physical or chemical properties [9] which can be particularly useful in the obtainment of a good adsorption matrix for the antigen of interest. Accordingly, the inclusion of chitosan will confer a more amphiphilic nature to the NPs, a characteristic that seems to be desirable for vaccine formulation purposes [10]. Moreover, chitosan's ability to stimulate cells of the immune system has been shown in many *in vitro* mechanistic studies [11, 12], but also in immunization studies with diverse antigens [7, 13]. Consequently, the inclusion of chitosan into PCL nanoparticles was expected to improve nanoparticle (NP) immunostimulatory effect. In our laboratory, the adjuvant effect of chitosan nanoparticles was validated with the hepatitis B antigen [14]. Additionally, we reported that the association of the CpG-ODN, a toll-like receptor 9 (TLR9) agonist, to the chitosan NP formulation induced a Th1/Th2 balanced immune response [14].

The purpose of the present study was to perform immunization studies with hepatitis B antigen to investigate the adjuvant properties of PCL/chitosan NPs and to explore some of the mechanisms that can be involved in the immune system stimulation by this nanoparticulate delivery system.

2. Materials and Methods

2.1. Materials

Chitosan (ChitoClear™ - 95 % DD and 8 cP viscosity measured in 1 % solution in 1 % acetic acid) was purchased from Primex Bio-Chemicals AS (Avaldsnes, NO). PCL (average MW 14000), 3-[4,5-dimethylthiazol-2-yl]-2,5-diphenyl tetrazolium bromide (MTT), D-(+)-Trehalose dehydrate (≥ 98.5 %), and 4-nitrophenyl N-acetyl- -D-glucosaminide (NAG), were obtained from Sigma-Aldrich Corporation (St. Louis, MO, USA). Cytosine-phosphate-guanine oligodeoxynucleotide (CpG-ODN) 1826, was acquired from InvivoGen (San Diego, CA, USA). Recombinant hepatitis B surface antigen (HBsAg), subtype adw with 25 kDa, was acquired from Aldevron (Fargo, ND, USA). Engerix-B was obtained from GlaxoSmithKline Biologicals (Rixensart, BE). All other chemicals and reagents were of analytical grade.

2.2. Methods

2.2.1. Nanoparticle preparation

Chitosan purification and PCL/chitosan NPs production were performed as previously described by us [15], with minor modifications concerning the NPs isolation steps. Briefly, after particle preparation NPs were isolated and concentrated by centrifugation at 16000 x g, for 75 min at 4 °C with a 200 L glycerol bed. Glycerol was eliminated by dialysis of the suspension against water for 48 h (Spectra®Por cellulose ester dialysis membrane, MWCO 300.000, Spectrum Europe B.V., Breda, NL). The resulting suspension was either freeze-dried (FreezeZone 6, Labconco Corporation, Kansas City, MO, USA) in the presence of trehalose, resulting in a powder with 5.7 % NPs, or re-suspended in a desired buffer volume for immediate utilization.

For *in vitro* cell activation studies, NPs were produced under lipopolysaccharide (LPS) free conditions and tested with endotoxin detection kit (Pyrogent™ gel clot Limulus Amebocyte Lysate (LAL) assay, 0.125 EU/mL, Lonza Group, Basel, CH).

To perform studies requiring fluorescence analysis with PCL/chitosan NPs (FITC-NPs), chitosan was previously labeled with fluorescein isothiocyanate (FITC) (Santa Cruz Biotechnology Inc., Heidelberg, DE), accordingly to a protocol described already by us [15].

HBsAg loaded PCL/chitosan NPs were prepared by incubation of concentrated PCL/chitosan NPs with HBsAg, in water under low stirring. The amount of protein adsorbed was calculated by the difference between the total protein added and the protein that remained in solution (after centrifugation), quantified by Pierce™ Biocinchoninic acid (BCA) Protein Assay Kit (Thermo Fisher Scientific Inc., Waltham, MA, USA), according to manufacturer's instructions. Size and zeta potential were measured by dynamic light scattering and electrophoretic light scattering, respectively, with a

Delsa™ Nano C (Beckman Coulter, Madrid, ES). Transmission electron microscopy was used to observe the HBsAg adsorbed NPs (stored in 4 % paraformaldehyde). Samples were placed in formvar coated nickel or cooper grids (300 mesh, TAAB Laboratories Equipment Ltd, Berkshire, UK), and observed under a FEI-Tecnai G2 Spirit Biotwin, a 20-120 kV transmission electron microscope (TEM) (FEI Company, Hillsboro, OR, USA).

2.2.2. Studies on monocytes: NPs uptake, TNF-α production and NPs cytotoxicity

Peripheral blood was kindly given by IPST,IP (Coimbra, PT) and was obtained from normal donors in heparinized syringes followed by serum depletion. Peripheral blood mononuclear cells (PMBC) were isolated on a density gradient with Lymphoprep™ (Axis-Shield, Dundee, SCT) according to the provider's guidance protocol, with minor modifications. Briefly, the blood dilution performed was 1:5 (v/v) in 0.09 % sodium chloride, the centrifugation step was performed at 1190 x g for 20 min (20 ℃) and the mononuclear cell dense ring was collected and washed with PBS (pH= 7.4 at 37 ℃) through consecutive centrifugations (487 x g, 10 min, 20 ℃) until the supernatant was clear. At the end, cells were suspended in RPMI 1640 medium supplemented with 1 % PenStrep and 10 % heat inactivated FBS, and seeded in 12 or 48-well plates at a concentration of 1×10^6 cells /mL in 1 mL or 0.5 mL, respectively. After 2 h incubation, non-adherent cells were aspirated and washed twice with supplemented RPMI 1640, before incubation with ice-cold PBS for 20 min at 4 ℃. Then, after new wash with ice-cold PBS, cells were incubated overnight with supplemented RPMI at 37 ℃ and used the next day.

The cellular uptake of two concentrations of FITC-labeled NPs was studied by flow cytometry using the 48-well plates (40 µg NPs/mL and 10 µg NPs/mL to 1×10^6 cells /mL, final volume: 0.5 mL). After a 4 h incubation period, cells were washed with 100 µL of PBS and detached from the wells with 100 µL of 0.25 % trypsin-EDTA solution (Gibco®, Life Technologies Corporation, Paisley, UK) and inactivated by 100 µL of supplemented culture medium. Cells from 12 wells were pooled in the same tube, centrifuged for 20 min at 487 x g, and re-suspended in 200 µL of ice-cold PBS and analyzed on BD FACSCalibur Flow Cytometer (BD Biosciences, Bedford, MA, USA). Prior to the analysis, 1.5 µL of 50 µg/mL propidium iodide (PI) solution was added to samples to evaluate cytotoxicity. Duplicates of the samples were also analyzed with 0.2 % trypan blue solution to exclude fluorescence at the surface of the cells. The mean fluorescence for a population of 20000 cells was collected and results were analyzed.

135

For the confocal laser scanning microscopy assay, cells previously seeded on glass coverslips in 12-well plates, were incubated with FITC-NPs (10 µg NPs/mL and 5 µg NPs/mL to 1 x 10^6 cells /mL, final volume: 1 mL) during 4 h and then labeled with Image-iT™ LIVE plasma membrane and nuclear labeling kit (Life Technologies Corporation, Paisley, UK) as previously described [15]. Samples were examined under a laser scanning inverted confocal microscope Carl Zeiss LSM 510 Meta with a Plan-Apochromat 63x/1.40 Oil DIC M27 objective (Carl Zeiss, Oberkochen, DE).

To test TNF- secretion induced by PCL/chitosan NPs (LPS free) in PBMCs, cells platted in 48 well-plates (1 x 10^6 cells /mL, final volume: 0.5 mL) were incubated with different NPs concentrations ranging from 40 µg/mL to 5 µg/mL. LPS was used as positive control at 0.2 µg/mL (0.5 EU/mL). After 24 h incubation, the supernatants were collected and stored at - 80 ºC until further TNF- quantification by ELISA according to manufacturer's instructions (Human TNF alpha ELISA Ready-SET-Go!™, eBioscience, San Diego, CA, USA). To examine the cytotoxicity associated with NPs stimulation, the culture medium was replaced with new medium, and MTT cell viability assay was performed according to manufacturer's protocol and cell viability (%) calculated according to equation 1:

$$Cell\ viability\ (\%) = \frac{(OD\ sample\ (540\ nm) - OD\ sample\ (630\ nm))}{(OD\ control\ (540\ nm) - OD\ control\ (630\ nm))}\ x\ 100 \qquad (Eq.1)$$

2.2.3. Mast cell activation

The human mast cell line HMC-1 was kindly provided by Dr. Butterfield, Mayo Clinic (Rochester, MN, USA) and maintained in Iscove's modified Dulbecco's medium (IMDM) at 37 ºC, 96 % relative humidity (RH), 5 % CO$_2$. The -hexosaminidase (-hex) release assay was performed as previously described by our group [7] with slight differences. HMC-1 cells were plated at a density of 6 x 10^6 cells/mL (100 L) per well in Tyrode's buffer and incubated during 45 min with particles suspended in the same buffer to a final concentration of 150 µg/mL, 80 µg/mL and 40 µg/mL. For comparison, PCL NPs prepared by the same technique as PCL/chitosan NPs but in the absence of chitosan, were used (150 µg/mL). Controls included C48/48 (positive control), 0.5 % Triton™ X-100 (total release) and unstimulated cells (basal release). After a brief centrifugation 30 µL of supernatant from each well were collected and incubated with 10 µL of NAG for 30 min at 37 ºC. Afterwards, 100 L of carbonate buffer (pH=10) induced a color change and optical density was read at 405 nm in a microplate reader (Multiskan EX Microplate, Thermo Fisher Scientific Inc., Waltham, MA, USA). -hex release was assessed using equation 2:

136

$$\beta - hex\ release(\%) = \frac{(OD\ sample\ \beta\text{-}hex\ release - OD\ control\ \beta\text{-}hex\ release)}{(OD\ TritonX\text{-}100\ \beta\text{-}hex\ release - OD\ control\ \beta\text{-}hex\ release)}\ x\ 100$$

<div align="right">(Eq.2)</div>

The level of granularity on HMC-1 cells was assessed by the analysis of cells stained with toluidine blue. After reproducing the above described protocol on poly-L-lysine coated coverslips, cells were washed with PBS, fixed with 4 % paraformaldehyde for 20 min, and stained with toluidine blue for 30 min. After staining, cells were washed repeatedly and mounted on microscope slides for further examination.

To evaluate if the HMC-1 degranulation and -hex release occurred due to NPs toxicity MTT assay was performed. The exact -hex release procedure described above was used and after 45 min incubation plates were briefly centrifuged (10 min, 800 x g) and the medium replaced by complete IMDM. MTT assay was performed right after the medium replacement for cell viability assessment.

To evaluate the NPs cellular uptake during the -hex release assay, the protocol was repeated and adapted to 24-well plates and FITC-NPs were used. Half of the HMC-1 cell samples were analyzed in a cytometer after the 45 min incubation with the particles. The other half, after the 45 min incubation, were washed and incubated for more 24 h in fresh culture medium before cytometry analysis. In both situations, cells were collected, centrifuged for 20 min at 487 x g, 20 ºC, and re-suspended in 200 µL of ice-cold PBS. Cell analysis was performed as described above on section 2.2.2..

2.2.4. Subcutaneous vaccination with HBsAg loaded PCL/chitosan nanoparticles

Eight-week-old C57BL/6 female mice from Charles River (Saint-Germain-Nuelles, FR) were housed in filter top cages with food and water provided *ad libitum.* All experiments were performed in accordance with FELASA guidelines and approved by the Ethical Animal Care Committee of the Center for Neuroscience and Cell Biology of Coimbra. Groups of 5 mice were used to test different subcutaneous (SC) vaccine formulations whose composition and immunization schedules are resumed in table 1. Immunizations were performed under light isoflurane anesthesia by SC injection (over the shoulders, back neck region) of 100 L formulations.

<p align="center">**Table 1:** Formulations for SC immunization of C57BL/6 mice.</p>

Formulation name	PCL/chitosan NPs (µg/animal)	HBsAg (µg/animal)	CpG-ODN (µg/animal)	SC immunization (prime & boost) (day)	Euthanasia (day)
403.5NPs	403.5	1.5	-	0, 14	42
807NPs	807	1.5	-	0, 14	42
1614NPs	1614	1.5	-	0, 14	42
807NPs+CpG	807	1.5	20	0, 14	42
HBsAg	-	1.5	-	0, 14	42
Engerix-B	-	1.5*	-	0, 14	42

*The volume of Engerix-B given to each mouse was adjusted so that HBsAg amount was 1.5 g/animal.

2.2.4.1.   Biological sample collection

Blood was collected by submandibular lancet method at day 14 and 42 from mice under light isoflurane anesthesia. After coagulate, blood was centrifuged at 4500 x g for 10 min for serum collection. At day 42, after blood collection mice were euthanized by cervical dislocation. Spleens were aseptically collected for cytokine production studies. Vaginal washes were collected at day 41 and 42 by instilling 100 µL of sterile PBS into the vaginal cavity and flushing the lavage fluid in-out 10 times before collection. Samples supplemented with phenylmethylsulfonyl fluoride (PMSF) and sodium azide (final concentration 1mM and 0.01 %, respectively), were centrifuged at 3300 x g for 10 min. The supernatants were collected and stored at 80 °C until further analysis.

2.2.4.2.   Determination of immunoglobulin titers

For serum HBsAg-specific IgG, IgG1, IgG2c, IgG3 and IgE determination, HBsAg coated plates were achieved by overnight incubation at 4 ºC of 0.1 µg/well HBsAg in 50 mM sodium carbonate/bicarbonate pH 9.6, on high-binding 96-well plates (Nunc MaxiSorp®, Thermo Fisher Scientific Inc., Waltham, MA, USA). Plates were washed 5 times with PBS-Tween 20 and blocked for 1 h at 37 °C. After washing, serial dilutions of serum were applied and incubated for 2 h at 37 °C. Following extensive washing, specific antibodies were detected using horseradish peroxidase (HRP) conjugated goat anti-mouse IgG (Bethyl Laboratories, Montgomery, TX, USA), IgG1 (Rockland Immunochemicals Inc., Limerick, PA, USA), IgG2c (GeneTex, Irvine, CA, USA), IgG3 (SouthernBiotech, Birmingham, AL, USA) or IgE (Nordic Immunological Laboratories, Susteren, NL), respectively, for 30 min at 37 °C according to the antibody dilution recommended by the suppliers. Next, o-phenylenediamine (OPD) solution (5 mg OPD to 10 mL citrate buffer and 10 µl H_2O_2) was incubated for

<p align="center">138</p>

10 min at room temperature. Reaction was stopped with 50 μL of 1M H_2SO_4 and absorbance was read at 492 nm with a microplate reader.

HBsAg-specific IgA in mucosal samples was determined according to the above described procedure using concentrated samples. Total IgA in mucosal samples was determined using a similar procedure, with minor modifications as described in Mouse IgA ELISA Quantitation Set protocol (Bethyl Laboratories, Montgomery, TX, USA). Vaginal and nasal IgA are presented as the ratio between specific anti-HBsAg IgA and total IgA for each mouse. Only mice whose IgA ratio was 2-fold higher than naïve mice ratio average were considered responders.

2.2.4.3.   Cytokine production by vaccinated mice spleen cells

Individual mice spleen cell suspensions were prepared as previously described by our group [7] without erythrocytes lysis. Spleen cell suspensions (0.25 x 10^6 cells/well) were cultured in 96-well plates, for incubation with and without stimulation of concanavalin A (con A) (1.25 g/well) and HBsAg (1 g/well). Duplicates of each condition were incubated at 37 ºC with 96 % relative humidity (RH) in the presence of 5 % CO_2, for 48 h (IL-17, IFN-) and 72 h (IL-4). After that period plates were centrifuged and the clear supernatants collected and stored at –80 ºC until further analysis. Cytokines were measured by ELISA technique according to kit manufacturer's instructions (Murine IL-4, IFN- and IL-17 standard ABTS ELISA development kits, PeproTech, Rocky Hill, NJ, USA).

2.2.5. Statistical analysis

Results were expressed as mean ± standard error of the mean (SEM) or standard error (SD), as indicated in each figure. Flow cytometry data were analyzed with CellQuest Modfit LT analysis software (BD Biosciences, Bedford, MA, USA). All other data was analyzed with GraphPad Prism v 5.03 (GraphPad Software Inc., La Jolla, CA, USA) by ANOVA, followed by a Tukey's post-test for multiple comparisons. P<0.05 was considered statistically significant difference).

3. Results and discussion

3.1. Characterization of PCL/chitosan NPs

PCL/chitosan NPs were achieved by the precipitation of PCL polymer, previously dissolved in acetone, in a diluted acetic acid solution containing chitosan, under high speed homogenization. The resultant unloaded particles, dispersed in water, had a mean diameter of 208.1 ± 28.7 nm, with low polydispersity index (0.18 ± 0.06) and a zeta potential of + 25.7 ± 2.9 mV, that suggests the chitosan influence at the NPs surface, as previously reported by other groups for chitosan modified PCL particles [16-18]. The loading of PCL/chitosan NPs with HBsAg antigen was performed with the particles dispersed in water, through simple incubation, aiming for HBsAg adsorption at NPs surface. The characterization of the different formulations according to its NPs:HBsAg (w/w) ratios, is illustrated in Figure 1A. CpG-ODN is a toll-like receptor 9 (TLR9) agonist, which is able to elicit innate immune responses alone or as a vaccine adjuvant. Studies performed in our laboratory showed that the association of CpG-ODN loaded chitosan nanoparticles with HBsAg loaded chitosan nanoparticles in same formulation was able to modulate the HBsAg-specific immune response towards a more balanced Th1/Th2 immune response [14]. To study if same effect would be observed with PCL/chitosan NPs, CpG-ODN was included in a formulation for vaccination studies. Therefore, results from the characterization of the formulation containing CpG-ODN are also included in Figure 1A. Similarly to unloaded PCL/chitosan NPs, HBsAg loaded NPs were monodisperse (PI ≤ 0.18) with a mean size around 200 nm and a zeta potential superior to + 18 mV. The exception was the 807NPs+CpG formulation, since the CpG-ODN presence shifted the overall surface charge of the NPs to highly negative values (- 35.45 mV). HBsAg adsorption on PCL/chitosan NPs surface was highly efficient (> 96 %) for all the formulations tested. Electrostatic force between chitosan positive amino groups and negative charges from HBsAg, together with hydrophobic interactions between the antigen and PCL explain the high surface adsorption [19]. Representative TEM images clearly illustrate the HBsAg VLPs adsorbed on PCL/chitosan NPs surface (Fig.1B).

A

	Formulations			
	403.5NPs	**807NPs**	**1614NPs**	**807NPs+CpG**
Size (nm)	201.7 ± 5.2	204.4 ± 4.5	203.1 ± 3.6	184.0 ± 4.7
PI[a]	0.18 ± 0.01	0.17 ± 0.01	0.17 ± 0.03	0.10 ± 0.05
ZP (mV)[b]	18.55 ± 2.31	18.22 ± 1.38	20.46 ± 0.04	-35.45 ± 0.02
HBsAg LE (%)[c]	≥ 96	≥ 96	≥ 96	≥ 96

[a] Polydispersity index, [b] Zeta Potential, [c] Loading efficacy

B
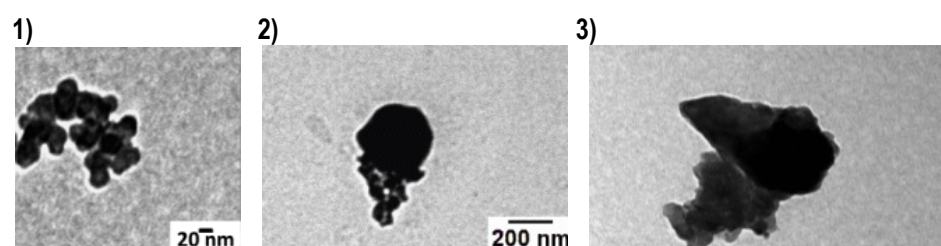
Figure 1: Characterization of formulations for vaccination studies. (A) Particle mean size distribution, zeta potential and HBsAg loading efficacy of 403.5NPs, 807NPs, 1614NPs and 807NPs+CpG formulations. Data are presented as mean ± SD, n =3. (B) Representative TEM images of HBsAg virus-like particles (1) and HBsAg loaded PCL/chitosan NPs after fixing, contrasting and embedding into formvar coated nickel electron microscope grids (2 and 3).

In a previous study [15], we showed *in vitro* PCL/chitosan NPs capability to be considered a protein delivery system. The present study aimed to explore the intrinsic immunostimulatory activity of PCL/chitosan NPs as to the best of author knowledge, nothing was reported until the moment.

3.2. PCL/Chitosan NPs are efficiently internalized but do not induce TNF-α production by human monocytes

Phagocytic cells, such as polymorphonuclear cells, macrophages and monocytes take up pathogens and particles. Therefore, the ability of PCL/chitosan NPs to be internalized by human PBMCs, particularly by monocytes (Fig. 2A, R2 gate) was investigated. These cells were chosen since they are, among others, normally recruited to the local of vaccine injection. After cell incubation with 2 different FITC-NP concentrations, cells were analyzed using flow cytometry. Less than 2 % of cells internalized propidium iodide (PI) (Fig. 2B, right Y axis), meaning that the 2 NP concentrations used revealed to be not toxic to the cells under the assay conditions. To quench the fluorescence of the particles adsorbed on cell surface and not internalized, a second analysis was performed using trypan

blue. Although, cells have been washed in order to eliminate NPs adsorbed on cell surface, the results showed that some particles remained on cell surface (Fig. 2B, left Y axis). In any case, a fluorescence approximately 4-fold and 7-fold higher than control was registered with 10 µg/mL and 20 µg/mL of NPs respectively, meaning that NPs were efficiently internalized and its cellular uptake seems to be related with the amount of NPs incubated with cells, considering the concentration range studied.

Following cellular interaction, NPs can be recognized as invaders and induce the generation of signals from innate immune system like the production of inflammatory mediators. To assess whether PCL/chitosan NPs had pro-inflammatory activity through the TNF- pathway, PBMCs were stimulated during 24 h with different NP concentrations (LPS free). TNF- is a pro-inflammatory cytokine generally viewed as an early mediator of inflammatory reactions [20]. Nonetheless, some particulate adjuvants have shown to create a local pro-inflammatory environment to recruit immune cells and the up-regulation of cytokines and chemokines is one of the mechanisms associated to it [21]. LPS was used in this experiment as a positive control for TNF- production and as expected induced elevated concentrations of this cytokine (Fig. 2D). In contrast, PCL/chitosan NPs did not induce TNF- production within the range of 5 µg/mL to 40 µg/mL, even with cell viability decreasing to values near 50 % with the highest NP concentration (Fig. 2E). To the best of author's knowledge, no previous reports tested the TNF- release from PBMCs after stimulation with PCL/chitosan NPs. However, in 1994 Otterlei et al. were the first to report chitosan's ability to induce TNF- production by monocytes accordingly to its molecular weight and deacethylation degree [22]. More recently, chitosan oligosaccharides (LPS free) were found to stimulate TNF- production by RAW264.7 macrophages [23]. In contrast, a report about the *in vitro* cellular responses induced by polyesters, showed only a low inflammatory response of J774 macrophages, after 48 h incubation with PCL pure polymer and made no reference to LPS contamination of the material [24]. PLGA, similarly to PCL, is a polyester and is widely used to prepare vaccine delivery systems. Xiong and co-workers [25] found that PLGA NPs with sizes superior to 100 nm, did not induce TNF- production on RAW264.7 macrophages after 24 h incubation, in contrast to 60 nm NPs. Another study also observed that bare and PEGylated PLGA NPs (> 300 nm) did not stimulate TNF- production by monocytes isolated from PBMCs [26]. Therefore, like other NPs already described, PCL/chitosan NPs did not induce an immune response through a mechanism dependent of inflammatory TNF- pathway.

142

A

B

C

D

E
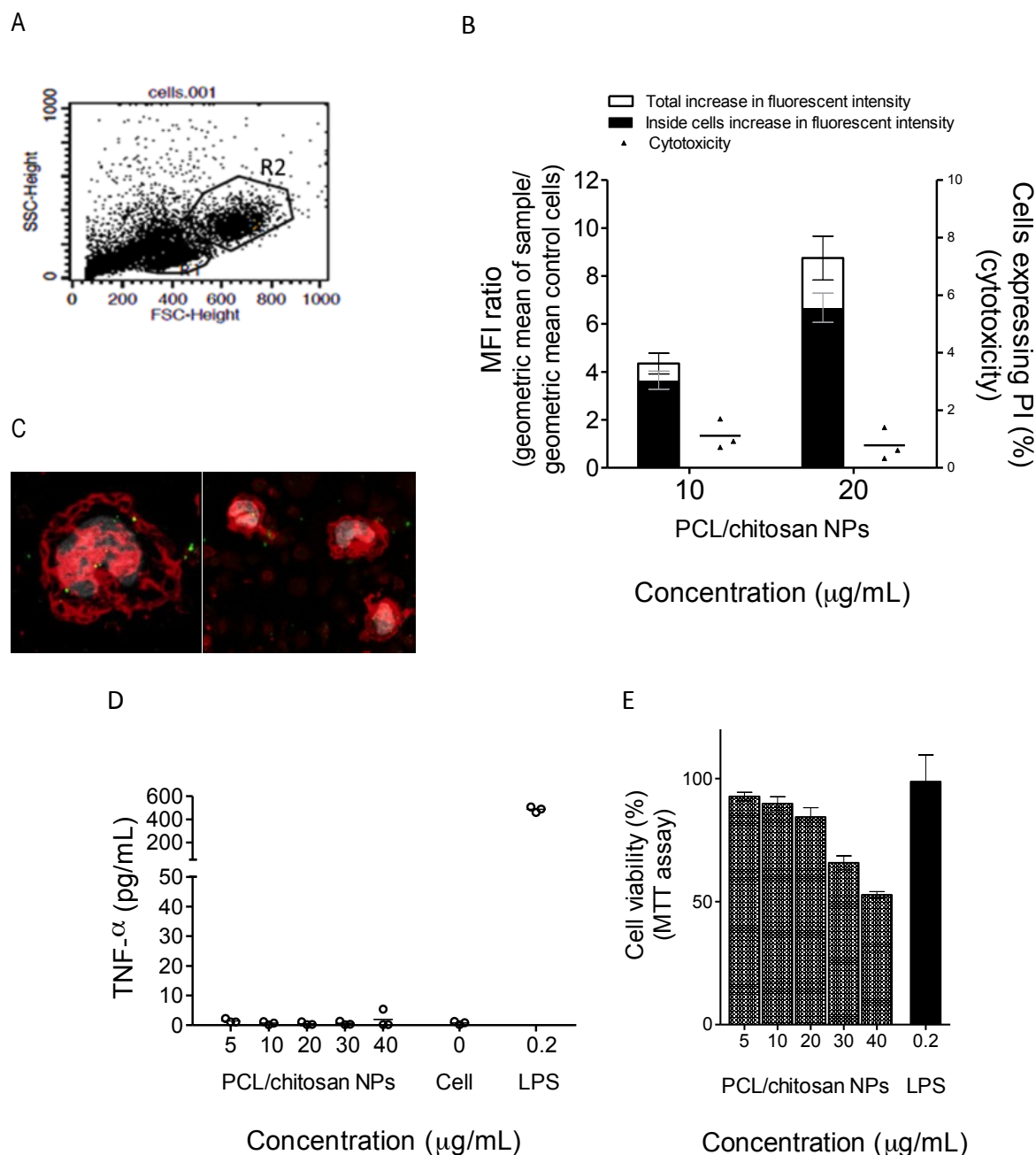
Figure 2: *In vitro* studies with PBMCs. (A) Flow cytometry setting regions used to identify PBMCs subpopulation: monocytes and lymphocytes were identified on a FSC vs SSC dot plot using free draw regions. (B) Flow cytometry analysis of NPs uptake by monocytes (R2 region) after 4 h incubation with PBMCs. NPs uptake (black) and cell surface interaction (white) were evaluated and the results expressed as mean fluorescence intensity (MFI) ratio (left Y axis) between the geometric mean of the sample and the geometric mean of the background. For cytotoxicity evaluation (right Y axis), the percentage of cells expressing PI were evaluated by the threshold criterion. Data are expressed as mean ± SEM, n= 3. (C) Confocal microscopy of FITC labeled PCL/chitosan NPs uptake by monocytes. Images represent the merging of z-stack slides, where it is possible to observe the nuclei in white, the cell membrane in red and the NPs in green. It is to note that while optimizing the NPs fluorescent

intensity with the merging option, the resulting images represent some NPs efficiently inside the cells while others are attached to the membrane. (D) TNF- release by PBMCs after stimulation with different concentrations of PCL/Chitosan NPs during 24 h. LPS was used as positive control. Basal TNF- production was considered the negative control. Data points correspond to replicates of 3 independent assays. (E) PBMCs were assessed for cell viability (%) under the conditions of TNF- release experiment through MTT cell viability assay. Data are expressed as mean ± SEM, n=5.

3.3. PCL/chitosan NPs are mast cell activators, inducing β-hexosaminidase release

Another type of cells that can be recruited for the local of injection during vaccination is mast cells. Their role in inflammation, allergic immune responses and as vaccine adjuvants is still not completely clarified. In fact, in recent years, mast cell activators have been described as good vaccine adjuvants [27, 28]. Mast cell degranulation occurs after cell stimulation by specific molecules and is characterized by the release of small vesicles containing inflammatory mediators. These vesicles have the ability to drain to local lymph nodes via lymphatics or activate APCs nearby which may result in the initiation of adaptive immune responses [6, 29]. To evaluate the capability of PCL/Chitosan NPs to act as mast cell activators several NP concentrations were tested with HMC-1 cells, a human mast cell line. C48/80, a well-known mast cell activator [27], was used on this experiment as a positive control. It was found that the percentage of -hex, released from HMC-1 cells, was dose-dependent (Fig. 3A, left Y axis). In particular, the lowest NP concentrations (40 µg/mL and 80 µg/mL) were able to induce as much -hex release as 40 µg/mL C48/80. On the other hand, the highest NP concentration (150 µg/mL) induced a -hex release statistically similar to 80 µg/mL C48/80. In order to understand the influence of chitosan and PCL in the mast cell activation, a control with PCL NPs (without chitosan) produced by the same production technique, was tested at a concentration of 150 µg/mL. Contrary to PCL/chitosan NPs, the value for -hex release induced by PCL NPs was statistically lower than 80 µg/mL C48/80, indicating that the chitosan included in NPs, might have an important role on mast cell activation. For all conditions tested, cell viability results were above 100 %, meaning that there was not any cytotoxic effect associated to the -hex release. Therefore, PCL/chitosan NPs are mast cell activators and do not depend on cell death to mediate its effects.

A

B

HMC-1 cells without stimullus

HMC-1 cells stimulated with C48/80

HMC-1 cells stimulated with PCL/chitosan NPs

C
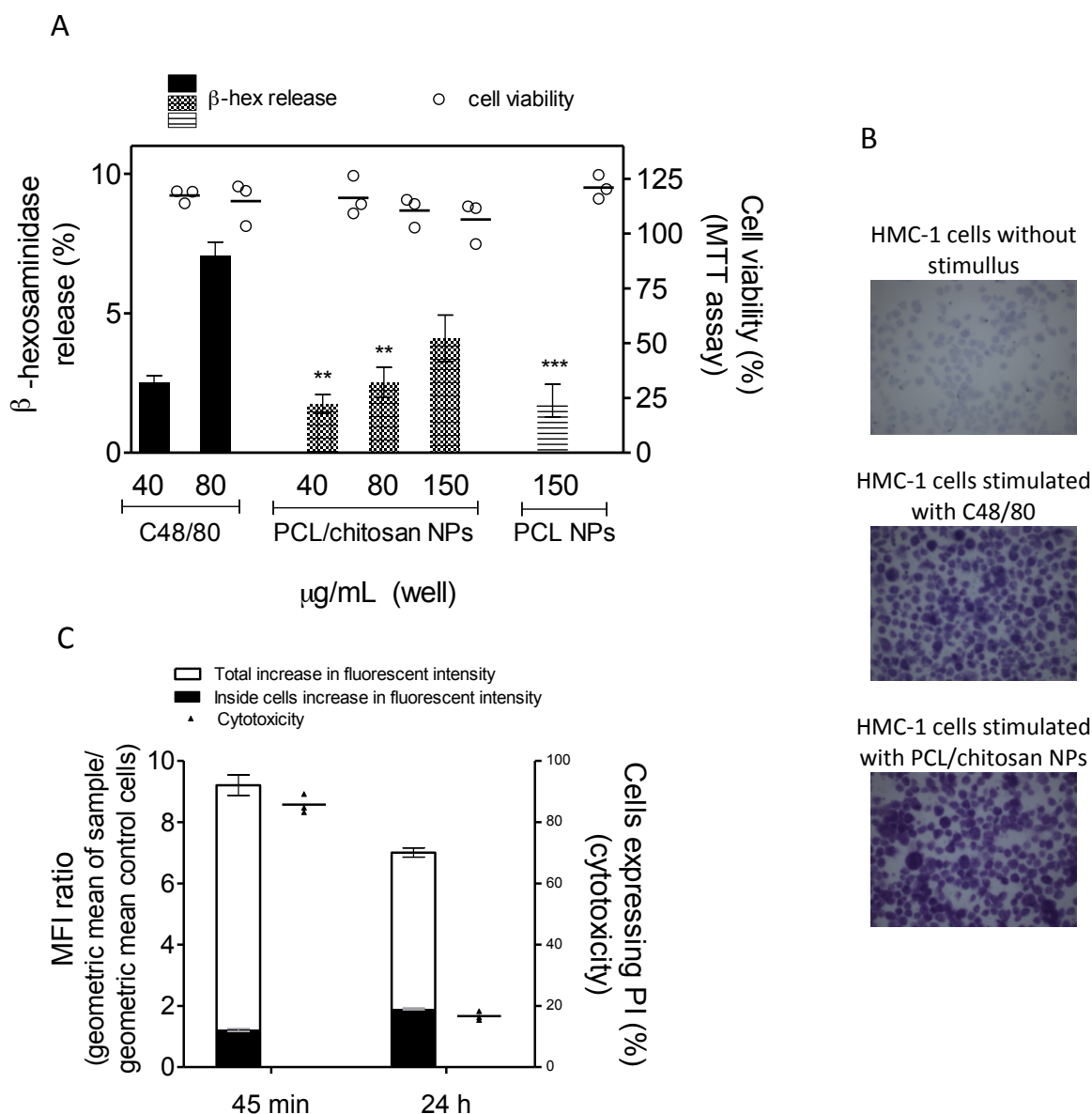
Figure 3: Evaluation of HMC-1 cellular activation. (A) Percentage of -hex release (left Y axis) and cell viability (right Y axis) induced on HMC-1 cell line by C48/80, PCL/chitosan NPs and PCL NPs at different concentrations. Data are presented as mean ± SEM, n≥3. ** $p < 0.01$ refers to NPs concentrations that differ from C48/80 at 80 g/mL. All other comparisons to positive controls present no statistical differences. (B) HMC-1 cell activation illustrated by the toluidine blue dye assay. From top to bottom: untreated cells, cells submitted to incubation with 80 μg/mL C48/80 and cells submitted to 80 μg/mL PCL/Chitosan NPs. Their granularity evidenced by toluidine blue staining after cell fixation was observed by microscopy on a Zeiss Axioskop 2 plus with a PlanNeofluar 20x objective (Carl Zeiss AG, Oberkochen, DE) and representative areas are presented. (C) Evaluation of HMC-1 cellular interaction with FITC-labeled PCL/chitosan NPs after 45 min incubation period and 24 h after incubation and medium replacement. Uptake (black) or cell surface interaction (white) were evaluated by the mean fluorescence intensity (MFI) ratio between the geometric mean of the sample and the geometric mean of the

background (left Y axis). At the same time intervals, the percentage of cells expressing PI was evaluated by the threshold criterion (right Y axis). Data are expressed as mean ± SEM, n= 3.

Regarding mast cell activation, although PCL/chitosan NPs had not been evaluated before, previous studies reported the effects of chitosan oligonucleotides and chitosan polysaccharide in rat basophilic leukemia cell line (RBL-2H3) [30]. These chitosan oligonucleotides demonstrated an inhibitory effect on mast cell activation through downregulation of the high-affinity receptor for IgE (Fc RI) expression [30]. Contrasting with this result, chitosan polysaccharide was able to induce activation on the same cell line [31]. Moreover, chitosan NPs were able to activate mast cells apparently due to the extensive adsorption on mast cells surface immediately after being added to the cells [7]. Considering PCL and mast cells interaction, PCL electrospun scaffolds coated with fibronectin have shown to be able to support mast cell adhesion [32]. However, on the PCL scaffold, mast cells only proliferated and increased cytokine production (TNF- , MIP-1 and IL-13), when stimulated with IgE and antigen (dinitrophenyl-human serum albumin) [32]. In present study PCL NPs showed that, although some activation was present, the effect was lower than for PCL/chitosan NPs. In line with what was said, PCL/chitosan NPs ability to activate mast cells may be enhanced due to chitosan presence at its surface, which may also influence NPs adsorption on the mast cell surface. Aridor and co-workers [33] suggested that the capacity to induce mast cell degranulation demonstrated by peptides and other polybasic molecules involves the insertion of their hydrophobic moiety into the membrane, enabling its positively charged domain to interact and directly activate G proteins in a receptor-independent manner. Since PCL/chitosan NPs present the hydrophobic properties of PCL associated to the positive chitosan charges, we may assume a similar activation mechanism.

In order to better explain HMC-1 activation by PCL/chitosan NPs flow cytometry studies were performed on cells after 45 min incubation with FITC labeled NPs, or 24 h after the incubation period. After 45 min incubation, results showed a major interaction of the NPs with cell surface, since the fluorescence detected was mostly quenched by trypan blue (Fig. 3C, left Y axis). This means NPs did not enter the cells to activate them. This observation withstands the fact that mast cells possess high-affinity binding receptors at their surface (Fc RI, Fc RIIB and Fc RIIIA), which may be responsible for the cell activation [34]. Surprisingly, when using PI to assess cell membrane integrity, the results demonstrated an elevated percentage of cells positive for this marker (Fig.3C, right Y axis). This result contradicts the MTT cell viability results previously presented (Fig. 3A, right Y axis) and therefore we theorized that this permeability was most likely associated to the -hex release and was not long-lasting. To confirm this, after the 45 min incubation with particles, cells were washed and incubated with complete culture medium for more 24 h before the flow cytometry analysis. While, right after the 45 min

incubation with particles, more than 80 % of cells presented a PI permeable membrane, after 24 h recovering at normal cell culture conditions, the permeability was restored to less than 20 %. On the other hand, the overall MFI ratio only showed a slight decrease. With these results, it was possible to conclude that PCL/chitosan NPs are effective mast cell activators, enhancing mast cell membrane permeability and consequent -hex release without causing irreversible damage to cells.

3.4. Subcutaneous vaccination with HBsAg loaded PCL/chitosan NPs induces a strong humoral immune response dependent on the adjuvant dose

In vitro mast cell activation studies suggested that PCL/chitosan NPs could act as a vaccine adjuvant. In order to validate this hypothesis, three test formulations, each with a different amount of NPs and equal antigen concentration, were subcutaneously administered (see table 1 for detailed dose information). A fourth group was also included in the study to evaluate if CpG-ODN loaded PCL/chitosan NPs were able to shift the immune response for a Th1 associated immune profile, similarly to CpG-ODN loaded chitosan NPs previously reported by us [14]. Control groups included the free HBsAg and the commercially available vaccine, Engerix-B. The free HBsAg was not able to induce the generation of detectable IgG endpoint-titers with a 1:128 serum dilution, after the first immunization (Fig.4A). However, we are aware HBsAg VLPs have intrinsic immunogenicity [35, 36] and a lower detection limit would most probably allow for the detection of anti-HBsAg IgG titers. Contrasting with this result, both the NPs adjuvanted HBsAg and the Engerix-B formulations were able to generate good anti-HBsAg IgG titers. In fact, no statistical difference was found between the IgG titers generated by the four NP-based formulations and the Engerix-B formulation, which contains aluminum hydroxide as adjuvant. These results from the prime immunization sustain the fact that PCL/chitosan NPs act as an efficient vaccine adjuvant that increase HBsAg immune response. At day 42, all mice efficiently presented detectable anti-HBsAg IgG titers and as expected, free HBsAg induced lower levels of antibodies compared to the other formulations (Fig.4B). Among the NPs-based formulations, the 1614NPs one was particularly important, since the titers induced by it were also statistically higher than the ones induced by Engerix-B ($p<0.05$).

147
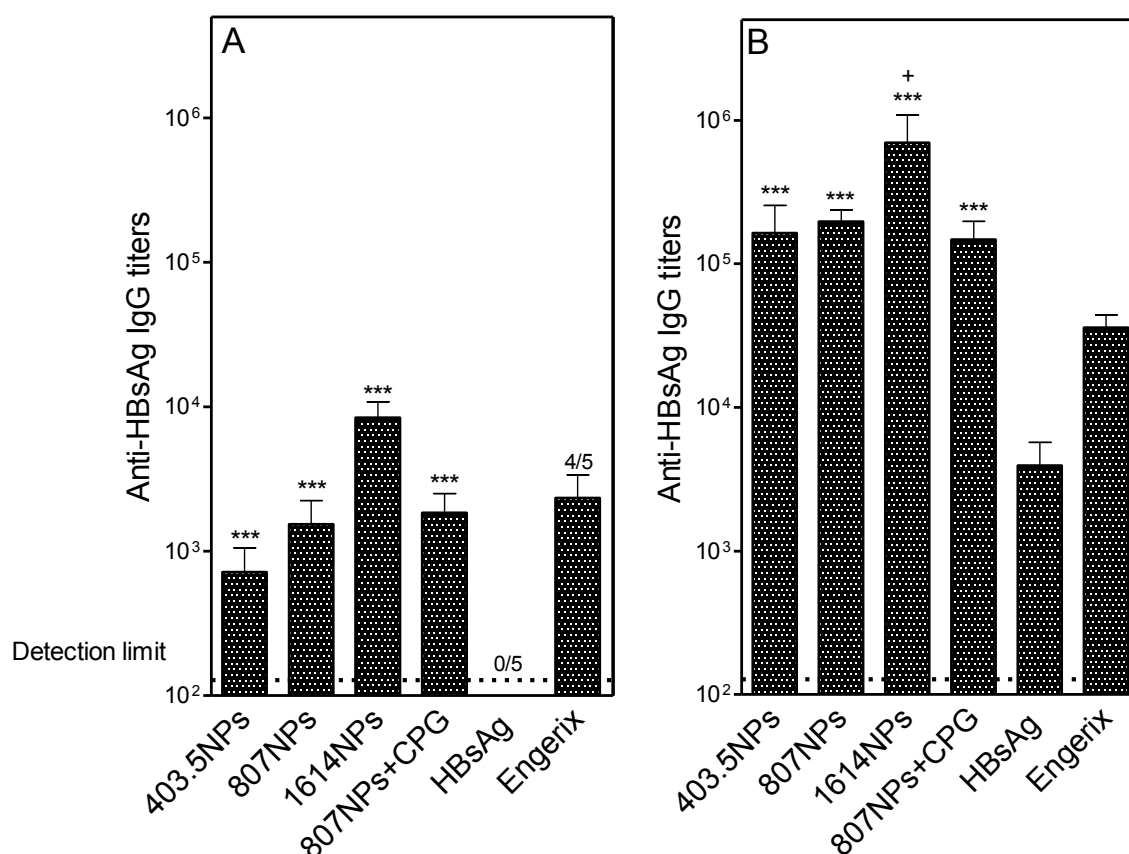
Figure 4: Immune response of SC immunized mice at day 14 (A) and day 42 (B). Serum anti-HBsAg IgG levels of mice immunized with formulations containing increasing amounts of PCL/chitosan NPs (403.5, 807 and 1614 g/dose) and 1.5 µg/dose of HBsAg, on days 0 and 14. Also, a formulation containing a second adjuvant (CpG-ODN, 20 g added to the 807 g/dose NPs formulation) was included in the study. Control corresponds to free HBsAg and Engerix-B, both dosed to 1.5 µg of antigen. Antibody levels were determined by ELISA as described in 'Materials and methods'. The end-point titer presented in the results represents the antilog of the last log 2 dilution for which the OD were at least two-fold higher than the value of the naive sample equally diluted. Numbers above bars represent the number of mice on which antibody levels were detected, if were not detected on all mice; Data are presented as mean ± SEM, n = 5. ***p < 0.001 indicates values that differ significantly from HBsAg control group. +p < 0.05 indicates values that differ significantly from Engerix-B control group.

3.5. HBsAg loaded PCL/chitosan NPs do not induce anti-HBsAg IgE production

PCL/chitosan NPs ability to activate MCs may generate a controversial discussion regarding the induction of IgE antibodies after vaccination. MCs are known to be involved in IgE mediated allergic responses, but they do not necessarily induce antigen specific IgE after vaccination [37]. Also, IgE responses in mice are normally transient and derived from short lived plasma cells resultant from a secondary encounter with an antigen [38]. Only in few situations a small population of long lived plasma

cells are located in the bone marrow and contribute to low levels of IgE sustained release [38]. However, since the non-desired IgE antibody production may be related to allergic or anaphylactic reactions upon antigen challenge [37], we evaluate our formulations regarding the induction of IgE at day 42, three weeks after the last vaccine boost. None of the formulations containing only HBsAg loaded PCL/chitosan NPs induced detectable IgE titers (Fig. 5A). These results are consistent with a previous report of our group, in which chitosan NPs formulated with or without C48/80 and presenting MC activation ability, did not induce IgE titers at day 42, after 3 intranasal immunizations with the *Bacillus anthracis* protective antigen [7]. Surprisingly, the HBsAg loaded PCL/chitosan NPs- adjuvanted with GpG, induced IgE titers in all immunized mice. CpG-ODN is a TLR-9 agonist capable of inducing Th1 based immune responses *in vitro* and *in vivo*. IgE in its turn, is a Th2 antibody downregulated by Th1 type cytokines meaning the adjuvant effect of CpG-ODN was expected to avoid this cytokine production [39]. Moreover, allergy studies sustain the use of CpG-ODN as vaccine adjuvants reducing IgE titers [39]. Nonetheless, a prophylactic vaccination study conducted by McGowen and co-workers [37] also observed that when using *Bacillus anthracis* protective antigen adjuvanted with 10 g of CpG-ODN by intradermal route, low IgE titers in 2 out of 4 mice were generated (2 immunizations, titers evaluated at day 42) [37]. In our study, we used a different immunization route and a 2-fold higher CpG-ODN dose which might explain detectable titers in all mice immunized with 807NPs+CpG formulation.

In the literature is widely reported the generation of IgE antibodies when aluminum salts are employed as vaccine adjuvants [3] and a recent study suggests the anti-HBV specific IgG and IgE responses are key factors for the persistent viral memory in children after HBV vaccination with the hepatitis B vaccine containing aluminum hydroxide [40]. However we found that the SC administration Engerix-B did not induce detectable specific IgE titers at day 42. We might suggest that the absence of IgE in this case may be related to the amount of aluminum hydroxide per dose which was 37.5 g for each 1.5 g HBsAg immunization dose. Yanase et al. [41] showed elevated IgE titers at day 35, on BALB/c mice subcutaneously vaccinated with 10 g ovalbumin and 200 g aluminum hydroxide (vaccines at day 0 and day 28). Next, at day 42 they reported that the IgE titers had diminished comparing to day 35, meaning the stronger IgE response may be transient. Our adjuvant dose was 5-fold less, and the evaluation of the IgE titer was 28 days after the last immunization. If IgE was induced, the titers might already be decreased at day 42 and therefore non-detectable.

Finally, considering the free HBsAg immunized mice, 2 animals developed IgE specific titers compatible with the detection limit of our test, which may be justified by the intrinsic immunostimulatory properties of HBsAg VLPs, expected to induce a Th2 immune response.

The anti-HBsAg IgG subtypes IgG1, IgG2c and IgG3, were also evaluated to understand the profile of immune response generated by each formulation. High serum specific IgG1 titers were found in all

groups, similar to the anti-HBsAg IgG titers (Fig. 5B). On the other hand, the generation of Th1 antibodies (IgG2c and IgG3) was low or inexistent in all immunized mice (Fig. 5C and 5D). Animals immunized with free HBsAg did not develop Th1 antibodies. Only one mouse from Engerix-B presented a low IgG2c titer, which was expected as the aluminum hydroxide adjuvant is typically responsible for Th2 type immune responses [42]. Regarding the animals immunized with the PCL/chitosan NPs-HBsAg formulations, one animal from each group presented serum specific IgG2c. On its turn, IgG3 was detected in 4 out of 5 animals immunized with the 807NPs+CpG formulation.
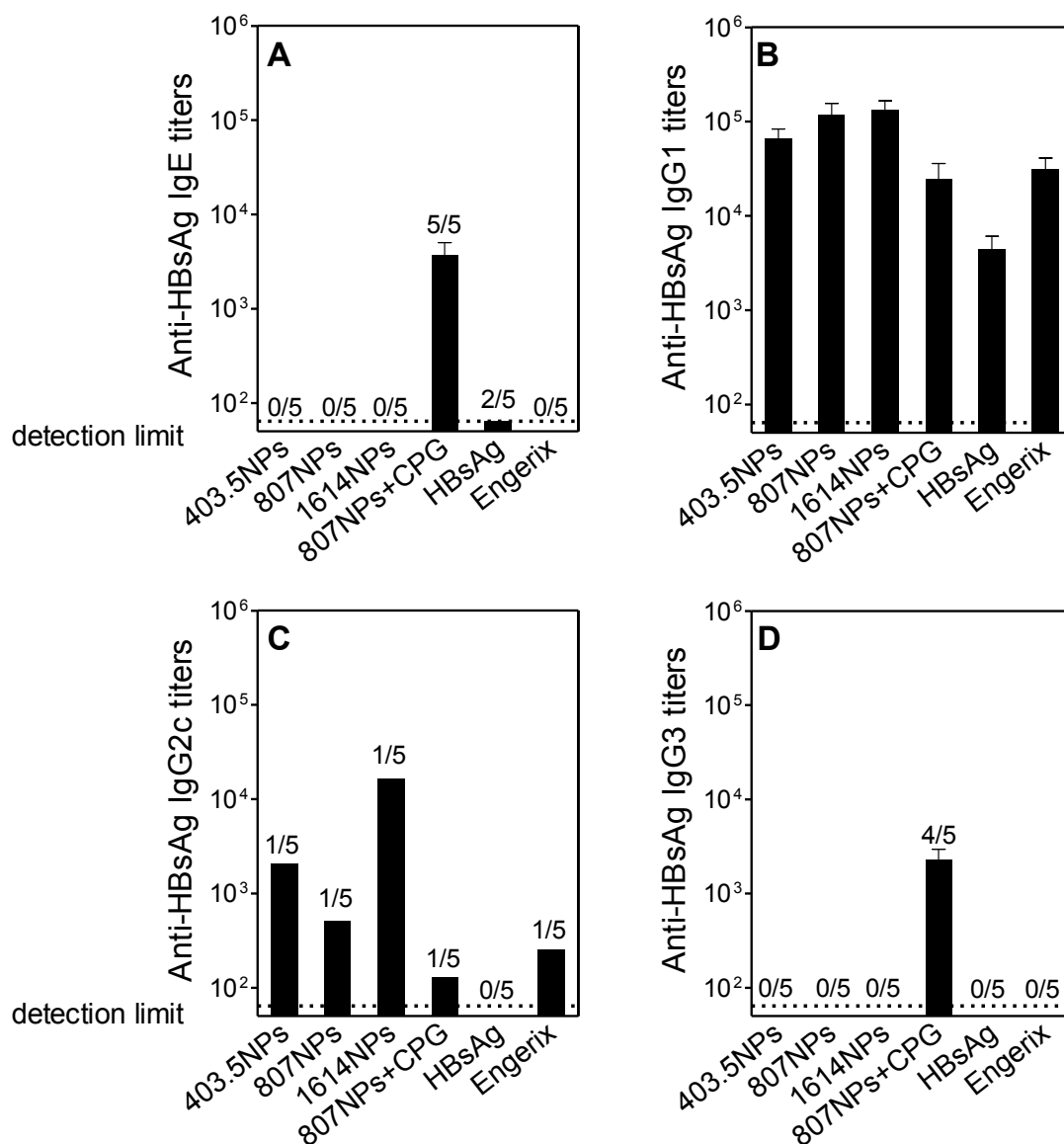
Figure 5: Immune response profile of SC immunized mice. Serum anti-HBsAg IgE (A), IgG1 (B), IgG2c (C) and IgG3 (D) levels of mice immunized with formulations containing increasing amounts of PCL/chitosan NPs (403.5, 807 and 1614 g/dose) and 1.5 μg/dose of HBsAg, on days 0 and 14. Also, a formulation containing a second adjuvant (CpG, 20 g added to the 403.5 g NP formulation) was included in the study. Control corresponds to free HBsAg and Engerix-B, both dosed to 1.5 μg of antigen as for the NPs. Blood was collected on days 14 and

42. IgG1 and IgG2c antibody levels at day 42 were determined by ELISA as described in 'Materials and methods'. The end-point titer presented in the results represents the antilog of the last log 2 dilution for which the OD were at least two-fold higher than the value of the naive sample equally diluted. Numbers above bars represent the number of mice on which antibody levels were detected, if were not detected on all mice; Data are presented as mean ± SEM, n= 5.

Considering the results we may hypothesize that the PCL/chitosan NPs adjuvant effect was not able to shift the antibody immune response to a more Th1 type. Nevertheless, in the 1614NPs group, the animal that presented IgG2c titers possessed a more balanced Th1/Th2 immune response with a ratio IgG2c/IgG1 of 0.76. The evaluation of the response induced by the 807NPs+CPG formulation revealed increased Th1 specific antibody titers in all animals. Calculating the ratios IgG3/IgG1 (from 4 out of 5 animals) or IgG2c/IgG1 (from 1 out of 5 animals) we reach a mean value of 0.76 which indicate that CpG was efficiently helping the formulation contributing to a more balanced Th1/Th2 immune response. These results are consistent with a previous work from our group [14] that reported an increase in the Th1/Th2 antibodies ratio from 0.1 to 1.0, when 20 g CpG-ODN were added to alginate coated chitosan NPs loaded with HBsAg.

So far results suggest that vaccines containing PCL/chitosan NPs were able to induce an increase in antibody titers against HBsAg, dependent on the NPs concentration. The titers were significantly higher than those induced by free HBsAg ($p<0.001$) and Engerix-B ($p<0.05$ for the 1614NPs formulation). Nevertheless, the humoral immune response Th-bias remained unchanged (Th2) for almost all animals, except for the group containing the extra Th1 adjuvant: CpG-ODN.

3.6. The adjuvant effect of PCL/chitosan NPs is characterized by a Th1/Th17 cellular immune response

Cytokines have a major role in cell mediated immune responses. CD4+ T cells may be divided in different populations according to the cytokines they secrete [43]. Th1 CD4+ T cells secrete IFN- and IL-2, are responsible for cell mediated immunity and provide helper function for specific IgG classes production involved in the virus neutralization and opsonization Th2 CD4+ T cells secrete mainly IL-4, and are responsible for B cell activation (T cell dependent activation) and consequent antibody production [43]. A third subset of CD4+ T cells produces IL-17 and IL- 22, and are implicated in protective cellular and memory responses, increasing immunity against a range of pathogens upon vaccination [44, 45]. In this report, cytokines production by immunized mice spleen cells after stimulation with HBsAg were analyzed for better understanding of adjuvant mechanism of PCL/chitosan NPs generated during vaccination.

151

A

B
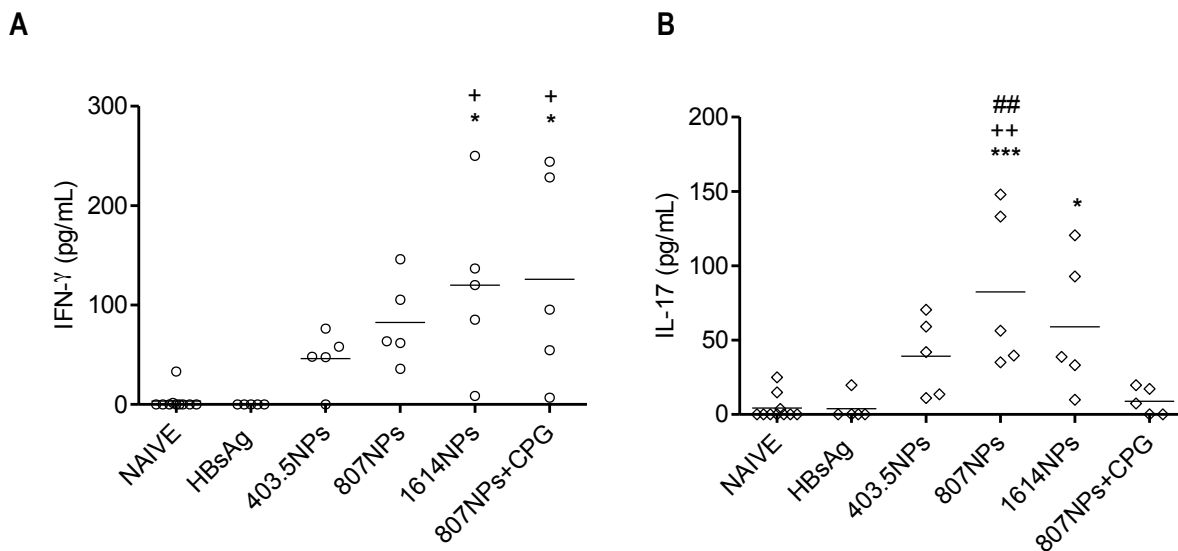
Figure 6: Spleen cells (0.25x10^6 cells/well) from both immunized and naïve C57/BL6 mice were stimulated with 1 g HBsAg as described in 'Materials and methods'. Supernatants were collected 72 h later and tested for IFN- and IL-17 by ELISA. Results are expressed as mean cytokine concentrations ± SEM, resulting from HBsAg stimulation (basal concentration subtracted) for each group of 5 immunized mice and 10 naïve mice. *p < 0.05 and ***p < 0.001 indicates values that differ significantly from naive group. +p < 0.05 and ++p < 0.01 indicates values that differ significantly from HBsAg control group. ##p ≤ 0.01 indicates values that differ significantly for the group containing CpG-ODN.

In regard to specific IL-4, there was no production of this cytokine upon re-stimulation with HBsAg (data not shown). On the other hand, specific IFN- production showed interesting differences. Spleen cells from mice immunized with free HBsAg did not produce IFN- upon re-stimulation with HBsAg. Conversely IFN- increased production seemed dependent on the amount of NPs used in the formulations (Fig. 6A). As a matter of fact, the IFN- production increase observed in spleen cells from mice immunized with the 1614NPs formulation was significantly different (p <0.05) from the production observed in naïve mice and in mice immunized with free HBsAg. This increased IFN- production was similar to the obtained in mice vaccinated with 807NPs+CpG formulation. Several reports have studied the effect of CPG in the re-direction of Th- bias of immune responses against several antigens, including HBsAg [14, 46-48]. Similarities between the 1614NPs and 807NPs+CpG formulation regarding IFN- production suggest that the adjuvant activity of PCL/chitosan NPs is directed for a Th1 cellular bias and is dose dependent. Other polymeric NPs have already showed advantages on cellular immune response redirection. In fact, poly(D,L-lactide) (PLA) NPs, when loaded with HBsAg lead to high levels of IFN- production and antibody isotypes, indicative of a Th1-type immune response [49]. Hydrophobic NPs based on poly(D,L-lactide-co-glycolide) (PLGA) modified with chitosan or its derivatives also increased IFN- production on vaccinated mice [50, 51].

While free HBsAg was not able to induce antigen specific IL-17 production in immunized mice, HBsAg loaded PCL/chitosan NPs formulations induced a Th17 profile cellular immune response (Fig. 6B). In fact, the 807NPs and 1614NPs formulations induced an increase in IL-17 titers statistically different from the naïve mice ($p \leq 0.05$) and from the HBsAg immunized mice (807NPs only, $p < 0.01$). Consistent with this, a recent publication from our group also showed that nasal immunization with chitosan nanoparticles containing *Bacillus anthracis* protective antigen (PA), caused IL-17 and IL-22 production in mice spleen cells, after re-stimulation with PA [7]. Nevertheless, authors have no knowledge of published work revealing the induction of IL-17 cytokine in mice vaccinated with HBsAg and polymeric NPs.

Interestingly, the 807NPs+CpG formulation did not induce increased IL-17 production upon stimulation. In fact, PCL/chitosan NPs contributed to a Th17 cellular based immune response but the addition of CpG-ODN containing formulation inhibited that pathway. In the literature, some controversial results regarding CpG-ODN adjuvant mechanism can be found. In accordance to our work, Verwaerde and co-workers [44] reported that the addition of CpG-ODN to a nanoparticulate carrier of heparin binding hemagglutinin antigen (HBHA) would increase IFN- but decrease IL-17 production on spleen cells of vaccinated mice, after HBHA stimulation. This inhibition may be related to the CpG-ODN adjuvant mechanism of action which comprises the secretion of IL-12 cytokine by APCs in order to polarize a Th1 immune response [52]. The increase in IL-12 secretion may be responsible for the negative regulation of Th17 cellular differentiation and therefore the abolishment of IL-17 production [52].

So far, *in vivo* we proved that PCL/chitosan NPs is a promising vaccine adjuvant, eliciting stronger systemic immune responses to HBsAg than simple HBsAg and even Engerix-B vaccine without inducing IgE antibodies. The adjuvant effect observed was dose dependent and significantly higher serum specific IgG titers were found when the maximum amount of NPs was used (1614 g/dose). Also, PCL/chitosan NPs induced higher IFN- and IL-17 cell production suggesting a Th1/Th17 cellular based immune response, different from what was observed with the additional use of CpG-ODN.

4. Conclusions

The most sough adjuvant effects in the vaccine field is the enhancement of antigen immunogenicity and modulation of the immune response; however they have much more capabilities. Vaccine adjuvants faster antibody production kinetics, prolong the achieved protection or even improve the responses among poor responder populations. Moreover, by providing a dose-sparing effect and reducing the need for booster immunizations, vaccine adjuvants may reduce immunization schedules and costs, and therefore expand vaccination benefits especially in developing countries [53]. In this study, PCL/chitosan NPs showed evident adjuvant ability, inducing higher anti-HBsAg IgG titers than the commercially available vaccine Engerix-B, using the same antigen dose. A key aspect of the results was the IFN- and IL-17 spleen cell production in mice immunized with HBsAg loaded PCL/chitosan NPs. The combination of strong humoral antigen levels, with cell mediated immune responses, represents the best way to achieve protection through vaccine immunization and may constitute a valuable alternative to alum-based vaccines. Finally, to the best of author's knowledge this is the first time a PCL based delivery system is described as a potential MC activator. For vaccine adjuvant purposes, the cellular activation mechanisms underlying the immunostimulatory effect of the delivery systems are of great importance to develop efficient vaccine formulations. Mechanistic approaches, concerning the polymeric NPs activation of the immune system, may provide essential knowledge for future vaccination strategies based on a rational vaccine design.

References

1.	Akagi, T., M. Baba, and M. Akashi, *Biodegradable Nanoparticles as Vaccine Adjuvants and Delivery Systems: Regulation of Immune Responses by Nanoparticle-Based Vaccine*, in *Polymers in Nanomedicine*, S. Kunugi and T. Yamaoka, Editors. 2012, Springer Berlin Heidelberg. p. 31-64.

2.	Joshi, V.B., S.M. Geary, and A.K. Salem, *Biodegradable particles as vaccine antigen delivery systems for stimulating cellular immune responses.* Hum Vaccin Immunother, 2013. **9**(12): p. 2584-90.

3.	Powell, B.S., A.K. Andrianov, and P.C. Fusco, *Polyionic vaccine adjuvants: another look at aluminum salts and polyelectrolytes.* Clin Exp Vaccine Res, 2015. **4**(1): p. 23-45.

4.	Abraham, S.N. and A.L. St John, *Mast cell-orchestrated immunity to pathogens.* Nat Rev Immunol, 2010. **10**(6): p. 440-52.

5.	St John, A.L., et al., *Synthetic mast-cell granules as adjuvants to promote and polarize immunity in lymph nodes.* Nat Mater, 2012. **11**(3): p. 250-7.

6.	Kunder, C.A., et al., *Mast cell-derived particles deliver peripheral signals to remote lymph nodes.* J Exp Med, 2009. **206**(11): p. 2455-67.

7.	Bento, D., et al., *Development of a novel adjuvanted nasal vaccine: C48/80 associated with chitosan nanoparticles as a path to enhance mucosal immunity.* Eur J Pharm Biopharm, 2015. **93**: p. 149-64.

8.	Staats, H.F., et al., *Mucosal targeting of a BoNT/A subunit vaccine adjuvanted with a mast cell activator enhances induction of BoNT/A neutralizing antibodies in rabbits.* PLoS One, 2011. **6**(1): p. e16532.

9.	Dash, T.K. and V.B. Konkimalla, *Poly-epsilon-caprolactone based formulations for drug delivery and tissue engineering: A review.* J Control Release, 2012. **158**(1): p. 15-33.

10.	Ulery, B.D., et al., *Rational design of pathogen-mimicking amphiphilic materials as nanoadjuvants.* Sci Rep, 2011. **1**: p. 198.

11.	Neumann, S., et al., *Activation of the NLRP3 inflammasome is not a feature of all particulate vaccine adjuvants.* Immunol Cell Biol, 2014. **92**(6): p. 535-42.

12.	Lin, Y.C., P.J. Lou, and T.H. Young, *Chitosan as an adjuvant-like substrate for dendritic cell culture to enhance antitumor effects.* Biomaterials, 2014. **35**(31): p. 8867-75.

13.	Scherliess, R., et al., *In vivo evaluation of chitosan as an adjuvant in subcutaneous vaccine formulations.* Vaccine, 2013. **31**(42): p. 4812-9.

14.	Borges, O., et al., *Alginate coated chitosan nanoparticles are an effective subcutaneous adjuvant for hepatitis B surface antigen.* Int Immunopharmacol, 2008. **8**(13-14): p. 1773-80.

15.	Jesus, S., G. Borchard, and O. Borges, *Freeze Dried Chitosan/ Poly- e-Caprolactone and Poly-e-Caprolactone Nanoparticles: Evaluation of their Potential as DNA and Antigen Delivery Systems.* J Genet Syndr Gene Ther 2013. **4**(164).

16.	Bilensoy, E., et al., *Intravesical cationic nanoparticles of chitosan and polycaprolactone for the delivery of Mitomycin C to bladder tumors.* Int J Pharm, 2009. **371**(1-2): p. 170-6.

17.	Florindo, H.F., et al., *The enhancement of the immune response against S. equi antigens through the intranasal administration of poly-epsilon-caprolactone-based nanoparticles.* Biomaterials, 2009. **30**(5): p. 879-91.

18.	Gupta, N.K., et al., *Development and characterization of chitosan coated poly-(varepsilon-caprolactone) nanoparticulate system for effective immunization against influenza.* Vaccine, 2011. **29**(48): p. 9026-37.

19.	Greiner, V.J., et al., *Characterization of the lipid and protein organization in HBsAg viral particles by steady-state and time-resolved fluorescence spectroscopy.* Biochimie, 2010. **92**(8): p. 994-1002.

20. Schulte, W., J. Bernhagen, and R. Bucala, *Cytokines in sepsis: potent immunoregulators and potential therapeutic targets--an updated view.* Mediators Inflamm, 2013. **2013**: p. 165974.

21. Awate, S., L.A. Babiuk, and G. Mutwiri, *Mechanisms of action of adjuvants.* Front Immunol, 2013. **4**: p. 114.

22. Otterlei, M., et al., *Characterization of binding and TNF-alpha-inducing ability of chitosans on monocytes: the involvement of CD14.* Vaccine, 1994. **12**(9): p. 825-32.

23. Zhang, P., et al., *Toll like receptor 4 (TLR4) mediates the stimulating activities of chitosan oligosaccharide on macrophages.* Int Immunopharmacol, 2014. **23**(1): p. 254-61.

24. Wu, J. and C.C. Chu, *Block copolymer of poly(ester amide) and polyesters: synthesis, characterization, and in vitro cellular response.* Acta Biomater, 2012. **8**(12): p. 4314-23.

25. Xiong, S., et al., *Size influences the cytotoxicity of poly (lactic-co-glycolic acid) (PLGA) and titanium dioxide (TiO(2)) nanoparticles.* Arch Toxicol, 2013. **87**(6): p. 1075-86.

26. Segat, D., et al., *Proinflammatory effects of bare and PEGylated ORMOSIL-, PLGA- and SUV-NPs on monocytes and PMNs and their modulation by f-MLP.* Nanomedicine (Lond), 2011. **6**(6): p. 1027-46.

27. Staats, H.F., et al., *A Mast Cell Degranulation Screening Assay for the Identification of Novel Mast Cell Activating Agents.* Medchemcomm, 2013. **4**(1).

28. McLachlan, J.B., et al., *Mast cell activators: a new class of highly effective vaccine adjuvants.* Nat Med, 2008. **14**(5): p. 536-41.

29. Fang, Y., et al., *Mast cells contribute to the mucosal adjuvant effect of CTA1-DD after IgG-complex formation.* J Immunol, 2010. **185**(5): p. 2935-41.

30. Vo, T.-S., et al., *Protective effect of chitosan oligosaccharides against FcεRI-mediated RBL-2H3 mast cell activation.* Process Biochemistry, 2012. **47**(2): p. 327-330.

31. Farrugia, B.L., et al., *The localisation of inflammatory cells and expression of associated proteoglycans in response to implanted chitosan.* Biomaterials, 2014. **35**(5): p. 1462-77.

32. Garg, K., J.J. Ryan, and G.L. Bowlin, *Modulation of mast cell adhesion, proliferation, and cytokine secretion on electrospun bioresorbable vascular grafts.* J Biomed Mater Res A, 2011. **97**(4): p. 405-13.

33. Aridor, M., L.M. Traub, and R. Sagi-Eisenberg, *Exocytosis in mast cells by basic secretagogues: evidence for direct activation of GTP-binding proteins.* J Cell Biol, 1990. **111**(3): p. 909-17.

34. Fang, Y., et al., *The immune complex CTA1-DD/IgG adjuvant specifically targets connective tissue mast cells through FcgammaRIIIA and augments anti-HPV immunity after nasal immunization.* Mucosal Immunol, 2013. **6**(6): p. 1168-78.

35. Boisgerault, F., G. Moron, and C. Leclerc, *Virus-like particles: a new family of delivery systems.* Expert Rev Vaccines, 2002. **1**(1): p. 101-9.

36. Chroboczek, J., I. Szurgot, and E. Szolajska, *Virus-like particles as vaccine.* Acta Biochim Pol, 2014. **61**(3): p. 531-9.

37. McGowen, A.L., et al., *The mast cell activator compound 48/80 is safe and effective when used as an adjuvant for intradermal immunization with Bacillus anthracis protective antigen.* Vaccine, 2009. **27**(27): p. 3544-52.

38. Wu, L.C. and A.A. Zarrin, *The production and regulation of IgE by the immune system.* Nat Rev Immunol, 2014. **14**(4): p. 247-59.

39. Peng, Z., et al., *CpG oligodeoxynucleotide vaccination suppresses IgE induction but may fail to down-regulate ongoing IgE responses in mice.* Int Immunol, 2001. **13**(1): p. 3-11.

40. Smith-Norowitz, T.A., et al., *IgE anti Hepatitis B virus surface antigen antibodies detected in serum from inner city asthmatic and non asthmatic children.* Hum Immunol, 2014. **75**(4): p. 378-82.

41. Yanase, N., et al., *OVA-bound nanoparticles induce OVA-specific IgG1, IgG2a, and IgG2b responses with low IgE synthesis.* Vaccine, 2014. **32**(45): p. 5918-24.

42. Michel, M.L. and P. Tiollais, *Hepatitis B vaccines: protective efficacy and therapeutic potential.* Pathol Biol (Paris), 2010. **58**(4): p. 288-95.

43. McNeela, E.A. and K.H. Mills, *Manipulating the immune system: humoral versus cell-mediated immunity.* Adv Drug Deliv Rev, 2001. **51**(1-3): p. 43-54.

44. Verwaerde, C., et al., *HBHA vaccination may require both Th1 and Th17 immune responses to protect mice against tuberculosis.* Vaccine, 2014. **32**(47): p. 6240-50.

45. Lin, Y., S.R. Slight, and S.A. Khader, *Th17 cytokines and vaccine-induced immunity.* Semin Immunopathol, 2010. **32**(1): p. 79-90.

46. Weeratna, R.D., et al., *CpG ODN can re-direct the Th bias of established Th2 immune responses in adult and young mice.* FEMS Immunol Med Microbiol, 2001. **32**(1): p. 65-71.

47. Brazolot Millan, C.L., et al., *CpG DNA can induce strong Th1 humoral and cell-mediated immune responses against hepatitis B surface antigen in young mice.* Proc Natl Acad Sci U S A, 1998. **95**(26): p. 15553-8.

48. Borges, O., et al., *Immune response by nasal delivery of hepatitis B surface antigen and codelivery of a CpG ODN in alginate coated chitosan nanoparticles.* Eur J Pharm Biopharm, 2008. **69**(2): p. 405-16.

49. Kanchan, V. and A.K. Panda, *Interactions of antigen-loaded polylactide particles with macrophages and their correlation with the immune response.* Biomaterials, 2007. **28**(35): p. 5344-57.

50. Pawar, D., et al., *Development and characterization of surface modified PLGA nanoparticles for nasal vaccine delivery: effect of mucoadhesive coating on antigen uptake and immune adjuvant activity.* Eur J Pharm Biopharm, 2013. **85**(3 Pt A): p. 550-9.

51. Thomas, C., et al., *Aerosolized PLA and PLGA nanoparticles enhance humoral, mucosal and cytokine responses to hepatitis B vaccine.* Mol Pharm, 2011. **8**(2): p. 405-15.

52. LeibundGut-Landmann, S., et al., *Syk- and CARD9-dependent coupling of innate immunity to the induction of T helper cells that produce interleukin 17.* Nat Immunol, 2007. **8**(6): p. 630-8.

53. Reed, S.G., M.T. Orr, and C.B. Fox, *Key roles of adjuvants in modern vaccines.* Nat Med, 2013. **19**(12): p. 1597-608.

Part 2. Exosomes as adjuvants for the recombinant hepatitis B antigen: first report in scientific literature

Abstract

Exosomes are a class of extracellular vesicles (EVs) with an important role in cell-to-cell communication. In this study we hypothesized that exosomes derived from immune cells may have an adjuvant effect when administered with a recombinant antigen. Exosomes isolated from LPS-stimulated human monocytic cell (THP-1) culture were included in vaccine formulations: a solution of hepatitis B recombinant antigen (HBsAg) or a suspension containing HBsAg loaded PCL/chitosan NPs. Anti-HBsAg IgG titers obtained after the subcutaneous (SC) administration of the vaccine formulations were of IgG1 type, similar in both mice groups and also similar to the observed on the experimental control group (HBsAg solution without exosomes). Therefore, this result suggests a weak or inexistent exosome immunomodulator effect, particularly on antigen-specific antibody generation. Moreover, the exosome presence together with the nanoparticulate formulation decreases the NPs adjuvant effect. On the other hand, exosomes stimulated a non-specific immunity (innate), characterized by the enhancement of IFN-secretion.

Keywords: Exosomes, extracellular vesicles, HBsAg, poly- -caprolactone/chitosan nanoparticles, vaccine adjuvant.

161

1. Introduction

In the last years, multiple classes of extracellular vesicles (EVs) with different sizes and biogenesis pathways were discovered and explored [1, 2]. Exosomes constitute one class of EVs, with a mean size range of 30 nm to 150 nm and present an endosomal origin [1-7]. They result from the inward budding of an endocytic vesicle membrane which creates multi-vesicular bodies (MVBs) which ultimately fuse with the plasma membrane allowing exosome cell release [2-5]. Most cell types are known to produce and secrete exosomes which membrane and cargo contents reflect that of the parent cells [3, 8]. The first role described for exosomes was the excretion of unnecessary proteins from the cells [9]. Presently, it is well established that exosomes have important roles in biological functions depending on the cell type from which they are released [8, 9]. Secreted exosomes may be captured or internalized by neighbor or close located cells, or they can enter the systemic circulation and reach different tissues and cells [9]. Either way, they are known to be an essential piece in cellular communication [3].

Both immune and non-immune cells secrete exosomes with important roles in immune regulation, whether for stimulation or suppression or even for the mediation of inflammatory and infectious diseases [2, 3, 8]. Since the parent cells influence exosome's biological effect, different exosomes may have antagonistic abilities, like the ability to stimulate or the ability to suppress the immune system [8]. One of the first reports on exosomes and their action on tumors, showed that tumor peptide-pulsed DC-derived exosomes result in inhibition of murine tumor growth, in a T cell-dependent manner when administered *in vivo* [10]. On the other hand, Bianco et al. [11], showed that exosomes derived from DCs are immunosuppressive and anti-inflammatory, capable of reversing established arthritis, if they possess a tryptophan-degrading enzyme acting, important for immune regulation and tolerance maintenance.

Exosomes are known to transport various molecules. Some are common to all types of exosomes and include molecules fundamental to the generation of MBVs, cytosolic proteins as tubulin and actin, protein kinase, heat shock proteins (HSP 70, HSP 90), Annexin and Rab family proteins, tetraspanins (CD9, CD63, CD81), and various transmembrane proteins molecules [9]. In its turn, evidence suggest that mainly exosomes derived from antigen presenting cells (APCs) carry MHC I and MHC II molecules and tetraspanin CD86 at their surface, which theoretically enables them to stimulate $CD8^+$ and $CD4^+$ T cells [3, 8, 12, 13]. Moreover, in the exosome membrane, some molecules may act as pathogen associated molecular patterns (PAMPs) contributing to the activation of immune cells [14].

The application of tumor derived exosomes in cancer therapy based on the fact that exosomes express MHC molecules together with co-stimulatory molecules that induce potent specific T cell and B cell responses as well as NK cell responses [15]. Moreover, tumor-derived exosomes are enriched in tumor antigens, and are being widely employed as a novel source of antigens for promoting cytotoxic T

lymphocyte (CTL) cross-priming [16]. Encouraging results in the cancer vaccine field are reinforced by the clinical trials (phase I and phase II) already developed using exosomes secreted by DCs [15]. Following a similar rationale, exosome acellular vaccines have also been tested in the context of infectious diseases. For instance, exosomes produced by diphtheria toxoid loaded DCs are able to induce a Th1 biased immune response against the bacterial pathogen infection, while the subunit based vaccine is able to induce only a Th2 immune response [17]. Also, indirectly OVA loaded exosomes proved to act as an adjuvant enhancing the humoral response to OVA, as well as changing the response to a Th1 type which cannot be achieved with the common adjuvants like Alum and LPS [12].

To conclude, exosomes ability to increase and modulate immune responses is extremely favorable for vaccination proposes. This natural and nanoscale vesicles, are able to stimulate both the innate and the adaptive immune system. They are able to activate granulocytes, DCs, macrophages or NK cells, and also to interact with CD8+, CD4+ and B cells in order to augment antigen specific immune responses [15].

With this work, it is our intention to test whether exosomes could efficiently act as vaccine adjuvants for subcutaneous (SC) vaccination with HBsAg recombinant protein, or with a nanoparticulate delivery system loaded with HBsAg. By contrast to the majority of published studies, the antigen would not be loaded in the exosomes, nor would the parent cells be sensitized or infected with the antigen or the virus. Consequently, we will address these exosomes as unmodified exosomes. For their production we chose a cell line of monocytes (THP-1 cell line) since they are important progenitor cells of APCs. Moreover, Pulliam and co-workers [18] showed that microvesicles released by THP-1 cells after stimulation with lipopolysaccharide (LPS) contained microRNAs involved in controlling viral infections and associated to IFN- increase. To test our approach, C57Bl/6 mice were vaccinated with 2 different doses of unmodified exosomes mixed with HBsAg or with HBsAg adsorbed PCL/chitosan nanoparticles (NPs) and the immune response was evaluated. PCL/chitosan NPs formulation was already studied by our group as a delivery system and immunostimulant adjuvant for HBsAg with success.

2. Materials and Methods

2.1. Materials

Chitosan (ChitoClear™ - 95 % DD and 8 cP viscosity measured in 1 % solution in 1 % acetic acid) was purchased from Primex Bio-Chemicals AS (Avaldsnes, Norway). PCL (average MW 14000), D-(+)-trehalose dehydrate ($\geq$ 98.5 %), RPMI 1640 medium, sodium pyruvate solution (100 mM), 2-mercaptoethanol, Lipopolysaccharides (LPS) from Escherichia coli 055:B5 and o-phenylenediamine (OPD) were obtained from Sigma-Aldrich Corporation (St. Louis, MO, USA). Fetal bovine serum (FBS) and PenStrep from Gibco® were purchased from Thermo Fisher Scientific Inc. (Waltham, MA, USA). Recombinant hepatitis B surface antigen (HBsAg), subtype adw was acquired from Aldevron (Fargo, ND, USA). THP-1 cell line was obtained from American Type Culture Collection (ATCC, Barcelona, ES). All other chemicals and reagents were of analytical grade.

2.2. Methods

2.2.1. Exosome production and isolation

Exosomes were produced by the human monocytic THP-1 cell line after the stimulus with LPS, following a protocol adapted from Thery et al. [19]. Briefly,THP-1 cells were cultured in RPMI supplemented with 10 % FBS, 1 % PenStrep, 1.4 g/L HEPES, 1.5 g/L sodium bicarbonate, 2.5 g/L glucose, 1 mM sodium pyruvate and 0.05 mM -mercaptoethanol. The cell culture medium for exosome production was supplemented with exosome-free-FBS which was previously centrifuged at 100000 x g (4 ºC) for 17 h, to eliminate contaminant exosomes derived from the serum. Cells were incubated overnight in petri dishes at a density of 8 x 10^5 cells /mL and then stimulated with LPS for 6 h. After this period, the supernatants (A) were collected by performing a 250 x g centrifugation for 5 min at room temperature. Cells were resuspended in the same volume of fresh FBS-exosome-free supplemented RPMI and incubated for additional 13 h (B). The supernatant A was centrifuged once more at 2000 x g for 10 min (4 ºC) and then at 10000 x g for 30 min (4 ºC) and both pellets were discarded. The resulting supernatant, free of cells and cell debris was again centrifuged, for 70 min at 110000 x g (4 ºC) to isolate the exosomes. Pellets correspondent to the various centrifuge tubes were pooled in a single tube filled with PBS pH 7.4 and centrifuged again (110000 x g, 70 min). The collected pellet (exosomes) was stored at 4 ºC, during 1 week maximum. The supernatant from the resuspended cells (B) was exposed to all the procedures previously described for the isolation of more exosomes and the cells were discarded.

2.2.1.1. Exosome characterization

Isolated exosomes were quantified according to their total protein content after lyse with lysis buffer (2 % Sodium dodecyl sulfate and 1 % Triton-X100 in 0.1 M Tris buffer, pH 7.4). Protein was measured by Pierce™ Biocinchoninic acid (BCA) Protein Assay Kit (Thermo Fisher Scientific Inc., Waltham, MA, USA) according to the manufacturer's instruction. The discarded supernatant derived from the last ultracentrifugation was also treated with lysis buffer and quantified for contaminant proteins that were not eliminated during the washing step. The final amount of exosomes was calculated following equation 1 (Eq. 1):

$$Exosomes\ (\mu g) = Isolated\ exosomes\ (\mu g\ protein) - Discarded\ supernatant\ (\mu g\ protein)$$

(Eq. 1)

Exosomes were observed in a transmission electron microscope (FEI-Tecnai G2 Spirit Biotwin, 20-120 kV - FEI company, Hillsboro, OR, USA) after contrasting the samples stored in 4 % paraformaldehyde following the protocol described by Thery et al. [19]. Briefly, 5 µL of the sample were placed in a formvar coated niquel grid (mesh size 300, 3.05 mm, TAAB Laboratory equipment Ltd, Berkshire, UK) and allowed to dry. Then, the grid was washed 4 times with PBS pH 7.4 and placed in 1 % glutaraldehyde for 5 min. Next, 8 washes with water were performed followed by 5 min incubation with uranyl-oxalate pH 7. Next the grid was placed in a mixture of methyl cellulose-uranyl acetate for more 10 min (on ice). Ending this time, the excess fluid was removed in paper filter and the grid was air dried for more 10 min before analysis [19].

2.2.2. Nanoparticle production

The procedure for the preparation of PCL/chitosan NPs in our laboratory as well as the chitosan purification method was previously described by us [20]. Regarding the isolation of the NPs after maturation a small modification was performed: the NPs suspended in the original medium were isolated and concentrated by centrifugation at 16000 x g, for 75 min at 4 °C with a 200 L glycerol bed. The glycerol was eliminated by dialysis of the suspension against water for 48 h, using Spectra®Por cellulose ester dialysis membrane (MWCO 300.000, Spectrum Europe B.V., Breda, NL) and the resulting suspension was concentrated by further centrifugation. HBsAg loaded PCL/chitosan NPs were prepared by the incubation of PCL/chitosan NPs with HBsAg, in water under low stirring (4035 µg/mL NPs and 15 µg/mL HBsAg in the final formulation). To calculate HBsAg loading efficacy, aliquots of the particle suspension were centrifuged (21000 x g, 20 min) and the HBsAg present in the supernatant

(non-bound) was quantified using Pierce™ Biocinchoninic acid (BCA) Protein Assay Kit. Loading efficacy (%) was calculated using the following equation (Eq. 2):

$$Loading\ efficacy\ (\%) = \frac{(total\ HBsAg\ \left(\frac{\mu g}{mL}\right) - non\ bound\ HBsAg\ \left(\frac{\mu g}{mL}\right))}{total\ HBsAg\ \left(\frac{\mu g}{mL}\right)}\ x\ 100$$

(Eq. 2)

Size and zeta potential were measured by dynamic light scattering and electrophoretic light scattering, respectively, with a Delsa™ Nano C (Beckman Coulter, Madrid, ES). Transmission electron microscopy was used to observe free HBsAg and HBsAg adsorbed NPs stored in paraformaldehyde 4 % as described for exosomes.

2.2.3. Subcutaneous vaccination of C57BL/6 mice

Eight-week-old female C57BL/6 mice were purchased from Charles River (Saint-Germain-Nuelles, FR). Animals were provided with food and water ad libitum and all experiments were in accordance with FELASA guidelines and approved by the Animal Care Committee of the Center for Neuroscience and Cell Biology of Coimbra. Groups of 5 mice were used to test three exosome vaccine formulations: 5 g exosomes with 1.5 g HBsAg (5 EXO HBsAg); 20 g exosomes with 1.5 g HBsAg (20 EXO HBsAg); and 20 g exosomes with 403.5 g PCL/chitosan NPs adsorbed with 1.5 g HBsAg (20 EXO NPs-HBsAg) and respective controls as detailed in Table 1. Immunization were performed with water based formulations under isoflurane anesthesia. Two control groups (without exosomes) were included in the study: 403.5 g PCL/chitosan NPs adsorbed with 1.5 g HBsAg (NPs-HBsAg); and 1.5 g of HBsAg alone (HBsAg).

Table 1: Formulations for SC immunization of C57BL/6 mice.

Formulation name	Exosomes (µg/animal)	PCL/chitosan NPs (µg/animal)	HBsAg (µg/animal)	SC immunization (prime & boost) (day)	Euthanasia (day)
EXO 5 HBsAg	5	-	1.5	0, 14	42
EXO 20 HBsAg	20	-	1.5	0, 14	42
EXO 20 NPs-HBsAg	20	403.5	1.5	0, 14	42
NPs-HBsAg	-	403.5	1.5	0, 14	42
HBsAg	-	-	1.5	0, 14	42

2.2.3.1.   Determination of serum IgG, IgG1 and IgG2c

Please see methods *section 2.2.4.2.*, *chapter 4, part 1* for details.

2.2.3.2.   Quantification of cytokines

Please see methods *section 2.2.4.3.*, *chapter 4, part 1* for details.

.

2.2.4. LPS evaluation

Limulus amebocyte lysate (LAL) assay (Pyrogent™ Gel Clot LAL Assay, 0.125 EU/mL sensitivity, Lonza Group, Basel, CH) was performed according to manufacturer's instructions for the detection of LPS presence on diverse samples including exosome samples.

2.2.5. Statistical analysis

Results were expressed as mean ± SEM. Data was analyzed by ANOVA test, followed by a Tukey´s post-test for multiple comparisons, with a value of $p \leq 0.05$ considered as a statistically significant difference. (GraphPad Prism v 5.03, GraphPad Software Inc., La Jolla, CA, USA).
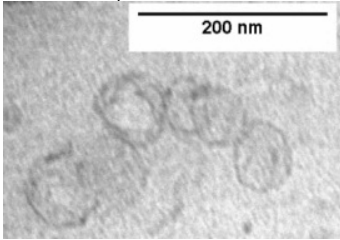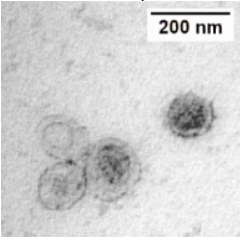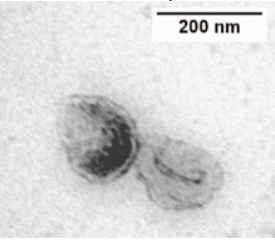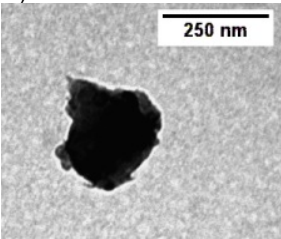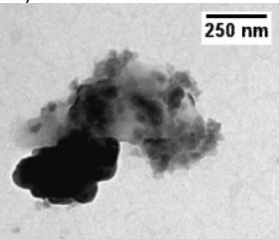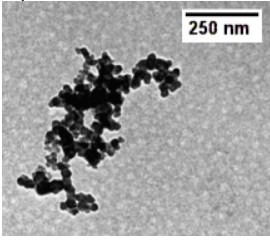
3. Results and discussion

3.1. Formulations for vaccination studies

Exosome secretion by cells was obtained by adapting a protocol on exosome secretion by peripheral blood monocyte cells (PBMCs) upon stimulation with LPS [21]. However, in order to achieve an exosome production yield more suitable for *in vivo* experiments, the use of the monocytic THP-1 cell line was preferred over the primary cell line of PBMCs [22]. By using a cell line, the exosome production becomes less time and resource consuming. Exosomes and other vesicles derived from THP-1 cells have already been studied for several immunotherapeutic applications [23-25]. Also, exosomes and microvesicles derived from LPS-stimulated THP-1 cells have been shown to contain IL-1 and inflammasome components and were demonstrated to be able to activate endothelial cells [23]. In another study these exosomes were also found to possess microRNAs able to induce the secretion of IFN- [18].

Exosome and PCL/chitosan NPs characterization were summarized in Figure 1. Exosome visualization by TEM microscopy revealed round vesicles with a lipid bilayer, with sizes varying from 80 nm to 200 nm (Fig. 1, images A, B and C). Some exosomes present a cup-shaped morphology resultant from the dehydration phenomena during the sample preparation and is frequently mistaken as a typical feature of exosomes [3, 6, 26].

Biodegradable polymeric delivery systems like PCL/chitosan NPs are being used as vaccine adjuvants for its ability to activate and enhance immune responses [27, 28]. In fact, previous studies developed by our group demonstrated the ability of antigen loaded PCL/chitosan NPs to increase the immune response achieved with HBsAg in C57BL/6 mice. The PCL/chitosan NPs formulation used in this study contained 1.5 µg HBsAg efficiently adsorbed to the surface of 403.5 µg NPs (loading efficacy ≥ 96 %) and presented a positive zeta potential (≈ + 19 mV) favoring cellular interactions, important for the immune response generation. In Figure 1, the images D and E illustrate PCL/chitosan NPs with an average size close to 200 nm loaded with HBsAg which is in agreement with the DLS data collected.

The recombinant antigen used for testing the adjuvant ability of exosomes was the HBsAg, a surface antigen of the hepatitis B virus used in the commercially available vaccines. This protein is produced in yeast cells and self assembles into 22 nm spherical virus-like particles (VLPs) stabilized by disulfide bounds [29, 30], that are illustrated in image F from Figure 1.

Adjuvant	Size (nm)	Zeta Potential (mV)	Loading efficacy (%)
	80-200 [a]	-	-
	A)	B)	C)
Exosomes			

Adjuvant	Size (nm)	Zeta Potential (mV)	Loading efficacy (%)
	201.65 ± 5.17 [b]	18.55 ± 2.31	≥ 96
	D)	E)	
PCL/chitosan NPs			

Antigen	Size (nm)	Zeta Potential (mV)	Loading efficacy (%)
	22 [c]	-	-
	F)		
HBsAg			

[a] Size determined by the evaluation of multiple representative TEM images. [b] Size determined by dynamic light scattering. [c] Size described in the scientific literature [29, 30].

Figure 1: Characterization of the adjuvants under study: exosomes and PCL/chitosan NPs; and the antigen: HBsAg. Exosomes size was estimated by the evaluation of multiple representative vesicles present on TEM images. Images A, B and C intend to illustrate the size dispersity of the vesicles observed. PLC/chitosan NPs size distribution and mean zeta potential value in milli-Q water and HBsAg loading efficacy (%). TEM images of PCL/chitosan NP adsorbed with HBsAg (D) and an agglomerate of PCL/chitosan NPs adsorbed with HBsAg (E). HBsAg size as described in bibliographic references and TEM images of the recombinant antigen assembled into VLPs (F).

3.2. Exosomes have low immunomodulator effect on HBsAg-specific antibody generation

A subcutaneous injection of HBsAg mixed with exosomes might have advantages, since both exosomes and HBsAg are likely to be transported to the same draining lymph nodes (LN) increasing the hypothesis of successful immune response [15]. In order to evaluate the influence of exosomes in the immune response generated against HBsAg mice were vaccinated through the SC route with 5 different vaccine formulations. Anti-HBsAg IgG titers were analyzed at day 14 and day 42 and the results obtained are presented in Figure 2. C57/BL6 mice vaccinated with a single dose of HBsAg (1.5 µg) did not generate detectable anti-HBsAg IgG. The inclusion of two doses (5 µg and 20 µg) of exosomes in the previous formulation allowed us to evaluate the role of the exosomes as HBsAg adjuvant. In fact, not all, but some mice from both experimental groups have developed anti-HBsAg IgG anti-HBsAg IgG titers at day 14. In a previous work, we observed that PCL/chitosan NPs is a good adjuvant for SC vaccination with HBsAg. Accordingly, all mice from the NPs-HBsAg group developed significant titers 14 days after the first injection. On the other hand, when we administered together the NPs-HBsAg and 20 g of exosomes in same formulation, the number of responder mice decreased to 2 (Fig. 2A). This may indicate a decrease in the adjuvant activity of NPs when mixed with the exosomes.

Four weeks after the boost at day 14, all mice from all experimental groups presented antibody titers against HBsAg (Fig. 2B). However, mice from the group immunized with HBsAg loaded NPs and exosomes attained similar antibody levels as mice from the groups immunized with exosome-containing formulations without NPs. Since the group immunized only with HBsAg loaded NPs presented significant higher antibody titers ($p < 0.05$) this result indicates a decrease of NPs adjuvant ability when in the presence of the exosomes. Additionally, exosomes seem not to interfere with the antibody isotype produced. Antigen VLPs induced the production of IgG1 antibodies which was not altered by the presence of diverse adjuvants (exosomes or NPs) in the antigen formulation (Fig. 2C). Therefore, in all cases only a Th2 humoral immune response was generated.

Nonetheless, previous studies had reported the induction of a balanced Th1 antibody response when using exosomes for vaccination. Indeed, modifying the exosomes with the antigen could possibly induce that adjuvant effect. For instance, Cheng and co-workers [31] found that exosomes obtained from the mouse macrophage cell line RAW 264.7, treated with M. tuberculosis culture filtrate proteins, were able to induce a higher IgG2c production in C57BL/6 mice than the BCG vaccine, when administered through the intranasal route. Also, Qazi et al. demonstrated that exosomes derived from bone marrow–derived dendritic cells (BMDCs) and directly loaded with ovalbumin (OVA) were able to induce an increased specific IgG2a antibody production in BALB/c mice, superior to the antigen

adjuvanted with LPS or alum, after intravenous vaccination. In these studies, exosomes were derived from infected cells or were primed with antigens, differences that may explain our contrasting results.
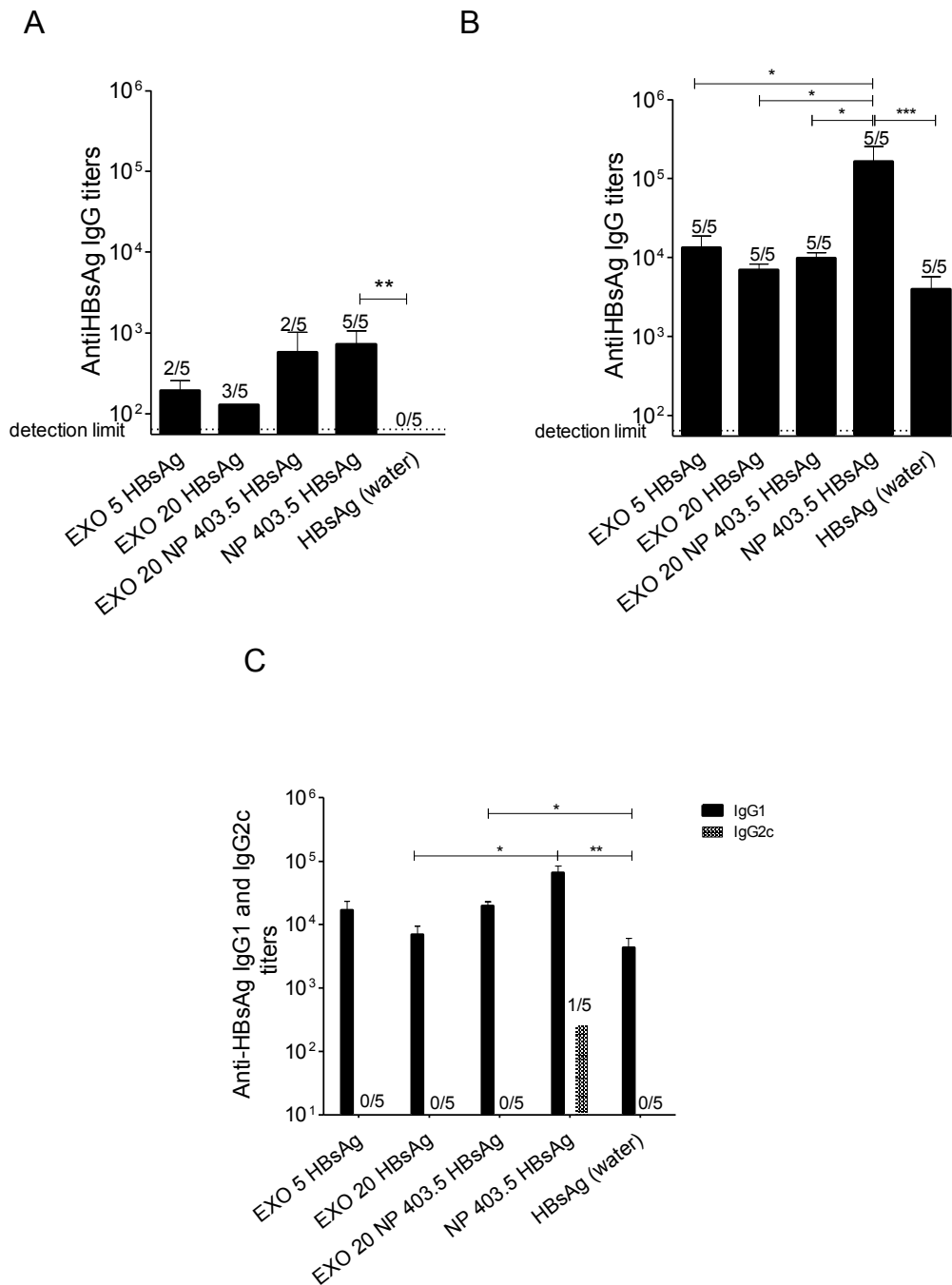
Figure 2: Immune response of SC immunized mice. Serum anti-HBsAg IgG levels of mice immunized on days 0 and 14 with formulations containing exosomes (5 and 20 g/dose) with 1.5 µg of HBsAg; exosomes (5 and 20 g/dose) with 403.5 µg PCL/chitosan NPs and 1.5 µg of HBsAg; and 403.5 µg PCL/chitosan NPs and 1.5 µg of HBsAg. Control corresponds to free HBsAg dosed to 1.5 µg of antigen as for the other formulations. Blood was collected on days 14 (A) and 42 (B). Antibody levels were determined by ELISA as described in 'Materials and methods'. The end-point titer in the results represents the antilog of the last log 2 dilution for which the OD were

171

at least two-fold higher than the value of the naive sample equally diluted. Numbers above bars represent the number of mice on which antibody levels were detected; Data (mean ± SEM) represents groups of 5 mice each. *, ** and *** indicates groups that are statistically different from each other with p ≤ 0.05, p ≤ 0.01 and p ≤ 0.001, respectively.

3.3. LPS-stimulated exosomes induced a Th1 cellular immune response against HBsAg

After animal euthanasia at day 42, spleens were aseptically removed and cultured for cytokine production analysis. The basal production of IL-4, IL-17 and IFN- were analyzed and the results obtained indicate that only IFN- presented differences among groups, including the control group (naïve). In fact, IFN- basal concentrations present on naïve mice spleen cell supernatants were very low. The same happened in groups immunized with HBsAg alone or HBsAg loaded NPs. By contrast, the 3 groups immunized with formulations containing exosomes presented an increased basal production of IFN- by spleen cells (Fig. 3). This increase was higher (p <0.001) in the group that was vaccinated with 20 g exosomes plus HBsAg. However, the immunization with this same amount of exosomes plus the HBsAg loaded NPs did not cause mice spleen cells to produce such higher IFN- basal concentrations. In fact, the NPs presence in the formulation seems to interfere with the non-specific exosome immune stimulation. IFN- is produced not only by CD8+ and CD4+ Th1 cells in the context of an adaptive immune response, but it is also produced by natural killer (NK) cells and natural killer T (NKT) cells in the context of innate immune responses [32]. The high increase in IFN- basal secretion in spleen cells of mice immunized with exosome containing formulations might suggest a stimulation of the innate immune response by these EVs, that can be important to control ongoing viral infections [32]. Moreover, this documented basal IFN- production might help the differentiation of CD8 and CD4 Th1 effector cells that are able to produce more IFN- after a second encounter with the antigen [32]. Nonetheless, we cannot disregard that an abnormal IFN- production has been associated with a number of autoimmune and inflammatory diseases [32]. To the best of the author's knowledge no other reports have focused on the increase of the basal IFN- after exosome vaccination for comparison to our results.
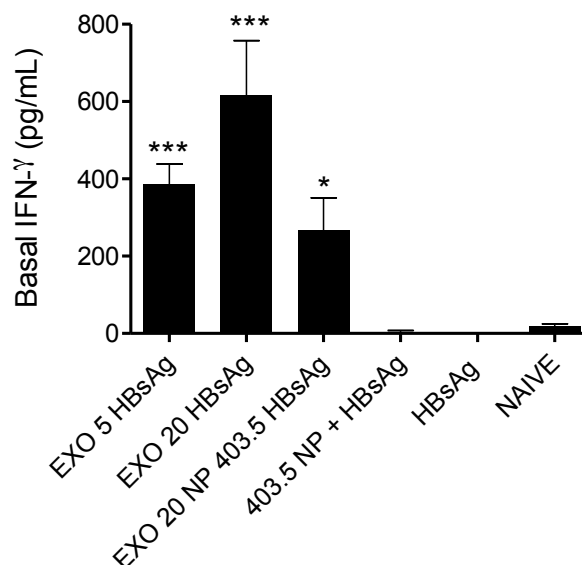
Figure 3: Basal production of IFN-γ. Spleen cells (0.25×10^6 cells/well) from both immunized and naïve C57/BL6 mice were cultured in complete RPMI. Supernatants were collected 72 hours later and tested for IFN-γ by ELISA. Results are mean cytokine concentrations ($\pm$ SEM) for each group of 5 immunized mice and 10 naïve mice. *$p \leq$ 0.05 and ***$p \leq$ 0.001 indicates values that differ significantly from naive group.

Cytokine production was also assessed after cell stimulation with HBsAg. Results from the IL-4 production by mice spleen cells showed no increase over the low basal cytokine levels (data not shown). On the other hand, in mice immunized with exosome containing formulations there was a tendency of increased IFN-γ production after spleen cells stimulation with HBsAg (Fig. 4A). In fact, the group 20 EXO HBsAg showed an increase in the specific IFN-γ production, statistically different from the naïve mice ($p < 0.01$) and from the free HBsAg immunized group ($p < 0.05$). This ability to produce elevated IFN-γ titers after a new encounter with the antigen is a valuable immune response with advantages on HBV vaccination. Regarding the NP 403.5 HBsAg immunized group, although no basal IFN-γ production had been observed, after HBsAg stimulation there was some increase in the production of this cytokine. Once more, the simultaneous presence of PCL/chitosan NPs and exosomes appears to have no advantage. Finally free HBsAg vaccinated mice spleen cells did not produce IFN-γ after stimulation with the antigen. With these results we can suggest that this exosomes have the ability to modulate the cellular immune response against HBsAg to a Th1 type. The same was already reported in the literature for vaccination strategies involving for instance dendritic cell derived exosomes [12] and macrophage derived exosomes [31] loaded with antigens.

173
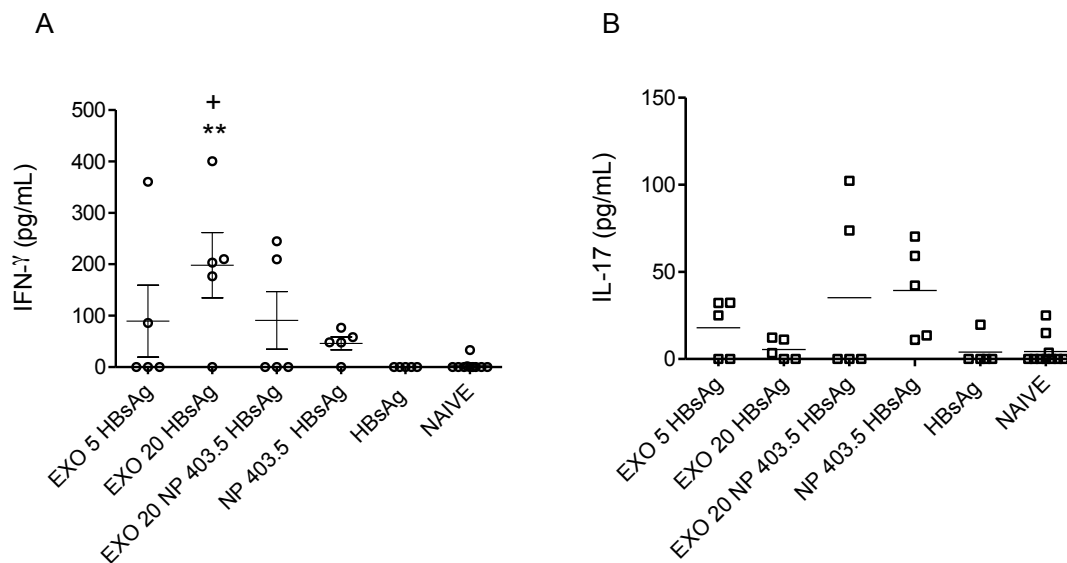
Figure 4: Spleen cells (0.25x10^6 cells/well) from both immunized and naïve C57/BL6 mice were stimulated with 1 g HBsAg as described in 'Materials and methods'. Supernatants were collected 72 hours later and tested for IFN- (A) and IL-17 (B) by ELISA. Results are cytokine concentrations resulting from HBsAg stimulation (basal concentration subtracted for each animal). Group of 5 immunized mice and 10 naïve mice are presented. **p ≤ 0.01 indicates values that differ significantly from naive group. +p ≤ 0.05 indicates values that differ significantly from HBsAg control group.

Concerning IL-17 cytokine, an increasing production tendency is observed only in some animals from the groups of mice immunized with NPs containing formulations (Fig. 4B). However, results present a great variability between mice from the same group. Nonetheless, the low IL-17 titers found in mice immunized with the formulations containing only exosomes and HBsAg suggest that the adjuvant ability of exosomes does not involve a Th17 cell-mediated immune response.

An important aspect to refer in this work is the presence of LPS (> 0.125 EU/mL) in the exosome containing formulations. This endotoxin is a TLR4 agonist with intrinsic immunostimulatory activity, which might be influencing the immune responses generated with exosome containing formulations [33]. In fact, results from a study on LPS loaded liposomes for HBsAg vaccination showed increased immune responses, particularly at a cellular level that was associated with the LPS content [34]. In the future, vaccination studies with LPS adjuvanted HBsAg or LPS free exosomes should be performed to elucidate the role of LPS in the tested exosome formulations.

4. Conclusions

Exosomes are important players in cell-to-cell communication and major attention has been given to its application in the biomedical field. Cancer vaccines based on the use of autologous or heterologous exosomes, with or without tumor epitopes and produced either by tumor cells or immune system cells, are being widely investigated and already showed encouraging results. In contrast, exosomes as adjuvants for prophylactic or therapeutic vaccines are not far discussed. In this report, we evaluated the effect of exosomes in the immune response generated against HBsAg. Important features were observed in this study namely the enhanced cellular immune response, illustrated by the increased IFN-γ concentrations. Exosomes adjuvant effect resulted in faster kinetic appearance of IgG antibody production when compared with free HBsAg. However, the antibody production induced by the different exosome containing formulations showed that the Th2 based response, typically associated with the recombinant HBsAg, remained unchanged. We may hypothesize that these results derive from the fact that the antigen was included in the formulation and not inside exosomes. Exosomes loaded with HBsAg may be a suitable future approach to generate different immunostimulant nano-vesicles. Loaded exosomes might carry intact HBsAg both inside and at its surface, allowing for stimulation of B cells, as described by Qazi et al. [12]. Also, the presentation of antigen epitopes at the surface at exosomes would be more efficient than its presentation with the native protein.

Further work involving exosome HBV loading and the characterization of co-stimulatory molecules present at the surface of unmodified and loaded exosomes should be able to bring new insights to this novel approach for hepatitis B vaccination.

References

1.   Wiklander, O.P., et al., *Extracellular vesicle in vivo biodistribution is determined by cell source, route of administration and targeting.* J Extracell Vesicles, 2015. **4**: p. 26316.

2.   Zhang, B., et al., *Immunotherapeutic potential of extracellular vesicles.* Front Immunol, 2014. **5**: p. 518.

3.   Robbins, P.D. and A.E. Morelli, *Regulation of immune responses by extracellular vesicles.* Nat Rev Immunol, 2014. **14**(3): p. 195-208.

4.   Johnsen, K.B., et al., *A comprehensive overview of exosomes as drug delivery vehicles - endogenous nanocarriers for targeted cancer therapy.* Biochim Biophys Acta, 2014. **1846**(1): p. 75-87.

5.   Qin, J. and Q. Xu, *Functions and application of exosomes.* Acta Pol Pharm, 2014. **71**(4): p. 537-43.

6.   Vlassov, A.V., et al., *Exosomes: current knowledge of their composition, biological functions, and diagnostic and therapeutic potentials.* Biochim Biophys Acta, 2012. **1820**(7): p. 940-8.

7.   Schageman, J., et al., *The complete exosome workflow solution: from isolation to characterization of RNA cargo.* Biomed Res Int, 2013. **2013**: p. 253957.

8.   Tran, T.H., et al., *Exosomes as nanocarriers for immunotherapy of cancer and inflammatory diseases.* Clin Immunol, 2015.

9.   De Toro, J., et al., *Emerging roles of exosomes in normal and pathological conditions: new insights for diagnosis and therapeutic applications.* Front Immunol, 2015. **6**: p. 203.

10. Zitvogel, L., et al., *Eradication of established murine tumors using a novel cell-free vaccine: dendritic cell-derived exosomes.* Nat Med, 1998. **4**(5): p. 594-600.

11. Bianco, N.R., et al., *Therapeutic effect of exosomes from indoleamine 2,3-dioxygenase-positive dendritic cells in collagen-induced arthritis and delayed-type hypersensitivity disease models.* Arthritis Rheum, 2009. **60**(2): p. 380-9.

12. Qazi, K.R., et al., *Antigen-loaded exosomes alone induce Th1-type memory through a B-cell-dependent mechanism.* Blood, 2009. **113**(12): p. 2673-83.

13. Li, X., et al., *Nanovesicular vaccines: exosomes.* Arch Immunol Ther Exp (Warsz), 2005. **53**(4): p. 329-35.

14. Anand, P.K., *Exosomal membrane molecules are potent immune response modulators.* Commun Integr Biol, 2010. **3**(5): p. 405-8.

15. Gehrmann, U., et al., *Harnessing the exosome-induced immune response for cancer immunotherapy.* Semin Cancer Biol, 2014. **28**: p. 58-67.

16. Wolfers, J., et al., *Tumor-derived exosomes are a source of shared tumor rejection antigens for CTL cross-priming.* Nat Med, 2001. **7**(3): p. 297-303.

17. Colino, J. and C.M. Snapper, *Exosomes from bone marrow dendritic cells pulsed with diphtheria toxoid preferentially induce type 1 antigen-specific IgG responses in naive recipients in the absence of free antigen.* J Immunol, 2006. **177**(6): p. 3757-62.

18. Pulliam, L. and A. Gupta, *Modulation of Cellular Function Through Immune-Activated Exosomes.* DNA Cell Biol, 2015. **34**(7): p. 459-63.

19. Thery, C., et al., *Isolation and characterization of exosomes from cell culture supernatants and biological fluids.* Curr Protoc Cell Biol, 2006. **Chapter 3**: p. Unit 3 22.

20. Jesus, S., G. Borchard, and O. Borges, *Freeze Dried Chitosan/ Poly- e-Caprolactone and Poly-e-Caprolactone Nanoparticles: Evaluation of their Potential as DNA and Antigen Delivery Systems.* J Genet Syndr Gene Ther 2013. **4**(164).

21. Ekström, K., et al., *Monocyte Exosomes Stimulate the Osteogenic Gene Expression of Mesenchymal Stem Cells.* PLoS ONE, 2013. **8**(9): p. e75227.

22. Gyorgy, B., et al., *Therapeutic applications of extracellular vesicles: clinical promise and open questions.* Annu Rev Pharmacol Toxicol, 2015. **55**: p. 439-64.

23.   Wang, J.G., et al., *Monocytic microparticles activate endothelial cells in an IL-1beta-dependent manner.* Blood, 2011. **118**(8): p. 2366-74.

24.   Wang, J., et al., *Evaluation of the Inflammatory Response in Macrophages Stimulated with Exosomes Secreted by Mycobacterium avium-Infected Macrophages.* BioMed Research International, 2015. **2015**: p. 9.

25.   Bhatnagar, S., et al., *Exosomes released from macrophages infected with intracellular pathogens stimulate a proinflammatory response in vitro and in vivo.* Blood, 2007. **110**(9): p. 3234-44.

26.   Raposo, G. and W. Stoorvogel, *Extracellular vesicles: exosomes, microvesicles, and friends.* J Cell Biol, 2013. **200**(4): p. 373-83.

27.   Akagi, T., M. Baba, and M. Akashi, *Biodegradable Nanoparticles as Vaccine Adjuvants and Delivery Systems: Regulation of Immune Responses by Nanoparticle-Based Vaccine*, in *Polymers in Nanomedicine*, S. Kunugi and T. Yamaoka, Editors. 2012, Springer Berlin Heidelberg. p. 31-64.

28.   Zhao, L., et al., *Nanoparticle vaccines.* Vaccine, 2014. **32**(3): p. 327-37.

29.   Chroboczek, J., I. Szurgot, and E. Szolajska, *Virus-like particles as vaccine.* Acta Biochim Pol, 2014. **61**(3): p. 531-9.

30.   Jain, N.K., et al., *Formulation and stabilization of recombinant protein based virus-like particle vaccines.* Adv Drug Deliv Rev, 2014.

31.   Cheng, Y. and J.S. Schorey, *Exosomes carrying mycobacterial antigens can protect mice against Mycobacterium tuberculosis infection.* Eur J Immunol, 2013. **43**(12): p. 3279-90.

32.   Schoenborn, J.R. and C.B. Wilson, *Regulation of interferon-gamma during innate and adaptive immune responses.* Adv Immunol, 2007. **96**: p. 41-101.

33.   McAleer, J.P. and A.T. Vella, *Educating CD4 T cells with vaccine adjuvants: lessons from lipopolysaccharide.* Trends Immunol, 2010. **31**(11): p. 429-35.

34.   Jain, V., et al., *Enhancement of T-helper type I immune responses against hepatitis B surface antigen by LPS derivatives adjuvanted liposomes delivery system.* J Drug Target, 2008. **16**(9): p. 706-15.

Chapter 5. Generation of an immune response with a reduced HBsAg recombinant protein dose, intranasally delivered by PCL/chitosan nanoparticles

Abstract

New strategies to increase HBV prophylactic vaccination especially in developing countries remain a major global health problem. Mucosal vaccination using polymeric nanoparticles (NPs) constitutes a valid approach to this issue. Specifically, poly- -caprolactone (PCL)/chitosan NPs present advantages as a mucosal vaccine delivery system: the high resistance of PCL against degradation in biological fluids and the mucoadhesive and immunostimulatory properties of chitosan. *In vitro* studies revealed these NPs were retained in a mucus-secreting pulmonary epithelial cell line and were capable to adsorb and enter differentiated epithelial cells. The intranasal (IN) administration of formulations based on PCL/chitosan NPs loaded with different amounts of HBsAg, generated in mice equal levels of serum anti-HBsAg IgG and nasal anti-HBsAg sIgA. PCL/chitosan NPs were found to increase the immune response of HBsAg and efficiently contribute to a dose reduction, making this formulation attractive for commercial purposes due to its decreased cost. The formulation surface characteristics, in particular, the positive zeta potential, are believed to be the basis for successful nasal immunization with antigen adsorbed to PCL/chitosan NPs.

Keywords: Nasal vaccination, polymeric nanoparticles, vaccine adjuvant, mucosa, immune response, poly- -caprolactone, chitosan.

1. Introduction

Commercially available hepatitis B virus (HBV) vaccines contain the hepatitis B surface antigen (HBsAg) and alum or aluminum hydroxide as adjuvant, and possess 90 % to 95 % efficacy. The immunization schedule comprises 3 intramuscular (IM) boosts and requires trained personnel and sterile injection materials, which still prevent many people to be vaccinated. Over the world, 2 billion people have been infected with HBV, with the major transmission routes being through sexual contact in low endemic areas, or through perinatal transmission in high endemic areas. Therefore, new strategies to increase HBV prophylactic vaccination especially in developing countries remain a major global health problem [1]. In contrast to commercially available IM vaccines, a mucosal vaccine against HBV would be advantageous regarding the administration procedure, would result in higher patient compliance, and would benefit the immune response generated by eliciting both systemic and mucosal immune responses [2]. The latter is mainly characterized by the production of secretory IgA (sIgA) at mucosal surfaces, which has the ability to resist protease and nuclease activity, allowing a prolonged protection compared to other antibodies [3]. For sexually transmitted HBV infection, sIgA production at the vaginal mucosa would play a decisive role in virus neutralization, preventing the infection [4]. The main challenge concerning mucosal vaccination is that mucosal surfaces have evolved in order to protect against external environment pathogens. They are constantly in a status of immunological surveillance against infections, inhibiting pathogens entrance through multiple unspecific strategies such as a mucus physical barrier, mucosal secretions containing proteases and nucleases and epithelial cells firmly organized with tight junctions [5, 6]. Hence, these mechanisms regulate the entrance of pathogens and also limit the success of mucosal vaccine delivery. In order to achieve a successful mucosal immunization, vaccines must overcome these initial barriers, and reach the integrated network of lymphoid and non-lymphoid cells and effector molecules that are responsible to prime innate and adaptive immune responses [6]. Moreover, mucosal vaccines generally depend on high amounts of antigen to induce an immune response, increasing the product costs and thereby reducing the interest by the pharmaceutical industry [5]. Therefore, the scientific community recognizes that technological solutions are an urgent need.

Polymeric particles have great ability to deliver highly purified recombinant antigens or pathogen subunits lacking intrinsic immunostimulatory activity [7]. In fact, their particulate nature is recognized for the enhancement of antigen uptake by antigen presenting cells (APCs) when used either in parenteral or mucosal vaccination strategies [8]. However, the ideal characteristics of a polymeric mucosal vaccine delivery system remain the subject of extensive research. Several studies agree that hydrophobic nanoparticles (NPs) are better taken up by intestinal Peyer's patches than more hydrophilic NPs [9] and

some suggested the presence of hydrophilic polymers on the surface of nanoparticles could increase the transport of these systems through mucosal surfaces [10].

Polymeric NPs comprising PCL and chitosan appear as a promising adjuvant delivery system for HBV mucosal vaccination, particularly through nasal route. These two well-known biodegradable polymers may have synergistic advantages in the generation of an immune response. PCL is a semicrystalline polyester, biodegradable but highly resistant to degradation in biological fluids [8, 11]. Its hydrophobicity may improve vaccine uptake by the nasal associated lymphoid tissue (NALT). Moreover, PCL, unlike other polyesters, namely poly(lactic-co-glycolic acid) (PLGA), does not generate an acidic environment on dissolution that could negatively affect the loaded molecule's antigenicity [10]. Chitosan has been extensively studied for its mucoadhesive properties as well as the ability to open intestinal and nasal mucosal tight junctions. The capacity to stimulate immune cells, its biocompatibility and abundant natural source, also represent positive features when used as a vaccine adjuvant [8, 12]. In the last years, HBsAg vaccines for nasal immunization have been developed and tested based on chitosan NPs [13, 14]. Also, approaches using chitosan, trimethyl chitosan and glycol chitosan to coat PLGA particles encapsulating HBsAg, have already shown better vaccination results through the nasal mucosa than uncoated PLGA particles [15, 16]. Using a similar rationale, it is our intention to use the hydrophobic nature of PCL to create a "pathogen mimicking" system, modified with chitosan, in order to achieve enhanced mucosal delivery of HBsAg. Previous work reported by Gupta and co-workers [17] for Influenza A virus (A/California/07/2009) H1N1 hemagglutinin (HA) protein showed chitosan coated PCL NPs entrapping HA by an emulsion-diffusion–solvent evaporation method efficiently leading to good Th1 biased systemic immune response and mucosal antibodies in the lung [17]. Florindo et al. [18] also used the double emulsion solvent evaporation method to produce PCL nanospheres modified with glycol chitosan or alginate, encapsulating or adsorbing *Streptococcus equi* antigens. Their results showed modified PCL nanospheres induced good specific antibody titers, and that the adsorption of the antigens compared to the encapsulation allowed for a faster generation of the immune response, after a single immunization [18]. Our work relies on the preparation of NPs containing both PCL and chitosan, using an easier method based on the direct nanoprecipitation of PCL in an aqueous solution containing chitosan. Moreover, the HBsAg antigen will be adsorbed to the NPs surface after production, in a nondestructive aqueous environment.

Preliminary *in vitro* studies were performed to investigate the capability of PCL/chitosan NPs as a mucosal delivery system. Furthermore, a nasal immunization study evaluated the systemic and mucosal immune response generated in C57BL/6 mice by HBsAg adsorbed onto PCL/chitosan NPs. With an antigen-dose response study, more than achieving a successful mucosal vaccine for HBV, we aimed to test a reduced antigen dose that would allow a decrease on the vaccine production costs.

2. Materials and Methods

2.1. Materials

Chitosan (ChitoClear™ - 95 % DD and 8 cP viscosity measured in 1 % solution in 1 % acetic acid) was purchased from Primex Bio-Chemicals AS (Avaldsnes, NO). PCL (average MW 14000), D-(+)-trehalose dehydrate (≥ 98.5 %), ovalbumin (≥ 98 %, grade V, ≈ 45 kDa), 3-[4,5-dimethylthiazol-2-yl]-2,5-diphenyl tetrazolium bromide (MTT), rhodamine B isothiocyanate (RBITC), basic fuchsin (dye content > 85 %) and mucin from porcine stomach Type III, were obtained from Sigma-Aldrich Corporation (St. Louis, MO, USA). Recombinant hepatitis B surface antigen (HBsAg), subtype adw of approximately 25 kDa, was acquired from Aldevron (Fargo, ND, USA). Calu-3 and Caco-2 cells were acquired from the American Type Culture Collection (BCN, ES). Fluorescein isothiocyanate (FITC) was purchased from Santa Cruz Biotechnology (Heidelberg, DE). All other chemicals and reagents were of analytical grade.

2.2. Methods

2.2.1. Nanoparticle preparation

Chitosan purification and PCL/chitosan NPs preparation by the nanoprecipitation of a PCL solution (4.5 mL, 0.2 % PCL) into a chitosan solution (13.5 mL, 0.1 % chitosan) , were performed as previously described by us, with minor modifications concerning the NPs isolation steps [19]. Therefore, after particle preparation, nanoparticles suspended in the original medium were isolated and concentrated by centrifugation at 16000 x g, for 75 min at 4 °C with a 200 L glycerol bed. The glycerol was eliminated by dialysis (cellulose ester dialysis membrane, MWCO 300.000 from Spectrum Europe B.V., Breda, NL) of the suspension against water, for 48 h. The resulting suspension was either freeze-dried in the presence of trehalose resulting in a 6 % NPs containing powder or centrifuged in 1.5 mL tubes, and ressuspended in miliQ water, for immediate usage. The former isolation technique was used for developing *in vitro* studies with cell lines, while fresh isolated NPs were used in all other experiments.

To perform studies requiring fluorescent analysis with PCL/chitosan NPs, chitosan was labeled with either FITC by a protocol previously reported by us, or with RBITC according to the same protocol with some modifications [19]. Briefly, for chitosan-RBITC equal volumes of 1 % (w/v) chitosan in 0.1 M of acetic acid and 0.069 % of RBITC in water-free methanol were mixed and stirred overnight in the dark. The mixture was then precipitated with 0.2 M NaOH at pH 10, and centrifuged for 5 min at 4500 x g and washed with water. The procedure was repeated until the supernatant's optical density at 556 nm was 0 and then the pellet was freeze-dried.

2.2.2. *In vitro* evaluation of PCL/chitosan NPs as mucosal delivery systems

2.2.2.1. Periodic acid: Schiff (PAS) colorimetric method

Mucin adsorption ability on PCL/chitosan NPs was determined by adapting an assay described elsewhere [20]. Briefly, 1 mg of NPs was incubated with mucin at several concentrations (50-300 µg/mL). The resulting suspensions were mixed and incubated at room temperature for 60 min. The suspension was then centrifuged at 21460 x g for 15 min and the supernatant quantified for free mucin content using the periodic acid: Schiff (PAS) colorimetric assay based on the adaptation of several references [15, 21, 22]. Briefly, Schiff reagent was prepared by mixing 100 mL of 0.5 % basic fuchsin aqueous solution and 10 mL of HCl 1 M. Prior to each assay 0.1 g of sodium metabisulphite were added to every 6 mL of Schiff reagent and the resultant solution was incubated at 37° C until it became pale yellow. Periodic acid reagent was freshly prepared every time by adding 0.14 mL of 50 % (w/v) periodic acid solution to 10 mL of 7 % (v/v) acetic acid solution. In order to quantify the mucin present in the samples, 90 µL of the diluted periodic acid was added to each 900 µL of supernatant and incubated for 75 min at 37 °C. Then 90 µL of Schiff reagent was added at room temperature and optical density measured at 550 nm after 30 min. Mucin standards (from 50 µg/mL to 250 µg/mL) were measured by the same procedure. The mucin adsorbed onto the NPs surface was calculated by subtracting the amount of free mucin from the total mucin content in the test mixture. Chitosan NPs and PCL NPs were also evaluated using the same protocol, to stablish comparisons with PCL/chitosan NPs. Chitosan NPs were produced according to [23] and PCL NPs by the same method as for PCL/chitosan NPs without adding chitosan. All NPs formulations were used fresh, as trehalose added as a protein stabilizer during freeze-dry would interfere with the colorimetric method.

2.2.2.2. Differentiated Calu-3 cell monolayers modeling the airway epithelial and mucosal barrier for *in vitro* studies

Calu-3 cells (passages 38-45) were cultured in Dulbecco's modified eagle medium (DMEM) supplemented with 10 % fetal bovine serum (FBS), 1 % PenStrep and 1.176 g/L sodium bicarbonate. To achieve a cell monolayer modeling the airway epithelial and a mucosal barrier, a protocol was adapted from several articles [24-27]. Briefly, Calu-3 cells detached from culturing flasks by 0.25 % trypsin-EDTA were subcultured in 12-well Transwell™ inserts (12 mm, 0.4 m PES, TC, Corning Incorporated, Corning, NY, USA). Cells were seeded at 2 X 10^5 cells/insert (500 L/well), on the apical side of the filter. The basolateral side was filled with 1.5 mL of complete DMEM. Calu-3 cells were attached to the filter for 24 h post seeding, and then the medium was removed from the apical compartment to allow cells to form a monolayer at an air-liquid interface. The differentiation stage during cultivation was followed by measuring the transepithelial electric resistance (TEER) using an EVOM epithelial

voltammeter (World Precision Instruments Inc., Hertfordshire, UK). Mucoadhesivity experiments were performed after 9–16 days, when mean TEER values were constant and around 400–500 .cm². One hour before adding RBITC-labeled NPs to the apical region, the basolateral medium was replaced by serum-free medium. 100 µL formulation suspended in serum-free medium was placed over the mucus layer, on the apical region and incubated for 6 h. After incubation, the cell monolayer surface was carefully washed with PBS pH 7.4 to eliminate non-bound particles and fixed with 4 % paraformaldehyde in PBS for 15 min at 37 ºC. The nuclei were labeled using Hoechst 33342 dye (Live Technologies Corporation, Paisley, UK) according manufacturer's instructions. After labeling, cells were washed twice with PBS and the filters were cut from the inserts and mounted in microscope slides with DAKO mounting medium. Samples were examined under an inverted confocal laser scanning microscope (CLSM) (Zeiss LSM 510 META, Carl Zeiss, Oberkochen, DE) with a EC Plan-Neofluar 40x/1.30 Oil DIC objective.

2.2.2.3. Differentiated and non-differentiated Caco-2 cell uptake of PCL/chitosan NPs and cytotoxicity studies

Caco-2 cells (passages 61-70) were cultured in DMEM supplemented with 10 % FBS, 1 % PenStrep and 1.176 g/L sodium bicarbonate. For non-differentiated cell studies, Caco-2 cells were seeded in a 48-well plate at a density of 1.5 x 10⁵ cells/well and stabilized for 24 h.

Before cytotoxicity experiments, medium was replaced with 250 L fresh medium. Samples of PCL/chitosan NPs suspended in 250 L serum-free medium (from 0.2 µg/mL to 500 µg/mL) were added to the cells. After 24 h incubation at 37 ºC, MTT assay was performed according to manufacturer's instructions and cell viability was determined as previously reported [19].

For uptake experiments, after 24 h cell stabilization, medium was replaced with 500 L serum-free medium and 20 L of FITC-labeled NPs were added to achive a final concentration of 40 g/mL per well, respectively. After 4 h or 18 h incubation period, medium was removed and cells were washed with 200 µL of PBS. Cells were detached from the wells using 100 µL of trypsin-EDTA solution 0.25 %, which was successively inactivated by 200 µL of complete medium. Cells from 2 wells were pooled in the same tube, centrifuged for 20 min at 250 x g (4 ºC), re-suspended in 200 µL of ice-cold PBS and analyzed on BD FACSCalibur Flow Cytometer (BD Biosciences, Bedford, MA, USA). Duplicates of the samples were also analyzed with trypan blue to exclude fluorescence at the surface of the cells. The mean fluorescence for a population of 20000 cells was collected and results were processed by CellQuest Modfit LT flow cytometry analysis software (BD Biosciences, Bedford, MA, USA).

For differentiated cell studies, Caco-2 cells were seeded in 48-well plate at a density of 8 x 10^4 cells/ well and incubated during 17 days allowing cells to differentiate. Medium was replaced every two days. On day 17 the uptake and the cytotoxicity assays were performed as described for non-differentiated cells.

2.2.3. Model antigen and HBsAg adsorption – size and surface charge characterization

Concentrated NPs were incubated with a solution of ovalbumin (OVA) for 30 min under low stirring. NPs : protein (w/w) ratios of 1614:10, 1614:5 and 1614:1.5 were used to measure size and surface charge of the resulting formulations. Similarly, PCL/chitosan NPs were incubated with HBsAg at the same (w/w) ratios. The resulting 3 vaccine formulations contained 107.6 mg/mL NPs and 0.67 mg/mL, 0.33 mg/mL or 0.1 mg/mL HBsAg and were prepared for the immunization study. The amount of protein adsorbed for each condition was calculated by the difference between the total protein added and the protein that remained in solution, which was quantified by Pierce™ BCA protein assay (Thermo Fisher Scientific Inc., Waltham, MA, USA) according to manufacturer's instructions. Size and zeta potential of NPs were measured by dynamic light scattering (presented as normalized intensity distribution) and electrophoretic light scattering (calculated by Smoluchowski approximation), respectively, with a Delsa™ Nano C (Beckman Coulter, Madrid, ES).

2.2.4. Immunization experiments

2.2.4.1. Intranasal (IN) vaccination of C57BL/6 mice

Female 8 weeks old C57BL/6 mice were purchased from Charles River (Saint-Germain-Nuelles, FR). Animals were provided with food and water ad libitum and all experiments were in accordance with FELASA guidelines and approved by the Animal Care Committee of the Center for Neuroscience and Cell Biology of Coimbra. Groups of 5 mice were used to test different formulations, whose composition and immunization schedules are listed in table 1. Intranasal immunizations were performed under isoflurane anesthesia by depositing 7.5 µL of the respective formulation in each mouse nostril. Attention was paid to administering a new drop only after the previous was inhaled.

Table 1: Formulations for intranasal (IN) immunization of C57BL/6 mice.

Formulation name	PCL/chitosan NPs (µg/animal)	HBsAg (µg/animal)	Immunization & boost (15 µL/animal) (day)	Euthanasia (day)
1614NPs-10	1614	10	0, 7, 21	42
1614NPs-5	1614	5	0, 7, 21	42
1614NPs-1.5	1614	1.5	0, 7, 21	42
10HBsAg	-	10	0, 7, 21	42

2.2.4.2.   Biological sample collection

Blood was collected from mice under slight isoflurane anesthesia, by submandibular lancet method at day 21 and 42. After coagulation, blood was centrifuged at 4500 x g for 10 min for serum collection. Vaginal washes were collected at day 41 and 42 by instilling 100 µL of sterile PBS into the vaginal cavity and triturating the lavage fluid 10 times before collection. Samples supplemented with phenylmethylsulfonyl fluoride (PMSF) and sodium azide (1 mM and 0.01 %, respectively), were centrifuged at 3300 x g during 10 min, supernatants collected and stored at 80 °C until further analysis. Nasal washes were collected at day 42 after mice euthanasia by cervical dislocation by flushing 200 µL of PBS into the mice trachea and collecting the out coming wash through the nose (see Figure A from supplementary material chapter 5 for more detail). Samples supplemented with phenylmethylsulfonyl fluoride (PMSF) and sodium azide (1 mM and 0.01 %, respectively), were centrifuged at 15700 x g during 20 min and supernatants collected and stored at 80 °C until further analysis.

2.2.4.3.   Determination of serum IgG

HBsAg coated plates were obtained by overnight incubation at 4 ºC of 100 µL HBsAg (1 µg/mL) in 50 mM sodium carbonate/bicarbonate pH 9.6, on high-binding 96-well plates (Nunc MaxiSorp®, Thermo Fisher Scientific Inc., Waltham, MA, USA). Plates were washed 5 times with PBS-polysorbate 20, and blocked for 1 h at 37 °C. After washing, serial dilutions of serum were applied and incubated for 2 h at 37 °C. Following extensive washing, specific antibodies were detected using horseradish peroxidase (HRP) conjugated goat anti-mouse IgG, for 30 min at 37 °C. Next, detection was performed with 5 mg o-phenylenediamine (OPD) suspended in 10 mL citrate buffer and 10 µL H_2O_2, for 10 min at room temperature and stopped with 1 M H_2SO_4. Absorbance was read at 492 nm with a microplate reader. Results were calculated as the antilog of the last log 2 dilution, for which the absorbance were at least two-fold higher than the value of the naive sample equally diluted.

2.2.4.4.   Quantification of IgA in mucosal samples

Antigen specific and total IgA were assessed by an Elisa procedure similar to the one described in the previous section with the following modifications: (1) the plates were coated with HBsAg (1 µg/mL) and also IgA (10 µg/mL); (2) vaginal and nasal washes were applied in both HBsAg and IgA coated plates without dilution; (3) mouse IgA serum reference was used to obtain calibration curves; HRP conjugated goat anti-mouse IgA was used for both specific and total IgA. Concentration of total and anti-HBsAg IgA were extrapolated from calibration curve. Vaginal and nasal IgA were presented as the ratio between specific anti-HBsAg IgA and total IgA for each mouse. Only samples whose IgA ratio was 2-fold higher than average naïve mice samples ratio were considered positive.

2.2.5. Statistical analysis

Results were expressed as mean ± standard error of the mean (SEM) or standard error (SD), as indicated for each assay. Data was analyzed by ANOVA, followed by Tukey´s post-test for multiple comparisons with $p \leq 0.05$ considered a statistically significant difference (GraphPad Prism v 5.03, GraphPad Software Inc., La Jolla, CA, USA).

3. Results and Discussion

3.1. PCL/chitosan NPs ability as a mucosal delivery system

PCL/chitosan NPs prepared by nanoprecipitation technique, presented in water a mean diameter of approximately 208 nm with low polydispersity (PI: 0.18) and a zeta potential of + 26 mV. These particles consist of two distinct polymers: PCL, a hydrophobic polymer; and chitosan, an extensively described mucoadhesive positively charged polymer. Our first experiment aimed at investigating mucin adsorption to the particle surface, as mucin is a glycosylated protein present in the mucus. To assess the influence of the dual polymeric composition of PCL/chitosan NPs, chitosan NPs and PCL NPs were used as controls on mucin adsorption assay.

Previous protein loading studies, performed in our laboratory on similar polymeric delivery systems, showed that the adsorption equilibrium takes place within a few minutes after the contact between particles and protein. Therefore, 1 mg of NPs were incubated at room temperature with different amounts of mucin during 60 min, in water. Results presented in Figure 1 show the amount of mucin adsorbed to NPs increased with increasing mucin concentration for the 3 types of NPs. Chitosan NPs presented the highest adsorption capacity for all the concentrations tested, while PCL NPs presented the lowest ($p < 0.05$ for all concentrations). PCL/chitosan NPs presented an intermediary mucin adsorption capacity result, compatible with the influence of both polymers. Indeed, while at lower mucin concentrations (50 µg/mL – 200 µg/mL) the adsorption capacity was lower than the demonstrated by chitosan NPs ($p < 0.001$), at higher mucin concentrations the results present no statistical difference to chitosan NPs. The different properties of the NP species are important to interpret these results. Chitosan NPs presented higher average size around 500 nm with zeta potential close to + 30 mV. In contrast, PCL and PCL/chitosan NPs presented sizes around 200 nm and zeta potentials (measured in water) of - 2.35 ± 3.21 mV and + 25.7 ± 2.9 mV, respectively. Whereas the higher positive charge presented by chitosan NPs may be beneficial mucin interaction, increased particle sizes diminish surface area, which is widely reported as a factor for diminishing protein adsorption [28]. Our results suggested that the high mucin adsorption demonstrated by chitosan NPs was compatible with the interaction of positively charged amino groups of chitosan with the negatively charged sialic acid substructure of mucin [29, 30]. On its turn, due to PCL polymer nature, the observed adsorption profile for PCL NPs was rather dependent on hydrophobic interactions of the polymer, with the hydrophobic domains of mucin. We may speculate that for PCL/chitosan NPs, chitosan is important for the mucin interaction, and higher mucin concentrations are necessary to overcome eventual repulsive forces by PCL. Additionally, the higher surface area resultant from the small particle size, contributed to an increase in the mucin interaction for higher mucin concentrations. Mazzarino et al. [31] recently used

quartz crystal microbalance with dissipation monitoring to evaluate the interaction between curcumin loaded PCL NPs with bovine submaxillary gland mucin (BSM). In their study they tested whether coating the NPs with different chitosans would influence BSM interaction, and concluded that chitosan, regardless of its molecular mass, was fundamental for the interaction [31].
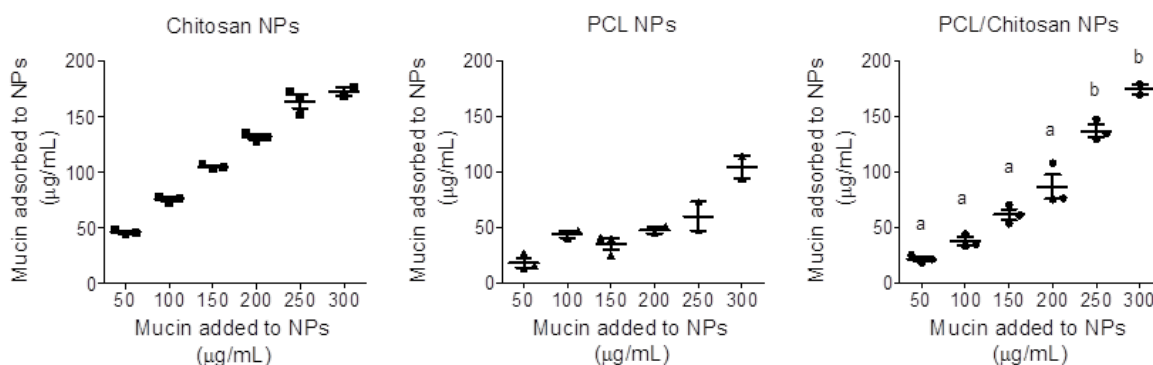

Figure 1: Mucin adsorption on 1 mg nanoparticles (PCL/chitosan NPs and on control chitosan NPs and PCL NPs). Data represent the average ± SEM of 3 individual assays. Statistical difference between means of PCL/chitosan NPs results and chitosan NPs results (a) or PCL NPs results (b) represent p<0.001.

The correct equilibrium between electric charge and hydrophobicity of the system is important to allow mucoadhesion but also diffusion through mucosal barriers [32]. Mucoadhesion may occur by multiple interaction forces between materials and the mucus like hydrogen bonding, electrostatic attraction, Van der Waals forces, mechanical interpenetration and entanglement and hydrophobic bonding [29, 30, 33]. There is not an ideal degree of mucoadhesion for the NPs that make them perfect mucosal delivery systems. In fact, the optimal mucoadhesion degree varies for each mucosa, depending on the thickness of the mucus layer and its specific clearance time [6]. The rationale behind the use of these polymeric NPs was to achieve a formulation suitable for mucosal vaccine delivery, whose surface properties were balanced by the dual polymer composition.

So far, we could only hypothesize that nanoprecipitated PCL/chitosan NPs would interact with mucus components. Therefore, *in vitro* experiments with mucus-producing epithelial cells aimed to demonstrate PCL/chitosan NPs mucoadhesivity. A human lung epithelial cell line, Calu-3, was used to perform confocal microscopy studies assessing particle ability to be retained at the mucus surface. This cell line was chose as Calu-3 cells, under air interface conditions, presents features of the airway epithelium (cilia, mucus production) [34]. In Figure 2, different slides of a z-stack (32 μm) illustrate increasingly deeper planes of the mucus covered cell monolayer. In the images, only nuclei and NPs are stained (blue and red, respectively). Mucus existence was inferred by the z-stack length of 32 m

191

between the top frame (where more particles were present) and the bottom frame (where most nuclei were present, indicating the cell monolayer). NPs agglomerates were visible at the mucus top surface and their presence decreased rapidly with the approximation to cell nucleus. Still, some particles were able to diffuse and reach the cell monolayer. These results suggest some retention of NPs, especially at the mucus surface.
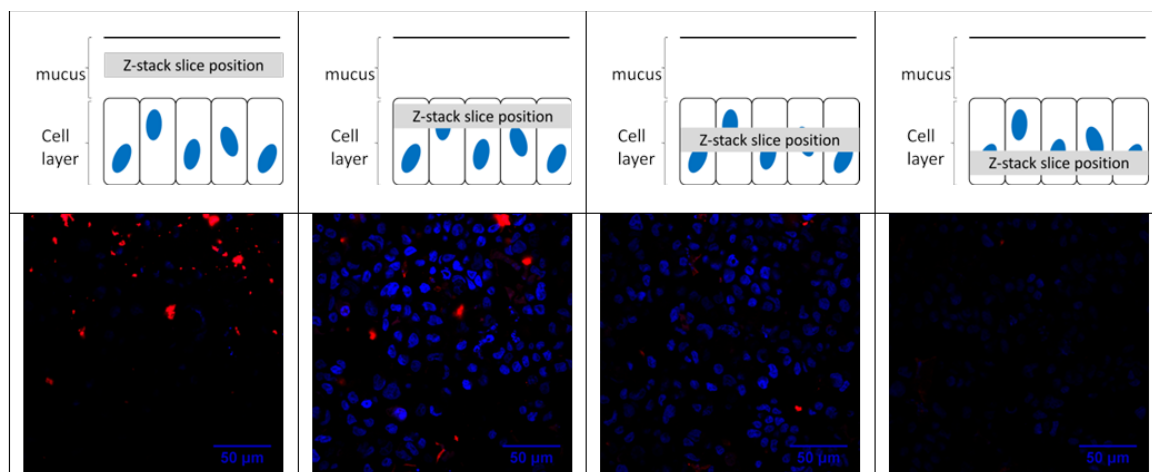

Figure 2: Calu-3 cells cultured on transwells at air-liquid interface conditions for differentiation and mucus production. After TEER values were constant around 400 .cm^2 to 500 .cm^2, 40 g/mL of fluorescently labeled nanoparticles (red) were placed on top of the mucus and incubation was kept for 6 h. At the end of the incubation period, apical medium was removed, the preparations fixed and cell nuclei were stained (blue). Confocal microscopy micrographs are representative of individual sections ('Z-stacks') taken across cell monolayer and apical mucus with a length of 32 μm.

3.2. Differentiated Caco-2 cells efficiently uptake PCL/chitosan NPs

The main purpose of this work was to evaluate PCL/chitosan NPs as adjuvant for nasal vaccination; however, the interaction of the delivery system with cells derived from intestinal mucosa was examined as well. The mucoadhesive property of the particles provides them the opportunity to be internalized, not only by the cells of the mucosa-associated lymphoid tissue, but also by epithelial cells. Differentiated Caco-2 cells possess morphological and functional features of small intestinal enterocytes constituted by a monolayer of polarized cells, coupled by tight junctions [35]. This way, Caco-2 cell also present similarities with nasal epithelium, and therefore were included in this report.

First of all, cell differentiation leads to phenotypic and genotypic changes evolving from a colon tumor-like pattern toward the profile of small intestinal tissue, which may alter the sensibility of the cells to the NPs [36, 37]. Therefore, a cell viability experiment was performed using non-differentiated and differentiated cells to evaluate the toxic effect of the NPs (Fig. 3). All NPs concentrations tested (ranging

from 0.1 µg/mL – 250 µg/mL) did not induce significant cytotoxicity, with cell viability superior to 70 % in all situations. The differences between non-differentiated and differentiated cells are around 10 % and are only statistically different for the 1, 10, 50 and 100 µg/mL concentrations. Similarly to our results, Gerloff et al. [38] demonstrated no significant different cytotoxicity mediated by 24 h incubation with ZnO NPs in non-differentiated and differentiated Caco-2 cells.
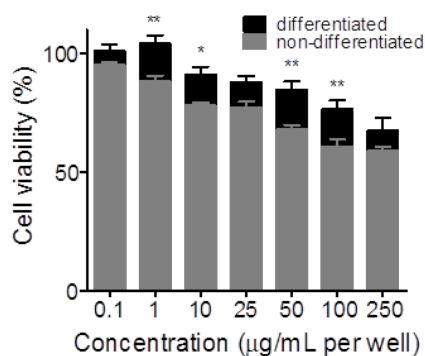

Figure 3: Differentiated (black) and non-differentiated (grey) Caco-2 cells were incubated for 24 h with diverse concentrations (ranging from 0.1 g/mL to 250 g/mL) of PCL/chitosan NPs. Cell viability (%) for each condition are expressed as mean ± SEM (n=6). Significant differences between differentiated and non-differentiated cells are marked by: *, $p < 0.05$ and **, $p < 0.01$.

To further evaluate the internalization of NPs by Caco-2 cells, uptake studies by flow cytometry analysis were developed. With the previous cytotoxicity results we were able to select a NPs concentration (40 µg/mL) to the uptake study that did not induce significant cell death, although uptake studies were performed with shorter incubation periods (4 h and 18 h) than cell viability ones (24 h). Figure 4 illustrates the uptake results and also show the fluorescent intensity geometric mean ratio (sample/background) calculated for the 3 independent assays performed. PCL/chitosan NPs labeled with FITC were able to enter non-differentiated cells more efficiently than non-differentiated cells (p <0.001). In fact, the NPs uptake in non-differentiated cells caused a mean fluorescent intensity increase ratio 2 or more folds higher, with or without the trypan blue treatment (to quench external fluorescence, resultant from membrane bound NPs). Differentiation diminishes the fluorescent intensity expressed by cells, meaning fewer particles are internalized or bound to the cell surface by differentiated cells. Nonetheless, the important observation to retain is that PCL/chitosan NPs were able to interact and enter differentiated Caco-2 cells.

An uptake study performed on non-differentiated Caco-2 cells with PCL NPs loaded with bovine serum albumin (BSA) labeled with FITC, showed that the hydrophobicity of the NPs was a beneficial factor for the uptake [11]. In fact, PCL NPs presented higher uptake than PLGA NPs obtained also by

193

w/o/w emulsion and both presented similar size and zeta potential. The difference remained only in the hydrophobicity, which was higher for PCL NPs [11]. By comparison, our NPs possessed the hydrophobic character of PCL, but also the influence of chitosan, which might further enhance the uptake by cells. A recent published study in differentiated Caco-2 cells revealed that trimethyl chitosan coating on PLGA NPs produced by w/o/w emulsion increased the NPs uptake by a adsorption mediated endocytosis, resultant from the positive charge conferred by chitosan to the formulation [39].
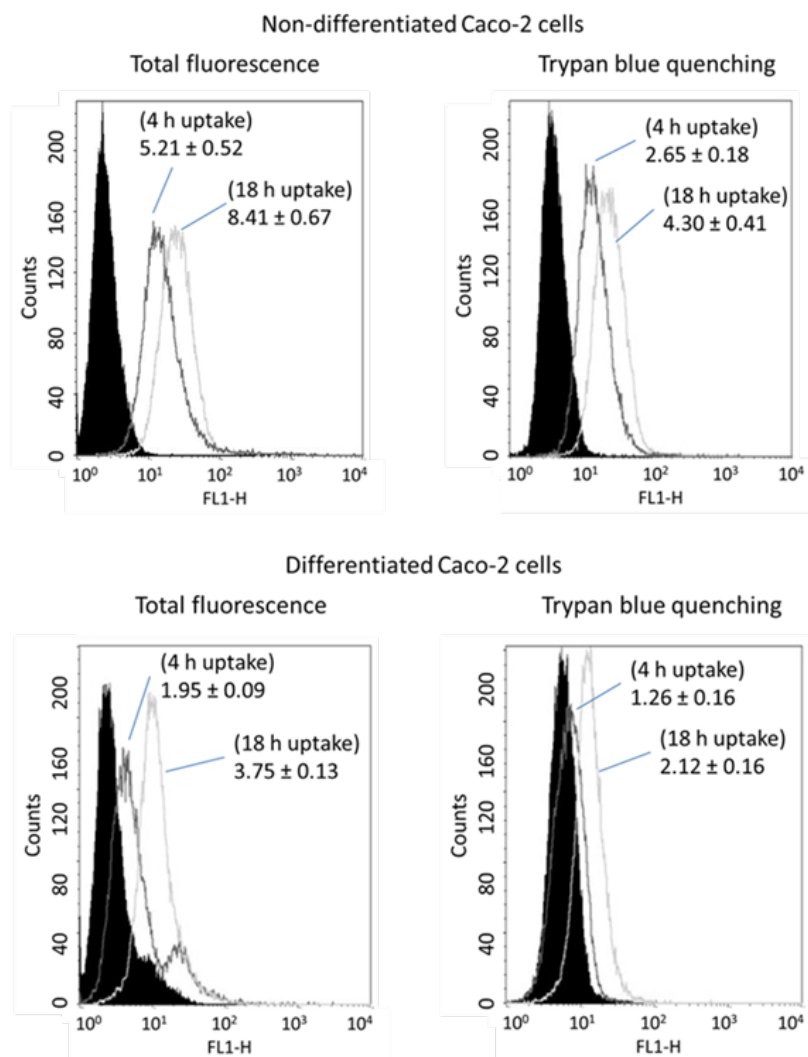
Figure 4: Differentiated and non-differentiated Caco-2 cell line uptake/interaction of 40 g/mL PCL/chitosan NPs fluorescently labeled with FITC at 4 h and 18 h incubation periods. Histograms represent the FITC mean fluorescent intensity (MFI) increase in the cell population under analysis. Black histograms represent the control cells; dark-grey lined histograms represent MFI increase after 4 h uptake assay; light-grey lined histogram represent MFI after 18 h uptake assay. Trypan blue quenching was exclude the fluorescence resultant from non-internalized NPs. The figure is a representative of 3 independent experiments with similar results. Close to each histogram curve, are presented the mean results of the ratio between sample and background (control cells)

geometric mean of the fluorescence, for the 3 assays performed, calculated according to [40]. Data are expressed as mean ± standard deviation.

3.3. Protein adsorption on PCL/chitosan NPs surface decreases its positive zeta potential

Zeta potential and average size of fresh NPs suspended in water and fresh NPs adsorbed with OVA, are described on the table 2. Model protein antigens, like OVA are commonly used for preliminary characterizations as they constitute a less expensive alternative and are highly antigenic in mice. Particularly in this case, it was chosen due to its similarities to HBsAg regarding isoelectric point and molecular weight. According to product information datasheet, OVA isoelectric point is between 4.4 and 4.9, while HBsAg isoelectric point is approximately 4.5 [41]. Therefore, although knowing the intrinsic differences between OVA and HBsAg do not allow for 100 % transposable results, the use of OVA as a model for the antigen adsorption studies can give us important insights in the expected behavior with HBsAg. To start with, OVA loading efficacy was near 100 % for all tested NPs:OVA ratios (w/w), meaning the short time period incubation procedure was efficient for loading the protein. Moreover, the size of all formulations was close to 200 nm and a decreasing size tendency was observed when protein is adsorbed. However, this phenomenon may be attributed to the reduction in hydrophilicity of the surface, once the evaluated parameter for size was the hydrodynamic diameter of the particles. Most authors agree the size between 100 nm and 500 nm is optimal for nanoparticles intended for mucosal delivery [10]. On the other hand, ideal surface properties, like hydrophobicity and charge are not consensual within the scientific community, and depend mostly on the polymer's nature [10]. Zeta potential values of NPs and protein adsorbed NPs show interesting variations. PCL/chitosan NPs when suspended in water present positive charge around + 25 mV, mainly due to the positively charged chitosan groups that influence surface characteristics of the NPs. When protein is adsorbed to the NPs, beyond hydrophobic interactions between hydrophobic regions of the protein and PCL polymer, electrostatic interactions are expected between the negative protein functional groups and the positive chitosan amine groups. When more protein is adsorbed to the same amount of PCL/chitosan NPs, it is likely that more chitosan amino groups are involved in the electrostatic interaction. Therefore, this phenomena might conduct to a decrease in the zeta potential of the NPs. Consistent with this theory, a decrease in zeta potential was confirmed for lower ratios. Indeed, a ratio 1614:10 generates surface charge values close to neutrality. A similar phenomenon was reported for PCL nanospheres modified with glycol chitosan. Without antigen, the zeta potential registered was + 38.7 mV while after adsorbing

an enzymatic extract of several antigenic proteins at an approximate ratio of 100:11 (w/w), the zeta potential decreased to low positive values (+ 5.4 mV) [18].

Table 2: Characterization of antigen adsorption at PCL/chitosan NPs surface. On the table are presented the Z-average particle size, zeta potential and model antigen (OVA) loading efficacy (%) for different ratios (w/w) NPs:OVA. Data are expressed as mean ± standard deviation.

Ratio NPs:OVA (w/w)	Average mean size (nm)	Polydispersity (PI)	Zeta potential (mV)	Loading efficacy (%)
1614:0	208.1 ± 28.7	0.18 ± 0.06	25.7 ± 2.9	> 96 %
1614:1.5	205.5 ± 5.0	0.09 ± 0.03	22.0 ± 2.4	> 96 %
1614:5	177.9 ± 2.5	0.12 ± 0.03	16.4 ± 0.5	> 96 %
1614:10	188.3 ± 1.2	0.13 ± 0.01	5.7 ± 1.5	> 96 %

After this initial characterization of the formulation using OVA as the model antigen, the adsorption of HBsAg at the NPs followed the same ratios and methodology. The adsorption of HBsAg VLPs on PCL/chitosan NPs, after simple incubation in aqueous media, avoids the encapsulation process, where the antigen is exposed to potential degradative environmental conditions. The same way as for OVA, loading efficacy with HBsAg was superior to 96 % for the 3 tested ratios. Florindo and co-workers [18] reported PCL nanospheres modified or not with glycol chitosan presented the same loading capacity for *Streptococcus equi* antigens. The reported differences, however, consisted in the interaction with the cargo, which was stronger for the modified ones, causing slower antigen release appropriate for nasal delivery.

3.4. Nasal vaccination mediated by PCL/chitosan NPs showed similar results with 10 µg or 1.5 µg of HBsAg per dose

Antigens, delivered by mucosal routes of administration, are generally diluted in mucosal fluids, captured in mucus gels, attacked by proteases, and excluded by epithelial barriers. Consequently, high amounts of antigen are needed to elicit a good immune response [5]. Moreover, the induction of the immune response at the NALT, benefits the isotype switching of B cells to IgA-producing plasma cells and further transport of sIgA to mucosal surfaces, where this antibody is fundamental for virus neutralization and opsonization [4]. IN immunization with HBsAg loaded PCL/chitosan NPs was expected to generate good systemic immunity as well as mucosal antibodies preventing the infection at a possible site of HBV entry (vaginal mucosa). In addition, we wanted to evaluate whether NPs administered through the nasal route, were able to reduce the amount of antigen required to generate the anti-HBsAg immune response.

196

In Figure 5A are presented serum anti-HBsAg IgG titers from mice immunized with formulations containing 1614 µg NPs/dose and either 1.5 µg, 5 µg or 10 µg HBsAg/dose in comparison to HBsAg (10 µg/dose) not associated with any adjuvant. Despite the overall weak outcome in the achievement of a systemic immune response, the results suggest an interesting finding. The formulation which contains lowest antigen amount (1614NPs-1.5) was the one that induced a higher number of responder mice. In fact, 4 out of 5 mice presented detectable specific IgG antibodies, while only 2 and 1 mice responded to the formulations containing 5 and 10 µg HBsAg/dose, respectively. So far, the antigen dose of 1.5 µg is much lower than the doses that are generally reported in the scientific literature for the HBsAg intranasal vaccination. Moreover, the antibody titer is not statistically different from the one obtained with mice, vaccinated with the high-dose HBsAg. Therefore, the differences observed in the total number of mice that were able to respond to the treatment should be related with formulation characteristics. A previous study using chitosan based NPs encapsulating HBsAg evaluated 2 different antigen doses: 10 and 20 g [42]. In general, their serum IgG results were low and no significant differences were found between the doses. They suggested the antigen interaction with the NPs caused a reduction of their cationic surface charge, decreasing the uptake and delivery from the nasal barrier [42]. In accordance with these authors, we concluded with the preliminary analysis performed with the model antigen OVA, that the increase of the antigen associated with the NPs had a direct influence on zeta potential of the NPs. Moreover, the same results were obtained with the zeta potential analysis of the formulations administered to the animals, which were the same NPs:protein (w/w) ratios. As is shown in Figure 5B, when 1.5 µg HBsAg are adsorbed to 1614 µg of PCL/chitosan NPs the zeta potential remains close to the one presented by unloaded NPs (+ 20.05 ± 0.6 mV). Yet, when 10 µg are adsorbed to the same amount of nanoparticles, the zeta potential decreases to values closer to neutrality. In this situation, the zeta potential differences may be enough to promote or diminish the efficacy of the adsorbed HBsAg when delivered through nasal mucosa. Once more, the results suggest the positive amino groups of chitosan present at NPs surface, contributing to the positive zeta potential may be blocked by the HBsAg. This blockage may be diminishing the ability of the vaccine formulation to generate an immune response as positive surface charge is an important aspect that increases the particle-cell interactions [43]. Furthermore, we can speculate that HBsAg presence at the surface of the NPs, may be preventing the mucoadhesive effect of chitosan, which is known to be dependent on the interaction of amino groups with the negative charged mucosae mucin [29]. In comparison, the 1614NPs-1.5 formulation possessed both the hydrophobic nature of PCL and the chitosan cationic influence, which resulted in higher number of animals presenting systemic immune responses.

Besides the systemic antibody titers evaluated after the nasal vaccination, specific anti-HBsAg sIgA was analyzed in the vaginal and nasal mucosa of immunized mice. To prevent errors from the variability

derived from the sample collection technique among mice, anti-HBsAg specific sIgA was normalized against total sIgA present in each sample. As illustrated in Figure 5C vaginal sIgA ratios were low (<0.06) and no statistical differences were found between the responder mice in the different groups. Surprisingly, 4 out of 5 mice from the group immunized with 10 g free HBsAg developed vaginal specific sIgA. Also, all animals from the 1614NPs-10 group presented vaginal specific sIgA. This may indicate higher amounts of antigen may be required to generate mucosal immune responses. Similar findings were found in our laboratory with a different antigen and delivery system [44]. In this previous study, chitosan NPs, incorporating a mast cell activator C48/80, were used as an anthrax protective antigen (PA) delivery system and it was observed that the mucosal immune response was antigen-dose dependent, while the systemic immune response was more dependent on the formulation characteristics.
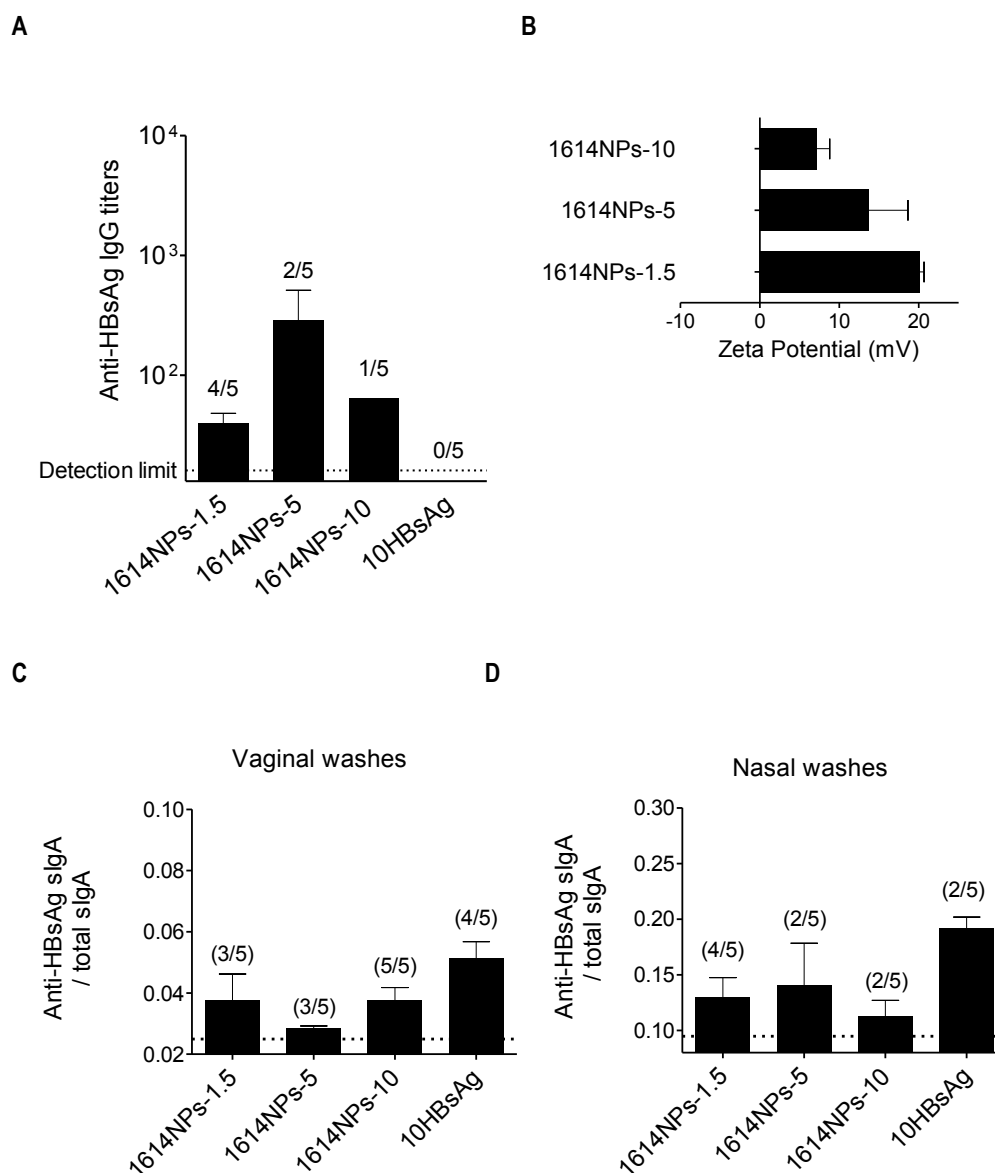
A

B

C

Vaginal washes

D

Nasal washes

Figure 5: Results from the *in vivo* studies evaluating PCL/chitosan NPs as HBsAg vaccine adjuvant. Mice were immunized with formulations containing increasing amounts of HBsAg (1.5, 5 and 10 g/dose) and 1614 µg/dose of PCL/chitosan NPs, on days 0, 7 and 21. Control group corresponds to mice immunized with free HBsAg dosed to the highest antigen amount tested: 10 µg/dose. (A) Serum anti-HBsAg IgG titers at day 42. The end-point titer presented in the results represents the antilog of the last log 2 dilution for which the OD were at least two-fold higher than the value of the naive sample equally diluted. Dotted line represents the detection limit. Numbers above bars represent the number of mice with detectable antibody levels. Results are presented as mean ± SEM. No statistical differences were found between groups. (B) Zeta potential of IN administered formulations. Measurements were performed after IN immunization with the remainder of each formulation. Data (mean ± SD) represents the three independent formulations from each boost. Vaginal (C) and nasal (D) anti-HBsAg sIgA (ng/mL) normalized against total sIgA (ng/mL) detected at day 4.2. Results were calculated performing the ratio of each individual mouse Anti-HBsAg sIgA/ Total sIgA concentration. Positive results were only considered for ratios

2-fold higher than naïve mice (represented by the dotted line). Numbers above bars represent the number of mice with positive antibody levels. Data (mean ± SEM). No statistical differences were found between groups.

Considering the nasal specific antibody production (Fig. 5D), a high number of mice presented anti-HBsAg sIgA/total sIgA ratios when the 1614NPs-1.5 formulation was used. Once more, a 10-fold increase in the antigen amount was ineffective probably because the formulation did not present optimal characteristics.

Results suggest that the zeta potential of the vaccine formulation has an important influence on the generation of the immune response. Similar conclusions are described in the literature regarding the immune response illustrated in this study. Recombinant hemagglutinin antigen (HA) from influenza virus was encapsulated into chitosan coated PCL NPs (+22.88 mV) and the immune response generated was compared with HA loaded PCL NPs (7.13 mV) [17]. Results showed both the systemic and the mucosal immune responses were stronger when chitosan was coating PCL NPs [17]. However, neither were the particles produced by the nanoprecipitation technique, nor was the antigen at the surface of the particles as in our experiment. We previously mentioned the contribution of *Streptococcus equi* antigens adsorbed at the surface PCL nanospheres modified with glycol chitosan for the zeta potential decrease (from + 38.7 mV to + 5.4 mV) [18]. In that report, the authors compared the immune response generated by this formulation with unmodified PCL nanospheres (without chitosan), that presented a zeta potential of -32.7 mV when adsorbed with antigens. Again, the immune response was higher when the formulation presented the cationic modification supporting the hypothesis that positively charged groups at the NPs surface, establish a decisive contribution for effective nasal vaccination. Nonetheless, the immune response they reported was derived from a *Streptococcus equi* enzymatic extract, which contains proteins and bacterial contaminants like LPS, a well-known immunopotentiator adjuvant, in addition to the desired antigens.

Bearing in mind the results obtained, in order to improve PCL/chitosan NPs as a nasal vaccine delivery system, the positive surface charge must be guaranteed after antigen adsorption. Additionally, nasal vaccination in mice should be performed with a reduced volume in order to prevent variable bioavailability due to the deposition of the formulation in the lung and lower respiratory tract [45]. However, some reports do not consider the volume an issue. A previous study reporting a nasal vaccine for HBV using glycol chitosan coated PLGA NPs encapsulating HBsAg suggested a good systemic immune response comparable to the immune response generated by SC administered alum adsorbed HBsAg. Also, they reported a strong mucosal sIgA production that was not accomplished with the SC administered control. The problem is the fact that they performed the immunization technique on BALB/c mice by inserting a small piece of polyethylene tubing, 0.2 cm into mice nostril (supine position)

and injected 0.5 mL of the formulation containing 10 g HBsAg into the nasal cavity. This formulation volume used is not recommended for nasal administration and consequently the results may not translate into an immune response initiated at the nasal mucosa region [15]. In the intranasal administration of PCL based nanospheres adsorbed with *S. equi* antigens, they used 50 L formulation although knowing other authors [46] have shown that 40 % of a 50 L intranasal dose reaches the lungs [18]. In order to avoid errors like this, we only administered 15 L of the PCL/chitosan NPs:HBsAg formulations to each mouse. However, a dose of 10 L per nostril would be mostly retained in the nose and would mean an increase of 25 % in the amount of antigen administered. This could be a strategy to improve our results. By using the 1614NPs-1.5 formulation and administering 20 L per mice, we could maintain the formulation positive zeta potential and induce an increase in the mucosal immune response as well as in the systemic production of antibodies. Another hypothesis to improve our results would be to further concentrate the NPs in the same volume in order to have a higher NPs/dose able to adsorb more antigen, without altering zeta potential of the final formulation. Though, this is more difficult to achieve since the NPs suspension was already highly concentrated.

4. Conclusions

New strategies to increase HBV vaccination especially in developing countries may be achieved by polymeric nanoparticle based vaccination for administration at mucosal sites, like the nasal mucosa. This accessible route would not need specialized personnel for the administration. Also, efficient nasal vaccination would induce sIgA antibody production at distant mucosal sites, increasing virus neutralization at mucosal entry sites. In the present paper we demonstrated the adjuvant ability of PCL/chitosan NPs as a nasal delivery system for HBsAg and the importance of the zeta potential of the formulation. All formulations tested generated equal immune responses, even with antigen doses 7-fold divergent. Although low, the immune response achieved with 1.5 µg antigen by IN administration route is an important realization, as recombinant antigens like HBsAg, are expensive biotechnological products, that highly increase the cost of modern vaccines. A dose-sparing activity of the formulations would therefore be beneficial in terms of a commercial approach of a nasal vaccine. The confirmation of the zeta potential influence, and a correct optimization of the formulation based on the attained conclusions, might enhance the PCL/chitosan NPs adjuvant activity as a mucosal delivery system with dose-sparing properties, becoming closer to an attractive and efficient HBV nasal vaccine.

References

1. MacLachlan, J.H. and B.C. Cowie, *Hepatitis B Virus Epidemiology.* Cold Spring Harb Perspect Med, 2015. **5**(5).

2. Borges, O., et al., *Mucosal vaccines: recent progress in understanding the natural barriers.* Pharm Res, 2010. **27**(2): p. 211-23.

3. Holmgren, J. and C. Czerkinsky, *Mucosal immunity and vaccines.* Nat Med, 2005. **11**(4 Suppl): p. S45-53.

4. Ogra, P.L., H. Faden, and R.C. Welliver, *Vaccination strategies for mucosal immune responses.* Clin Microbiol Rev, 2001. **14**(2): p. 430-45.

5. Neutra, M.R. and P.A. Kozlowski, *Mucosal vaccines: the promise and the challenge.* Nat Rev Immunol, 2006. **6**(2): p. 148-58.

6. Woodrow, K.A., K.M. Bennett, and D.D. Lo, *Mucosal vaccine design and delivery.* Annu Rev Biomed Eng, 2012. **14**: p. 17-46.

7. Zaitseva, M., et al., *Use of human MonoMac6 cells for development of in vitro assay predictive of adjuvant safety in vivo.* Vaccine, 2012. **30**(32): p. 4859-65.

8. De Souza Reboucas, J., et al., *Nanoparticulate adjuvants and delivery systems for allergen immunotherapy.* J Biomed Biotechnol, 2012. **2012**: p. 474605.

9. Ensign, L.M., R. Cone, and J. Hanes, *Oral drug delivery with polymeric nanoparticles: the gastrointestinal mucus barriers.* Adv Drug Deliv Rev, 2012. **64**(6): p. 557-70.

10. des Rieux, A., et al., *Nanoparticles as potential oral delivery systems of proteins and vaccines: a mechanistic approach.* J Control Release, 2006. **116**(1): p. 1-27.

11. Singh, J., et al., *Diphtheria toxoid loaded poly-(epsilon-caprolactone) nanoparticles as mucosal vaccine delivery systems.* Methods, 2006. **38**(2): p. 96-105.

12. Borges, O., et al., *Induction of lymphocytes activated marker CD69 following exposure to chitosan and alginate biopolymers.* Int J Pharm, 2007. **337**(1-2): p. 254-64.

13. Tafaghodi, M., et al., *Hepatitis B surface antigen nanoparticles coated with chitosan and trimethyl chitosan: Impact of formulation on physicochemical and immunological characteristics.* Vaccine, 2012. **30**(36): p. 5341-8.

14. Pawar, D. and K.S. Jaganathan, *Mucoadhesive glycol chitosan nanoparticles for intranasal delivery of hepatitis B vaccine: enhancement of mucosal and systemic immune response.* Drug Deliv, 2014: p. 1-11.

15. Pawar, D., et al., *Development and characterization of surface modified PLGA nanoparticles for nasal vaccine delivery: effect of mucoadhesive coating on antigen uptake and immune adjuvant activity.* Eur J Pharm Biopharm, 2013. **85**(3 Pt A): p. 550-9.

16. Pawar, D., et al., *Evaluation of mucoadhesive PLGA microparticles for nasal immunization.* Aaps j, 2010. **12**(2): p. 130-7.

17. Gupta, N.K., et al., *Development and characterization of chitosan coated poly-(varepsilon-caprolactone) nanoparticulate system for effective immunization against influenza.* Vaccine, 2011. **29**(48): p. 9026-37.

18. Florindo, H.F., et al., *The enhancement of the immune response against S. equi antigens through the intranasal administration of poly-epsilon-caprolactone-based nanoparticles.* Biomaterials, 2009. **30**(5): p. 879-91.

19. Jesus, S., G. Borchard, and O. Borges, *Freeze Dried Chitosan/ Poly- e-Caprolactone and Poly-e-Caprolactone Nanoparticles: Evaluation of their Potential as DNA and Antigen Delivery Systems.* J Genet Syndr Gene Ther 2013. **4**(164).

20. Martinac, A., et al., *Development and bioadhesive properties of chitosan-ethylcellulose microspheres for nasal delivery.* Int J Pharm, 2005. **291**(1-2): p. 69-77.

21. Mantle, M. and A. Allen, *A colorimetric assay for glycoproteins based on the periodic acid/Schiff stain [proceedings].* Biochem Soc Trans, 1978. **6**(3): p. 607-9.

22. Dhawan, S., A.K. Singla, and V.R. Sinha, *Evaluation of mucoadhesive properties of chitosan microspheres prepared by different methods.* AAPS PharmSciTech, 2004. **5**(4): p. e67.

23. Borges, O., et al., *Preparation of coated nanoparticles for a new mucosal vaccine delivery system.* Int J Pharm, 2005. **299**(1-2): p. 155-66.

24. Borchard, G., et al., *Transport and local metabolism of budesonide and fluticasone propionate in a human bronchial epithelial cell line (Calu-3).* J Pharm Sci, 2002. **91**(6): p. 1561-7.

25. Haghi, M., et al., *Time- and passage-dependent characteristics of a Calu-3 respiratory epithelial cell model.* Drug Dev Ind Pharm, 2010. **36**(10): p. 1207-14.

26. Vllasaliu, D., et al., *Tight junction modulation by chitosan nanoparticles: comparison with chitosan solution.* Int J Pharm, 2010. **400**(1-2): p. 183-93.

27. Teijeiro-Osorio, D., C. Remunan-Lopez, and M.J. Alonso, *Chitosan/cyclodextrin nanoparticles can efficiently transfect the airway epithelium in vitro.* Eur J Pharm Biopharm, 2009. **71**(2): p. 257-63.

28. Rahman, M., et al., *Protein-Nanoparticle Interactions.* Springer Series in Biophysics, ed. B. Martinac. Vol. 15. 2013: Springer-Verlag.

29. Patil, S., et al., *Mucoadhesive chitosan microspheres of carvedilol for nasal administration.* J Drug Target, 2010. **18**(4): p. 321-31.

30. Chuah, L.H., et al., *Curcumin-containing chitosan nanoparticles as a potential mucoadhesive delivery system to the colon.* Pharm Dev Technol, 2013. **18**(3): p. 591-9.

31. Mazzarino, L., et al., *On the mucoadhesive properties of chitosan-coated polycaprolactone nanoparticles loaded with curcumin using quartz crystal microbalance with dissipation monitoring.* J Biomed Nanotechnol, 2014. **10**(5): p. 787-94.

32. Petrovsky, N. and J.C. Aguilar, *Vaccine adjuvants: current state and future trends.* Immunol Cell Biol, 2004. **82**(5): p. 488-96.

33. Shaikh, R., et al., *Mucoadhesive drug delivery systems.* J Pharm Bioallied Sci, 2011. **3**(1): p. 89-100.

34. Florea, B.I., et al., *Drug transport and metabolism characteristics of the human airway epithelial cell line Calu-3.* J Control Release, 2003. **87**(1-3): p. 131-8.

35. Ferruzza, S., et al., *A protocol for differentiation of human intestinal Caco-2 cells in asymmetric serum-containing medium.* Toxicol In Vitro, 2012. **26**(8): p. 1252-5.

36. Speckmann, B., et al., *Proinflammatory cytokines down-regulate intestinal selenoprotein P biosynthesis via NOS2 induction.* Free Radic Biol Med, 2010. **49**(5): p. 777-85.

37. Saaf, A.M., et al., *Parallels between global transcriptional programs of polarizing Caco-2 intestinal epithelial cells in vitro and gene expression programs in normal colon and colon cancer.* Mol Biol Cell, 2007. **18**(11): p. 4245-60.

38. Gerloff, K., et al., *Influence of simulated gastrointestinal conditions on particle-induced cytotoxicity and interleukin-8 regulation in differentiated and undifferentiated Caco-2 cells.* Nanotoxicology, 2013. **7**(4): p. 353-66.

39. Sheng, J., et al., *N-Trimethyl Chitosan Chloride-Coated PLGA Nanoparticles Overcoming Multiple Barriers to Oral Insulin Absorption.* ACS Appl Mater Interfaces, 2015. **7**(28): p. 15430-41.

40. Leslie, G., *Flow cytometry - a basic guide.* 2006, Institute of Medical Biology, University of Southern Denmark.

41. Jezek, J., et al., *A heat-stable hepatitis B vaccine formulation.* Hum Vaccin, 2009. **5**(8): p. 529-35.

42. Prego, C., et al., *Chitosan-based nanoparticles for improving immunization against hepatitis B infection.* Vaccine, 2010. **28**(14): p. 2607-14.

43. Zhao, L., et al., *Nanoparticle vaccines.* Vaccine, 2014. **32**(3): p. 327-37.

44. Bento, D., H.F. Staats, and O. Borges, *Effect of particulate adjuvant on the anthrax protective antigen dose required for effective nasal vaccination.* Vaccine, 2015.

45.   Coombes, A.G., et al., *Single dose, polymeric, microparticle-based vaccines: the influence of formulation conditions on the magnitude and duration of the immune response to a protein antigen.* Vaccine, 1996. **14**(15): p. 1429-38.

46.   Eyles, J.E., et al., *Analysis of local and systemic immunological responses after intra-tracheal, intra-nasal and intra-muscular administration of microsphere co-encapsulated Yersinia pestis sub-unit vaccines.* Vaccine, 1998. **16**(20): p. 2000-9.

Chapter 6. Concluding remarks and future perspectives

Concluding remarks

The work presented in this thesis was devoted to the study of the biodegradable PCL/chitosan NPs as a vaccine adjuvant, focusing on its abilities as a delivery system and as an immunopotentiator. In particular, PCL/chitosan NPs adjuvanticity was analyzed in the context of the development of an improved hepatitis B vaccine.

So far, NPs based on the physical blend of PCL and chitosan had never been studied and used as a delivery system for any hepatitis B antigen. Moreover, all similar particles described in vaccination studies involving other antigens were prepared by complex procedures. Their preparation comprises diverse techniques, like emulsification followed by diffusion and/or evaporation of the organic solvent. By contrast, in the present work the nanoprecipitation technique was the selected method for PCL/chitosan NPs preparation due to its simplicity, since demanding and time consuming techniques are not attractive as simple and fast ones. In fact, the major advantage of this technique is the rapid formation of the NPs in a one-step procedure. In addition, it may avoid prolonged stirring rates, sonication or increased temperatures, and does not require water immiscible solvents, nor the generation of oily-aqueous interfaces [1]. Also, simple techniques are generally more reproducible.

During the initial preparation phase, it was possible to observe that the PCL/chitosan NPs prepared, formed a visually stable formulation, with no aggregation and no deposition during several days. These NPs were also stable to temperature oscillations, even during the production stage. Therefore, PCL/chitosan NPs present advantages over chitosan NPs, which are widely studied and were previously characterized and described by our group. By contrast to PCL/chitosan NPs, chitosan NPs stability and reproducibility is highly influenced by the room temperature.

In the scientific literature, several evidences suggest that the incorporation of a hydrophilic polymer (chitosan) in hydrophobic-based NPs (PCL NPs) would benefit a "pathogen-mimicking effect" of the delivery system, advantageous for the immune response generation [2-4]. Moreover, diverse strategies involving chitosan were reported during the last years and their success was mainly derived from its mucoadhesive and immunostimulatory properties. These properties are particularly advantageous for the mucosal delivery of vaccines. Therefore, the rationale behind the choice to include this polymer in PCL particles was entirely justified. The zeta potential value of + 21.7 ± 0.5 mV, obtained with PCL/chitosan NP water suspension proved chitosan presence into particles and its influence on particle surface, since PCL NPs water suspension presented a neutral zeta potential. This positive charge given by chitosan amino groups, increases the interaction with the negatively charged cell surfaces [5] and the negatively charged sialic acid present in the mucus [6]. In fact, results of the studies presented along

this thesis and performed with different cell lines (A549, PBMC, Caco-2, HMC-1) revealed good cell surface interaction and cellular uptake of PCL/chitosan NPs. In comparison to PCL NPs, the blend NPs demonstrated higher adsorption ($p <0.001$) of porcine mucin type III, a glycoprotein found in mucus secretions. Moreover, these NPs were found to adhere to a differentiated monolayer of Calu-3 epithelial cell line, with mucus-producing ability.

The favorable results from the characterization of PCL/chitosan NPs instigated the progression of the work and the evaluation of these NPs as adjuvant nanocarriers for antigens. The adsorption was the preferred loading procedure during all the work developed. This simple adsorption method performed after NPs production and isolation, avoided the exposure of cargo molecules to harmful environmental conditions, such as the organic solvent necessary for PCL dissolution during production. Most of the work described in the literature about vaccines comprising PCL and chitosan particles, use the encapsulation method to load the antigens. However, Florindo et al. [7] had already tried this approach but with an enzymatic extract containing protein antigens, instead of purified proteins or recombinant antigens. The adsorption of the recombinant hepatitis B virus surface antigen (HBsAg) on PCL/chitosan NPs was highly efficient, as we expected from the results achieved previously with model proteins. Moreover, after 1 month storage of freeze dried HBsAg loaded PCL/chitosan NPs, the recombinant antigen presented no major alteration of its secondary structure (see Figure A from the supplementary material chapter 6), a result also similar to the ones obtained during a 6 month storage study with ovalbumin loaded PCL/chitosan NPs. Interestingly, we could found that the zeta potential of the NPs in water was highly influenced by the protein adsorption: increasing amounts of protein at the NPs surface induced a progressive decrease in zeta potential surface charge, ultimately reaching negative values. Thus, for the vaccination studies it was hypothesized that a NP:antigen (w/w) ratio allowing the conservation of the positive zeta potential of the NPs would be beneficial for the cellular interaction and the NPs uptake by antigen presenting cells (APCs).

Vaccination studies using HBsAg recombinant protein, showed the adjuvant ability of PCL/chitosan NPs, through the subcutaneous (SC) route of administration. Indeed, PCL/chitosan NPs induced a dose-dependent adjuvant effect for the hepatitis B recombinant antigen. The highest NP dose clearly induced a systemic humoral immune response higher than the free antigen and, most importantly, higher than the commercially available vaccine, Engerix-B®. Moreover, the cellular immune response generated was characterized by a Th1/Th17 profile, which was revealed by the production of IFN- and IL-17 cytokines by vaccinated mice spleen cells, after re-stimulation with the antigen. Major challenges in the development of new prophylactic or therapeutic vaccines for hepatitis B virus (HBV) reside in the generation of strong cellular immune responses [8]. Accordingly, the work developed demonstrates that PCL/chitosan NPs induced an important adjuvant effect during HBsAg SC vaccinations, by stimulating

both the humoral and cellular arm of the immune response. Moreover, in the literature, no evidence suggests that the Th1 cellular response occurs for alum-adjuvanted vaccines, like Engerix-B® [9]. On the other hand, Th17 cellular response was not proved for conventional protein antigens adjuvanted with alum [9, 10]. In fact, the ability of alum to promote Th17 responses appears to be dependent on the nature of the vaccine antigen and for instance, killed bacteria may synergize with alum to promote Th17 responses [11]. Regarding HBsAg vaccination, only one report from Saade et al. [9] evaluated the IL-17 production after mice vaccination with HBsAg mixed with a novel adjuvant Advax™ (polysaccharide adjuvant based on delta inulin). Likewise, they found increased IL-17 production in their interest group as compared to free HBsAg and alum-adjuvanted HBsAg groups. Consequently, the stimulation of Th1 and Th17 cytokines by PCL/chitosan NPs when used as nanocarriers for HBsAg vaccination together with the higher IgG titers may provide better protection that the existing alum-adjuvanted HBV vaccines.

PCL/chitosan NPs adjuvant ability demonstrated in the SC vaccination studies instigated exploratory experiments with the aim of revealing the immunological mechanism associated to the particles effect. Until the moment, the intrinsic immunostimulatory properties of the PCL/chitosan NPs were barely discussed in the literature. The studies performed in this thesis, showed endotoxin-free PCL/chitosan NPs had no pro-inflammatory effect on mononuclear cells isolated from human blood (PBMCs). Therefore, it can be suggested that the adjuvant effect of these NPs do not depend on the activation of inflammatory pathways involving TNF- secretion (such as the nuclear factor κ (NF-κ) or the mitogen activated protein kinase (MAPK) pathways [12]), decreasing the risk of tissue damage at the site of administration. In fact, although the induction of TNF- production may be beneficial for recruiting immune cells (monocytes, macrophages, DCs, neutrophils, NK and T memory cells) to the administration site increasing the immune response, in some situations, it may cause toxic effects. On the other hand, it was observed that PCL/chitosan NPs cause -hexosaminidase release from HMC-1 cells, which is a signal of mast cell (MC) activation. In fact, MCs mainly located at the host–environment interface, respond to pathogen stimulation releasing preformed mediators that activate the innate immune system and further direct immune cells to the site of infection and to draining lymph nodes [13]. The finding that PCL/chitosan NPs are MC activators constitutes an important element to understand the mechanistic concepts behind the NPs adjuvant activity, but it also instigates research concerning other nanoparticulate systems. Until now, among polymeric delivery systems, only chitosan NPs had been described as MC activators [13], in a study performed by elements of our group. Now, we demonstrated that PCL/chitosan NPs are also MC activators and that chitosan is a key element for this effect. Indeed, PCL NPs induced a much lower -hexosaminidase release and its only difference to PCL/chitosan NPs is the absence of the polysaccharide.

211

The ability of PCL/chitosan NPs to activate MCs *in vitro* suggested a mucosal vaccine adjuvant activity, due to the extensive presence of MCs at mucosal surfaces [14]. Furthermore, the encouraging SC results achieved, confirmed the intrinsic immunostimulatory capability of PCL/chitosan NPs. Consequently, a nasal vaccination study was performed but the serum IgG titers found on intranasally immunized mice were low in comparison to the titers found on subcutaneously immunized mice, and not all mice responded. Nonetheless, among the 3 formulations tested by nasal route (containing equal NP doses), the highest rate of responders was found with the vaccine formulation that presented the lowest dose of antigen (1.5 µg). Notably, this formulation was similar to a formulation used in the SC vaccination study, except for the volume. The realization that an immune response was induced through nasal vaccination, with a dose of HBsAg equal to what was used subcutaneously is extremely important. The dose reduction of expensive biotechnological products, as recombinant antigens, is an asset when researching vaccines whose targets are predominantly developing countries. The first problem associated with the success of this nasal vaccination strategy was the concentration of the formulation in reduced volumes (i.e., 15 µL), so that the vaccine is deposited in the mice nasal mucosa, instead of being swallowed or instilled into the lungs. The 3 formulations tested were extremely concentrated, with 1614 µg of NPs in 15 µL and varied in the amount of antigen adsorbed. As stated, the zeta potential was dependent on the amount of antigen adsorbed, and in this case the nanoparticulate formulation with the lowest antigen dose (equal to SC vaccination) presented a positive zeta potential (> 20 mV), while the one with the highest antigen dose (10 µg) presented a neutral zeta potential. The adsorption of the antigen, although contributing to a better and faster exposition of antigenic epitopes to APCs, changed the surface charge of the NPs, possibly decreasing its mucoadhesive capacity and its ability to stablish cellular interactions with cells. Consequently, higher antigen doses did not induce better immune responses, highlighting the importance of the adjuvants and the formulation characteristics in challenging strategies like mucosal vaccination.

Taking under consideration the successful results achieved with the SC recombinant vaccine, a pDNA vaccine was developed using the same PCL/chitosan NP delivery system and the same immunization route. However, the formulation containing PCL/chitosan NPs complexes prepared with pDNA encoding for HBsAg generated no systemic immune response. In fact, these results were consistent with the preliminary *in vitro* results. Despite the good pDNA loading ability, *in vitro* studies with a luciferase plasmid complexed with PCL/chitosan NPs showed low transfection efficiency. Altogether, the results suggest that the surface charge of the complexes might be in the origin of the negative outcome. During the preparation and characterization of the vaccine formulation, the pDNA loading ability was found to be exclusively dependent on the presence of chitosan at the NPs surface, since PCL NPs (prepared without chitosan) were not able to complex pDNA. Though, due to the highly

negative nature of pDNA, chitosan presence in the NPs was not able to maintain the positive surface charge of the complexes, even at NP:pDNA ratios (w/w) of 500:1, which probably resulted in a reduced cellular interaction.

The co-administration of immunological adjuvants with polymeric NPs is a well-known strategy to improve or even re-direct the type of immune response generated against HBV infection. Accordingly, it was explored the co-administration of CpG-ODN and of exosomes with the subcutaneous HBsAg loaded PCL/chitosan NP vaccine formulation.

The vaccination with the nanoparticulate formulation containing CpG-ODN generated an immune response compatible with the presence of the co-adjuvant, which was characterized by both Th2 and Th1 antibodies and IFN- secretion.

In its turn, the use of exosomes as co-adjuvants to the HBsAg loaded NPs induced a significantly higher IFN- production by spleen cells. This cytokine production was greatly enhanced particularly at the basal level, indicating a non-specific stimulation of the innate immune system. So far, in the literature, encouraging results of exosomes in infectious vaccination field rely on their use as delivery systems, this is, natural nano-vesicles containing antigens, either directly (antigens pulsed into exosomes) or indirectly loaded (exosomes pulsed into exosomes precursor cells). In contrast, our approach involved the use of exosomes without previous contact with the target antigen as vaccine adjuvants. Based on the results, this hypothesis needs further investigation.

Interestingly, in both situations described the use of a co-adjuvant seems to somehow limit the adjuvant effect induced by each component, rather than causing a synergistic effect. In fact, the vaccination of mice with exosomes plus HBsAg loaded PCL/chitosan NPs induced lower IFN- titers than the vaccination with HBsAg and exosomes in the absence of NPs, and induced lower antibody titers than the vaccination of mice with HBsAg loaded NPs in the absence of exosomes. Similarly, the vaccination with HBsAg loaded PCL/chitosan NPs co-adjuvanted with CpG-ODN did not induce IL-17 secretion, which opposes to the response generated in the absence of this immunopotentiator.

To conclude, the work performed in this thesis encountered the main objectives initially proposed. PCL/chitosan NPs were proved to be good vaccine adjuvants for recombinant antigens. Specifically, they were able to increase the humoral and cellular immune responses to HBsAg and therefore, can be suggested as an alternative to aluminum salts, used in the commercially available vaccines. Although the exact mechanism of action of PCL/chitosan NPs remains to be fully characterized, the induction of cytokines characteristic of a Th1/Th17 based immune response against the HBsAg suggests that this might be an advantageous vaccination strategy, in particular for hepatitis B.

Future perspectives

Indubitably, the studies performed on the course of this thesis brought new insights into the "nanovaccinology" field and as expected, each conclusion opened the door to new questions and challenges.

The adjuvant effect of PCL/chitosan NPs for the recombinant hepatitis B surface antigen was demonstrated on this PhD project, particularly when the formulations were administered by the SC route. Nonetheless, in the future, further mechanistic studies should be done to complete the knowledge about PCL/chitosan NPs adjuvant ability. Moreover, it could be advantageous to study the vaccination with lower antigen doses, maintaining the elevated amounts of NPs and using for instance a single administration regimen. This proof of concept should be important to demonstrate the vaccine superior efficacy. These studies, together with tests ensuring the quality and evaluating the toxicity of the adjuvant and the adjuvant /antigen combination, would be fundamental to meet some of the requirements of the guideline on adjuvants in vaccines for human use, recommended by the European Medicines Agency (EMEA/CHMP/VEG/134716/2004). The toxicity assessment, in particular the local tolerance upon administration, would be particularly important for establishing comparisons with the currently available HBsAg vaccines adjuvanted with aluminum hydroxide. In fact, despite being used in several available vaccines, aluminum based adjuvants have been associated with severe local reactions such as subcutaneous nodules or granulomatous inflammation.

The use of exosomes as a non-specific adjuvant for HBsAg vaccine was the part of the work which still involves a larger number of questions. New studies have already been hypothesized. To start with, a detailed characterization of the surface markers expressed by the described exosomes has to be done. Also, in the future it should be assessed the influence of the LPS that was used as a stimulus for exosome production, in the immune response generated. Lastly, exosome production by stimulating cells with HBsAg antigen could be beneficial if we could load the antigen into the exosomes and simultaneously present the adjuvant and the antigen to the same APC. Nonetheless, in this situation the strategy would be to use the exosome as the antigen delivery system.

References

1.	Bilati, U., E. Allemann, and E. Doelker, *Development of a nanoprecipitation method intended for the entrapment of hydrophilic drugs into nanoparticles.* Eur J Pharm Sci, 2005. **24**(1): p. 67-75.
2.	Ulery, B.D., et al., *Rational design of pathogen-mimicking amphiphilic materials as nanoadjuvants.* Sci Rep, 2011. **1**: p. 198.
3.	Petersen, L.K., et al., *Activation of innate immune responses in a pathogen-mimicking manner by amphiphilic polyanhydride nanoparticle adjuvants.* Biomaterials, 2011. **32**(28): p. 6815-22.
4.	Jiao, Q., et al., *Immunomodulation of nanoparticles in nanomedicine applications.* Biomed Res Int, 2014. **2014**: p. 426028.
5.	Zhao, L., et al., *Nanoparticle vaccines.* Vaccine, 2014. **32**(3): p. 327-37.
6.	Patil, S., et al., *Mucoadhesive chitosan microspheres of carvedilol for nasal administration.* J Drug Target, 2010. **18**(4): p. 321-31.
7.	Florindo, H.F., et al., *The enhancement of the immune response against S. equi antigens through the intranasal administration of poly-epsilon-caprolactone-based nanoparticles.* Biomaterials, 2009. **30**(5): p. 879-91.
8.	Khatri, K., et al., *Plasmid DNA loaded chitosan nanoparticles for nasal mucosal immunization against hepatitis B.* Int J Pharm, 2008. **354**(1-2): p. 235-41.
9.	Saade, F., et al., *A novel hepatitis B vaccine containing Advax, a polysaccharide adjuvant derived from delta inulin, induces robust humoral and cellular immunity with minimal reactogenicity in preclinical testing.* Vaccine, 2013. **31**(15): p. 1999-2007.
10.	Hogenesch, H., *Mechanism of immunopotentiation and safety of aluminum adjuvants.* Front Immunol, 2012. **3**: p. 406.
11.	Mori, A., et al., *The vaccine adjuvant alum inhibits IL-12 by promoting PI3 kinase signaling while chitosan does not inhibit IL-12 and enhances Th1 and Th17 responses.* Eur J Immunol, 2012. **42**(10): p. 2709-19.
12.	Smith, R.E., et al., *A novel MyD-1 (SIRP-1alpha) signaling pathway that inhibits LPS-induced TNFalpha production by monocytes.* Blood, 2003. **102**(7): p. 2532-40.
13.	Bento, D., et al., *Development of a novel adjuvanted nasal vaccine: C48/80 associated with chitosan nanoparticles as a path to enhance mucosal immunity.* Eur J Pharm Biopharm, 2015. **93**: p. 149-64.
14.	McLachlan, J.B., et al., *Mast cell activators: a new class of highly effective vaccine adjuvants.* Nat Med, 2008. **14**(5): p. 536-41.

Supplementary material

Chapter 2

4.5 ml, 0.1 %
PCL solution
added dropwise

13.5 ml, 0.1%
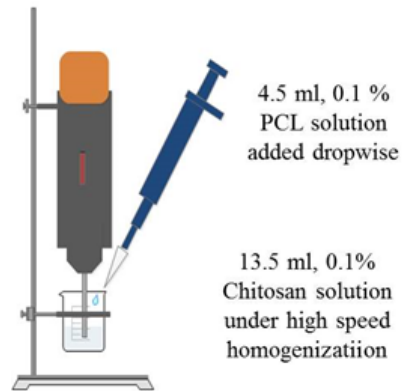Chitosan solution
under high speed
homogenizatiion

Figure A: PCL/chitosan NPs are produced by placing the high speed homogenizer probe into a beaker containing 13.5 ml chitosan aqueous solution and adding 4.5 ml PCL solution dropwise. The high speed homogenization is continued 1 min after complete PCL addition. Particles maturate 45 min under magnetic stirring before usage.
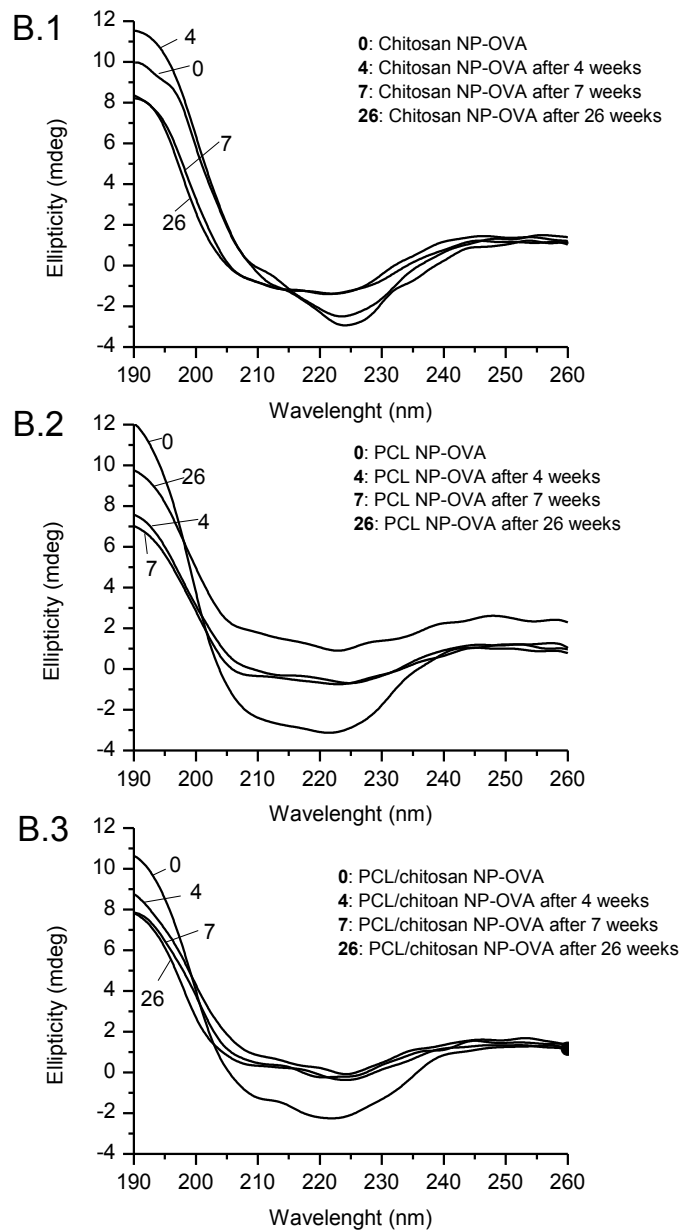
Figure B: CD spectra of Ovalbumin adsorbed to NPs over time at 4 ºC (B.1 - chitosan NPs; B.2 – PCL NPs; B.3 - PCL/chitosan NPs).
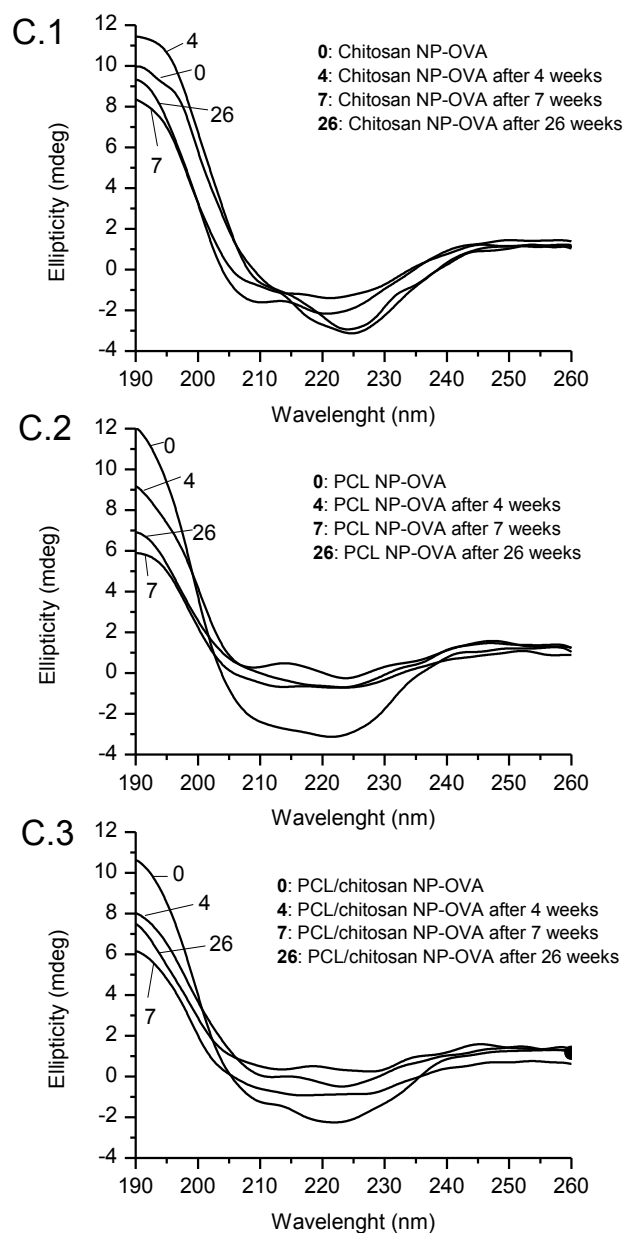
Figure C: CD spectra of Ovalbumin adsorbed to NPs over time at 45 ºC (C.1 - chitosan NPs; C.2 – PCL NPs; C.3 - PCL/chitosan NPs).
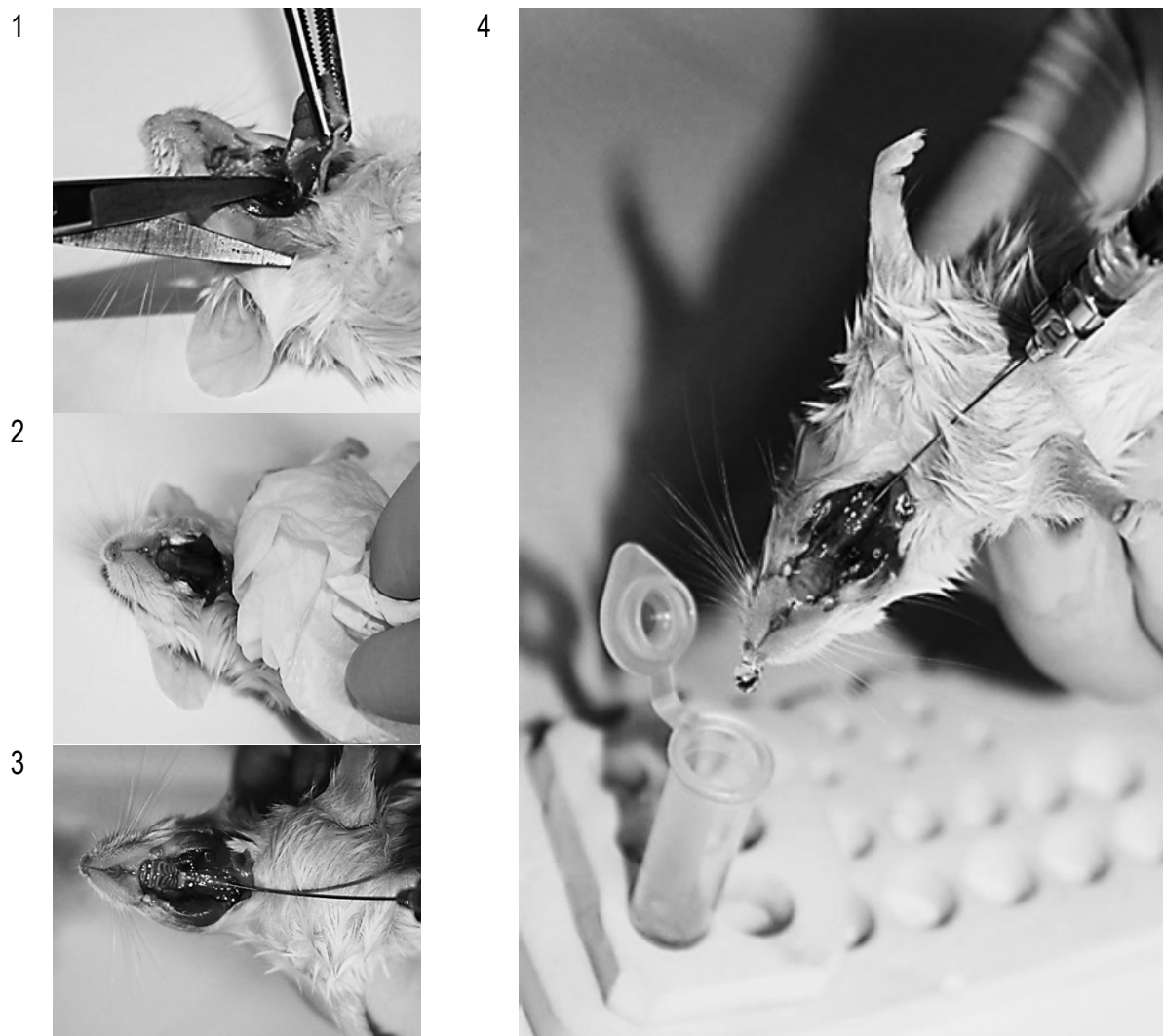
Chapter 5

Figure A: Representative images of the nasal wash technique performed in order to evaluate mucosal immune response in mice nasal mucosa after vaccination. Steps leading to the collection of the nasal wash are illustrated. 1) After the animal euthanasia the jaw is carefully removed by cutting the mouth sideways until the trachea shows up accessible without disruption. The separated jaw and tongue are transversally cut for better approach; 2) Blood present in the oral cavity is cleaned using PBS and medical compresses or absorbent paper; 3) A small hole in the trachea is done with a 19 G needle in order to further insert a mouse oral gavage needle; 4) The mice is positioned vertically to the collection tube, while the mouse oral gavage needle is inserted cautiously in the animal trachea. PBS is then flushed through the needle, passing the mice nasal cavity and exiting its nostrils to the collection tube.
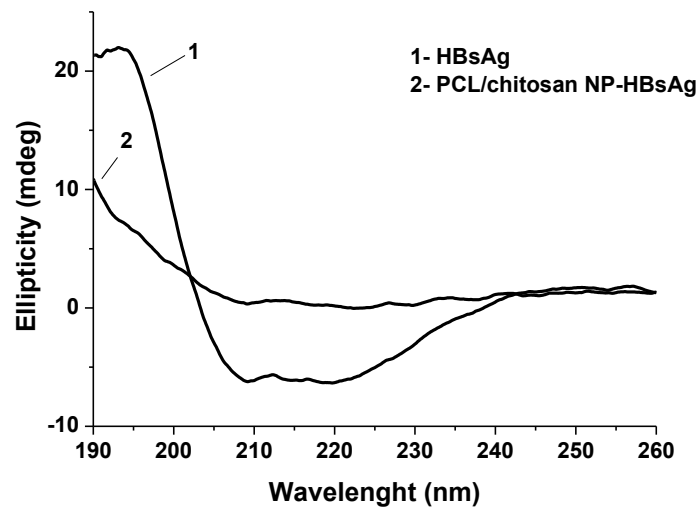
Chapter 6

Figure A: Circular dichroism analysis of hepatitis B recombinant protein. CD spectra of HBsAg in solution and after resuspension of a freeze-dried formulation of HBsAg adsorbed to PCL/chitosan NPs. The analysis was performed 1 month after freeze-drying and the powder was kept at room temperature.

225